Detection and characterization of nanoparticles released from municipal wastewater treatment plants and paints using single particle inductively coupled plasma mass spectrometry

Arshath Abdul Rahim

Doctor of Philosophy

Department of Civil Engineering and Applied Mechanics,

McGill University

Montreal, Quebec, Canada

August 2021

A thesis submitted to McGill University in partial fulfillment of the requirements of the degree of Doctor of Philosophy

Table of Contents

List of Tables

List of Tables in Supplementary Information

List of Figures

List of Figures in Supplementary Information

List of Figures in Appendix

Abstract

Engineered nanoparticles (ENPs) are being used extensively in a variety of industrial and consumer products due to their high specific surface area. Currently, some of the most common nanomaterials used are nanoscale titanium dioxide, copper, and silver. Titanium dioxide nanoparticles ($nTiO_2$) are attractive for their properties of photocatalytic activity and UV-protection. Copper and silver nanoparticles are largely used for their antimicrobial properties. Copper-based nanoparticles (nCu) are found in marine antifouling paints, agricultural biocides, textiles, and wood preservatives. Silver nanoparticles (nAg) are used in paints, medical bandages, textiles, and food containers. The widespread use of NPs in various products leads to their release to the environment during use of the products and as a consequence of their end-of-life disposal. A significant fraction of these ENPs used in products enter municipal wastewater treatment plants (WWTPs), which is eventually discharged to the environment primarily with waste sludge from settling tanks and to a smaller extent with effluent waters. It is estimated that 70-99% of the NPs entering the WWTP settle out with sludge. Biosolids derived from WWTP sludge are applied on agricultural lands as fertilizers and a significant fraction of the ENPs from sludge are retained in the biosolids. However, due to the limited quantitative data that is available on ENPs in sludge and biosolids, assessment of environmental risks and bio-uptake of ENPs is difficult.

The first objective of this research involves the development and optimization of methods to detect the size, particle size distribution and concentration of metal (Ag and Cu) ENPs in biosolids through the application of various extraction procedures and the subsequent analysis of aqueous extracts by single particle mode in inductively coupled plasma mass spectrometry (spICP-MS). The analysis was optimized and validated by performing control experiments with biosolids aqueous extracts spiked with gold NPs (nAu) of different sizes and development of this method enabled the detection of metallic nAg concentration of $2.6 \pm 0.0004 \times 10^7$ to $8.2 \pm 0.001 \times 10^8$ NPs/g of dry biosolids (mass concentration: 1.2 to 91.1 ng/g), with a mean size of approximately 16.0 ± 0.2 to 41.3 ± 0.5 nm measured for biosolids. Similarly, the measured concentration of nAg in sludge was $1.2 \pm 0.5 \times 10^7$ to $3.9 \pm 0.1 \times 10^9$ NPs/g in dry sludge with a mean size of approximately 21.8 ± 0.2 to 39.7 ± 2.1 nm. nCu was also detected in the sludge and biosolids matrices with a mean size ranging from 42.9 ± 0.3 to 109.7 ± 1.7 nm and particle number concentration of $2.8 \pm 0.001 \times 10^7$ to $2.7 \pm 0.02 \times 10^9$ NPs/g in dry biosolids, compared to a mean

size of 67.3 ± 1.1 to 142.8 ± 1.8 nm, with concentration of $6.4 \pm 0.4 \times 10^{7}$ to $1.7 \pm 0.004 \times 10^{10}$ NPs/g in dry sludge. For all WWTPs, measured nAg and nCu concentrations were lower than the predicted no observed effect concentration (PNEC) in soils. This is a step forward to understand how much NPs get released into the environment through the WWTP biosolids and will be a helpful input for policy makers. Furthermore, this study advances analytical capabilities for environmental fate and transformation of NPs in complex environmental matrices.

The second objective of this thesis focuses on the detection and the characterization of nAg and nCu using spICP-MS in wastewater (WW) effluent samples, by using sequential cycles of centrifugal ultrafiltration (CUF) to concentrate NPs into a smaller volume to improve detectability. Sequential cycles of CUF was found to be more efficient than cloud point extraction (CPE) using surfactants, an alternative approach that has been used to concentrate NPs from aqueous samples. WW effluent from 9 different Canadian municipal WWTPs were analysed for nAg and nCu using spICP-MS. Concentration of nCu varied from 0.1 ng/L to 12 ng/L depending on the WWTP effluent with size varying from 34.6 ± 1.3 to 68.0 ± 0.3 nm. Concentration of nAg detected ranged from 0.08 to 0.43 ng/L with mean size 19.3 ± 0.1 to 34.7 ± 7.2 nm lower than previously reported studies. These measured concentrations of NPs in WW effluent are 10^{3} to 10^{7} folds lower than in WW biosolids. Even though these NP concentration are below PNEC (nAg - 12 ng/L and nCuO - 340 ng/L) in freshwater, constant loading can lead to bioaccumulation of NPs in the organisms by constant exposure to WW effluent. The data reported here can be used for future modelling, exposure assessment and toxicology studies.

ENPs are being extensively used in paints and coatings to improve specific performance attributes, and thus are released in the environment over time. Little information is available on how the environmental risks of ENPs or its dissolved form released from products differ from pristine (as manufactured) ENPs. The third objective was to quantify the fraction of Ag released as ENPs or as dissolved species from painted surfaces over time due to contact with different pH solutions and/or direct exposure to sunlight; and to compare the colloidal stability and bacterial toxicity of the pristine nAg and released nAg from painted surface embedded in the paint matrix.. nAg releases increased over time at all pH conditions, with highest nAg concentrations observed at acidic pH of 3.5 at $2.16 \pm 0.78 \times 10^{7}$ NP/mL/g at the end of day 16, compared to basic pH ~8.5

with 3.86 ± 0.21 × 10^6 NP/mL/g or DI water pH ~5.8 with 2.07 ± 0.09 × 10^6 NP/mL/g. Thus, the release of nAg at acidic pH was 10-folds higher than with neutral pH and 5.6-folds higher than at basic pH. nAg released with acid pH was smaller in size, with mean diameter of 37.1 ± 2.1 nm compared to 64.6 ± 4.3 nm with neutral pH. The paint-released nAg was significantly more colloidally stable and resistant to dissolution compared to pristine nAg, at neutral pH. Finally, toxicity tests with *E. coli D21* suspended in aqueous extracts (neutral pH) of painted surfaces showed that cells were non-culturable after 3 hours, whereas no impact on culturability of cells exposed to pristine nAg was found over 42 h. Thus, the physico-chemical properties and ecotoxicological potential of paint-released and pristine nAg are significantly different.

nTiO_2 is one of the major ENPs used in paints for its photocatalytic properties and UV protection. About one third of global nTiO_2 produced is used in paints and coating, improving the products' properties. The paint's weight is composed of 10 to 30% of nTiO_2. The behavior of pristine nTiO_2 and released nTiO_2 from the painted surface should be analysed to understand their fate and toxicity. The fourth objective was to quantify the fraction of nTiO_2 released from painted surfaces (commercial and custom-made paints) over time due to contact with different pH solutions and/or direct exposure to sunlight; and to compare the colloidal stability and bacterial toxicity of the pristine nTiO_2 and released nTiO_2 from painted surface embedded (custom-made paint) in the paint matrix. Comparison of four commercial paints with unknown concentration of nTiO_2 showed that B-NP ext. (claimed to have NPs) released 11 to 16 times lower nTiO_2 of 1 to 2 ng/mL of water/g of dry paint compared to other commercial paints ~ 10 to 30 ng/mL/g. At acidic pH 3.5-4.2, nTiO_2 released from commercial paint on surfaces were 20 to 42% more compared to neutral or basic for three paints except for A ext. paint. As different commercial paints released dissimilar amounts of nTiO_2 under different pH conditions, no observable patterns of release were detected for all four paints. Custom made paint at acidic pH of ~3.5 and basic pH ~8.5 lead to aggregation and settling of nTiO_2 compared to DI water (pH ~5.8). Sonication of the collected wash water from acidic pH ~3.5 released twice the particle number compared to basic pH ~8.5 and DI water at pH ~5.8 at the end of 11 days. Custom made paint with nTiO_2 behaves similarly to commercial paint B-NP ext., with concentrations of ENP released around ~1 ng/mL/g in quiescent systems exposed to DI water, acidic and basic conditions. Finally, disinfection tests on survival of *E. coli D21* showed that nTiO_2 released from paint were toxic after 6 hours compared to base paint (which recorded survival up to 18 h) and pristine $nTiO_2$, where the *E. coli D21* survival was present through the experiment period of 42 h.

Overall, this research gives a better understanding of the release of NPs from paints and presents newly developed techniques to detect and measure NPs in one of the major environmental sinks (WWTPs). The thesis explores the difference in stability and disinfection properties between pristine NPs and NPs released from paints. In addition, it established new methods to concentrate and detect NPs in complex matrices in WWTPs like WW effluent, sludge and biosolids.

Résumé

Les nanoparticules de synthèse (NPs) sont intensivement utilisées dans une multitude de produits industriels et de consommation, grâce à leur grande surface spécifique. Actuellement, les nanoparticules les plus populaires sont les nanoparticules de dioxyde titane, de cuivre et d'argent. Les nanoparticules de dioxyde de titane ($nTiO_2$) sont surtout utilisées pour leur activité photocatalytique et leur protection contre les rayons ultraviolets. Les nanoparticules de cuivre (nCu) sont trouvées dans les peintures antisalissures marines, les biocides agricoles, les textiles et les préservatifs de bois. Les nanoparticules d'argent (nAg) sont utilisées dans les produits de peinture, les bandages médicaux, textiles et les contenants alimentaires. L'usage répandu de nanoparticules (NPs) dans divers produits aboutit à leur rejet dans l'environnement lors de l'usage des produits et comme une conséquence de rejet de fin de vie. Une grande partie de ces NPs utilisés dans plusieurs produits se jette dans les stations de traitement des eaux usées (STEP), et finit par être rejetée dans l'environnement principalement avec les boues provenant des bassins de décantations, et avec les effluents dans une moindre mesure. En effet, 70 à 99% des NPs affluents aux STEP sont éliminées par décantation. Les biosolides dérivées des boues des STEP sont appliquées en tant que fertiliseurs dans les terres agricoles, et une proportion importante des NPs des boues est retenue dans les biosolides. Cependant, les données quantitatives disponibles sur les NPs dans les boues et les biosolides sont limitées, rendant ainsi l'évaluation du risque environnemental et de l'absorption biologique des NPs plus difficiles.

Le premier objectif de cette thèse est de développer et d'optimiser des méthodes pour détecter la taille, la distribution de tailles des particules et la concentration en NPs de métaux (Ag et Cu) dans les biosolides, à travers l'application de plusieurs procédures d'extraction et d'analyse subséquente des extraits aqueux avec la spectrométrie de masse par plasma à couplage inductif à une seule particule (spICP-MS). L'analyse a été optimisée et validée en effectuant des expériences de contrôle avec des extraits aqueux de biosolides additionnés avec des NPs en or (nAu) de tailles différentes, et le développement de cette technique a permis la détection de nAg métallique avec une concentration de $2.6 \pm 0.0004 \times 10^7$ à $8.2 \pm 0.001 \times 10^8$ NPs/g de biosolides secs (concentration en masse : 1.2 à 9.1 ng/g), avec une taille moyenne de 16.0 ± 0.2 à 41.3 ± 0.5 nm nm mesurée pour les biosolides. Pareillement, la concentration en nAg mesurée était de $1.2 \pm 0.5 \times 10^7$ à $3.9 \pm 0.1 \times 10^9$ NPs/g dans les boues sèches avec une taille moyenne de 21.8 ± 0.2 à 39.7 ± 2.1 nm. Des

particules de nCu ont été aussi détectées dans les matrices de boues et des biosolides, avec une taille moyenne entre 42.9 ± 0.3 et 109.7 ± 1.7 nm et une concentration de nombre de particules de $2.8 \pm 0.001 \times 10^7$ à $2.7 \pm 0.02 \times 10^9$ NPs/g pour les biosolides secs, comparées à une taille moyenne entre 67.3 ± 1.1 et 142.8 ± 1.8 nm et une concentration de $6.4 \pm 0.4 \times 10^7$ à $1.7 \pm 0.004 \times 10^{10}$ NPs/g dans les boues sèches. Pour tous les STEP, les concentrations en nAg et nCu étaient inférieures à la concentration prévisible sans effet (CPSE) dans les sols. Ceci constitue une méthode innovative pour comprendre la quantité de NPs rejetée dans l'environnement à travers les biosolides des STEP et sera contribution utile aux décideurs politiques. De plus, cette étude avance les capacités analytiques pour l'évaluation du devenir et de la transformation des NPs dans les matrices complexes environnementales.

Le deuxième objectif de cette thèse concerne la détection et la caractérisation des nAg et nCu à l'aide de la spICP-MS dans les échantillons d'effluents d'eaux usées, en utilisant les cycles séquentiels d'ultrafiltration centrifuge (UCF) pour concentrer les NPs dans de plus petits volumes et améliorer ainsi leur détectabilité.La technique des cycles séquentielles d'UCF s'est révélée être plus efficace que le procédé d'extraction au point trouble (EPT); ce dernier est basé sur l'utilisation d'agents de surface, qui est une autre approche utlisée pour concentrer les NPs dans les échantillons aquatiques. Des échantillons d'effluents d'eaux usées ont été extraits de 9 différentes STEPs municpales Canadiennes et analysés pour nAg et nCu à l'aide de la spICP-MS. La concentration en nCu variait entre 0.1 ng/L et 12 ng/L, dépendamment sur l'échantillon d'effluent d'eaux usées, avec la taille variant entre 34.6 ± 1.3 et 68.0 ± 0.3 nm nm. La concentration en nAg était détectée entre 0.08 et 0.43 ng/L avec une taille moyenne entre 19.3 ± 0.1 et 34.7 ± 7.2 9 nm, qui sont des valeurs inférieures à celles reportées dans les études antérieures. Ces concentrations de NPs mesurées dans l'effluent d'eaux usées ont été trouvées 10^3 à 10^7 fois plus inférieures à celles dans les biosolides des eaux usées. Même si ces valeurs de concentrations de NPs sont bien au-dessous du CPSE (nAg - 12 ng/L et nCuO -340 ng/L) dans les eaux douces, leur chargement continu aboutirait à la bioaccumulation de NPs dans les organismes à travers l'exposition continue aux effluents d'eaux usées. Les données reportées dans cette étude pourraient être utiles dans les modélisations futures ainsi que dans les études d'évaluation de l'exposition et de toxicologie.

Les NPs sont intensivement utilisés dans les produits de peinture et de revêtement afin d'améliorer leurs attributs de perfomance, et par conséquent, seront rejetés dans l'environnement avec le temps. Peu d’informations sont disponibles concernant le risque environnemental lié au rejet des NPs et la façon dont leur forme dissolue émise des produits diffère de la forme intacte des NPs. Ainsi, pour le troisième objectif de cette thèse, les particules de nAg et de nAg dissolues émises des surfaces peintes dans les solutions aqueuses de chimie variante pour une période de 15 jours, étaient charctérisées à l’aide sw la spICP-MS. Les rejets de nAg augmentent avec le temps sous toutes les conditions de pH, où la concentration la plus élevée de nAg mesurée était dans un pH acide de 3.5, de l’ordre de 2.16 ± 0.78 × 10^7 NP/mL/g à la fin du $16^{ème}$ jour, comparé au pH basique de ~8.5 avec une concentration de 3.86 ± 0.21 × 10^6 NP/mL/g, ou de l’eau DI (pH ~5.8) avec 2.07 ± 0.09 × 10^6 NP/mL/g. Ainsi, le rejet de nAg dans un pH acide était 10 fois plus élevé que celui dans un pH neutre et 5.6 fois plus élevé que celui dans un pH basique. Les particules de nAg émises dans le pH acide étaient plus petites de taille, avec un diamètre moyen de 37.1 ± 2.1 nm, comparé à 64.6 ± 4.3 nm dans le pH neutreLes nAg émises des surfaces de peinture étaient considérablement plus stables au niveau des colloïdes et résistantes à la dissolution, comparées aux nAg intactes dans un pH neutre. Finalement, des tests de toxicité avec l’*E. coli D21* suspendu dans des extraits aqueux (pH neutre) des surfaces peintes, montrent que les cellules devenaient non-cultivables après 3 heures, tandis qu’aucun impact est reporté sur la cultivabilité des cellules exposées aux nAg intactes durant 24 heures. Ainsi, les propriétés physico-chimiques et le potentiel écotoxicologique des nAg intactes et celles émises des surfaces peintes sont considérablement différents.

Les particules de $nTiO_2$ sont notamment utilisées dans les produits de peinture pour leurs propriétés photocatalytiques et leur protection contre les rayons ultraviolets. Environ un tiers des $nTiO_2$ produites sont utilisées pour la peinture et le revêtement, améliorant ainsi les propriétés des produits. En fait, le poids de la peinture est composé de 10 à 30% de $nTiO_2$. Le comportement des $nTiO_2$ intactes et de celles émises des surfaces peintes doit être analysé afin de comprendre leur devenir et leur toxicité. Pour le quatrième objectif de cette thèse, les $nTiO_2$ émises des surfaces peintes, en utilisant des peintures commerciales et des peintures faites sur mesures, ont été analysées sous différentes conditions de pH pour caractériser leur tailles, concentrations et la distribution des tailles de particules, en analysant des échantillons de lavage aqueux avec la spICP-MS. L’analyse de 4 échantillons de peintures commerciales, parmi lesquels un produit est marqué d’avoir de la peinture contenant des NPs tandis que les autres ne le sont pas, a montré que le produit de peinture à base de NP émet 11 à 16 fois moins de $nTiO_2$ avec une concentration de 1 à 2 ng/mL d'eau/g de peinture sèche, comparée aux autres peintures commerciales ~ 10-30 ng/mL/g. Dans un pH acide de ~3.5, les $nTiO_2$ émises de 3 peintures commerciales, appliquées sur des surfaces modèles, étaient de 20 à 42% de plus que celles émises sous un pH neutre ou basique; cependant, ces tendances n'étaient pas observées pour le 4ème échantillon de peinture. Puisque les différentes peintures commerciales ont émis de différentes quantités de $nTiO_2$ sous différent PHaucun patron d'émission était remarqué pour les quatre échantillons de peinture. Les peintures faites sur mesure sous un pH acide de ~3.5 et basique de ~8.5 ont abouti à une agrégation et une décantation de $nTiO_2$, comparé à l'eau DI (pH ~5.8). La sonification des eaux de lavage collectées d'un pH acide de ~3.5, rejetait deux fois plus le nombre de particules comparé au pH basique ~8.5 et l'eau DI ayant un pH ~5.8, à la fin du 11ème jour d'analyse. Les peintures faites sur mesure avec le $nTiO_2$ se comportent de façon similaire à la peinture commerciale B-NP ext., avec des concentrations de NPs émises de ~1 ng/mL dans les systèmes à repos exposés à l'eau DI, et à des conditions acides et basiques. Finalement, des tests de désinfection concernant la survie de l'*E. Coli D21* montrent que les $nTiO_2$ émises des peintures étaient toxiques après 6 heures comparées aux peintures de base (enregistrant une durée de survie de 18h) et aux $nTiO_2$ intactes, où la survie d'*E. coli D21* était toujours présente tout au long de la période de l'expérience de 42 heures.

En conclusion, cette thèse fournit une meilleure compréhension concernant l'émission des NPs des peintures, et présente de nouvelles techniques développées pour détecter et mesurer les NPs dans un des lieux environnementaux les plus importants (les STEPs). Cette thèse identifie la différence dans les propriétés de stabilité et de désinfection entre les NPs intactes et celles émises des peintures. De plus, de nouvelles méthodes sont présentées pour concentrer et détecter les NPs dans les matrices complexes de STEPs, telles que l'effluent d'eaux usées, les boues et les biosolides.

Acknowledgment

I would like to express my sincere gratitude and appreciation to my supervisor, Prof. Subhasis Ghoshal, for giving me the opportunity to pursue a PhD degree and whose continuous support, guidance, and patience during the course of my dissertation. I would like to thank him again for opportunity he has given me to work on multiple projects with numerous collaborators, which has helped to widen my research skill and abilities.

I would like to thank all the collaborators, Dr. Ali Akbari, Dr. Sanaz Alizadeh, Dr. Sarayu Rao, Dr. Krittika Mittal, Dr. Xiaoyu Gao, Mariana Umpiérrez-Failache, and Anirban Kundu, for their expertise and insights into completions of the various research projects. A sincere thanks to David Liu (McGill University) and Jean-Philippe Masse (École Polytechnique de Montréal) for the help with microscopic analysis of my complex samples. I would like to thank Jorge Sayat, Dr. William Cook, John Bartczak, Daina Brumelis, William Dumais and Dr. Pinar Ozcer for their help with technical assistance. I would like to acknowledge the financial support from McGill Engineering Doctoral Award (MEDA), John M. Bishop and family Fellowships for Sustainability in Engineering and Design, Lars & Alberta Firing Graduate Fellowships in Engineering, McGill Sustainability Systems Initiative (MSSI) Material Research Theme Graduate Award, CREATE in Green Chemistry and finally, Natural Science and Engineering Research Council of Canada (NSERC), Environment and Climate Change Canada (ECCC), Hydro Quebec funding through Prof. Subhasis Ghoshal.

A special thanks to all my current and previous research colleagues, namely, Dr. Ali Akbari for his role as a mentor in the initial stages of my PhD, Dr. Sai Rajasekar Chandrasekar Rajajayavel, Dr. Sanaz Alizadeh, Dr. Sarayu Rao and Mariana Umpiérrez-Failache for the heart warming friendship and support, Dr. Sourjya Bhattacharjee, Dr. Mehrnoosh Azodi, Dr. Yanyan Zhang, Anirban Kundu, Vinicius Bueno, Aude Bechu and others for their support. I would also like to thank all the graduate students in the Environmental Engineering office and lab for creating a great productive work environment.

I am grateful for all my friends in Montreal (Jai, Rias, Ferose, Varun and many others) and back home in India (Dinu, Abhilash, Sooraj and many others) for their continuous support during my PhD journey. My deepest thanks go to my partner Sarah El Outayek, for her amazing support

and love. Last but not least, I am thankful for the love and encouragement of my parents (Abdul Rahim and Sakeena) and my brother (Ashik), without which I would not have completed this degree.

Preface and Contribution of Authors

Preface

In accordance with the *"Guidelines for Thesis Preparation"*, this thesis is presented in a manuscript-based format. Chapters 1 and 2 include the introduction and literature review, followed by the discussion of the results presented in a manuscript format in chapters 3-6. Chapter 7 presents the summary and conclusion of this thesis and the potential for future work. The manuscripts presented in Chapters 3 to 6 have been or are in preparation to be submitted to different peer reviewed journals. In all the publications stated above, the author of the manuscript is the primary author of this thesis. A detailed description of the efforts and contributions to new knowledge of all authors are presented below.

Contribution of Authors

- Findings from Chapter 3 are in preparation for submission to the following journal: Environmental Pollution.

Rahim, A.A., and Ghoshal, S. (2021), "Silver and copper nanoparticles in sludge and biosolids from municipal wastewater treatment plants"

- Rahim, A.A. - Designed and conducted experiments, analysed data, and wrote the manuscript.
- Ghoshal S. - Experimental design, research supervision, discussion of experimental results, and revision of manuscript.
- Findings from Chapter 4 are in preparation for submission to the following journal: Science of the Total Environment.

Rahim, A.A. and Ghoshal, S. (2021), "Concentration of silver and copper nanoparticles in WW effluent from municipal wastewater treatment plants"

- Rahim, A.A. - Designed and conducted experiments, analysed data, and wrote the manuscript.
- Ghoshal S. - Experimental design, research supervision, discussion of experimental results, and revision of manuscript.

- Findings from Chapter 5 are in preparation for submission to the following journal: Science of the Total Environment.

Rahim, A.A., Kundu, A. and Ghoshal, S. (2021), “Stability and disinfection of silver nanoparticles released from paint compared to pristine nanoparticles.”

- Rahim, A.A. - Designed and conducted experiments, analysed data, and wrote the manuscript.
- Kundu, A. - Assisted with *E. Coli* disinfection studies, discussion of experimental results.
- Ghoshal S. - Experimental design, research supervision, discussion of experimental results, and revision of manuscript.
- Findings from Chapter 5 are in preparation for submission to the following journal: Science of the Total Environment

Rahim, A.A., Kundu, A. and Ghoshal, S. (2021), “Release of titanium dioxide nanoparticles from custom-made and commercial painted surface in water and associated disinfection studies”

- Rahim, A.A. - Designed and conducted experiments, analysed data, and wrote the manuscript.
- Kundu, A. - Assisted with *E. Coli* disinfection studies, discussion of experimental results.
- Ghoshal S. - Experimental design, research supervision, discussion of experimental results, and revision of manuscript.
- Findings from Chapter 6 are in preparation for submission to the following journal: Science of the Total Environment

Contribution to Knowledge

The specific contributions to new knowledge from four chapters which are to be submitted for publication are listed below.

- **Chapters**
    - Chapter 3 - Silver and copper nanoparticles in sludge and biosolids from municipal wastewater treatment plants
    - Chapter 4 - Concentration of silver and copper nanoparticles in WW effluent from municipal wastewater treatment plants
    - Chapter 5 - Stability and disinfection of silver nanoparticles released from paint compared to pristine nanoparticles
    - Chapter 6 - Release of titanium dioxide nanoparticles from custom-made and commercial painted surface in water and associated disinfection studies

1. **Extraction and characterization of nAg and nCu particles in complex matrix like sludge and biosolids of municipal wastewater treatment plants from 11 plants across Canada using single particle ICP-MS.** There is a lack of reports in the literature of reliable data from direct measurements of the size and concentration of ENPs in municipal WWTP sludge and biosolids, which are expected to contain high loads of ENPs. This study identified an efficient method for extraction of NPs from sludge and biosolids, that enabled subsequent detection and characterization of nAg and nCu particle size distributions and concentrations by single particle mode in Inductively coupled mass spectrometer (spICP-MS). Finally, characterization of nAg and nCu size, particle size distribution and concentrations from sludge and biosolids from eleven WWTPs across Canada were performed. This is the first report of systematic ENP characterization in sludge and biosolids across several regional WWTPs anywhere in the world.
2. **Development of techniques to pre-concentrate NPs (nAg and nCu) in low NP concentrated wastewater effluent from municipal wastewater treatment plants across Canada. The concentrated NPs are detected for size and concentration single particle ICP-MS.** Several studies have estimated that significant fractions of NPs released from various products are released to sewers and eventually to wastewater treatment plants. It is estimated that 70-99% of the NPs entering the municipal WWTP settle out with sludge

generated at the plants. A smaller fraction of the NPs entering the municipal WWTP is released with WW effluent to water bodies. However, given the large volumes of WW effluents; the release with effluents still constitutes a significant flux. In this study, we characterized nAg and nCu using spICP-MS in WW effluent samples by developing methods to concentrate them in aqueous samples. This is the first report of systematic characterization of NPs in multiple WW effluent in Canada. This data is an important step in enabling future risk assessment and modelling studies.

3. **Comparative study on the stability and reactivity of pristine nAg to nAg released from paints.** In previous studies on toxicity, transformation and stability of NPs have been generally characterized using pristine NPs, instead of NPs released from nano-enabled products. In this study, nAg released from paint applied on surfaces under various environmental aging and aqueous chemistry conditions were characterized for size and concentration by analyses of the aqueous phase in contact with painted surfaces by ICP-MS in single particle mode. This study showed that the nAg released from paint, after detaching from the paint matrix, have different physico-chemical and biological properties compared to pristine nAg. No significant change over time was observed with released nAg from painted surfaces in terms of aggregate/particle sizes, ENP concentration, stability, and dissolution activity. Pristine nAg, however, demonstrated significant aggregation and dissolution over time. This contributes to the understanding of the distinct behaviour of released ENPs from products and pristine ENPs. Furthermore, this study showed that nAg released from paint have higher toxicity to *E. coli D21* compared to base paint, and pristine nAg. Our results signify the necessity of toxicity and fate studies using released ENPs from products, rather than pristine ENPs. This report proves that current approaches of using pristine ENPs do not represent the real scenario of ENPs released from products.
4. **nTiO_2 used in commercial paints behaved differently from macro size TiO_2. nTiO_2 released from painted surfaces are different from pristine nTiO_2**. The literature on studies related to stability, transformation, and toxicity of nTiO_2 were generally characterized using pristine NPs, instead of NP released from nano-enabled products. In addition, most of the past published research reports characterization of nTiO_2 using total metal analysis and microscopic techniques without particle sizing and NP concentration

information in complex matrix. In this thesis, the release of $nTiO_2$ from painted surfaces using both commercial and custom-made paint under various pH conditions was characterized for size, concentration, and particle size distribution by analyses of the aqueous wash samples by ICP-MS in single particle mode. This study characterized the concentration of $nTiO_2$ released from a declared nano-enabled commercial paint to be 10 to 16 times lower compared to commercial paints that do not mention any information of the TiO_2 particle sizes used. Even though a high concentration (10% w/v) of $nTiO_2$ is used to produce the nano paint, only less 1% NPs was released from the surface with exposure to water of different pH, implying satisfactory binding of NP with the resins in the paint matrix. In addition, this study showed that $nTiO_2$ released from paint have higher toxicity to *E. coli D21* compared to base paint, and pristine $nTiO_2$.

List of Abbreviations

AAS: Atomic absorption spectroscopy

CPE: Cloud point extraction

CUF: Centrifugal ultrafiltration

DI: De-ionized

DLS: Dynamic light scattering

DOC: Dissolved organic carbon

EDS: Energy dispersive X-ray spectroscopy

ENP: Engineered Nanoparticle

ICP-MS: Inductively coupled plasma mass spectrometry

ICP-OES: Inductively coupled plasma optical emission spectrometry

KNO_3: Potassium nitrate

LB agar: Luria–Bertani agar

NOM: Natural organic matter

nAg: Silver nanoparticles

nAu: Gold nanoparticles

nCu: Copper nanoparticles

$nTiO_2$: Titanium dioxide nanoparticles

NOM: Natural organic matter

NP: Nanoparticle

NTA: Nanoparticle tracking analysis

PVP: Polyvinylpyrrolidone

ROS: Reactive oxygen species

SEM: Scanning electron microscopy

spICP-MS: Single Particle Inductively Coupled Plasma Mass Spectrometer

TEM: Transmission electron microscopy

UV: Ultraviolet

WW effluent: Wastewater effluent

WWTP: Wastewater treatment plants

CHAPTER 1   INTRODUCTION

1.1.   Introduction

Nanotechnology is one of the major areas for industrial growth, with engineered nanoparticles (ENPs) used in wide range of fields. Nanoparticles (NPs) are defined as chemical substances having one or more dimensions less than 100 nm [1, 2]. The properties of NPs are significantly different from those of other materials due to quantum effects and other unique properties (e.g. reactivity, optical and electrical characteristics) arising from the high specific surface area where a significantly larger number of atoms are exposed to the surface compared to larger particles or the bulk forms of the materials. In the environment, NPs can occur naturally (e.g. volcanic ash), and can be produced unintentionally through anthropogenic activity, mostly from combustion and industrial mechanisms (e.g., diesel engines) or in the case of ENPs can be synthesized or manufactured with specific sizes, shapes and composition [3, 4].

The potential areas of use of ENPs is extensive, which can include cosmetics, textiles, electronics, medical, paints and coatings, water treatment, soil remediation, food, packaging and many more. The major types of ENPs used in different fields of expertise include carbon NPs (fullerenes and carbon nanotubes), metal and metal oxide NPs (titanium dioxide, silica, silver, copper, etc.), semiconductor NPs (quantum dots), polymeric NPs (organic based) and lipid-based NPs [5-7]. Based on the research report of nanotechnology market forecast of 2020, global nanotechnology market between 2020 and 2025 is expected to have a compound annual growth rate of more than 14.3% with investments close to $121 billion [8].

Despite the success of this emerging technology, there is insufficient information regarding the health and environmental risks related to the ENPs [9, 10]. The extensive use of ENP-enabled products leads to the release of ENPs from various products during their use or end-of-life into the environment without full knowledge of their fate, behaviour and impacts on the environment and biota [10-12]. The small size and large surface areas of NPs enhance their ability to cross cell membranes [13]. Also, the similarity of ENPs in size-to-cellular components might trigger allosteric interactions with proteins and nucleic acids, which could interrupt vital processes (gene translation, transcription, and enzyme function) [14, 15]. In addition, the large surface area of NPs can boost the chemical reactivity and reactive oxygen species generations [16, 17], making them contaminants-carriers through a fast and long-range transport.

Several studies have indicated the release of these NPs from nano-enabled products into the environment through various pathways [18, 19]. Municipal wastewater treatment plants (WWTPs) are considered one of the main acceptors of NPs released during the processes of manufacturing, using or disposing of NP-based products [20, 21]. Studies have reported that 17 and 34% of the total metal NPs that are manufactured are released to WWTPs [18, 19, 22, 23]. NP concentrations in wastewater effluent samples extracted from 10 municipal facilities across the USA were found to be ranging between <2 to 20 μg/L [20, 24-26]. Furthermore, probabilistic material flow analysis, applied to estimate the concentrations of NPs in the effluents of different WWTPs across USA and Europe, reported the following NPs concentration values: $nTiO_2$ (1.8 to 4.3 ng/L), nZnO (0.3 to 0.4 ng/L), nAg (21.0 to 42.5 ng/L), carbon nanotubes (8.6 to 14.8 ng/L) and fullerenes (3.8-5.2 ng/L) [18, 22, 23].

Despite the low concentration of NPs currently measured in wastewater, these numbers are expected to increase due to the growth of the global production of NP-based products in the near future. The released NPs reach WWTPs, where they are eliminated from effluent through settling, biosorption, aggregation, precipitation and other biomass mediated techniques to sludge [20, 24, 27-30]. Therefore, an increase in the WW influent NP concentrations will result in an increase of NPs in the effluent and sewage sludge. Mainly, WWTPs are responsible for removing phosphorus, nitrogen, and organic matter. The sewage sludge, outcome of the wastewater treatments, requires stabilization through sewage sludge digestion preceding the final disposal (e.g. landfilling) [31]. Hence the importance of assessing the potential impacts of NPs on the sewage sludge digestion processes and the biological wastewater treatment.

The detection and characterization of NPs in complex matrices is challenging and can be achieved through several available methods. First, imaging techniques, such as Scanning Electron Microscopy (SEM) and Transmission Electron Microscopy (TEM), are used for the detection of NPs in clean matrices. However, these methods require extensive sample preparation (removal of solids and concentrating NPs in the sample), especially in complex matrices (ex. soils, biosolids), and do not provide reliable quantitative information about the ENP concentrations due to their low concentrations and the small sample size analyzed [32, 33]. Particle sizing techniques, such as Dynamic Light Scattering (DLS) and Nanoparticle Tracking Analysis (NTA) are commonly used in NP analysis, and yet have some limitations regarding the analysis of NPs in environmental samples representing complex media, due to their inability to distinguish target NPs from background natural colloids, such as clays and mineral oxide particles. In fact, these methods rely on the light scattering intensity, which is proportional to the sixth power of the particle size. Thus, the presence of a small amount of background natural colloids, that is larger than the NPs, will lead to biased higher estimates of NPs size [34]. Finally, the single particle inductively coupled plasma mass spectrometry (spICP-MS) is considered a powerful technique to measure metal NP sizes and concentrations in relatively pure aqueous samples at sub parts per billion concentrations [35-42].

Several studies have reported on the toxicity of pristine NPs to model organisms (e.g. algae, zebrafish) [43, 44]. For example, silver NPs (nAg) have shown toxic effects in WW biofilm at constant loading concentrations as low as 10 and 22 µg/L [45]. No observed effect concentration (NOEC) of nAg in algae is 250 µg/L [46]. Effect concentration at 10% effect (EC_{10}) of nAg in *Daphnia magna* is ~12 µg/L [46]. Similarly, copper NPs (nCu) have shown toxic effects in fish at concentrations as low as 20 µg/L [47]. NOEC of copper toxicity on algae, invertebrates (*Daphnia magna*) and fish are 22, 14.9 and 15.6 µg/L, respectively [48]. However, despite the presence of these extensive studies, the evaluation of toxicities of NPs to microbes in WW treatment processes remains in early analysis phase. In fact, these microbial systems are more complex compared to the previously studied pure cultures, since they contain different microbes, organic and inorganic matters. Hence, previous studies on the NP-induced toxicity to paradigm organisms cannot be used to assess accurately the toxicity of NPs to microbes in wastewater treatment processes. Toxic effects of NPs are contributed by both nanospecific (due to the size and reactive oxygen species generation) [49-53] and ion release [53-55]. Toxicity of free ions is shown in many organisms and complexation may result in the reduction of ions, leading to lower toxic effects [56, 57]. Additionally, dissolved ions form insoluble or sparingly insoluble inorganic complex that may sediment from the system [52, 58]. Therefore, WW effluent with high organic matter can still be dangerous to aquatic organisms with nanospecific toxic effects. Nonetheless, since wastewater treatment processes are well engineered, the potential negative impacts of NPs can be reduced by improving the design process and/or operational conditions.

The more ENPs are used in consumer products, the higher their release into the environment. NP detection and characterization is challenging in WWTP samples due to the low concentrations and complex matrices. Nevertheless, there is a lack of measured concentration and size of NPs in municipal WWTP and their related impacts on the environment. Material flow models rely on the life cycle of nano-enabled products to give estimates of the total mass of ENPs being discharged into different environmental matrices [59], without distinguishing between dissolved fractions, single, transformed and agglomerated ENPs [60]. Hence, as part of environmental risk assessment, appropriate analytical techniques need to be developed, in order to measure and assess transformed ENPs at their predicted environmental concentrations in WW effluent, sludge and biosolids from municipal WWTPs. This is a major fate process disregarded by material flow models, leading to a lack of measured concentration of NPs in WW effluent, sludge and biosolids. Furthermore, transformation of NPs from products can influence the bioavailability and toxicity. Sulfidation of nAg in WWTPs is an example of a transformation process, as it reduces the bioavailability of nAg caused by the formation of insoluble Ag_2S, slowing down the release of dissolved Ag [61, 62]. However, incomplete sulfidation may continuously release dissolved ions, leading to toxicity to target organisms [61, 63]. In comparison, nCu were found to be more soluble with the formation of nCuS, which can lead to toxicity and bioavailability due to formation of dissolved Cu [64]. Thus, it is essential to detect and characterize the transformation of NPs in WWTPs to determine their fate in the environment. Specifically, a detailed comprehension of measured size and concentration on NPs on WW effluent, sludge and biosolids in WWTPs is required.

1.2. Knowledge Gaps

There is a consensus in literature that approximately 70-99% of the NPs entering the WWTP settle out with sludge [65-67]. A minor fraction of the NPs entering the WWTP is released with WW effluent to water bodies; however, given the large volumes of WW effluents, the release with effluents still constitutes a significant flux. The characterization of the concentration, sizes and compositions of NPs in WW effluents have not been thoroughly assessed in the literature. NP detection in complex environmental matrices (such as biosolids or sludge) is difficult, as the concentration in the environment is low and it is hard to identify and measure them in the matrix. The reported data on NP size and particle concentration data (including nAg or nCu) in the complex matrix like sludge or biosolids is minimal, and thus detection and characterization of NPs is very challenging.

Approximately 50-60% of WWTP sludge generated in North America is used for land application [68, 69], and thus, the assessment of the NPs present in waste sludge and biosolids, prepared for land application, is important for assessing the incremental risks posed by NPs to biota and humans. There are currently no demonstrated methods for extraction and characterization of NP concentrations and size in complex matrices like WW sludge and biosolids. There is a need to assess the effects of NP concentration, size, and composition as well as contact time with sludge and biosolids. Furthermore, various treatment techniques applied for stabilization of sludge from WWTPs to make biosolids (e.g. alkaline sludge stabilization, composting, pasteurization, anaerobic digestion), can cause physical and chemical transformations of NPs. However, the extent and nature of the transformations, along with the diversity in size and composition of specific ENPs caused by different biosolids treatments, are not yet known.

To evaluate ENPs along with their fate in WWTPs, it is important to assess the characteristics of ENPs released from different sources, in addition, to the differences from their pristine counterparts, which are often, employed in laboratory fate and toxicity studies. One of the major sources of NPs released in the environment is from outdoor paints and coating applied on buildings, automobiles, pipes, etc. There is scarce published information on the concentration of ENPs likely to be readily released and the aggregation, dissolution, transformation, distribution behavior and toxicity of these ENPs released from nano-enabled products compared to their pristine counterparts.

1.3. Research Objectives

The overall goal is to develop reliable techniques for the detection and characterization of NPs released from nano-enabled products into municipal WWTPs, and to use these techniques to improve the understanding of the fate of NPs in WWTPs. The specific objectives are:

1. To develop methods for extraction and characterization of size, concentration, and chemical composition of nAg and nCu in highly chemically complex matrices of WWTP sludge and biosolids where the NPs are present in low concentrations, and to characterize them in sludge and biosolids samples from multiple Canadian WWTPs using spICP-MS, electron microscopy and X-ray analyses.
2. To develop methods for extraction and characterization of size, concentration, and composition of nAg and nCu in WW effluents from several Canadian WWTPs.
3. To compare the aggregation, dissolution, and disinfection capabilities of nAg, and $nTiO_2$ released from paints and coatings to pristine (as-manufactured) forms in different pH conditions.

1.4. Thesis Overview

Chapter 2 – This chapter provides a literature review on the analytical techniques used for NP detection in environment, predicted and measured concentrations of NPs in WW effluent and biosolids, review on the fate, transformation and toxicity of NPs in WW sludge and biosolids; and finally, released NPs from product matrix is different in size, stability and toxicity from the pristine NPs.

Chapter 3 - This chapter describes the development and optimization of methods to detect the size, particle size distribution and concentration of metal (Ag and Cu) ENPs in biosolids, through the application of various extraction procedures and the subsequent analysis of aqueous extracts by spICP-MS. Furthermore, the study evaluates the capability of spICP-MS for determination of the concentration, size, and its limit of detection of NPs in the biosolids matrix. Finally, a systematic study is presented, focusing on the detection and characterization of nAg and nCu size, particle size distribution and concentrations from sludge and biosolids from 11 WWTPs across Canada.

Chapter 4 – This chapter focuses on the detection and characterization of nAg and nCu in WW effluent samples using spICP-MS by developing methods to concentrate NPs in several Canadian WWTPs. Methods developed to concentrate NPs by spiking nAg in DI water and WW effluent are described. The developed pre-concentration technique is used to measure nAg and nCu size, particle size distribution and concentration of NPs in WW effluent from 11 WWTPs across Canada using spICP-MS.

Chapter 5 – This chapter describes studies, where nAg released from painted surfaces under various aging and aqueous chemistry conditions were characterized for size and concentration by analyses of the aqueous wash samples by spICP-MS. The change in stability of nAg released from painted surfaces was compared to that of pristine nAg in DI water conditions, for a period of 15 days. Finally, disinfection tests on survival of *E. coli D21* between nAg released from paint, base paint and pristine nAg were compared over an experiment period of 42 h.

Chapter 6 – This chapter describes studies, where $nTiO_2$ released from painted surfaces under various aging and aqueous chemistry conditions were characterized for size and concentration by analyses of the aqueous wash samples by spICP-MS. The chapter also includes a comparison of 4 commercial paints (3 external and 1 internal) with unknown concentration of $nTiO_2$, for $nTiO_2$ released under different pH conditions. Finally, disinfection tests on survival of *E. coli D21* between $nTiO_2$ released from paint, base paint and pristine $nTiO_2$ were compared over an experiment period of 42 h.

Chapter 7 – This chapter contains the overall summary of the thesis and general conclusion of this doctoral research work

1.5. Publications

- Rahim, A.A. and Ghoshal, S. (2021), "Silver and copper nanoparticles in sludge and biosolids from municipal wastewater treatment plants" *In preparation for submission to* **Environmental Pollution**.
- Rahim, A.A. and Ghoshal, S. (2021), "Concentration of silver and copper nanoparticles in WW effluent from municipal wastewater treatment plants" *In preparation for submission to* **Science of the Total Environment**.
- Rahim, A.A., Kundu, A. and Ghoshal, S. (2021), "Stability and disinfection of silver nanoparticles released from paint compared to pristine nanoparticles." *In preparation for submission to* **Science of the Total Environment**.

- Rahim, A.A., Kundu, A. and Ghoshal, S. (2021), “Release of titanium dioxide nanoparticles from custom-made and commercial painted surface in water and associated disinfection studies” *In preparation for submission to* **Science of the Total Environment.**

1.6. References

1. Moore, M.N., *Do nanoparticles present ecotoxicological risks for the health of the aquatic environment?* Environment International, 2006. **32**(8): p. 967-976.
2. Roco, M.C., *Nanotechnology: convergence with modern biology and medicine.* Current Opinion in Biotechnology, 2003. **14**(3): p. 337-346.
3. Farré, M., J. Sanchís, and D. Barceló, *Analysis and assessment of the occurrence, the fate and the behavior of nanomaterials in the environment.* TrAC Trends in Analytical Chemistry, 2011. **30**(3): p. 517-527.
4. Montaño, M.D., et al., *Current status and future direction for examining engineered nanoparticles in natural systems.* Environmental Chemistry, 2014. **11**(4): p. 351-366.
5. Bhatia, S., *Nanoparticles Types, Classification, Characterization, Fabrication Methods and Drug Delivery Applications*, in *Natural Polymer Drug Delivery Systems: Nanoparticles, Plants, and Algae*, S. Bhatia, Editor. 2016, Springer International Publishing: Cham. p. 33-93.
6. Jeevanandam, J., et al., *Review on nanoparticles and nanostructured materials: history, sources, toxicity and regulations.* Beilstein journal of nanotechnology, 2018. **9**: p. 1050-1074.
7. Weinberg, H., A. Galyean, and M. Leopold, *Evaluating engineered nanoparticles in natural waters.* TrAC Trends in Analytical Chemistry, 2011. **30**(1): p. 72-83.
8. Industryarc, *Nanotechnology Market report – Forecast (2020-2025)*. 2020: Report Code: ESR 0048.
9. Bystrzejewska-Piotrowska, G., J. Golimowski, and P.L. Urban, *Nanoparticles: Their potential toxicity, waste and environmental management.* Waste Management, 2009. **29**(9): p. 2587-2595.
10. Tiede, K., et al., *Considerations for environmental fate and ecotoxicity testing to support environmental risk assessments for engineered nanoparticles.* Journal of Chromatography A, 2009. **1216**(3): p. 503-509.
11. Aiken, G.R., H. Hsu-Kim, and J.N. Ryan, *Influence of Dissolved Organic Matter on the Environmental Fate of Metals, Nanoparticles, and Colloids.* Environmental Science & Technology, 2011. **45**(8): p. 3196-3201.
12. Buffet, P.-E., et al., *A marine mesocosm study on the environmental fate of silver nanoparticles and toxicity effects on two endobenthic species: The ragworm Hediste diversicolor and the bivalve mollusc Scrobicularia plana.* Science of The Total Environment, 2014. **470-471**: p. 1151-1159.
13. Vasir, J.K. and V. Labhasetwar, *Quantification of the force of nanoparticle-cell membrane interactions and its influence on intracellular trafficking of nanoparticles.* Biomaterials, 2008. **29**(31): p. 4244-4252.

14. Saptarshi, S.R., A. Duschl, and A.L. Lopata, *Interaction of nanoparticles with proteins: relation to bio-reactivity of the nanoparticle.* Journal of Nanobiotechnology, 2013. **11**(1): p. 26.
15. Du, W., et al., *TiO2 and ZnO nanoparticles negatively affect wheat growth and soil enzyme activities in agricultural soil.* Journal of Environmental Monitoring, 2011. **13**(4): p. 822-828.
16. Dinesh, R., et al., *Engineered nanoparticles in the soil and their potential implications to microbial activity.* Geoderma, 2012. **173–174**(0): p. 19-27.
17. Manke, A., L. Wang, and Y. Rojanasakul, *Mechanisms of Nanoparticle-Induced Oxidative Stress and Toxicity.* BioMed Research International, 2013. **2013**: p. 15.
18. Gottschalk, F., et al., *Modeled environmental concentrations of engineered nanomaterials (TiO2, ZnO, Ag, CNT, fullerenes) for different regions.* Environmental Science & Technology, 2009. **43**(24): p. 9216-9222.
19. Keller, A.A. and A. Lazareva, *Predicted releases of engineered nanomaterials: From global to regional to local.* Environmental Science & Technology Letters, 2013. **1**(1): p. 65-70.
20. Westerhoff, P., et al., *Occurrence and removal of titanium at full scale wastewater treatment plants: implications for TiO 2 nanomaterials.* Journal of Environmental Monitoring, 2011. **13**(5): p. 1195-1203.
21. Kim, B., et al., *Discovery and Characterization of Silver Sulfide Nanoparticles in Final Sewage Sludge Products.* Environmental Science & Technology, 2010. **44**(19): p. 7509-7514.
22. Gottschalk, F. and B. Nowack, *The release of engineered nanomaterials to the environment.* Journal of Environmental Monitoring, 2011. **13**(5): p. 1145-1155.
23. Gottschalk, F., T. Sun, and B. Nowack, *Environmental concentrations of engineered nanomaterials: Review of modeling and analytical studies.* Environmental Pollution, 2013. **181**: p. 287-300.
24. Li, L., et al., *To What Extent Can Full-Scale Wastewater Treatment Plant Effluent Influence the Occurrence of Silver-Based Nanoparticles in Surface Waters?* Environmental Science & Technology, 2016. **50**(12): p. 6327-6333.
25. Mitrano, D.M., et al., *Detecting nanoparticulate silver using single-particle inductively coupled plasma–mass spectrometry.* Environmental Toxicology and Chemistry, 2012. **31**(1): p. 115-121.
26. Hadioui, M., V. Merdzan, and K.J. Wilkinson, *Detection and characterization of ZnO nanoparticles in surface and waste waters using single particle ICPMS.* Environmental science & technology, 2015. **49**(10): p. 6141-6148.
27. Li, L., et al., *Quantification of nanoscale silver particles removal and release from municipal wastewater treatment plants in Germany.* Environmental science & technology, 2013. **47**(13): p. 7317-7323.
28. Westerhoff, P.K., M.A. Kiser, and K. Hristovski, *Nanomaterial removal and transformation during biological wastewater treatment.* Environmental Engineering Science, 2013. **30**(3): p. 109-117.
29. Chen, Y., et al., *Long-term effects of copper nanoparticles on wastewater biological nutrient removal and N2O generation in the activated sludge process.* Environmental science & technology, 2012. **46**(22): p. 12452-12458.

30. Ganesh, R., et al., *Evaluation of nanocopper removal and toxicity in municipal wastewaters.* Environmental science & technology, 2010. **44**(20): p. 7808-7813.
31. Wang, D. and Y. Chen, *Critical review of the influences of nanoparticles on biological wastewater treatment and sludge digestion.* Critical reviews in biotechnology, 2016. **36**(5): p. 816-828.
32. Hassellöv, M., et al., *Determination of Continuous Size and Trace Element Distribution of Colloidal Material in Natural Water by On-Line Coupling of Flow Field-Flow Fractionation with ICPMS.* Analytical Chemistry, 1999. **71**(16): p. 3497-3502.
33. Tiede, K., et al., *Detection and characterization of engineered nanoparticles in food and the environment.* Food Additives and Contaminants, 2008. **25**(7): p. 795-821.
34. Domingos, R.F., N. Tufenkji, and K.J. Wilkinson, *Aggregation of Titanium Dioxide Nanoparticles: Role of a Fulvic Acid.* Environmental Science & Technology, 2009. **43**(5): p. 1282-1286.
35. Mitrano, D.M., et al., *Silver nanoparticle characterization using single particle ICP-MS (SP-ICP-MS) and asymmetrical flow field flow fractionation ICP-MS (AF4-ICP-MS).* Journal of Analytical Atomic Spectrometry, 2012. **27**(7): p. 1131-1142.
36. Lee, S., et al., *Nanoparticle size detection limits by single particle ICP-MS for 40 elements.* Environmental science & technology, 2014. **48**(17): p. 10291-10300.
37. Montaño, M., et al., *Improvements in the detection and characterization of engineered nanoparticles using spICP-MS with microsecond dwell times.* Environmental Science: Nano, 2014. **1**(4): p. 338-346.
38. Montaño, M.D., et al., *Single Particle ICP-MS: Advances toward routine analysis of nanomaterials.* Analytical and Bioanalytical Chemistry, 2016. **408**(19): p. 5053-5074.
39. Degueldre, C. and P.Y. Favarger, *Thorium colloid analysis by single particle inductively coupled plasma-mass spectrometry.* Talanta, 2004. **62**(5): p. 1051-1054.
40. Degueldre, C., P.Y. Favarger, and C. Bitea, *Zirconia colloid analysis by single particle inductively coupled plasma–mass spectrometry.* Analytica Chimica Acta, 2004. **518**(1): p. 137-142.
41. Degueldre, C., P.Y. Favarger, and S. Wold, *Gold colloid analysis by inductively coupled plasma-mass spectrometry in a single particle mode.* Analytica Chimica Acta, 2006. **555**(2): p. 263-268.
42. Montaño, M.D., et al., *Opportunities for examining the natural nanogeochemical environment using recent advances in nanoparticle analysis.* Journal of Analytical Atomic Spectrometry, 2019. **34**(9): p. 1768-1772.
43. Griffitt, R.J., et al., *Exposure to copper nanoparticles causes gill injury and acute lethality in zebrafish (Danio rerio).* Environmental Science & Technology, 2007. **41**(23): p. 8178-8186.
44. Aruoja, V., et al., *Toxicity of nanoparticles of CuO, ZnO and TiO2 to microalgae Pseudokirchneriella subcapitata.* Science of the total environment, 2009. **407**(4): p. 1461-1468.
45. Alizadeh, S., et al., *Impacts of Continuous Inflow of Low Concentrations of Silver Nanoparticles on Biological Performance and Microbial Communities of Aerobic Heterotrophic Wastewater Biofilm.* Environmental Science & Technology, 2019.
46. Sohn, E.K., et al., *Aquatic toxicity comparison of silver nanoparticles and silver nanowires.* BioMed Research International, 2015. **2015**.

47. Malhotra, N., et al., *Review of Copper and Copper Nanoparticle Toxicity in Fish.* Nanomaterials, 2020. **10**(6): p. 1126.
48. European Chemicals Agency. *Acute & chronic ecotoxicity of soluble copper species in view of hazard classification of copper and copper compounds*. 2021; Available from: https://echa.europa.eu/documents/10162/13626/attachment_4_copper_flakes_en.pdf.
49. Shi, J., et al., *To duckweeds (Landoltia punctata), nanoparticulate copper oxide is more inhibitory than the soluble copper in the bulk solution.* Environmental Pollution, 2011. **159**(5): p. 1277-1282.
50. Hanna, S.K., et al., *Accumulation and toxicity of metal oxide nanoparticles in a soft-sediment estuarine amphipod.* Aquatic toxicology, 2013. **142**: p. 441-446.
51. Buffet, P.-E., et al., *A mesocosm study of fate and effects of CuO nanoparticles on endobenthic species (Scrobicularia plana, Hediste diversicolor).* Environmental science & technology, 2013. **47**(3): p. 1620-1628.
52. Conway, J.R., et al., *Aggregation, dissolution, and transformation of copper nanoparticles in natural waters.* Environmental science & technology, 2015. **49**(5): p. 2749-2756.
53. Hadrup, N., A.K. Sharma, and K. Loeschner, *Toxicity of silver ions, metallic silver, and silver nanoparticle materials after in vivo dermal and mucosal surface exposure: A review.* Regulatory Toxicology and Pharmacology, 2018. **98**: p. 257-267.
54. Blinova, I., et al., *Ecotoxicity of nanoparticles of CuO and ZnO in natural water.* Environmental Pollution, 2010. **158**(1): p. 41-47.
55. Franklin, N.M., et al., *Comparative toxicity of nanoparticulate ZnO, bulk ZnO, and ZnCl2 to a freshwater microalga (Pseudokirchneriella subcapitata): the importance of particle solubility.* Environmental science & technology, 2007. **41**(24): p. 8484-8490.
56. Sunda, W., *Relationship between cupric ion activity and the toxicity of copper to phytoplankton, 168 pp*. 1975, Ph. D. Thesis, Massachusetts Institute of Technology, Cambridge.
57. Moore, M., et al., *Responses of the mussel Mytilus edulis to copper and phenanthrene: interactive effects.* Marine Environmental Research, 1984. **14**(1-4): p. 167-183.
58. Liu, J., et al., *Controlled Release of Biologically Active Silver from Nanosilver Surfaces.* ACS Nano, 2010. **4**(11): p. 6903-6913.
59. Giese, B., et al., *Risks, release and concentrations of engineered nanomaterial in the environment.* Sci. Rep., 2018. **8**(1): p. 1565.
60. Nowack, B., et al., *Progress towards the validation of modeled environmental concentrations of engineered nanomaterials by analytical measurements.* Environmental Science: Nano, 2015. **2**(5): p. 421-428.
61. Kraas, M., et al., *Long-term effects of sulfidized silver nanoparticles in sewage sludge on soil microflora.* Environmental toxicology and chemistry, 2017. **36**(12): p. 3305-3313.
62. Starnes, D.L., et al., *Distinct transcriptomic responses of Caenorhabditis elegans to pristine and sulfidized silver nanoparticles.* Environmental Pollution, 2016. **213**: p. 314-321.
63. Baalousha, M., et al., *Transformations of citrate and Tween coated silver nanoparticles reacted with Na2S.* Science of the total environment, 2015. **502**: p. 344-353.
64. Ma, R., et al., *Sulfidation of copper oxide nanoparticles and properties of resulting copper sulfide.* Environmental Science: Nano, 2014. **1**(4): p. 347-357.
65. Kaegi, R., et al., *Behavior of Metallic Silver Nanoparticles in a Pilot Wastewater Treatment Plant.* Environmental Science & Technology, 2011. **45**(9): p. 3902-3908.

66. Ma, R., et al., *Fate of Zinc Oxide and Silver Nanoparticles in a Pilot Wastewater Treatment Plant and in Processed Biosolids.* Environmental Science & Technology, 2014. **48**(1): p. 104-112.
67. Barton, L.E., et al., *Monte Carlo simulations of the transformation and removal of Ag, TiO2, and ZnO nanoparticles in wastewater treatment and land application of biosolids.* Science of The Total Environment, 2015. **511**: p. 535-543.
68. Sarafadeen, A.O., et al., *Biosolids Land Application.* Pensee, 2014. **76**(9).
69. Canadian Water and Wastewater Association (CWWA). *FAQ on Biosolids*. 2012 [cited 2017 January 4th]; Available from: http://www.cwwa.ca/faqbiosolids_e.asp.

CHAPTER 2 LITERATURE REVIEW

2.1. Analytical techniques for characterizing NPs in environmental matrices

Detection and characterization of NPs in complex matrices is challenging. Imaging techniques, such as scanning electron microscopy (SEM) and transmission electron microscopy (TEM), provide direct evidence of NPs in clean matrices but require extensive sample preparation in complex matrices such as soils and biosolids. The samples prepared for microscopic techniques should have less background matrix (removal of background) and have enough concentration of NPs (concentrating NPs in the sample) to be easily visible. Furthermore, they do not provide reliable quantitative information about ENP concentrations, given the small sample size analysed and low concentration of ENPs present in environmental matrices [1, 2]. Particle sizing techniques, such as dynamic light scattering (DLS) and nanoparticle tracking analysis (NTA), have limitations for analysis of ENPs in environmental samples representing complex media, because of their inability to distinguish target NPs from background natural colloids such as clays and mineral oxide particles. The light scattering intensity is proportional to the sixth power of particle size, and even the presence of a small amount of background natural colloids larger than NPs will lead to biased higher estimates of NPs size [3].

Centrifugal ultrafiltration (CUF) (using filters with low cut off size such as 3 kDa - 1 to 3 nm) has been used to determine the dissolved ion concentrations in NPs or colloidal suspensions. In this method, the concentration of the (dissolved) metals in the filtrate is subtracted from the total concentration of metals (particulate and dissolved) measured by acid digestion of the whole samples, to provide an estimate of the concentration of the metals present in particulate form [4-6]. However, if significant amounts of metals are bound to natural organic matter (NOM) (macromolecules) which are retained on the filter, a gross over-estimation of NP concentrations can occur because of the error in the estimation of the dissolved fraction. There is also the possibility that background colloids may contain the same element that the NPs are comprised of and contribute to over estimation of the NP concentration in the initial solution.

Single particle mode inductively coupled plasma mass spectrometry (spICP-MS) is a powerful technique for measuring metal NP sizes and concentrations in relatively pure aqueous samples at sub parts per billion concentrations [7-14]. In contrast to standard mode ICP-MS, samples introduced to spICP-MS are not acid digested or acidified. In standard ICP-MS, acid digested samples are measured for dissolved metal concentrations, whereas samples in spICP-MS are introduced directly without large colloids and need to be diluted to the point that only a few droplets contain single particle. The liquid sample is aerosolized into small droplets before entering the high temperature plasma. In spICP-MS, the metal NPs passing through the high temperature plasma are atomized and ionized, then separated by their mass-to-charge ratios (m/z) in the mass spectrometer, enabling the identification and quantification of elements present as dissolved and particulate material. The cloud of ions generated by ionized NPs is identified as a large peak compared to the nearly constant background signal from dissolved ions. The target element is allowed to pass through the quadrupole mass filter with the specific m/z ratio, while neglecting other elements. The time spent to acquire mass spectra data to be integrated for reporting as a single datum point, is known as dwell time. Depending on the element measured, the length of the dwell time affects the minimum detectable size of the NPs [7, 15]. The larger the dwell time used for measurement, the more likely it is to have multiple NPs coinciding in a single peak. The dwell time should be small enough and in an appropriate range to help determine and distinguish between multiple NPs reaching the detector in close sequence. The mass signals generated from each dwell time are calibrated for concentration and size, using previously analysed dissolved or NP calibration [12-14]. Sizes as low as 20 nm of spiked nAg at a concentration of 10 ppb in wastewater samples could be reliably characterized using a short dwell time of 100 µs [16].

However, the concentrations of the NPs analyzed in many environmental matrices, such as natural waters and wastewater effluents (WW effluent), are expected to be lower due to dilution in the receiving water body and therefore, there is a need to concentrate these environmental samples to enable detection and quantification, even by sensitive instruments such as spICP-MS or electron microscopy. Cloud point extraction (CPE) is a technique employed to concentrate NPs in environmental water samples [17, 18]. CPE is an extraction method relying on the micelle-analyte (micelle-NP) interactions. The concentration of surfactant at which micelles start forming is called the critical micelle concentration (CMC), and the temperature above which the formed micelles are immiscible in water is called the lowest critical solution temperature (LCST). CPE involves three fundamental steps: (1) Association of the analytes (NPs), present in the original matrix, within the micellar aggregates; (2) increase in temperature above the LSCT, which causes separation of the coacervative phase from the bulk aqueous phase; and finally, (3) phase separation using centrifugation and decanting [19]. The surfactant with the concentrated NPs is analysed to obtain the concentration.

The limit of detection of silver NPs (nAg) spiked into wastewater samples concentrated by CPE was found to be 12.9 ng/L for influent water and 0.7 ng/L for effluent wastewater measured using graphite furnace atomic absorption spectroscopy (AAS) [17, 20]. Liu et al. (2009) reported that the presence of humic acids (0−30 mg/L dissolved organic carbon) had no effect on the extraction of nAg using CPE and there was negligible interference from Ag^+ [18]. Copper oxide NPs (nCuO) spiked at concentration of 20 to 100 µg/L in wastewater were extracted by CPE with recovery efficiency ranging from 80.4% to 108.2 %. Relatively lower recovery of NPs (59.2 to 69.4%) were observed for samples spiked with a lower concentration of 5µg/L [21]. *In general, it is important to have an effective technique to concentrate and measure the NPs in complex environmental samples.*

2.2. Predicted and measured concentrations of NPs in WW effluent and biosolids

The detected or estimated concentrations of NPs in environmental aquatic samples are usually at the ng/L levels. A few studies have reported metal NP concentrations in WWTP effluents with the assumption that the total metal present in the filtrate after 0.45 µm filtration is nanoparticulate [22-25]. This can lead to inaccurate measurement of NP concentration as some of the metal may be present as sub-micron sized particles larger than ~100 nm, the metal phases present in other sub-micron colloids or even dissolved ions bound with organic matter molecules (metal ligand complexes) that cannot pass through 0.45 µm filters. The total metal in the filtrate is typically characterized by AAS or inductively coupled plasma optical emission spectroscopy (ICP-OES) or ICP-MS after acid digestion. Using this approach, TiO_2 in WW effluent was detected at concentrations of 1-100 µg/L [22-24] and nAg in WW effluent at 4-10 ng/L [25]. However, this NP concentration characterization technique has significant shortcomings because it does not take into account the loss of the NPs on the filters, and accounts for dissolved ions (or complexed to dissolved organic matter trapped in the filter) as nanoparticulate. Thus, while such techniques can be used for completely insoluble metals such as TiO_2, they cannot be used for NPs of more labile metals such as Cu and Ag. Furthermore, these techniques do not provide particle size information, nor direct measurements of concentration.

Detection of carbonaceous nanomaterial (CNM) in environmental samples are difficult, as there is a limit of analytical capabilities and lack of methods for quantifying CNM in the presence of other carbonaceous materials. Therefore, analysis of CNM's from environmental samples requires an elaborate extraction procedure. A study detected fullerenes using liquid chromatography–mass spectrometry (LC-MS) at concentrations ranging from 1 to 70,000 ng/L in WW effluent samples from different treatment plants [26]. The LC-MS analysis was performed on concentrated toluene extracts of the retentate of effluent samples that were passed through a 0.45 µm filter. The filters were oven dried and ultra sonicated prior to toluene extraction. The range of nAg concentrations measured in the WW effluents varied between studies: from 1 to 10 ng/L using CPE and measurement with AAS [20], to 100 to 200 ng/L using direct spICP-MS analyses [27]. Hadioui et al. (2015) observed nZn of 160 to 210 nm diameter and concentrations of approximately 50 ng/L using spICP-MS [28]. In that study, the detection limits of nZnO were improved by removing dissolved metals from the samples by elution through an in-line ion exchange column. Total Ti was analysed in WW effluent by digestion using ammonium persulfate and analysis using ICP-MS for indirect concentration measurement of $nTiO_2$, which gave values of 1.6 to 1.8 µg/L [29]. The study assumes that all the TiO_2 present in WWTP is in the form of NPs. Another study calculated the concentration of nAg in filtered wastewater influent using field flow fractionation and standard ICP-MS, to be1.9 µg/L with 9.3 nm as size [30]. A recent study using fast multielement spICP-MS detected 13 metals for size and concentration in various compartments in WWTP in south California, USA [31]. This study used centrifugation as a method to separate solids from complex samples and measured for the metal concentration and particle size distribution in WW effluent, with nAg concentration of 1.8 ± 0.01 ng/L with a mean size of 13.4 ± 0.1 nm and copper NPs (nCu) concentration of 25.6 ± 1.7 ng/L with a mean size of 94.3 ± 0.2 nm [31]. Concentrations of other NPs (Cd, Co, Al, Au, Ni, Zn, Ce, Mn, Ti, Fe and Mg) in the WW effluent were also reported in the range of 0.24 ± 0.07 to 70229 ± 4893 ng/g and mean sizes varying from 13.4 ± 0.1 to 1734.2 ± 23.4 nm. A recent study on the detection of nAg in a river (using CPE and spICP-MS), immediately downstream of the WW effluent discharge outfall, reported concentrations of 2.0 to 8.6 ng/L compared to 0.9 to 2.3 ng/L upstream of the plant [20].

Despite the concentration of the NPs in WW effluent being in the range of ng/L, the significant volume of the WW effluent released into the water sources could pose risks to the environment from discharge of ENPs. Although prior studies have confirmed the presence of NPs in WW effluents, they have emphasized on the development of detection methods, rather than obtaining a robust assessment of their concentrations in effluents from different WWTPs. Therefore, there is scarcity of information regarding NP size and concentration data.

Unlike WW effluent, the reported data on NPs in the sludge or biosolids is minimal because biosolids are very complex matrices, and thus detection and characterization of NPs becomes very challenging and appropriate analytical methods have not yet been developed. Currently, there are only few studies that have reported concentrations of TiO_2 in sludge. The concentration of particulate TiO_2 in the sludge at approximately 300 to 10,000 mg/kg was reported in several studies by acid digestion of the sludge followed by ICP-MS or ICP-OES analysis, with the assumption that Ti would exist only in particulate form [22-24]. Another study reported total titanium concentrations by digestion using ammonium persulfate and subsequent analysis with ICP-MS, for the indirect calculation of $nTiO_2$, as 317.4 µg/g in biosolids [29]. However, this approach does not provide any size information for the particulate TiO_2 and thus, its NP concentrations were not determined. A recent study has used fast multielement single particle inductively coupled plasma mass spectroscopy to characterize 13 metal NP concentrations with concentration and particle size distribution in different compartments (influent, post primary effluent, secondary effluent, reclaimed water, waste sludge and anaerobic sludge) of a WWTP in southern California, USA.[31]. The study analysed the supernatant of the samples from different compartments for mass concentration and particle size distribution. That study reported concentrations and sizes in WW sludge of nAg (4.3 ± 0.2 ng/g total suspended solids (TSS), 16.7 ± 0.3 nm) and nCu (76.5 ± 30.1 ng/g, 132.8 ± 1.1 nm) and in anaerobic sludge of nAg (442.7 ± 0.2 ng/g, 14.7 ± 0.7 nm) and nCu (4234.8 ± 30.1 ng/g, 66.6 ± 8.1 nm). Concentrations and sizes of other NPs (Cd, Co, Al, Au, Ni, Zn, Ce, Mn, Ti, Fe and Mg) were reported in the waste sludge (0.13 ± 0.03 to 22585.4 ± 1225.4 ng/g, 39.0 ± 0.1 to 1680.4 ± 54.4 nm) and anaerobic sludge ranged (1.9 ± 1.5 to 10874.8 ± 4492.1 ng/g, 33.5 ± 3.4 to 326.5 ± 35.4 nm).

Some estimates have been provided from model predictions based on approximate worldwide or regional NP production and consumption volumes, and materials flow analyses from the products to different environmental compartments. Predicted concentrations of $nTiO_2$ in WW effluents varied between 2 to 7 µg/L [32, 33] and 1200 to 1300 µg/L [34] in others. nAg concentrations of 1 to 75 ng/L [32, 33, 35], 10 to 300 ng/L [36] and 70 µg/L [34] were estimated in WW effluent. The concentrations of carbon nanotube (CNT) and cerium dioxide NPs ($nCeO_2$) were in the range of 0.01 to 1 ng/L. Sewage sludge was predicted to contain higher concentrations of NP relative to effluents. $nTiO_2$ was found to be the most abundant NP in sewage sludge, with concentrations in the range of 3 to 600 µg/g [32-34]. Predicted nAg concentrations in biosolids from different studies were in the range of 1.5 to 6 µg/g [32, 33], 0.3 to 13 ng/g [35], 4.5 to 1700 ng/g [33, 35] and 50 ng/g [34]; and for nCu in biosolids the concentration values were in the range of 1 to 20 ng/g [36] and 0.01 to 0.15 ng/g [36]. A modeling study by Hendren et al. (2013) showed that surface characteristics and the type of coating on the ENP could influence their release from WWTPs [35]. Dynamic multimedia fate and transport model (nanoFate) reported that sufficient concentration of ENPs (TiO_2, CuO, ZnO and CeO_2) can be accumulated exceeding the minimum toxicity levels in freshwater and soils [37]. nanoFate model also reports that ENPs are aggregated or dissolved in sediments and agricultural fields applied with biosolids. *Overall, these predicted NP concentrations vary by several orders of magnitude from one study to another, and thus there is a need to site-specific data from direct measurements. Consequently, there is a need for information on the measured NP size and concentration from real wastewater samples to be able to assess how they affect the environment around us. In addition, this data will be helpful in further modelling and toxicity studies.*

2.3. Attachment and settling of NPs to sludge biomass in WWTPs

NPs extensively attach to microbial flocs and sludge in WWTPs and settle out from the mixed liquor in sedimentation tanks with the biomass or as independent particles and aggregates. The NPs collide with themselves and with other suspended colloids, bacteria and its flocs due to their brownian movement leading to homo- and heteroaggregation [38, 39]. The extents of this attachment are influenced by NP surface chemistry, surface charge, size, concentrations and aqueous chemistry [40-44]. Approximately, 70-99% of Ag are settled with wastewater sludge due to attachment to biomass, aggregation and sedimentation in systems spiked with nAg [38, 41, 45, 46]. Surface functionalization also influences the attachment to sludge biomass, as evidenced by 90% settling of polyvinylpyrrolidone (PVP)-coated nAg, compared to 70% of gum arabic (GA)-

functionalized nAg [45]. Similar results were reported by a study on nAg with different particle coating (polyvinylpyrrolidone and citrate) in sewage sludge, which did not have an impact on neither partitioning (~99%) nor aggregation state [47]. Attachment of NPs to biomass varies widely with the NP type, with reported extents of attachment and settling being 88% for fullerenes, 23% for $nTiO_2$ and 13% for fullerol [41]. In another study, bare $nCeO_2$ and $nTiO_2$ were extensively (95 to 100%) attached and settled with sludge, but lower removal extents were observed with citrate-functionalized $nCeO_2$ (85%) and GA-functionalized nAg (70%) [48]. nAg spiked in different soils (forest and agricultural soils) had strong sorption on soil ligands, later leading to the release of dissolved Ag into soils suspended in water, either due to the oxidation of nAg or the detachment of sorbed dissolved Ag from soils [49]. Approximately 90% of the nAg (~30 μg/L) were dosed daily once in a sequence batch reactor partitioned with solids fraction of mixed liquor suspended solids, and transformed into AgS NPs [50]. More than 80% of the (10 μg/L) nAg and (100 μg/L) $nTiO_2$ particles separated to effluent solids in a labscale WWTP [51]. A study on size dependence removal of nAg (5 to 10 nm and 40 nm) spiked at 5 or 50 μg/L in batch WWTP systems reported that 5-10nm nAg precipitated instantly and were found to be stable, whereas, 40 nm nAg aggregated (without dissolution) with solids in the system leading to sedimentation, suggesting importance of size of NPs in fate dynamics [52]. A recent study on nAg (20, 60 and 100 nm at 50 μg/L) mobility in soils with and without sludge reported ~10 times lower mobility in sludge amended soils [53].

Fate models of $nTiO_2$ in freshwater systems report probable homo-aggregation and also, heteroaggregation with suspended particle matter [54]. The nanoFate model predicts that ENPs in biosolids applied to agricultural fields, are aggregated and their concentration is several orders of magnitude higher compared to the ones just receiving NPs from atmospheric deposition [37]. Other NP fate models predicted separation of NPs due heteroaggregation followed by sedimentation with natural particles in water systems [55-57]. Another material flow model reported adsorption of nAg and dissolved Ag from socks to WWTP biomass [58]. Material flow models predicted separation of ~95% of NPs from effluents into sludge [33, 35, 43]. The NPs released from WWTPs are distributed between the WW effluent and sludge, but the effects of concentration, size, and type of NPs on the distribution ratio are not understood. Furthermore, the studies mentioned above have assessed the distribution of NPs in the aqueous phase and in the biomass using total metals analyses, and as well have spiked NPs at concentrations (~mg/L) significantly higher than the range of actual concentrations (low ~µg/L) measured for ease of analyses. *Thus, it is quite likely that the distribution of NPs in WWTPs estimated in the above-mentioned studies is not applicable to low concentrations of NPs typically found in municipal WWTPs. In addition, there is a need to assess the concentration of NPs entering WWTPs between WW effluent and biosolids.*

2.4. Transformation of NPs in WW effluent and biosolids

NPs undergo various physical and chemical transformations when in contact with environmental matrices. Many metal NPs release ions from the surface under conditions favorable for dissolution such as low pH, chemical matrix or presence of strong agents depending on the NP [38, 42, 59]. A study has shown that nAg dissolution can lead to reformation and precipitation of new NPs in the presence of inorganic and organic sulfides in wastewater effluent [16]. Several other studies have demonstrated that dissolved Ag present in reducing conditions with natural organic matter like humic and fulvic acids, leads to the formation of nAg [60-62]. Various factors for aggregation, dissolution and transformation of nCu in the environment include copper valence speciation, natural organic matter (NOM), pH of the solution and ionic strength of aqueous media [63-66]. Conway et al. (2015) reported that nCuO (20-100 nm) aggregated instantly to form sizes of 250 to 400nm in eight natural waters, whereas nCu (100-1000 nm) and $nCu(OH)_2$ (100-100 nm) particles formed sizes larger that 1000 nm [66]. Dissolution rate of nCu particle (nCu, nCuO and $nCu(OH)_2$) was the highest at low pH of 4 and lowest at basic pH of 11, with presence of extra polymeric substance (EPS) increasing the dissolution [64]. Dissolution of nCu leads to formation of complexes with NOM, carbonates and hydroxides [63, 64, 66].

A previous study has reported nanoscale silver sulfide colloids of 5 to 20 nm, using TEM in sewage sludge from WWTP [67]. nAg entering WWTPs are transformed to nAg_2S, and during thermal treatment of biosolids, the partial formation of Ag_2SO_4 and Ag-sulfhydryl groups along with some residual Ag^0 was observed by X-ray photo spectroscopy [68]. nAg, nCu and nZn entering the sewers undergo significant changes to their surface chemistry, due to sulfidation or reactions with other inorganic wastewater constituents as well as dissolved organic matter such as humic and fulvic acids, polysaccharides, proteins, extracellular polymeric substances etc. [16, 38, 46, 47, 69]. nZn transformed into Zn−Fe oxy/hydroxide $Zn_3(PO4)_2$ and ZnS, with more Zn associated with sulfide in anaerobic conditions and higher concentration of Zn-Fe oxy/hydroxide under aerobic conditions [68]. $nTiO_2$ (44 to 120 nm) were reported to be found in sludge and biosolids as aggregates [70] and without any chemical transformation [43]. Other NPs, such as $nCeO_2$ transformed from Ce(IV) to Ce(III) in biosolids [44].

nAg (~30 µg/L) were dosed daily once in a sequence batch reactor transformed into AgS NPs in activated sludge treatment, and did not affect the efficient functioning of the reactor [50]. However, transformed AgS NPs impacted microbiome population in anaerobic digestor [50]. Different nAg particles (nAg - ~10nm (polyvinyl sulphonate, mercaptosuccinic acid and citrate coated), nAgCl - 200 nm) with different coatings spiked at environmentally realistic concentration of 50 µg/g in sewage sludge, reported that neither surface coating nor nAg composition inhibited the formation of nAg_2S [71]. Fate of nAg (~50 nm, continuously injected at 18 µg/g and 400 µg/g) in sludge amended soils for cultivation of plants (wheat and rape) showed that nAg completely transformed into stable fraction of Ag_2S observed by X-ray absorption spectroscopy [72]. The same study also reports the presence of amorphous Ag_2S and/or Ag-thiol complexes (~20 to 35 %) as well as nanosized metallic sulfides in WW sludge, biosolids and soil amended with biosolids [72]. The stability of nAg_2S particles depends on the environmental conditions with incineration of biosolids transforming 20 to 50 % Ag^o [69, 73, 74] and high levels of chloride reduces the stability of nAg_2S particles by formation of AgCl complexes [75]. Similar results were obtained from other studies spiked with nAg, reporting Ag_2S formation in WWTPs [16, 38, 46, 67]. nCu speciation is observed at the end stages of sewage sludge, whereas oxidation of sulfides was increasingly observed in aerobic condition [76]. Another study on pristine nCuO particles (50nm) reported the formation of amorphous nCu_xS to eventually re-crystalline to CuS with comparable sizes [77]. The sulfidation of nCuO particles (40 nm, 100mg/L) in water showed predominant formation of soluble copper sulfate hydroxide NPs cluster with sizes between 5 and 10 nm, which are more bioavailable and toxic due to the high dissolution of CuS in environmentally relevant conditions [78]. *The size, concentration and transformation of NPs leaving WWTPs will inform about what is released into the environment and will be valuable inputs for fate and risk studies and models.*

2.5. Toxicity of NPs in wastewater and biosolids

WW effluents are released into natural water bodies, and waste sludge from WWTP is often converted to biosolids and applied to agricultural fields. A wide range of biota is directly exposed to NPs present in effluents and biosolids. Several studies have attributed the toxicological responses observed in various microorganisms to dissolution of metal NPs and their uptake [5, 79, 80]. Furthermore, fullerenes, CNT and several metal NPs have been shown to cause toxicity through oxidative stress resulting from the formation of radicals, and reactive oxygen species (ROS) or due to nano size-specific reactivity properties of these NPs [81, 82].

Several studies have reported toxicity of ENPs in wastewater and biosolids matrices at higher than environmentally relevant concentrations [83-86]. Studies with WWTP biosolids spiked with 62.5 µg/kg of nAg and $nTiO_2$ (close to predicted environmental concentrations from modelling studies) of diameters ranging between 35 and 55 nm, revealed changes in the microbial community composition [33, 87]. Other studies showed significant reduction of microbial growth with increase in concentration of nAg, $nTiO_2$ and nZn [88-90]. A study of toxicity of nAg and Ag^+ on filter feeder organisms found in WWTPs, suggested an EC_{50} of approximately 2 and 0.75 mg/L, respectively, with nAg as a source of ion depending on the size, surface coating and environment [91]. A study on toxicity of planktonic and bacterial biofilm culture in the presence of nAg (10 to 40 mg/L) demonstrated cell death of 99.9% despite significant aggregation and attachment [92]. Toxic effects of NPs are mostly related to both nanospecific (size and reactive oxygen species genereation) [66, 93-96] and dissolved ion release [79, 96, 97]. Additionally, silver and copper ions form insoluble, or sparingly insoluble, inorganic complex, prone to sedimentation from the system [66, 98]. Therefore, WW effluent with high organic matter can still be dangerous to aquatic organisms with nanospecific toxic effects. Predicted no observed effect concentrations (PNEC) of nAg and nCuO in freshwater are estimated to be 12 and 340 ng/L, respectively [99]. PNEC in soil, calculated based on the sludge pathway, is nAg 30 µg/g [100]. There is no data on the PNEC of nCu in soils, but a PNEC of 26 µg/g for total Cu in soil has been reported [101].

The adsorption of pollutants in a real WW effluent onto spiked $nTiO_2$ and $nSiO_2$ increased toxic effects of those NPs to cyanobacteria *Anabaena variabilis* due to additive effects [102]. Several studies showed similar results of increased toxicity in organism exposed to NPs absorbed with toxic compounds [103-106]. On the other hand, multi element NPs of size 30 to 35 nm, comprised of an Au core and an

Ag and AgCl shell, showed photo degradation of toxic compounds like ibuprofen and clofibric acid present in wastewater samples [107].

The transformation of NPs in WW matrices alters their toxicity potential. nAg in the wastewater systems transform into nAg_2S in the presence of sulfide and the sulfidated nAg were found to be less toxic than pristine nAg [108]. Several studies have shown that sulfidation reduces the toxicity of nAg particles in both aquatic (zebrafish and killifish) and terrestrial (earthworms and duck week) organisms [109-112]. However, a recent study on the long term effects of sulfidized nAg at 1 mg/L concentration in sewage sludge on soil microflora showed toxicity [113]. Biosolids amended soils with varying concentrations (1, 10, or 100 µg/g) of NPs (nAg, nZnO, $nTiO_2$ or nCuO), reported that nZnO and nCuO had no significant effect on soil enzyme activity, whereas $nTiO_2$ had a slight reduction in enzyme activity, and nAg at 100 µg/g had inhibition effects on select enzyme activity [114]. The presence of organic molecules like humic and fulvic acid, mitigated the toxicity of some NPs to the microorganisms by reducing the amount available for exposure [81, 115]. The aggregation of NPs reduces their ion release rate along with their potential to be delivered to the cell surface, and thereby lowers their antimicrobial activities [85]. *It is important to comprehend the transformation of these NPs in the WWTP to assess the risks towards the environment.*

2.6. NPs in paints and coatings

There is a need to characterize the release of NPs from high-volume products such as paints and coatings, which are main NPs sources entering WWTPs and surface water. NPs (based on their specific properties) introduced in paint, are expected to improve the existing properties of the product. Currently, the most relevant nanomaterials for the paint industry are nanoscale TiO_2, SiO_2 and Ag. $nTiO_2$ particles are used for their properties of photocatalytic activity and UV-protection [116]. $nSiO_2$ particles impart macro- and micro-hardness, abrasion, scratch and weather resistance in paint [117, 118]. nAg particles provide antimicrobial effects in paints [119]. The NPs are used at varying concentrations, varying from 1 to 15% by weight of paint along with various binders (15 to 29%), for stabilization and dispersion. The constituents of the paint affect the properties of the NPs as well as their stability in the paint [116, 120]. During environmental exposures to precipitation, solar and temperature conditions, the NPs are released along with binders into the environment [121] with some studies showing large aggregates of $nSiO_2$ [121, 122] and others showing nAg less than 15nm being removed from the surface [119]. Extensive studies have been conducted to assess the toxic effects of pristine NPs used in products and mechanisms of toxicity on several model aquatic and terrestrial organisms [86, 123, 124]. Studies have shown the stability and toxicity of NPs depends on the particle size and aggregation state [125-129].

Holtz et al. (2012) [130] prepared coatings containing 1% (wt./v) silver nitrate and ammonium vanadate NPs in water-based paints, and observed a broad-spectrum antibacterial activity against *S.aureus*, *E.faecalis*, *E.coli*, and *S.enterica* with minimum inhibitory concentration values of 3.15 mg/L recorded (as opposed to 100 ppm with commonly-used antibiotics). Similar results were observed when Kumar et al. (2008) [131] inoculated glass slides coated with nAg added to oil-based paint with cells of *S.aureus* and *E.coli*, where minimal to no growth was observed after overnight incubation, indicating strong anti-bacterial activity. In parallel, loss of the active species (in this case, Ag^+) from such coatings have spurned research into slow-release or triggered mechanisms. Tiller et al. (2005) [132] synthesized materials such as adhesives, resins etc. which when impregnated with biocides interact with the latter through pore-size and/or hydrophobic interactions and serve as slow-release frameworks. In a related study, Aymonier et al. (2002) [133] coated glass surfaces with hybrid composites of nAg on amphiphilic macromolecules and sprayed *E.coli* cells on these slides. After overnight incubation, bacterial colony counts were seen to fall by 98% due to the release of Ag^+ from the hybrid composites. Elechiguerra et al. (2005) [134] employed High Angle Annular Dark Field scanning transmission electron microscopy to show size-dependent (1-10 nm) interaction of nAg with glycoprotein residues on HIV-1 capsid. Several other studies have also shown that nAg in pristine form are toxic against viruses like Hepatitis B virus-AD38 [135], HIV-1 caspid [134], murine norovirus (MNV) [136], adenovirus serotype 2 and H1N1 influenza A [137].

Studies have shown that the stability and toxicity of $nTiO_2$ depend on the particle size and aggregation state [125-128]. Incorporation of $nTiO_2$ in commercial paints and coatings imparts antimicrobial activity and prevents degradation and deterioration of external surfaces and facades [138]. When exposed to UV light, generation of reactive oxygen species (ROS) occurs in surfaces coated with TiO_2-containing paints which inactivates viruses and bacteria. This is also in part due to the two crystalline forms of $nTiO_2$-anatase and rutile that show different photoactive behaviors [139]. Paint coatings modified to contain $nTiO_2$ photocatalysts prepared by Sousa et al. (2013)

[140] showed above 98% loss in E.coli viability after 10 W/m^2 UV-A exposure for 40 minutes. Base paint formulations without photocatalysts exhibited only 45 to 55% cell viability loss. 5-micron thick TiO_2 coatings prepared by Chung et al. (2008) [141] showed reduction in viable bacterial counts by order of 10^4 from 10^5 in 40 h; the coating had an antimicrobial activity for *S.aureus* and *E. coli*. Ueda et al. (2017) [142] prepared a dispersion liquid containing $nTiO_2$ and cuprous oxide NPs, phosphate-ester surfactant, and organic solvent. Coatings containing this liquid and a binder resin were prepared and studies with *E. coli* and bacteriophage Q-beta reported anti-bacterial and anti-viral activities at 3 h. In another study, Chen et al. (2014) [143] incorporated 15 nm size $Cu/nTiO_2$ NPs into latex paint as a slow-release antibacterial agent. Minimum inhibitory concentrations of these NPs for *E. coli* and *S. aureus* strains were reported to be 21 mg/L and 14 mg/L respectively. Synergistic presence of Cu and TiO_2 enhanced ROS generation, leading to greater lipid peroxidation and leakage of intracellular matter. $Cu/nTiO_2$ NPs incorporated in latex paint showed 90% antibacterial activity even after 35 days, implying sustained activity. Antiviral activity of $nTiO_2$ was shown by Levina et al. (2015) [144], who synthesized composites containing DNA fragments non-covalently bound to 5 nm $nTiO_2$ which could bind selectively to nucleic acids in Influenza A virus, leading to a 99% inhibition of virus reproduction. Hydroxyapatite-TiO_2 composites synthesized by Monmaturapoj et al. (2018) [145] showed decrease in H1N1 Influenza A viral titers by 2 log at a dose of 0.5 mg/L in presence of UV exposure for 3 h. The composite improved TiO_2 binding of virus particles; ROS disrupted the membrane proteins and viral nucleic acids. $nTiO_2$ released from paint surfaces comes along with paint matrix, which may perhaps change its toxicity and fate in the environment compared to pristine $nTiO_2$.

Studies have shown that pristine NPs released into the environment are transformed under various environmental conditions [16, 38, 45, 48]. NPs released from functionalized surfaces and products will likely carry some of the product matrix [58, 146, 147], which could alter its environmental fate and toxicity behavior [148-151]. Although various studies have shown ENP releases from paint, most studies [146, 147, 152] have largely relied on electron microscopy techniques, which do not provide reliable data for concentrations and size distributions of the ENPs released. Previous studies on ENP release from painted surface reported the total metal concentration (indirect quantitative) and/or microscopic data (qualitative) with no information on size, particle size distribution and dissolved metal concentration [119, 121, 146, 147, 152-156]. A recent study on the characterization of $nTiO_2$ released from outdoor paints exposed to rainfall and snow, using single particle mode inductively coupled plasma mass spectrometry (spICP-MS), has reported a release of NPs with sizes ranging between 20 and 60 nm, and concentrations less than 0.0001% released from the painted surfaces [157]. Similarly, another study reported $nTiO_2$ release from painted surfaces after precipitation, with sizes ranging between 15 and 120 nm, and association with Al (20%) and Zr (1%) from the paint; these results were obtained using spICP-MS and spICP-time of flight-MS (spICP-TOF-MS) to directly measure the particle size distribution, concentration of NPs and association with other metals [158]. Although this is a reliable approach for assessing the mass concentrations of ENPs of insoluble metals such as $nTiO_2$, it offers no information on the size and aggregation state of the ENPs being released. nAg released from functionalized surfaces and products will likely carry some of the product matrix which could influence its environmental transformation, mobility and toxicity behavior of nAg [148-151]. *There is a lack of knowledge regarding the concentration and size of NPs released from nano-enabled products like paints and coatings. There is a need to assess how released NPs from painted surface are different in size, stability, and toxicity compared to the pristine NPs.*

2.7. References

1. Hassellöv, M., et al., *Determination of Continuous Size and Trace Element Distribution of Colloidal Material in Natural Water by On-Line Coupling of Flow Field-Flow Fractionation with ICPMS.* Analytical Chemistry, 1999. **71**(16): p. 3497-3502.
2. Tiede, K., et al., *Detection and characterization of engineered nanoparticles in food and the environment.* Food Additives and Contaminants, 2008. **25**(7): p. 795-821.
3. Domingos, R.F., N. Tufenkji, and K.J. Wilkinson, *Aggregation of Titanium Dioxide Nanoparticles: Role of a Fulvic Acid.* Environmental Science & Technology, 2009. **43**(5): p. 1282-1286.
4. Ma, R., et al., *Size-controlled dissolution of organic-coated silver nanoparticles.* Environmental science & technology, 2011. **46**(2): p. 752-759.
5. Navarro, E., et al., *Toxicity of silver nanoparticles to Chlamydomonas reinhardtii.* Environmental science & technology, 2008. **42**(23): p. 8959-8964.
6. Li, X., J.J. Lenhart, and H.W. Walker, *Aggregation kinetics and dissolution of coated silver nanoparticles.* Langmuir, 2011. **28**(2): p. 1095-1104.
7. Mitrano, D.M., et al., *Silver nanoparticle characterization using single particle ICP-MS (SP-ICP-MS) and asymmetrical flow field flow fractionation ICP-MS (AF4-ICP-MS).* Journal of Analytical Atomic Spectrometry, 2012. **27**(7): p. 1131-1142.
8. Lee, S., et al., *Nanoparticle size detection limits by single particle ICP-MS for 40 elements.* Environmental science & technology, 2014. **48**(17): p. 10291-10300.

9. Montaño, M., et al., *Improvements in the detection and characterization of engineered nanoparticles using spICP-MS with microsecond dwell times.* Environmental Science: Nano, 2014. **1**(4): p. 338-346.
10. Montaño, M.D., et al., *Single Particle ICP-MS: Advances toward routine analysis of nanomaterials.* Analytical and Bioanalytical Chemistry, 2016. **408**(19): p. 5053-5074.
11. Montaño, M.D., et al., *Opportunities for examining the natural nanogeochemical environment using recent advances in nanoparticle analysis.* Journal of Analytical Atomic Spectrometry, 2019. **34**(9): p. 1768-1772.
12. Degueldre, C. and P.Y. Favarger, *Thorium colloid analysis by single particle inductively coupled plasma-mass spectrometry.* Talanta, 2004. **62**(5): p. 1051-1054.
13. Degueldre, C., P.Y. Favarger, and C. Bitea, *Zirconia colloid analysis by single particle inductively coupled plasma–mass spectrometry.* Analytica Chimica Acta, 2004. **518**(1): p. 137-142.
14. Degueldre, C., P.Y. Favarger, and S. Wold, *Gold colloid analysis by inductively coupled plasma-mass spectrometry in a single particle mode.* Analytica Chimica Acta, 2006. **555**(2): p. 263-268.
15. Hineman, A. and C. Stephan, *Effect of dwell time on single particle inductively coupled plasma mass spectrometry data acquisition quality.* Journal of Analytical Atomic Spectrometry, 2014. **29**(7): p. 1252-1257.
16. Azodi, M., Y. Sultan, and S. Ghoshal, *Dissolution Behavior of Silver Nanoparticles and Formation of Secondary Silver Nanoparticles in Municipal Wastewater by Single-Particle ICP-MS.* Environmental Science & Technology, 2016. **50**(24): p. 13318-13327.
17. Liu, J.-f., et al., *Triton X-114 based cloud point extraction: a thermoreversible approach for separation/concentration and dispersion of nanomaterials in the aqueous phase.* Chemical Communications, 2009(12): p. 1514-1516.
18. Liu, J.-f., et al., *Cloud point extraction as an advantageous preconcentration approach for analysis of trace silver nanoparticles in environmental waters.* Analytical Chemistry, 2009. **81**(15): p. 6496-6502.
19. Raynie, D.E., *Surfactant-Mediated Extractions, Part I: Cloud-Point Extraction.* LCGC North America, 2016. **34**(1): p. 14-18.
20. Li, L., et al., *To What Extent Can Full-Scale Wastewater Treatment Plant Effluent Influence the Occurrence of Silver-Based Nanoparticles in Surface Waters?* Environmental Science & Technology, 2016. **50**(12): p. 6327-6333.
21. Majedi, S.M., B.C. Kelly, and H.K. Lee, *Evaluation of a cloud point extraction approach for the preconcentration and quantification of trace CuO nanoparticles in environmental waters.* Analytica Chimica Acta, 2014. **814**(0): p. 39-48.
22. Kiser, M., et al., *Titanium nanomaterial removal and release from wastewater treatment plants.* Environmental science & technology, 2009. **43**(17): p. 6757-6763.
23. Westerhoff, P., et al., *Occurrence and removal of titanium at full scale wastewater treatment plants: implications for TiO 2 nanomaterials.* Journal of Environmental Monitoring, 2011. **13**(5): p. 1195-1203.
24. Johnson, A.C., et al., *An assessment of the fate, behaviour and environmental risk associated with sunscreen TiO 2 nanoparticles in UK field scenarios.* Science of the Total Environment, 2011. **409**(13): p. 2503-2510.
25. Johnson, A., et al., *Exposure assessment for engineered silver nanoparticles throughout the rivers of England and Wales (CB0433).* Centre for Ecology and Hydrology, UK, 2011.

26. Farré, M., et al., *First determination of C 60 and C 70 fullerenes and N-methylfulleropyrrolidine C 60 on the suspended material of wastewater effluents by liquid chromatography hybrid quadrupole linear ion trap tandem mass spectrometry.* Journal of Hydrology, 2010. **383**(1): p. 44-51.
27. Mitrano, D.M., et al., *Detecting nanoparticulate silver using single-particle inductively coupled plasma–mass spectrometry.* Environmental Toxicology and Chemistry, 2012. **31**(1): p. 115-121.
28. Hadioui, M., V. Merdzan, and K.J. Wilkinson, *Detection and characterization of ZnO nanoparticles in surface and waste waters using single particle ICPMS.* Environmental science & technology, 2015. **49**(10): p. 6141-6148.
29. Khosravi, K., et al., *A novel approach for determining total titanium from titanium dioxide nanoparticles suspended in water and biosolids by digestion with ammonium persulfate.* Analytica Chimica Acta, 2012. **713**: p. 86-91.
30. Hoque, M.E., et al., *Detection and characterization of silver nanoparticles in aqueous matrices using asymmetric-flow field flow fractionation with inductively coupled plasma mass spectrometry.* Journal of Chromatography A, 2012. **1233**: p. 109-115.
31. Huang, Y., et al., *Fast Multielement Quantification of Nanoparticles in Wastewater and Sludge Using Single-Particle ICP-MS.* ACS ES&T Water, 2021. **1**(1): p. 205-213.
32. Gottschalk, F., et al., *Modeled environmental concentrations of engineered nanomaterials (TiO2, ZnO, Ag, CNT, fullerenes) for different regions.* Environmental Science & Technology, 2009. **43**(24): p. 9216-9222.
33. Gottschalk, F., T. Sun, and B. Nowack, *Environmental concentrations of engineered nanomaterials: Review of modeling and analytical studies.* Environmental Pollution, 2013. **181**: p. 287-300.
34. Tiede, K., et al., *Review of the Risks Posed to Drinking Water by Man-Made Nanoparticels*. 2012, FERA, UK. p. 170.
35. Hendren, C.O., et al., *Modeling nanomaterial fate in wastewater treatment: Monte Carlo simulation of silver nanoparticles (nano-Ag).* Science of The Total Environment, 2013. **449**: p. 418-425.
36. Keller, A.A. and A. Lazareva, *Predicted releases of engineered nanomaterials: From global to regional to local.* Environmental Science & Technology Letters, 2013. **1**(1): p. 65-70.
37. Garner, K.L., S. Suh, and A.A. Keller, *Assessing the Risk of Engineered Nanomaterials in the Environment: Development and Application of the nanoFate Model.* Environmental Science & Technology, 2017. **51**(10): p. 5541-5551.
38. Kaegi, R., et al., *Fate and transformation of silver nanoparticles in urban wastewater systems.* Water Research, 2013. **47**(12): p. 3866-3877.
39. Markus, A., et al., *Modeling aggregation and sedimentation of nanoparticles in the aquatic environment.* Science of the Total Environment, 2015. **506**: p. 323-329.
40. Furtado, L.M., et al., *Environmental Fate of Silver Nanoparticles in Boreal Lake Ecosystems.* Environ Sci Technol, 2015. **49**(14): p. 8441-50.
41. Kiser, M.A., et al., *Biosorption of nanoparticles to heterotrophic wastewater biomass.* Water Research, 2010. **44**(14): p. 4105-4114.
42. Brar, S.K., et al., *Engineered nanoparticles in wastewater and wastewater sludge – Evidence and impacts.* Waste Management, 2010. **30**(3): p. 504-520.

43. Barton, L.E., et al., *Monte Carlo simulations of the transformation and removal of Ag, TiO2, and ZnO nanoparticles in wastewater treatment and land application of biosolids.* Science of The Total Environment, 2015. **511**: p. 535-543.
44. Barton, L.E., et al., *Heteroaggregation, transformation and fate of CeO2 nanoparticles in wastewater treatment.* Environmental Pollution, 2015. **203**: p. 122-129.
45. Barton, L.E., et al., *Transformation of Pristine and Citrate-Functionalized CeO2 Nanoparticles in a Laboratory-Scale Activated Sludge Reactor.* Environmental Science & Technology, 2014. **48**(13): p. 7289-7296.
46. Kaegi, R., et al., *Behavior of Metallic Silver Nanoparticles in a Pilot Wastewater Treatment Plant.* Environmental Science & Technology, 2011. **45**(9): p. 3902-3908.
47. Whitley, A.R., et al., *Behavior of Ag nanoparticles in soil: Effects of particle surface coating, aging and sewage sludge amendment.* Environmental Pollution, 2013. **182**: p. 141-149.
48. Barton, L.E., *Fate and transformation of metal-(oxide) nanoparticles in wastewater treatment.* 2014: Duke University.
49. Benoit, R., K.J. Wilkinson, and S. Sauvé, *Partitioning of silver and chemical speciation of free Ag in soils amended with nanoparticles.* Chemistry Central Journal, 2013. **7**(1): p. 75.
50. Doolette, C.L., et al., *Transformation of PVP coated silver nanoparticles in a simulated wastewater treatment process and the effect on microbial communities.* Chemistry Central Journal, 2013. **7**(1): p. 46.
51. Georgantzopoulou, A., et al., *Ecotoxicological effects of transformed silver and titanium dioxide nanoparticles in the effluent from a lab-scale wastewater treatment system.* Environmental science & technology, 2018. **52**(16): p. 9431-9441.
52. Tuoriniemi, J., et al., *Size dependence of silver nanoparticle removal in a wastewater treatment plant mesocosm measured by FAST single particle ICP-MS.* Environmental Science: Nano, 2017. **4**(5): p. 1189-1197.
53. Bolaños-Benítez, V., et al., *Engineered silver nanoparticle (Ag-NP) behaviour in domestic on-site wastewater treatment plants and in sewage sludge amended-soils.* Science of The Total Environment, 2020. **722**: p. 137794.
54. Praetorius, A., M. Scheringer, and K. Hungerbühler, *Development of Environmental Fate Models for Engineered Nanoparticles・A Case Study of TiO2 Nanoparticles in the Rhine River.* Environmental science & technology, 2012. **46**(12): p. 6705-6713.
55. Meesters, J.A.J., et al., *Multimedia environmental fate and speciation of engineered nanoparticles: a probabilistic modeling approach.* Environmental Science: Nano, 2016. **3**(4): p. 715-727.
56. Bouchard, D., et al., *Simulating multiwalled carbon nanotube transport in surface water systems using the water quality analysis simulation program (WASP).* Environmental science & technology, 2017. **51**(19): p. 11174-11184.
57. Meesters, J.A., et al., *Multimedia modeling of engineered nanoparticles with SimpleBox4nano: model definition and evaluation.* Environmental science & technology, 2014. **48**(10): p. 5726-5736.
58. Benn, T.M. and P. Westerhoff, *Nanoparticle Silver Released into Water from Commercially Available Sock Fabrics.* Environmental Science & Technology, 2008. **42**(11): p. 4133-4139.
59. Montaño, M.D., et al., *Current status and future direction for examining engineered nanoparticles in natural systems.* Environmental Chemistry, 2014. **11**(4): p. 351-366.

60. Akaighe, N., et al., *Humic acid-induced silver nanoparticle formation under environmentally relevant conditions.* Environmental science & technology, 2011. **45**(9): p. 3895-3901.
61. Maurer, F., et al., *Reduction and Reoxidation of Humic Acid: Influence on Speciation of Cadmium and Silver.* Environmental Science & Technology, 2012. **46**(16): p. 8808-8816.
62. Hou, W.-C., et al., *Sunlight-Driven Reduction of Silver Ions by Natural Organic Matter: Formation and Transformation of Silver Nanoparticles.* Environmental Science & Technology, 2013. **47**(14): p. 7713-7721.
63. Ameh, T. and C.M. Sayes, *The potential exposure and hazards of copper nanoparticles: A review.* Environmental Toxicology and Pharmacology, 2019. **71**: p. 103220.
64. Adeleye, A.S., et al., *Influence of Extracellular Polymeric Substances on the Long-Term Fate, Dissolution, and Speciation of Copper-Based Nanoparticles.* Environmental Science & Technology, 2014. **48**(21): p. 12561-12568.
65. Torres-Duarte, C., et al., *Developmental effects of two different copper oxide nanomaterials in sea urchin (Lytechinus pictus) embryos.* Nanotoxicology, 2016. **10**(6): p. 671-679.
66. Conway, J.R., et al., *Aggregation, dissolution, and transformation of copper nanoparticles in natural waters.* Environmental science & technology, 2015. **49**(5): p. 2749-2756.
67. Kim, B., et al., *Discovery and Characterization of Silver Sulfide Nanoparticles in Final Sewage Sludge Products.* Environmental Science & Technology, 2010. **44**(19): p. 7509-7514.
68. Ma, R., et al., *Fate of Zinc Oxide and Silver Nanoparticles in a Pilot Wastewater Treatment Plant and in Processed Biosolids.* Environmental Science & Technology, 2014. **48**(1): p. 104-112.
69. Impellitteri, C.A., et al., *Transformation of silver nanoparticles in fresh, aged, and incinerated biosolids.* Water Research, 2013. **47**(12): p. 3878-3886.
70. Kim, B., et al., *Characterization and environmental implications of nano-and larger TiO 2 particles in sewage sludge, and soils amended with sewage sludge.* Journal of Environmental Monitoring, 2012. **14**(4): p. 1128-1136.
71. Lombi, E., et al., *Transformation of four silver/silver chloride nanoparticles during anaerobic treatment of wastewater and post-processing of sewage sludge.* Environmental Pollution, 2013. **176**: p. 193-197.
72. Pradas del Real, A.E., et al., *Fate of Ag-NPs in Sewage Sludge after Application on Agricultural Soils.* Environmental Science & Technology, 2016. **50**(4): p. 1759-1768.
73. Meier, C., et al., *Transformation of silver nanoparticles in sewage sludge during incineration.* Environmental science & technology, 2016. **50**(7): p. 3503-3510.
74. Yin, Y., et al., *Photo-and thermo-chemical transformation of AgCl and Ag2S in environmental matrices and its implication.* Environmental Pollution, 2017. **220**: p. 955-962.
75. Wang, P., et al., *Silver Nanoparticles Entering Soils via the Wastewater–Sludge–Soil Pathway Pose Low Risk to Plants but Elevated Cl Concentrations Increase Ag Bioavailability.* Environmental Science & Technology, 2016. **50**(15): p. 8274-8281.
76. Donner, E., et al., *X-ray Absorption and Micro X-ray Fluorescence Spectroscopy Investigation of Copper and Zinc Speciation in Biosolids.* Environmental Science & Technology, 2011. **45**(17): p. 7249-7257.

77. Gogos, A., et al., *Sulfidation kinetics of copper oxide nanoparticles.* Environmental Science: Nano, 2017. **4**(8): p. 1733-1741.
78. Ma, R., et al., *Sulfidation of copper oxide nanoparticles and properties of resulting copper sulfide.* Environmental Science: Nano, 2014. **1**(4): p. 347-357.
79. Franklin, N.M., et al., *Comparative toxicity of nanoparticulate ZnO, bulk ZnO, and ZnCl2 to a freshwater microalga (Pseudokirchneriella subcapitata): the importance of particle solubility.* Environmental science & technology, 2007. **41**(24): p. 8484-8490.
80. George, S., et al., *Use of a rapid cytotoxicity screening approach to engineer a safer zinc oxide nanoparticle through iron doping.* ACS nano, 2009. **4**(1): p. 15-29.
81. Dinesh, R., et al., *Engineered nanoparticles in the soil and their potential implications to microbial activity.* Geoderma, 2012. **173–174**(0): p. 19-27.
82. Manke, A., L. Wang, and Y. Rojanasakul, *Mechanisms of Nanoparticle-Induced Oxidative Stress and Toxicity.* BioMed Research International, 2013. **2013**: p. 15.
83. Reidy, B., et al., *Mechanisms of Silver Nanoparticle Release, Transformation and Toxicity: A Critical Review of Current Knowledge and Recommendations for Future Studies and Applications.* Materials, 2013. **6**(6): p. 2295.
84. Sajid, M., et al., *Impact of nanoparticles on human and environment: review of toxicity factors, exposures, control strategies, and future prospects.* Environmental Science and Pollution Research, 2015. **22**(6): p. 4122-4143.
85. Yang, Y., C. Zhang, and Z. Hu, *Impact of metallic and metal oxide nanoparticles on wastewater treatment and anaerobic digestion.* Environmental Science: Processes & Impacts, 2013. **15**(1): p. 39-48.
86. Klaine, S.J., et al., *Nanomaterials in the environment: behavior, fate, bioavailability, and effects.* Environmental Toxicology and Chemistry, 2008. **27**(9): p. 1825-1851.
87. Shah, V., et al., *Response of soil bacterial community to metal nanoparticles in biosolids.* Journal of Hazardous Materials, 2014. **274**: p. 399-403.
88. Murata, T., M. Kanao-Koshikawa, and T. Takamatsu, *Effects Of Pb, Cu, Sb, In and Ag Contamination on the Proliferation of Soil Bacterial Colonies, Soil Dehydrogenase Activity, and Phospholipid Fatty Acid Profiles of Soil Microbial Communities.* Water, Air, and Soil Pollution, 2005. **164**(1-4): p. 103-118.
89. Ge, Y., J.P. Schimel, and P.A. Holden, *Evidence for Negative Effects of TiO2 and ZnO Nanoparticles on Soil Bacterial Communities.* Environmental Science & Technology, 2011. **45**(4): p. 1659-1664.
90. Throbäck, I.N., et al., *Silver (Ag+) reduces denitrification and induces enrichment of novel nirK genotypes in soil.* FEMS Microbiology Letters, 2007. **270**(2): p. 189-194.
91. Burkart, C., et al., *Nanoparticles in wastewater treatment plants: a novel acute toxicity test for ciliates and its implementation in risk assessment.* Environmental Science and Pollution Research, 2015. **22**(10): p. 7485-7494.
92. Choi, O., et al., *Interactions of nanosilver with Escherichia coli cells in planktonic and biofilm cultures.* Water Research, 2010. **44**(20): p. 6095-6103.
93. Shi, J., et al., *To duckweeds (Landoltia punctata), nanoparticulate copper oxide is more inhibitory than the soluble copper in the bulk solution.* Environmental Pollution, 2011. **159**(5): p. 1277-1282.
94. Hanna, S.K., et al., *Accumulation and toxicity of metal oxide nanoparticles in a soft-sediment estuarine amphipod.* Aquatic toxicology, 2013. **142**: p. 441-446.

95. Buffet, P.-E., et al., *A mesocosm study of fate and effects of CuO nanoparticles on endobenthic species (Scrobicularia plana, Hediste diversicolor).* Environmental science & technology, 2013. **47**(3): p. 1620-1628.
96. Hadrup, N., A.K. Sharma, and K. Loeschner, *Toxicity of silver ions, metallic silver, and silver nanoparticle materials after in vivo dermal and mucosal surface exposure: A review.* Regulatory Toxicology and Pharmacology, 2018. **98**: p. 257-267.
97. Blinova, I., et al., *Ecotoxicity of nanoparticles of CuO and ZnO in natural water.* Environmental Pollution, 2010. **158**(1): p. 41-47.
98. Liu, J., et al., *Controlled Release of Biologically Active Silver from Nanosilver Surfaces.* ACS Nano, 2010. **4**(11): p. 6903-6913.
99. Lützhøft, H.-C.H., et al., *Environmental Effects of Engineered Nanomaterials: Estimations of Predicted No-Effect Concentrations (PNECs).* 2015.
100. Schlich, K., et al., *Hazard assessment of a silver nanoparticle in soil applied via sewage sludge.* Environmental Sciences Europe, 2013. **25**(1): p. 17.
101. Caetano, A.L., et al., *Copper toxicity in a natural reference soil: ecotoxicological data for the derivation of preliminary soil screening values.* Ecotoxicology, 2016. **25**(1): p. 163-177.
102. Martin-de-Lucia, I., et al., *Reverse Trojan-horse effect decreased wastewater toxicity in the presence of inorganic nanoparticles.* Environmental Science: Nano, 2017. **4**(6): p. 1273-1282.
103. Yang, W.-W., A.-J. Miao, and L.-Y. Yang, *Cd2+ toxicity to a green alga Chlamydomonas reinhardtii as influenced by its adsorption on TiO2 engineered nanoparticles.* PLoS One, 2012. **7**(3): p. e32300.
104. Recillas, S., et al., *Use of CeO2, TiO2 and Fe3O4 nanoparticles for the removal of lead from water: Toxicity of nanoparticles and derived compounds.* Desalination, 2011. **277**(1): p. 213-220.
105. Martín-de-Lucía, I., et al., *Reverse Trojan-horse effect decreased wastewater toxicity in the presence of inorganic nanoparticles.* Environmental Science: Nano, 2017.
106. Denet, E., et al., *Metal oxide nanoparticles for the decontamination of toxic chemical and biological compounds.* International Journal of Pharmaceutics, 2020. **583**: p. 119373.
107. Devi, T.B. and M. Ahmaruzzaman, *Bio-inspired facile and green fabrication of Au@Ag@AgCl core–double shells nanoparticles and their potential applications for elimination of toxic emerging pollutants: A green and efficient approach for wastewater treatment.* Chemical Engineering Journal, 2017. **317**: p. 726-741.
108. Liu, J., K.G. Pennell, and R.H. Hurt, *Kinetics and Mechanisms of Nanosilver Oxysulfidation.* Environmental Science & Technology, 2011. **45**(17): p. 7345-7353.
109. Reinsch, B., et al., *Sulfidation of silver nanoparticles decreases Escherichia coli growth inhibition.* Environmental science & technology, 2012. **46**(13): p. 6992-7000.
110. Kaphle, A., et al., *Nanomaterials for agriculture, food and environment: applications, toxicity and regulation.* Environmental chemistry letters, 2018. **16**(1): p. 43-58.
111. Ubaid, K.A., et al., *Fate and risk of metal sulfide nanoparticles in the environment.* Environmental Chemistry Letters, 2020. **18**(1): p. 97-111.
112. Levard, C., et al., *Sulfidation of silver nanoparticles: natural antidote to their toxicity.* Environmental science & technology, 2013. **47**(23): p. 13440-13448.
113. Kraas, M., et al., *Long-term effects of sulfidized silver nanoparticles in sewage sludge on soil microflora.* Environmental Toxicology and Chemistry, 2017: p. n/a-n/a.

114. Asadishad, B., et al., *Amendment of Agricultural Soil with Metal Nanoparticles: Effects on Soil Enzyme Activity and Microbial Community Composition.* Environmental Science & Technology, 2018. **52**(4): p. 1908-1918.

115. Fabrega, J., et al., *Silver Nanoparticle Impact on Bacterial Growth: Effect of pH, Concentration, and Organic Matter.* Environmental Science & Technology, 2009. **43**(19): p. 7285-7290.

116. Marolt, T., et al., *Photocatalytic activity of anatase-containing facade coatings.* Surface and Coatings Technology, 2011. **206**(6): p. 1355-1361.

117. Künniger, T., et al., *Release and environmental impact of silver nanoparticles and conventional organic biocides from coated wooden façades.* Environmental Pollution, 2014. **184**: p. 464-471.

118. Zhou, S., et al., *The change of the properties of acrylic-based polyurethane via addition of nano-silica.* Progress in Organic Coatings, 2002. **45**(1): p. 33-42.

119. Kaegi, R., et al., *Release of silver nanoparticles from outdoor facades.* Environ Pollut, 2010. **158**(9): p. 2900-5.

120. Tiarks, F., et al., *Formulation effects on the distribution of pigment particles in paints.* Progress in organic coatings, 2003. **48**(2): p. 140-152.

121. Zuin, S., et al., *Leaching of nanoparticles from experimental water-borne paints under laboratory test conditions.* Journal of nanoparticle research, 2014. **16**(1): p. 2185.

122. Mizutani, T., et al., *Application of silica-containing nano-composite emulsion to wall paint: A new environmentally safe paint of high performance.* Progress in Organic Coatings, 2006. **55**(3): p. 276-283.

123. Shoults-Wilson, W.A., et al., *Evidence for avoidance of Ag nanoparticles by earthworms (Eisenia fetida).* Ecotoxicology, 2011. **20**(2): p. 385-396.

124. Cox, A., et al., *Silver and titanium dioxide nanoparticle toxicity in plants: A review of current research.* Plant Physiology and Biochemistry, 2016. **107**: p. 147-163.

125. Zhang, Y., et al., *Stability of commercial metal oxide nanoparticles in water.* Water Research, 2008. **42**(8): p. 2204-2212.

126. Zhang, Y., et al., *Impact of natural organic matter and divalent cations on the stability of aqueous nanoparticles.* Water Research, 2009. **43**(17): p. 4249-4257.

127. Warheit, D.B., et al., *Health effects related to nanoparticle exposures: Environmental, health and safety considerations for assessing hazards and risks.* Pharmacology & Therapeutics, 2008. **120**(1): p. 35-42.

128. Ottofuelling, S., F. Von Der Kammer, and T. Hofmann, *Commercial Titanium Dioxide Nanoparticles in Both Natural and Synthetic Water: Comprehensive Multidimensional Testing and Prediction of Aggregation Behavior.* Environmental Science & Technology, 2011. **45**(23): p. 10045-10052.

129. Gorth, D.J., D.M. Rand, and T.J. Webster, *Silver nanoparticle toxicity in Drosophila: size does matter.* International journal of nanomedicine, 2011. **6**: p. 343-350.

130. Holtz, R.D., et al., *Nanostructured silver vanadate as a promising antibacterial additive to water-based paints.* Nanomedicine: Nanotechnology, Biology and Medicine, 2012. **8**(6): p. 935-940.

131. Kumar, A., et al., *Silver-nanoparticle-embedded antimicrobial paints based on vegetable oil.* Nature materials, 2008. **7**(3): p. 236-241.

132. Tiller, J., C. Sprich, and L. Hartmann, *Amphiphilic conetworks as regenerative controlled releasing antimicrobial coatings.* Journal of Controlled Release, 2005. **103**(2): p. 355-367.

133. Aymonier, C., et al., *Hybrids of silver nanoparticles with amphiphilic hyperbranched macromolecules exhibiting antimicrobial properties.* Chemical Communications, 2002(24): p. 3018-3019.
134. Elechiguerra, J.L., et al., *Interaction of silver nanoparticles with HIV-1.* Journal of nanobiotechnology, 2005. **3**(1): p. 6.
135. Lu, L., et al., *Silver nanoparticles inhibit hepatitis B virus replication.* Antiviral therapy, 2008. **13**(2): p. 253.
136. Park, S., et al., *Antiviral properties of silver nanoparticles on a magnetic hybrid colloid.* Appl. Environ. Microbiol., 2014. **80**(8): p. 2343-2350.
137. Mori, Y., et al., *Antiviral activity of silver nanoparticle/chitosan composites against H1N1 influenza A virus.* Nanoscale research letters, 2013. **8**(1): p. 93.
138. Kaiser, J.-P., S. Zuin, and P. Wick, *Is nanotechnology revolutionizing the paint and lacquer industry? A critical opinion.* Science of the total environment, 2013. **442**: p. 282-289.
139. Toma, F.L., et al., *Comparative study on the photocatalytic behaviour of titanium oxide thermal sprayed coatings from powders and suspensions.* Surface and Coatings Technology, 2009. **203**(15): p. 2150-2156.
140. Sousa, V.M., et al., *Photoinactivation of various antibiotic resistant strains of Escherichia coli using a paint coat.* Journal of Photochemistry and Photobiology A: Chemistry, 2013. **251**: p. 148-153.
141. Chung, C.J., et al., *An antimicrobial TiO2 coating for reducing hospital-acquired infection.* Journal of Biomedical Materials Research Part B: Applied Biomaterials: An Official Journal of The Society for Biomaterials, The Japanese Society for Biomaterials, and The Australian Society for Biomaterials and the Korean Society for Biomaterials, 2008. **85**(1): p. 220-224.
142. Ueda, T., D. Yamashina, and K. Kinugawa, *Copper complex titanium oxide dispersion liquid, coating agent composition, and antibacterial/antiviral member*. 2017, Google Patents.
143. Chen, S., et al., *Synergistic antibacterial mechanism and coating application of copper/titanium dioxide nanoparticles.* Chemical Engineering Journal, 2014. **256**: p. 238-246.
144. Levina, A.S., et al. *TiO2～DNA nanocomposites as efficient site-specific antiviral agents against influenza A virus in cell culture*. in *2015 IEEE 15th International Conference on Nanotechnology (IEEE-NANO)*. 2015. IEEE.
145. Monmaturapoj, N., et al., *Antiviral activity of multifunctional composite based on TiO2-modified hydroxyapatite.* Materials Science and Engineering: C, 2018. **92**: p. 96-102.
146. Al-Kattan, A., et al., *Release of TiO2 from paints containing pigment-TiO2 or nano-TiO2 by weathering.* Environmental Science: Processes & Impacts, 2013. **15**(12): p. 2186-2193.
147. Al-Kattan, A., et al., *Behavior of TiO2 Released from Nano-TiO2-Containing Paint and Comparison to Pristine Nano-TiO2.* Environmental Science & Technology, 2014. **48**(12): p. 6710-6718.
148. Saber, A.T., et al., *Nanotitanium dioxide toxicity in mouse lung is reduced in sanding dust from paint.* Particle and Fibre Toxicology, 2012. **9**(1): p. 4.
149. Smulders, S., et al., *Toxicity of Nanoparticles Embedded in Paints Compared with Pristine Nanoparticles in Mice.* Toxicological Sciences, 2014. **141**(1): p. 132-140.
150. Smulders, S., et al., *Toxicity of nanoparticles embedded in paints compared to pristine nanoparticles, in vitro study.* Toxicology Letters, 2015. **232**(2): p. 333-339.

151. Starnes, D.L., et al., *Distinct transcriptomic responses of Caenorhabditis elegans to pristine and sulfidized silver nanoparticles.* Environmental Pollution, 2016. **213**: p. 314-321.
152. Al-Kattan, A., et al., *Characterization of materials released into water from paint containing nano-SiO2.* Chemosphere, 2015. **119**: p. 1314-1321.
153. Kägi, R., et al., *Synthetic TiO2 nanoparticle emission from exterior facades into the aquatic environment.* Environmental pollution, 2008. **156**(2): p. 233-239.
154. Adeleye, A.S., et al., *Release and detection of nanosized copper from a commercial antifouling paint.* Water Research, 2016. **102**: p. 374-382.
155. Clar, J.G., et al., *Release and transformation of ZnO nanoparticles used in outdoor surface coatings for UV protection.* Science of The Total Environment, 2019. **670**: p. 78-86.
156. Zhang, X., et al., *Effects of weathering and rainfall conditions on the release of SiO2, Ag, and TiO2 engineered nanoparticles from paints.* Journal of Nanoparticle Research, 2017. **19**(10): p. 338.
157. Azimzada, A., et al., *Release of TiO2 nanoparticles from painted surfaces in cold climates: characterization using a high sensitivity single-particle ICP-MS.* Environmental Science: Nano, 2020. **7**(1): p. 139-148.
158. Azimzada, A., et al., *Single- and Multi-Element Quantification and Characterization of TiO2 Nanoparticles Released From Outdoor Stains and Paints.* Frontiers in Environmental Science, 2020. **8**(91).

Connecting text between Chapter 2 and Chapter 3

ENPs are being used extensively in a variety of industrial and consumer products due to their high specific surface area. Two of the major ENPs used in products are silver (nAg) and copper (nCu). A significant fraction of these ENPs used in products are entering municipal wastewater treatment plants (WWTPs), which is removed (approximately 70 to 99%) with settled sludge. Biosolids prepared from these sludges (50 to 60%) are applied on agricultural lands as fertilizers. There are currently no demonstrated methods for extraction and characterization of NP concentrations and size in complex matrices like WW sludge and biosolids. There is a need to assess the effects of NP concentration, size, and composition as well as contact time with sludge and biosolids. However, due to the limited quantitative data that is available on ENPs in municipal biosolids, assessment of environmental risk and bio-uptake is difficult. This study involves the development and optimization of methods to detect the size, particle size distribution and concentration of metal (Ag and Cu) ENPs in biosolids through the application of various extraction procedures and the subsequent analysis of aqueous extracts by single particle mode in ICP-MS (spICP-MS).

CHAPTER 3 SILVER AND COPPER NANOPARTICLES IN SLUDGE AND BIOSOLIDS FROM MUNICIPAL WASTEWATER TREATMENT PLANTS

Abstract

Engineered nanoparticles (ENPs) are being used extensively in a variety of industrial and consumer products due to their high specific surface area. Two of the major ENPs used in products are silver (nAg) and copper (nCu). A significant fraction of these ENPs used in products are entering municipal wastewater treatment plants (WWTPs), which is removed with settled sludge. Biosolids prepared from these sludges are applied on agricultural lands as fertilizers. However, due to the limited quantitative data that is available on ENPs in sludge and biosolids, assessment of environmental risks and bio-uptake of ENPs is difficult. This study involves with the development and optimization of methods to detect the size, particle size distribution and concentration of metal (Ag and Cu) ENPs in biosolids, through the application of various extraction procedures, and the subsequent analysis of aqueous extracts by spICP-MS. ENPs in aqueous extracts of biosolids were detected with an approximate mean size ranging from 16.0 ± 0.2 to 41.3 ± 0.5 nm for Ag and 42.9 ± 0.3 to 109.7 ± 1.7 nm for Cu, with a concentration in the range of 10^7 to 10^9 NPs/g of dry biosolids from eight municipal WWTPs across Canada. In parallel, NPs in sludge had a similar mean size and number concentration to those in biosolids with 21.8 ± 0.2 to 39.7 ± 2.1 nm for Ag and 67.3 ± 1.1 to 142.8 ± 1.8 nm for Cu, and a concentration of 10^7 to 10^{10} NPs/g of dry sludge. This data is an important input to future risk assessment and modelling studies. This is a step forward to understand how much NPs get released into the environment through the WWTP biosolids and will be a helpful input for policy makers and furthermore, advances analytical capabilities for detection and characterization NPs in complex environmental matrices.

3.1. Introduction

Engineered nanoparticles (NPs) or materials has been extensively used in various consumer and commercial products [1-4]. Currently, an approximate number of 7,000 NP-containing products are being commercially produced and used in 52 countries across the world [5]. Silver nanoparticles (nAg) are used in paints, medical bandages, textiles and food containers for their antimicrobial properties [6] and copper-based nanoparticles (nCu) are used in marine antifouling paints, antimicrobial textiles and wood preservatives [7]. Several studies have demonstrated the release of these NPs from NP-enabled products into the environment through various pathways [4, 8]. One of the major routes of this release is through discharges of effluents, sludge and biosolids from municipal wastewater treatment plants (WWTP). Keller and Lazareva (2013) suggested that between 17 and 34% of the total metal NPs that are manufactured are released to WWTPs following their use [8], of these, 44% are nAg and 18% are nCu [9]. In WWTPs, there is a significant attachment of NPs to sludge biomass. Approximately 70 to 99% of systems spiked with nAg are found to be attached and settle with wastewater biomass [10-13]. Depending on the WWTP facility, the sludge is stabilized using various processes to biosolids, for its application on agricultural fields, or disposal in landfills, or incineration [13], and thus NPs associated with sludge are released into different environmental compartments [14]. In North America, about 50 to 60 % of biosolids generated from WWTPs are used on agricultural fields as fertilizers [15, 16].

NP detection in complex environmental matrices (such as biosolids or sludge) is difficult since the concentration in the environment is low and it is hard to identify and measure them in the matrix. The most popular technique to quantify NPs in environment water samples is cloud point extraction (CPE) that has been employed to concentrate NPs and then merged with analytical techniques to report NP concentrations [17-19]. The reported data on NP size and particle concentration data (including nAg or nCu) in the complex matrix like sludge or biosolids is minimal, and thus detection and characterization of NPs is very challenging. Currently, there are only a few studies that have reported concentrations of TiO_2 (a commonly used NP) in sludge [20]. The concentration of particulate TiO_2 in the sludge at approximately 300 to 10,000 mg/kg was reported in several studies by acid digestion of the sludge followed by ICP-MS or ICP-OES analysis, with the assumption that Ti would exist only in particulate form [20-23]. However, this approach does not provide any size information for the particulates and thus the concentrations of the nanoparticulate fraction could not be confirmed. A recent study has used fast multielement single particle inductively coupled plasma mass spectroscopy (spICP-MS) to characterize 13 metal NP size and concentration (Cd, Co, Al, Au, Ni, Zn, Ce, Mn, Ti, Fe and Mg) with concentration and particle size distribution in different compartments (influent, post primary effluent, secondary effluent, reclaimed water, waste sludge and anaerobic digester sludge) of a WWTP in southern California, USA.[24]. The study analysed the supernatant of the samples from different compartments for mass concentration and particle size distribution. That study reported concentrations and sizes in WW sludge of nAg (4.3 ± 0.2 ng/g total suspended solids (TSS), 16.7 ± 0.3 nm) and nCu (76.5 ± 30.1 ng/g, 132.8 ± 1.1 nm), and in anaerobic digester sludge of nAg (70.5 ± 0.03 ng/g, 14.7 ± 0.7 nm) and nCu (705.8 ± 5.0 ng/g, 66.6 ± 8.1 nm). Concentrations and sizes of some other relevant NPs in the waste sludge are 0.13 ± 0.03 ng/g, 39.0 ± 0.1 nm for nCd, 2.7 ± 0.9 ng/g, 48.6 ± 3.2 nm for Au, 17.0 ± 0.9 ng/g, 91.6 ± 0.6 nm for Al, 57.1 ± 1.3 ng/g, 99.9 ± 1.3 nm for Zn, 54.7 ± 4.1 ng/g, 39.0 ± 0.1 nm for Ce, 359.8 ± 8.6 ng/g, 255.7 ± 1.2 nm for Ti, and 9263.9 ± 281.5 ng/g, 479.6 ± 4.1 nm for Fe. For anaerobic digester sludge, the reported concentrations for some relevant NPs were 0.3 ± 0.2 ng/g, 58.4 ± 5.0 nm for nCd, 3.7 ± 0.1 ng/g, 44.8 ± 0.8 nm for Au, 61.4 ± 10.9 ng/g, 44.0 ± 6.8 nm for Al, 339.8 ± 19.5 ng/g, 52.5 ± 11.0 nm for Zn, 172.1 ± 99.4 ng/g, 43.2 ± 0.9 nm for Ce, 1094.4 ± 174.7 ng/g, 98.4 ± 30.0 nm for Ti, and 1440.1 ± 427.8 ng/g, 144.9 ± 15.3 nm for Fe. Some modeling studies have predicted a concentration of nAg in biosolids in the range of 4.5 to 1700 ng of nAg/g biosolids [25, 26] and 0.01 to 0.15 ng of nCu/g biosolids [8].

Extensive studies have been conducted to understand the toxic effects of NPs on several model aquatic and terrestrial organisms and the mechanisms of their toxicity [27-29]. However, there is a lack of data on the concentration of NPs present in various environmental compartments [26, 30]. This is particularly true for NPs in sludge and biosolids from municipal WWTPs, which are considered to be important compartments contributing NPs to agricultural soils (from land application of biosolids) [16, 31], land fill disposal [2, 9] and to the atmosphere (from incineration of sludge) [32, 33]. The data on concentration as well as hazard, derived from toxicity tests, are both important for estimation of human health and environmental risks. In addition to the concentration of NPs, the characterization of their size and surface chemistry is vital to understand the environmental impacts of NPs in wastewater systems and in the environment. For example, higher bioavailability and uptake of nAg_2S in soils were observed in elevated Cl compared to soils with low Cl [34]. nAg and nCu may release their ions into wastewater due to dissolution which may contribute significantly to their toxicity [35, 36], however the surface chemistry of NPs can be modified by reactions and adsorption of organic and inorganic components of wastewater and sludge, which can lead to altered dissolution and toxicity [6, 12, 13, 30, 37-41].

This study is aimed at the characterization of size and concentration of nAg and nCu in WWTP sludge and biosolids. nAg and nCu were chosen for their wide use in nano enabled products [6-8, 25, 26, 42] and significant toxicity in the environment [43-51]. The size and concentration of nAg and nCu in sludge and biosolids, in 11 different WWTPs, were characterized to capture the differences due to sizes of the WWTPs, the treatment and sludge stabilization technologies employed and regional differences. Biosolids and sludge samples were spiked with nAu with various size over different contact times to optimize NP extraction efficiency. In addition, to assess the effect of the matrix in the detection of NPs, nAg or nCu were spiked in DI water controls and compared to biosolids. Furthermore, nAg or nCu were spiked in biosolids and extracted with enzyme digestion to assess the change in size and composition in biosolids with contact time.

spICP-MS was used for the characterization of nAg and nCu in the sludge and biosolids extracts. spICP-MS is a powerful technique for measuring metal NP sizes and concentrations in aqueous samples at sub parts per billion (environmentally relevant) concentrations [52-60]. Imaging techniques provide direct evidence of NPs in clean matrices but require extensive sample preparation in complex matrices such as soils and biosolids. Particle sizing techniques have limitations for analysis of ENPs in environmental samples representing complex media, because of their inability to distinguish target NPs from background natural colloids such as clays and mineral oxide particles. spICP-MS has significant advantages over other techniques (microscopy, light scattering techniques, total metal measurement using ICP-OES and ICP-MS) for NP analysis, because it can measure NP size, type, and concentration simultaneously. The detection limit of size varies depending on the element, with nCu having an approximate theoretical limit of 40 nm and nAg around 20 nm, and these size detection limits are attainable with complex environmental matrices [53]. For example, sizes as low as 20 nm at a concentration of 10 ppb in spiked wastewater samples were reliably characterized using a short dwell time of 100 µs [37]. The detection limit of nCu in soil matrix using spICP-MS was reported to be close to 35 nm [7].

3.2. Materials and Methods

3.2.1. Sludge and biosolids sample collected

Sludge and biosolids samples were collected from 11 different WWTPs (8 samples of biosolid and 8 of sludge - Table 3-1) across Canada by Environment and Climate Change Canada. The samples were collected in the provinces of Alberta (3), Ontario (2), Quebec (2), Manitoba (2) and Nova Scotia (2), to understand the variation between provinces. Composited samples from a 3-day sampling period from each municipal WWTP were obtained to minimized bias related to heterogeneity in the samples and possible time-based fluctuations in NP concentration. Upon collection, the samples were frozen at a temperature of -80℃ until analysis. Freezing and storage of aqueous suspension samples had no impact on the measured NPs concentrations and sizes (Table S3-1).

Table 3-1 Details of sludge generation and treatment processes used in different WWTPs across Canada

WWTPs	*Bioreactor*	*Settling tank*	*Sludge treatment*	*Population of city*
Plant A, AB	Activated sludge	Secondary Clarifier	Anaerobic digester and settling lagoons	1290000
Plant B, AB	Activated sludge	Secondary Clarifier	Anaerobic digester and settling lagoons	1290000
Plant C, AB	Activated sludge	Secondary Clarifier	Anaerobic digester and settling lagoons	1290000
Plant D, ON	Biological Aeration filtration facility	Secondary Clarifier	Mechanical dewatering and sludge cake pumping	217185
Plant E, ON	Activated sludge	Secondary clarifier	Mechanical dewatering, heat dried and pelletized sludge	217185
Plant F, QC	Activated sludge	Secondary Clarifier	Alkaline stabilization and mechanical dewatering	23357

Plant G, QC	Activated sludge	Secondary Clarifier	Anaerobic digester and composting	53236
Plant H, MB	Activated sludge	Secondary Clarifier	Anaerobic digester and mechanical dewatering	404,000
Plant I, MB	Activated sludge	Secondary Clarifier	Anaerobic digester and mechanical dewatering	86000
Plant J, NS	Activated sludge	Secondary Clarifier	Mechanical dewatering and Alkaline stabilization blended with dewatering (N-Viro technology)	403130
Plant K, NS	Activated sludge	Secondary Clarifier	Mechanical dewatering and Alkaline stabilization blended with dewatering (N-Viro technology)	52344

3.2.2. Extraction of NPs in biosolids

Biosolids and sludge cannot be directly analyzed for NPs by spICP-MS, as large particulate sizes and high solids concentrations can clog the nebulizer. Thus, NPs were extracted into water and then analysed by spICP-MS. The feasibility of extraction of NPs in aqueous media was evaluated using gold NPs (nAu) due to its chemical stability, and its absence in the WW samples. In addition, nAu does not have any intrinsic any interferences from other elements in ICP-MS. Three procedures for extracting NPs from sludge and biosolids were evaluated using nAu; (i) DI water with mixing, (ii) DI water with sonication and (iii) enzyme (protease) digestion of the organic matter followed by DI water extraction with sonication. Biosolids were spiked with 100 µg/L of uniformly sized 30 nm or 55 nm of nAu (Nanocomposix) for a contact period of 30 days. The contact period was chosen to be in the range of the average residence time for sludge in a typical wastewater treatment plant (10 to 15 days) [61, 62] and in the range of the sludge residence time (15 to 40 days) in anaerobic digestors [63]. For DI water with mixing, 0.5 g of the biosolid samples were diluted using 2 mL DI water, vortexed for 1 min and allowed to settle for 10 min. The supernatant was then sampled and directly analyzed in the sp ICP-MS. For the DI water with sonication extraction, the DI water (2 mL) diluted biosolid sample (0.5 g) was placed in ultrasonic bath for 60 min at 37 Hz under pulse mode to release the NPs trapped in the biosolids matrix. Then the sample was allowed to settle 10 min and the supernatant was sampled. The enzyme digestion procedure was adapted from elsewhere [64] used proteinase from *Aspergillus melleus* at 30 mg/mL (Sigma Aldrich) in a solution of 50 mM ammonium bicarbonate buffer (Sigma Aldrich) and 5 mg/mL sodium dodecyl sulfate (SDS) (Fischer Scientific) to degrade biomass in the biosolids sample to aid the release of NPs into aqueous phase. The biosolids sample with the proteinase solution was incubated at 37°C for 4 hours. The biosolid enzyme mixture was then sonicated in an ultrasonic bath for 10 min at 37 Hz under pulse mode, to further NPs release into the supernatant. The sample was allowed to settle 10 min and the supernatant was sampled. Aliquots of the supernatants were sampled immediately and analyzed using spICP-MS. Multiple biosolid samples (Plant B, AB; Plant F, QC; and Plant H, MB) from WWTPs based on different technologies for preparation of biosolids were analysed to assess the impact of the biosolid extraction techniques.

3.2.3. Characterization of nAg and nCu spiked in biosolids

To assess the effects of contact time on the size and concentration of nAg and nCu in biosolids on the change in size and composition, 100 µg/L of polyvinylpyrrolidone (PVP)-coated 80 nm nAg and 2 mg/L of 50 nm nCuO were spiked into biosolids. A higher concentration of mg/L spiked nCu was used to remove the influence of background concentration in biosolids. The biosolids were sampled at time points 1, 10 days or 12 days, 20 and 30 days and analyzed for change in particle size and concentration. Enzyme-based digestion (proteinase from *Aspergillus melleus*) was used to release NPs into the supernatant. Aliquots of the supernatants were sampled immediately and analyzed using spICP-MS. In addition, to assess the effect of matrix in detection of NPs, 10 ng/L of PVP-coated 80 nm nAg and 3 µg/L of 50 nm nCuO was spiked into biosolids and compared to DI water and unamended biosolids. The samples were collected immediately, were diluted accordingly, and measured in triplicates using spICP-MS.

3.2.4. Transformation of nAg in biosolids

To assess the effects of biosolids contact time on transformation of nAg size and composition, 100 µg/L of polyvinylpyrrolidone (PVP)-coated 80 nm nAg spiked into biosolids. The biosolids were sampled at time points of 1, 3, 8, 15, 21 and 30 days and analysed for change in particle size and concentration. Enzyme-based digestion (proteinase from *Aspergillus melleus*) was used to release NPs into the supernatant. Aliquots of supernatant were sampled and analysed using TEM-EDS and spICP-MS.

3.3. Instrumentation and Characterization

3.3.1. spICP-MS analysis

NP characterization was performed using PerkinElmer NexION 300x ICP-MS in single particle mode supported by Syngistix software (ver 1.1). This analysis provided the NP size distribution, NP concentration and dissolved metal concentration in the samples. An integration dwell time of 100 µs with sampling time of 100-150 s was used. The dwell time was chosen to distinguish between multiple nanoparticles reaching the detector in close sequence at the concentration ranges present in the samples [52, 65]Standard reference nAu (NIST) of diameter 60 nm or ultra uniform nAu (nanocomposix) of particle diameter 30 or 55 nm at a concentration of 10^5 particles/mL were diluted in DI water/ biosolids aqueous extract matrix from the reactors to find the transport efficiency (4.0 to 9.5%) for spICP-MS. Other main instrumental settings and conditions are provided in the SI (Table S3-2).

The calibration for silver or copper between the concentration range of 50 ng/L to 2 µg/L was prepared using standard dissolved silver or copper ions of 1000 mg/L (SCP Science PlasmaCAL). The biosolid aqueous extracts were diluted accordingly, and measured in triplicates using spICP-MS. The spiked nAg, spiked nCuO, background controls and stock solution were measured along with the biosolid aqueous extract.

3.3.2. Sample Digestion and Element Analysis

Biosolid samples were acid digested using ICP grade nitric acid (SCP Science) and hydrogen peroxide (Fisher Scientific) was added in the ratio of 5:1 in volume. The digested samples were analysed along with quality controls; spiked with 100 µg/L dissolved Ag and 100 µg/L nAg and background controls (DI water and acid blanks) using hot block digestion at 95 °C for 60 minutes. The digested samples were diluted to the required volume and measured using standard mode in Perkin Elmer NexION 300x ICP-MS and Perkin Elmer 8000x ICP-OES. Each biosolid extract sample was digested in duplicate and each digested sample was measured in triplicate.

3.3.3. Transmission Electron Microscopy (TEM)

TEM analysis was performed using a FEI Tecnai G2 F20 S/TEM equipped with Gatan Ultrascan 4000 4k × 4k CCD Camera System (Model 895). An EDAX Octane T Ultra W/Apollo XLT2 SDD system was used for energy dispersive X-ray spectroscopy (EDS) measurements. 10 µL of the sample concentrate was deposited on the Cu/Au TEM grids (Electron Microscopy Sciences, Carbon film 200 mesh Cu/Au grids). The grids were allowed to dry and multiple drops were applied for samples to concentrate the nanoparticles. The samples were rinsed with DI water to clean background debris, and air-dried again prior to their analysis using TEM and EDS.

3.3.4. UV−Vis Spectroscopy

The optical absorption spectra of water-soluble cuprous ion complex from sludge and biosolids samples using Pierce^{TM} BCA protein assay were measured at absorbance of 562 nm by Ultrospec 3300 pro UV/Visible spectrophotometer.

3.4. Results and discussion

3.4.1. Extraction efficiency of spiked Au NPs from biosolids

Enzyme (proteinase from *Aspergillus melleus*) digestion of biosolids resulted in higher extraction efficiency from the biosolids matrix (95.8 ± 6.3 %) compared to enzyme-free DI water extraction with mixing (44.8 ± 9.7 %) or sonication (71.4 ± 11.2%) for nAu of 30 nm and 55 nm mean diameter, as shown in Figure 3-1. The extraction efficiencies resulting from enzyme digestion was unchanged for both sizes of the NPs and for contact time (0 to 30 days) of nAu with the biosolids. There was greater variability in the extraction efficiency for DI water extraction by mixing or sonication, compared to enzyme digestion. For 30 nm nAu, increasing contact time of nAu with biosolids resulted in lower extraction efficiencies by sonication. As shown in previous studies [64, 66, 67], there was no loss or interference in the measurement of NPs after enzyme digestion. In enzyme-based extraction, no observed loss in efficiency was observed from left over carbohydrates or fats in the samples, as the extraction efficiency was close to 95%. As enzyme digestion was more efficient than the other methods for extracting the nAu into the aqueous supernatant, this technique was used to extract nAg and nCu from the different municipal WWTP sludge and biosolids.

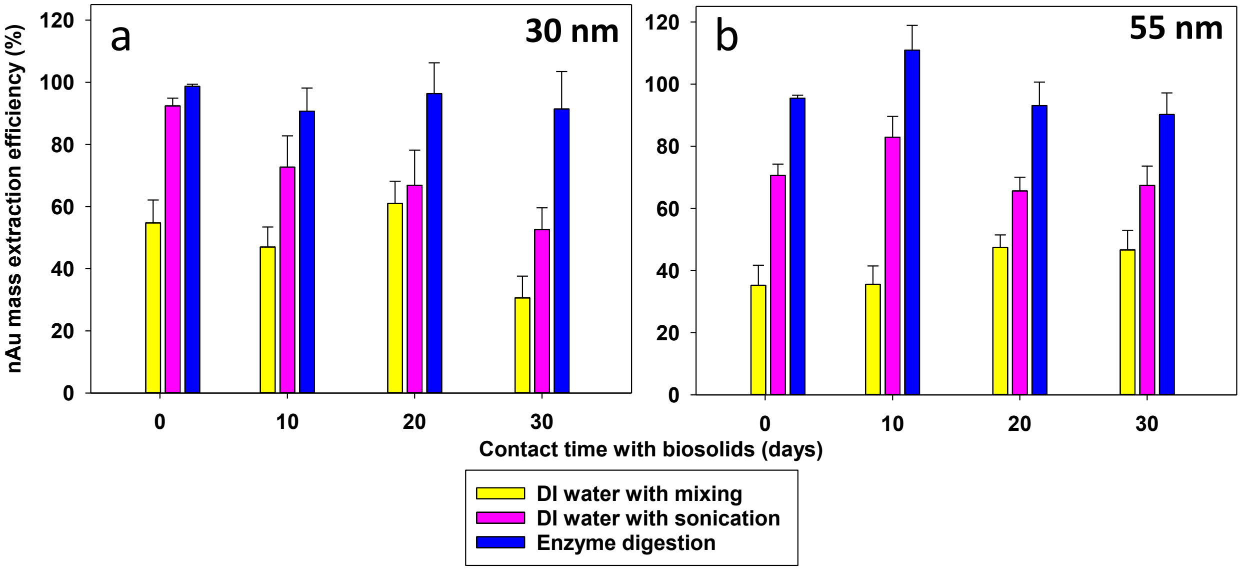

Figure 3-1 Extraction efficiency of nAu (mass basis) of different sizes in biosolids from different extraction techniques over the period of 30 days (a) 30 nm nAu and b) 55 nm nAu (sample replicates, n = 3 and measurement replicate = 3)

3.4.2. Extractable nAg and nCu measurement in sludge and biosolids

The nAg concentration of 10^7 to 10^8 NPs/g of dry biosolids (mass concentration: 1.2 to 91.1 ng/g - Table S3-3) with a mean size of 16.0 ± 0.2 to 41.3 ± 0.5 nm was measured for biosolids (Figure 3-2). The error values represent the standard deviation (both triplicates of sample and measurement) mean size of the particle size distribution. Similarly, the measured concentration of nAg in sludge was 10^7 to 10^9 NPs/g in dry sludge with a mean size of 21.8 ± 0.2 to 39.7 ± 2.1 nm. The mass concentration of nAg (1.5 to 785.9 ng/g) in the sludge and biosolids are provided in Table S3-3. These measured nAg mass concentrations were in the low range of the predicted concentrations of 1.6 ng/g to 3 mg/g from various materials flow analyses studies [4, 8, 25, 26, 68].

nCu was also detected in the sludge and biosolids matrix with mean size ranging from 42.9 ± 0.3 to 109.7 ± 1.7 nm with particle number concentration of 10^7 to 10^9 NPs/g in dry biosolids and mean size of 67.3 ± 1.1 to 142.8 ± 1.8 nm with concentration of 10^7 to 10^{10} NPs/g in dry sludge as shown in Figure 3-2. The measured values (mass concentration: 1.3 ng/g to 14.7 µg/g - Table S3-3) in sludge and biosolids were in the range of predicted concentration 10 to 800 ng/g for some WWTPs but for the other WWTPs were up to 10 times more than the predicted concentration [8]. Several quality assurance and quality control steps were taken to identify the effects of size, concentration and matrix effects of the biosolids extract on measurement accuracy. These are discussed in SI section 3.7.1).

A recent study characterized concentrations and sizes of NPs in WW sludge from a WWTP in southern California, USA and the concentrations and mean diameters of nAg (4.3 ± 0.2 ng/g, 16.7 ± 0.3 nm) and nCu (76.5 ± 30.1 ng/L, 132.8 ± 1.1 nm) [24]. The concentration for nAg and nCu were in the lower range of our measured data and NP size are in the range of our measured data.

The effect of matrix on recovery and detection of size of nAg and nCu in this study was found to be negligible. nAg particles (30 nm and 80 nm) were found have recoveries of 88.3 ± 2.5% (25.0 ± 0.5 nm) and 85.1 ± 4.6 % (73.2 ± 2.5 nm) in the biosolids matrix compared to 99.0 ± 5.2% (24.5 ± 0.1 nm) and 93.2 ± 3.5% (71.6 ± 0.9 nm) DI water with no change in particle size (Figure S3-1). Similarly, nCu had recovery of 103.5 ± 6.9% (109.4 ± 1.7 nm) in biosolid matrix compared to 88.0 ± 5.1% (110.5 ± 1.2 nm) in DI water (Figure S3-2).

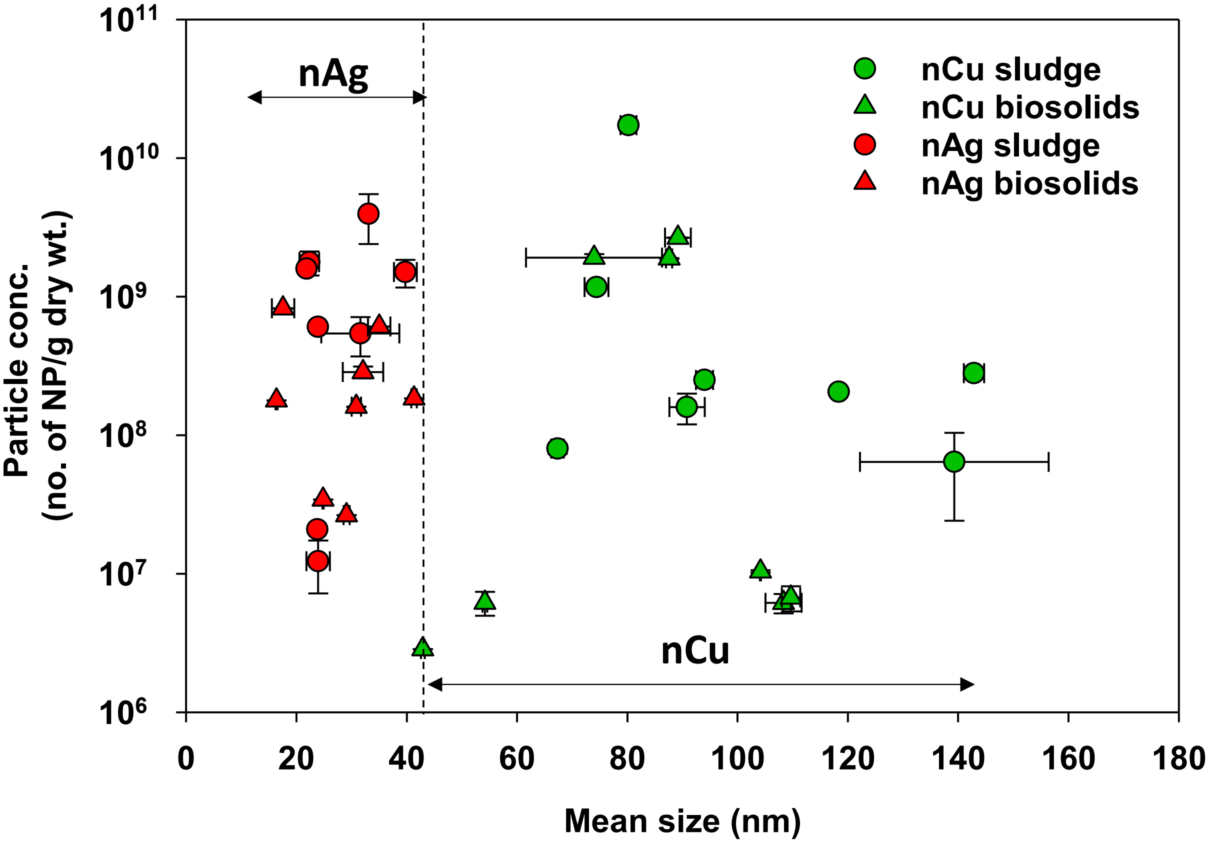

Figure 3-2 Mean size and NP concentration of nAg and nCu in biosolids and sludge aqueous extract using enzyme buffer extraction from various WWTP across Canada

The predicted no observed effect concentration (PNEC) in soil, calculated based on the sludge exposure pathway, is nAg 30 µg/g [69]. There is no reported data on the PNEC of nCu in soils, but a PNEC of 26 µg/g for total Cu in soil has been reported [70]. The measured concetrations were lower compared to PNEC for soil, and yield a a risk quotient of less than 1. Although for a few WWTPs the nCu values were comparable to the PNEC, for most WWTPs nCu values were orders of magnitude lower. For all WWTPs nAg concentrations were at least two order of magnitude lower than the PNEC. However, it should be noted that PNEC of nAg and nCuO in freshwater is 12 and 340 ng/L, respectively [71]. Thus the water extractable NPs from sludge and biosolids be mobilized and may contribute to toxicity in natural aqueous environments.

The concentrations of nAg and nCu represented approximately only ~ 0.01 to 5% of total mass of the metals obtained by acid digestion (Table S3-4), which suggests that the remaining metal in the biosolids was in the form of un-extracted nano or larger particles, or as dissolved complexes with organic matter or organometal compounds. The total Ag and Cu concentration measured was in a similar range to other studies for sludge and biosolids from different WWTPs [72, 73]. Soil quality guidelines for protection of environment and human health (SQG) by the Canadian Council of Ministers of the Environment (CCME) reports concentration below 63 µg/g for Cu and 20 µg/g for Ag [74]. The Bureau de Normalisation du Quebec (BNQ), in accordance with the requirements of the Standard Council of Canada (SCC), recommends trace metal concentration of 1500 µg/g for Cu in soil amendments with alkaline or dried municipal biosolids, whereas Ag is an unregulated metal in biosolids [75]. The United States Environmental Protection Agency (US EPA) regulates Cu concentration of 3750 µg/g in biosolids, while Ag is unregulated [76]. The concentrations of total Cu in biosolids measured in all our plants are below the recommended 1500 µg/g (BNQ) or 3750 µg/g (US EPA) for Cu.

The mean diameter of nAg particles (16.0 ± 0.2 to 41.3 ± 0.5) in various WWTPs were smaller than nCu (47 .1 ± 0.3 to 142.1 ± 1.8 nm), which is evident from Figure 1-2. This was unexpected given that Cu has a higher solubility than Ag in natural waters. The most frequent sizes of nAg (14 to 32 nm) and nCu (34 to 116 nm) were skewed towards to lower sizes compared to the mean size (calculated as mass weighted average). Particle size distributions of nAg and nCu in sludge and biosolids varied between plants and are presented in Figure S3-6, Figure S3-7, Figure S3-8, and Figure S3-9. No trends in size or concentration between sludge and biosolids for nAg or nCu from the different WWTPs by location or treatment techniques were observed (Figure 3-3).

Box plots of data for mass concentrations and mean particle sizes for nAg and nCu from all WWTPs showed no significant difference in the overall mean values between sludge and biosolids for each NP (Figure 3-3). The difference in means of mass and particle size were tested using pairwise Tukey t test ($p<0.05$). The median mass concentration in sludge was however ~26.7 times larger than the that for biosolids for nCu, and ~3.7 times higher for nAg.

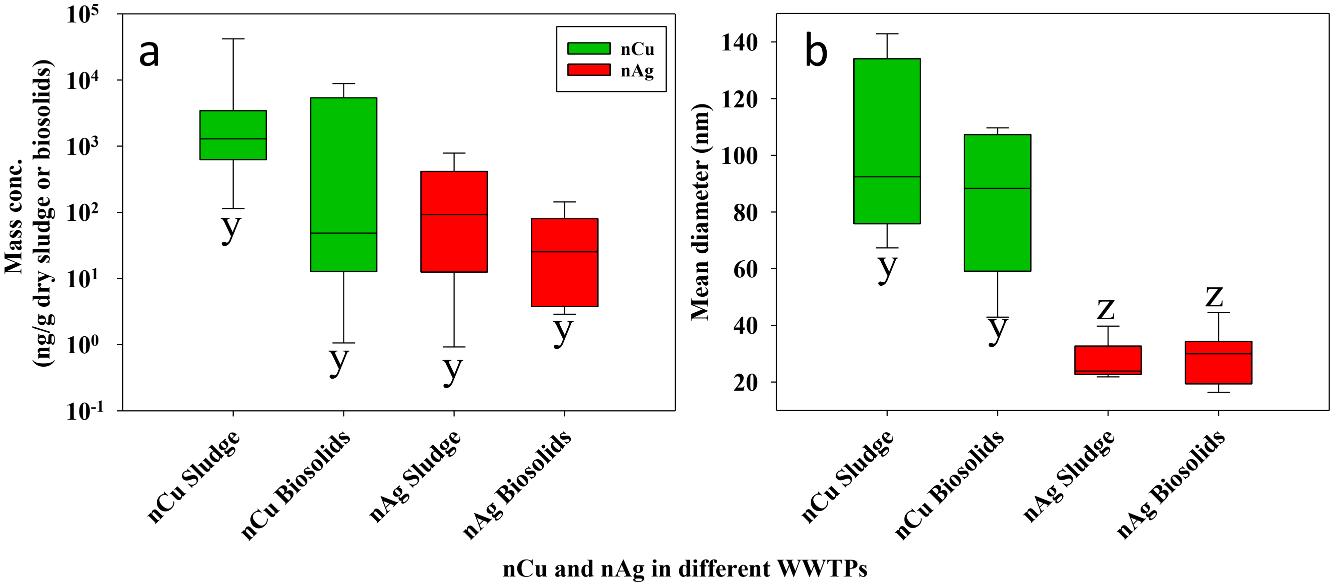

Figure 3-3 Boxplot of mass concentration (a) and mean diameter (b) of nCu and nAg in WW sludge and biosolids across Canada . Lower case letters (y and z) indicate differences between treatments ($p < 0.05$, one-way ANOVA)

One of the limitation of spICP-MS is that there is element specific detection limit for size (10 nm for nAg and 30 nm nCu) and thus, the mean sizes may be over-estimated if there are significant numbers of particles below the detection limit. Conversely, larger hetero- and homoaggregates that settle easily are unlikely to detected.

TEM analysis of biosolids show presence of NPs of Cu, Ti, Al, Si and Sn (Figure S3-5). However no nAg particles were detected even with an extensive search of multiple samples and image frames. It is likely that the low concentrations nAg made them difficult to identify in the matrix of dense organic matter and other colloids. This raises the question if the nAg counts detected in the sp ICP MS spectra were artefacts, for example, of Ag-organic matter complexes. To investigate this, 50 ng/L dissolved Ag was spiked in biosolids suspension and analyzed using spICP-MS. The addition of dissolved Ag only contributed to counts attributable to dissolved Ag and did not alter the counts attributable to nAg, i.e., the particle size distribution of nAg was not altered from that of the unspiked biosolids. The recovery of dissolved Ag was 90.2 ± 5.8 % (Table

S3-7). This suggests that Ag complexes with organic matter do not provide dense and large enough Ag atom clusters that can generate spICP MS signals corresponding to particles.

nCu detected in unspiked biosolid samples which was found to be associated with sulfur (EDS data) as per the previous studies [77] (Figure 3-4). The number concentration of nCuO spiked in biosolids decreased with contact time, increasing the dissolved Cu (Figure S3-4). TEM-EDS of the spiked nCu showed that it converted to nCuS from nCuO, similar results to unspiked nCu.

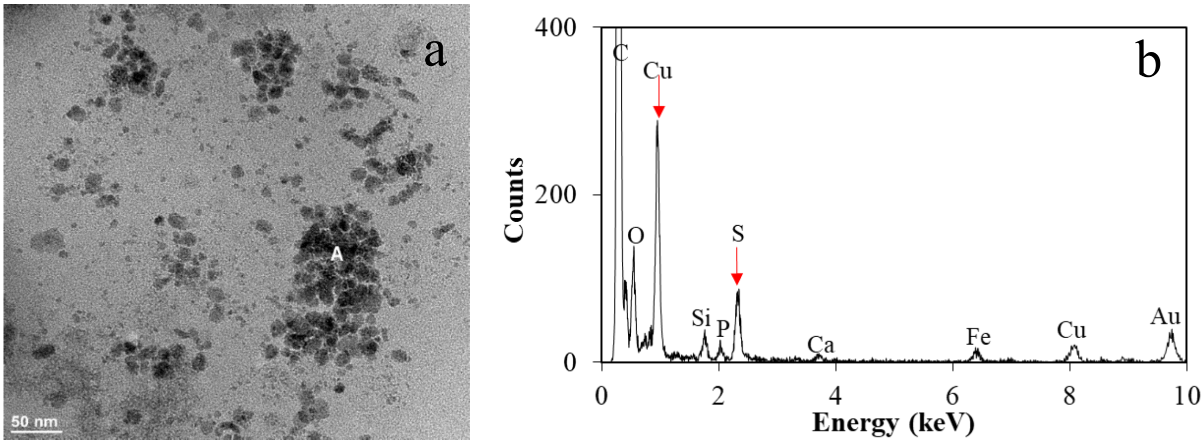

Figure 3-4 nCu in unspiked biosolids using TEM and EDS in gold grid (a) TEM image of nCu (b) EDS of the sample showing the association with sulfur.

3.4.3. Transformation of nAg

The transformation of the size and composition of 80 nm PVP-coated nAg (100 µg/L) in biosolids was assessed over time to characterize temporal transformations of nAg. A decrease in size of the individual nAg spiked in biosolids over 8 days was observed in the TEM images in Figure 3-5a-c. Individual nAg diameters decreased from 80 nm to approximately 30 nm over this time period. The TEM image of the nAg at day 8 also shows significant aggregation. At longer contact times (above 8 days), it was difficult to identify enough nAg in TEM to quantify its size in a statistically relevant manner. spICP-MS analysis of enzyme extracted biosolids also confirmed a gradual decrease in size to ~30 nm over 30 days (Figure 3-d). The diameter measurement of spiked nAg in biosolids using spICP-MS changed from 71.2 ± 3.2 nm on day 1 to 33.1 ± 1.3 nm on day 30. The rate of change in size of the spiked nAg in the TEM images and the spICP-MS are different, but is expected because of the vastly different number of nanoparticles analysed by the two techniques, and also because spICP-MS provides the size of the free particles as present in their dispersed or aggregated form. spICP-MS analysis showed that the mass fraction of Ag present as NPs in the biosolids decreased from 92.9 ± 1.4 % on day 1 to 7.0 ± 0.4% on day 30, as shown in Figure S3-3. Thus, the decrease in size overtime is attributable to dissolution of the NPs in the water rich biosolids (approximately 96% water content). The dissolution of nAg in wastewater samples and sludge has been observed in several studies [37, 78, 79]. It is noteworthy that with time the nAg appears to be associated with S as seen in the EDS spectra taken on the nAg. (Figure 3-5e,f). Several other studies have also reported that nAg in sludge and biosolids was sulfidated by inorganic and organic (thiol) sulfur [12, 30, 37, 38, 80]. It is likely that the nAg in unspiked biosolids was completely sulfidated. Ag_2S and other species of sulfidated Ag have low solubility, and thus may have contributed to the persistence of the nAg colloids [37, 81]. Kim et al. [82] reported TEM images of Ag_2S nanocrystals of size range ~5-20 nm in sewage sludge.

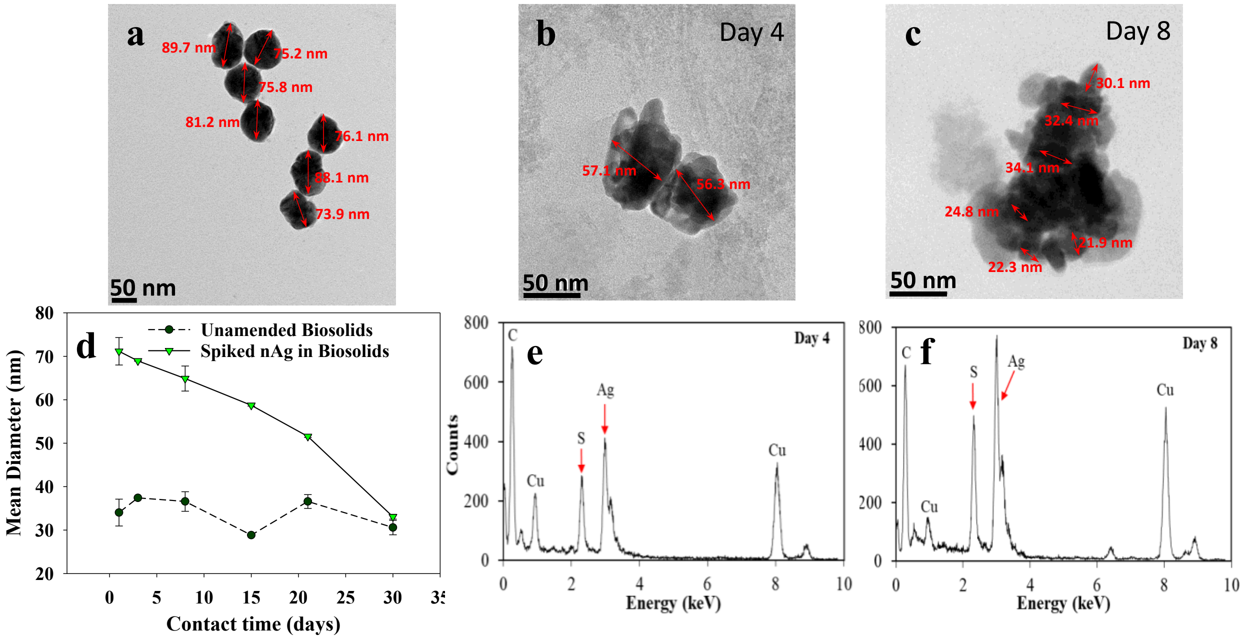

Figure 3-5 Change in spiked 80 nm PVP coated nAg in the biosolids using spICP-MS, TEM and EDS (a) TEM of nAg, before addition to biosolids, (b & c) TEM and EDS after 4 days of

contact time, (d) change in mean size of nAg with contact time using spICP-MS, (e & f) EDS analysis on nAg after 8 days of contact with biosolids.

3.5. Implications

This is a first study that reports NP particle size distribution and concentration in sludge and biosolids in Canadian municipal WWTPs. Biosolids are a sink for NPs entering WWTPs. Depending on the concentration of NPs in biosolids applied onto agricultural fields, the NPs may contribute to the toxicity from other contaminants present in biosolids,to micro- and larger organisms present in the soil and even to crops. There is a possibility of the NPs in biosolids to be released to surface water and/or ground water either as NPs or its dissolved forms. Presently, the measured concentration of NPs (nAg and nCu) reported in the study has a risk quotient (measured conc./ PNEC) way less than 1. The significance of this data is that it is an important input to the risk assessment modelling and analyses. Other NPs observed in unspiked biosolids from TEM-EDS analysis such as Ti, Al, Si and Sn NPs were detected. The study contributes to the understanding of how much NPs get released into the environment through the WWTP biosolids and will be a helpful input for policy makers.

These sulfidized nAg was more stable as there was less dissolution because of the surface transformation. Sulfidized nAg were found to be less toxic and more stable compared to the pristine nAg [80, 83]. Several other studies have shown reduced toxic effects at concentration of 50 to 500 ppb on micro organism of nAg_2S compared to nAg [84-87]. However, sulfidation of the nAg to nAg_2S does not render it completely benign [88]. Recent long-term exposure studies of 1 mg/L of nAg_2S have shown toxic effects of these persistent NPs [84, 85, 87]. Similarly, nCu which was found to be associated with sulfur, can also contribute to toxicity. Li et al.[89] reported that sulfidized nCu is more toxic than pristine nCu. Only ~ 0.01 to 5% of the total mass of the metals are easily available in NP form, while the rest of the metals in the biosolids are in the form of un-extracted nano or larger particles, complexes with organic matter or organometal compounds. This is a step forward to understand how much NPs get released into the environment through the WWTP biosolids and will be a helpful input for policy makers. Furthermore, this study advances analytical capabilities for environmental fate and transformation of NPs in complex environmental matrices.

3.6. Acknowledgements

We acknowledge the assistance of David Liu, McGill university and Jean-Philippe Masse, École Polytechnique de Montréal for TEM/EDS analysis. Environment and Climate Change Canada for providing with samples from 11 different municipal WWTPs. The research was supported by the Natural Sciences and Engineering Research Council of Canada and Environment and Climate Change Canada. Dr. Ali Akbari provided comments for improvement of the manuscript and figures. A. A. R was supported by McGill Engineering Doctoral Award.

3.7. Supplementary information

Table S3-1 nAg conc. before and after freeze storing in at -80 C

Measurement	Most Freq. Size (nm)	Mean Size (nm)	nAg Part. Conc. (NP/mL)
Before freezing at -80 C	13.2 ± 0.1	17.8 ± 0.1	3.6 ± 0.9 x 10^7
After Freeze thaw	11.8 ± 0.1	16.4 ± 0.2	3.3 ± 0.3 x 10^7

Table S3-2 spICP-MS instrumental parameters used for measurements

Parameter Value	
Sample Uptake Rate	0.28-0.34 mL/min
Nebulizer gas flow	0.97-1.03 L/min
Nebulizer	Meinhard Glass Concentric

Spray Chamber	Meinhard Glass Cyclonic
RF Power	1600 W
Analyte	Ag107, Cu63
Analysis time	100-150 s
Dwell time	100 μs

Table S3-3 Mass concentration of nAg and nCu recovered from 11 different WWTPs across Canada

WWTPs	Mass concentration recovery of NPs (ng/g of dry sludge or biosolids)			
	nAg		**nCu**	
	Sludge	**Biosolids**	**Sludge**	**Biosolids**
Plant A, AB	93.8 ± 2.9	143.6 ± 0.1	978.2 ± 57.4	10701.9 ± 908.2
Plant B, AB	-	51.8 ± 4.9	-	14688.1 ± 2005.5
Plant C, AB	108.4 ± 21.2	24.5 ± 0.2	114.3 ± 9.2	7212.1 ± 148.7
Plant D, ON	0.9 ± 0.4	3.6 ± 0.1	1603.3 ± 30.4	41.3 ± 3.5
Plant E, ON	1.5 ± 0.1	2.9 ± 0.1	812.3 ± 50.6	47.9 ± 9.6
Plant F, QC	-	4.3 ± 0.1	-	5.2 ± 1.1
Plant G, QC	-	25.9 ± 0.3	-	59.2 ± 0.1
Plant H, MB	519.2 ± 11.7	89.3 ± 0.4	41917.3 ± 102.8	1.3 ± 0.1
Plant I, MB	785.9 ± 30.8	143.6 ± 0.1	562.1 ± 14.9	10701.9 ± 908.2

Plant J, NS	91.0 ± 2.6	-	3833.7 ± 306.1	-
Plant K, NS	45.2 ± 2.5	-	2263.8 ± 18.6	-

Table S3-4 Percentage of NP detected in spICP-MS to total concentration of metal in the biosolids

Different WWTPs	**Copper in Biosolids**			**Silver in Biosolids**		
	nCuconc. (ng/g dry solids)	**Total Cu (ng/g of dry solids)**	**Cu in NPs to Total Cu (%)**	**nAg conc. (ng/g dry solids)**	**Total Ag (ng/g dry solids)**	**Ag in NP to Total Ag (%)**
Plant A, AB	8.9 ± 0.05x10^{3}	2.9 ± 0.3x10^{5}	**3.1 ± 0.2**	3.2 ± 0.04x10^{2}	2.9 ± 0.5x10^{3}	**5.0 ± 0.01**
Plant B, AB	3.6 ± 0.2x10^{3}	1.8 ± 0.1x10^{5}	**2.0 ± 2.3**	6.5 ± 0.5x10^{1}	2.3 ± 0.8x10^{3}	**2.3 ± 0.6**
Plant C, AB	5.9 ± 0.05x10^{3}	1.4 ± 0.01x10^{6}	**0.4 ± 02**	1.9 ± 0.01x10^{2}	1.2 ± 0.5x10^{4}	**0.2 ± 0.01**
Plant D, ON	3.7 ± 0.6x10^{1}	4.3 ± 0.2x10^{5}	**0.01 ± 0.003**	2.7 ± 0.01	2.4 ± 0.2x10^{3}	**0.2 ± 0.05**
Plant E, ON	4.2 ± 0.8x10^{1}	2.3 ± 0.3x10^{5}	**0.02 ± 0.003**	1.9 ± 0.01	1.4 ± 0.01x10^{3}	**0.2 ± 0.01**
Plant F, QC	4.6 ± 0.9	2.9 ± 0.7x10^{5}	**0.002 ± 0.0001**	1.6 ± 0.02	6.0 ± 0.4x10^{2}	**0.7 ± 0.03**
Plant G, QC	5.5 ± 0.1x10^{1}	6.3 ± 0.1x10^{5}	**0.01 ± 0.001**	1.9 ± 0.1	1.1 ± 0.4x10^{3}	**2.4 ± 0.03**
Plant H, MB	1.6 ± 0.1	4.6 ± 0.1x10^{5}	**0.0002 ± 0.00005**	1.4 ± 0.03	4.1 ± 0.2x10^{3}	**2.2 ± 0.05**

Table S3-5 Protein concentration measured in various sludge and biosolids by PierceTM BCA protein assay

WWTPS	***Protein conc. (mg/g of dry sludge)***	***Protein conc. (mg/g of dry biosolids)***
Plant A, AB	95.0 ± 3.2	29.0 ± 1.6
Plant B, AB		12.5 ± 0.8

Plant C, AB	61.0 ± 5.8	15.7 ± 2.1
Plant D, ON	32.8 ± 1.2	6.2 ± 0.5
Plant E, ON	37.3 ± 2.4	8.9 ± 0.5
Plant F, QC		38.7 ± 0.9
Plant G, QC		20.5 ± 1.2
Plant H, MB	20.7 ± 1.5	15.2 ± 1.1
Plant I, MB	62.8 ± 4.5	
Plant J, NS	205.3 ± 8.9	
Plant K, NS	310.4 ± 12.2	

The NPs present in sludge and biosolids are released by digestion of the protein in the system. The amount of protein in water extract of both sludge and biosolids were determined by the Pierce^{TM} BCA protein assay with quality controls and BSA calibrations. The amount of protein was calculated to determine if NPs can be released from the sludge or biosolids matrix using proteinase enzyme based digestion (Table S3-5). Mechanical dewatering (due to loss of proteins in dewatering) and anaerobic digestion (loss of protein due to reduction of biomass) of sludge might be possible reasons for lower concentration of proteins in biosolids compared to sludge.

Table S3-6 Number recovery percentage of 10 ng/L 30nm nAg spiked in aqueous extract matrix and measured using spICP-MS to assess the detection limit of nAg due to matrix effect in different sludge and biosolids

WWTPs	***Number concentration recovery of 10ng/L spiked 30nm nAg (%)***	
	Sludge	**Biosolids**
Plant A, AB	90.4 ± 1.5	102.5 ± 5.2
Plant B, AB		95.8 ± 7.5
Plant C, AB	94.3 ± 2.3	94.2 ± 4.2
Plant D, ON	88.4 ± 3.6	126.9 ± 11.7
Plant E, ON	120.3 ± 12.9	135.2 ± 5.3
Plant F, QC		100.1 ± 4.9

Plant G, QC		88.6 ± 3.8
Plant H, MB	102.4 ± 5.6	93.3 ± 2.1
Plant I, MB	94.5 ± 7.7	95.4 ± 7.8
Plant J, NS	113.2 ± 8.8	-
Plant K, NS	112.5 ± 9.5	-

Table S3-7 Recovery of spiked dissolved Ag in the biosolids aqueous extract.

Biosolids Suspension	**Measured Dissolved Ag Conc. (ppt)**	**AgNP Mean Size (nm)**
Unspiked	-	26.8 ± 2.1
Spiked with 50 ng/L Ag+ ion (Contact = 1 h)	45.1 ± 2.9	27.3 ± 1.2

Table S3-8 Percentage water content in sludge and biosolids to calculate dry weight

WWTPS	***Percentage water content in sludge (%)***	***Percentage water content in biosolids (%)***
Plant A, AB	98.0 ± 0.4	98.0 ± 0.4
Plant B, AB		93.3 ± 0.1
Plant C, AB	98.4 ± 0.7	96.7 ± 0.5
Plant D, ON	71.7 ± 1.3	5.6 ± 0.1
Plant E, ON	91.5 ± 0.1	46.3 ± 0.7
Plant F, QC		81.3 ± 1.3
Plant G, QC		77.6 ± 0.2
Plant H, MB	96.3 ± 0.1	71.4 ± 0.4

Plant I, MB	97.6 ± 0.6
Plant J, NS	95.3 ± 0.2
Plant K, NS	96.1 ± 0.1

Table S3-9 nAg and nCu measured in various unspiked municipal WWTP sludge using proteinase enzyme digestion and measured using spICP-MS (sample replicates, n = 3 and measurement replicates = 3)

WWTPs	*Number concentration (NP/g of dry sludge)*		*Mean size of NP in sludge (nm)*	
	nCu	**nAg**	**nCu**	**nAg**
Plant A, AB	$2.5 \pm 0.1 \times 10^{8}$	$5.4 \pm 1.7 \times 10^{8}$	94.0 ± 1.5	31.6 ± 7.1
Plant C , AB	$7.9 \pm 0.6 \times 10^{7}$	$1.8 \pm 0.3 \times 10^{9}$	67.3 ± 1.1	22.3 ± 1.8
Plant D, ON	$2.1 \pm 0.03 \times 10^{8}$	$1.2 \pm 0.5 \times 10^{7}$	118.3 ± 0.7	23.9 ± 2.1
Plant E, ON	$6.4 \pm 0.4 \times 10^{7}$	$2.1 \pm 0.05 \times 10^{7}$	139.3 ± 17.1	23.8 ± 0.1
Plant H, MB	$1.7 \pm 0.001 \times 10^{10}$	$1.5 \pm 0.3 \times 10^{9}$	80.2 ± 1.4	39.7 ± 2.1
Plant I, MB	$1.6 \pm 0.4 \times 10^{8}$	$3.9 \pm 1.5 \times 10^{9}$	90.8 ± 3.2	33.1 ± 0.5
Plant J, NS	$2.8 \pm 0.2 \times 10^{8}$	$1.6 \pm 0.04 \times 10^{9}$	142.9 ± 1.8	21.8 ± 0.2
Plant K, NS	$1.2 \pm 0.001 \times 10^{9}$	$6.1 \pm 0.3 \times 10^{8}$	74.4 ± 2.2	23.8 ± 0.2

Table S3-10 nAg and nCu measured in various unspiked municipal WWTP biosolids using proteinase enzyme digestion and measured using spICP-MS (sample replicates, n = 3 and measurement replicates = 3)

WWTPs	*Number concentration (NP/g of dry biosolids)*		*Mean size of NP in biosolids (nm)*	
	nCu	**nAg**	**nCu**	**nAg**
Plant A, AB	$2.7 \pm 0.01 \times 10^{9}$	$6.1 \pm 0.001 \times 10^{8}$	89.2 ± 2.3	35.0 ± 2.0
Plant B, AB	$1.9 \pm 0.1 \times 10^{9}$	$2.9 \pm 0.2 \times 10^{8}$	73.9 ± 12.3	32.1 ± 3.7
Plant C , AB	$1.9 \pm 0.01 \times 10^{9}$	$8.2 \pm 0.001 \times 10^{8}$	87.6 ± 0.5	17.5 ± 2.0
Plant D, ON	$6.2 \pm 0.9 \times 10^{6}$	$2.6 \pm 0.001 \times 10^{7}$	108.3 ± 3.3	29.1 ± 0.5
Plant E, ON	$6.7 \pm 1.3 \times 10^{6}$	$3.4 \pm 0.001 \times 10^{7}$	109.7 ± 1.7	24.8 ± 0.1
Plant F, QC	$6.2 \pm 1.2 \times 10^{6}$	$1.8 \pm 0.001 \times 10^{8}$	54.2 ± 0.4	16.4 ± 0.2
Plant G, QC	$1.0 \pm 0.2 \times 10^{5}$	$1.6 \pm 0.001 \times 10^{8}$	104.2 ± 0.1	30.8 ± 0.8
Plant H, MB	$2.8 \pm 0.001 \times 10^{6}$	$1.8 \pm 0.001 \times 10^{8}$	42.9 ± 0.3	44.5 ± 0.5

Table S3-11 Spiked 55nm nAu recovery using enzyme based digestion on multiple municipal WWTPs.

WWTPs	**55nm nAu recovery after enzyme based digestion from biosolids**
Plant B, AB	93.2 ± 8.2
Plant F, QC	92.3 ± 7.6
Plant H, MB	95.3 ± 5.4

3.7.1. Detection limit and matrix effect of NPs in biosolids aqueous extract

To assess the effect of the matrix of the solution, size and concentration of the NP in measurements using spICP-MS, we spiked 30 and 80nm PVP- coated nAg in both DI water, and biosolids extract at a concentration of 10 ng/L. The measured concentration of 30 nm nAg varied from 99.0 ± 5.2 % in DI water to 88.3 ± 2.5% in biosolids matrices, as shown in Figure S3-1a & c. The measured concentration of 80 nm nAg in DI water and biosolids matrix was 93.2 ± 3.5% and 85.1 ± 4.6%, respectively as shown in Figure S3-1b & d. Thus, the size of (30 and 80nm) nAg did not influence the concentration or size measurements in biosolids matrix using spICP-MS.

Similar recovery trends can be observed when 3 µg/L of nCu particles (particle size spICP-MS: 110.5 ± 1.2 nm) were spiked in the biosolids matrix and compared with control biosolids matrix and DI water. Higher concentrations of nCu were used to account for the high background dissolved concentration in the biosolids matrix. The recovery of nCu varied from 88.0 ± 5.1 % in DI to 103.5 ± 6.9 % in biosolids matrix as shown in Figure S3-2, with almost no change in the particle mean size. These results from both nAg and nCu indicate that the particle number recovery of nAg and nCu is not affected by the biosolids matrix.

The naturally occurring nAg (Figure S3-1e) were observed in unamended biosolids. Spiking pristine 80nm (10 ng/L) into unamended biosolids showed that background peak of 22.2 ± 1.2 nm co-existed with spiked 80nm nAg peaks as shown in Figure S3-1d. Furthermore, spiking

10 ng/L of 30 nm nAg into unamended biosolids, added on nAg particle peak frequency (to around ~450 frequency - Figure S3-1c) to pre-existing natural nAg particle peak frequency (from around ~250 frequency - Figure S3-1e). These results from Figure S3-1c & d suggest that the background peaks observed in unamended biosolids are naturally occurring nAg and not background noise observed in spICP-MS.

10 ng/L of 30nm nAg was spiked into 9 biosolids and 9 sludge to see if different sludge and biosolids matrix had influence on detection using spICP-MS. Recovery of spiked nAg in different sludge/biosolid matrices varied between 88.4 ± 3.6 to 135.2 ± 5.3 % recovery (Table S3-6). The recovery higher than 100% suggesting the presence of pre-existing natural nAg in the samples. Thus, different sludge/biosolids matrix had minimal effect on detection on NP using spICP-MS.

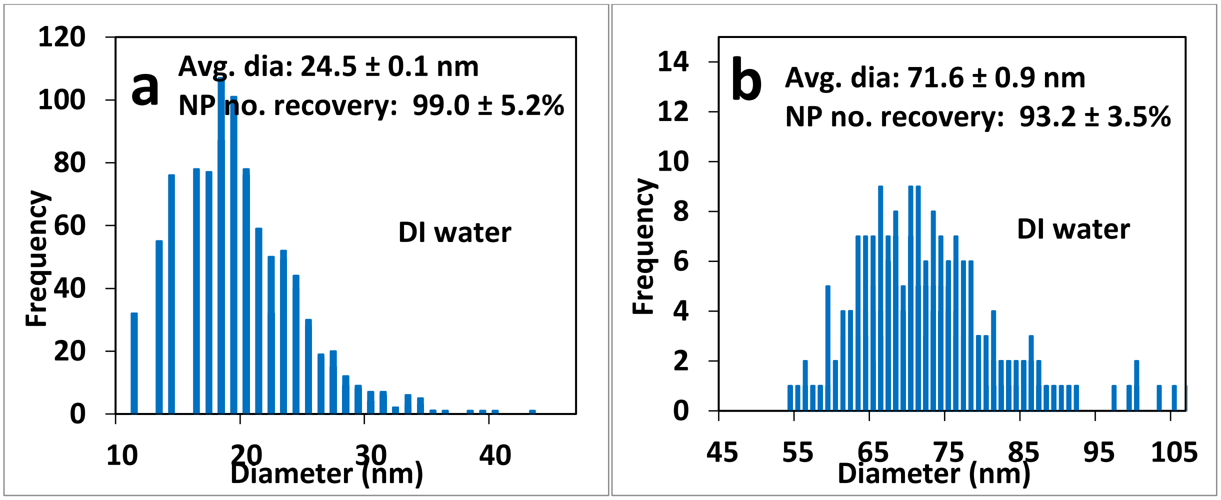

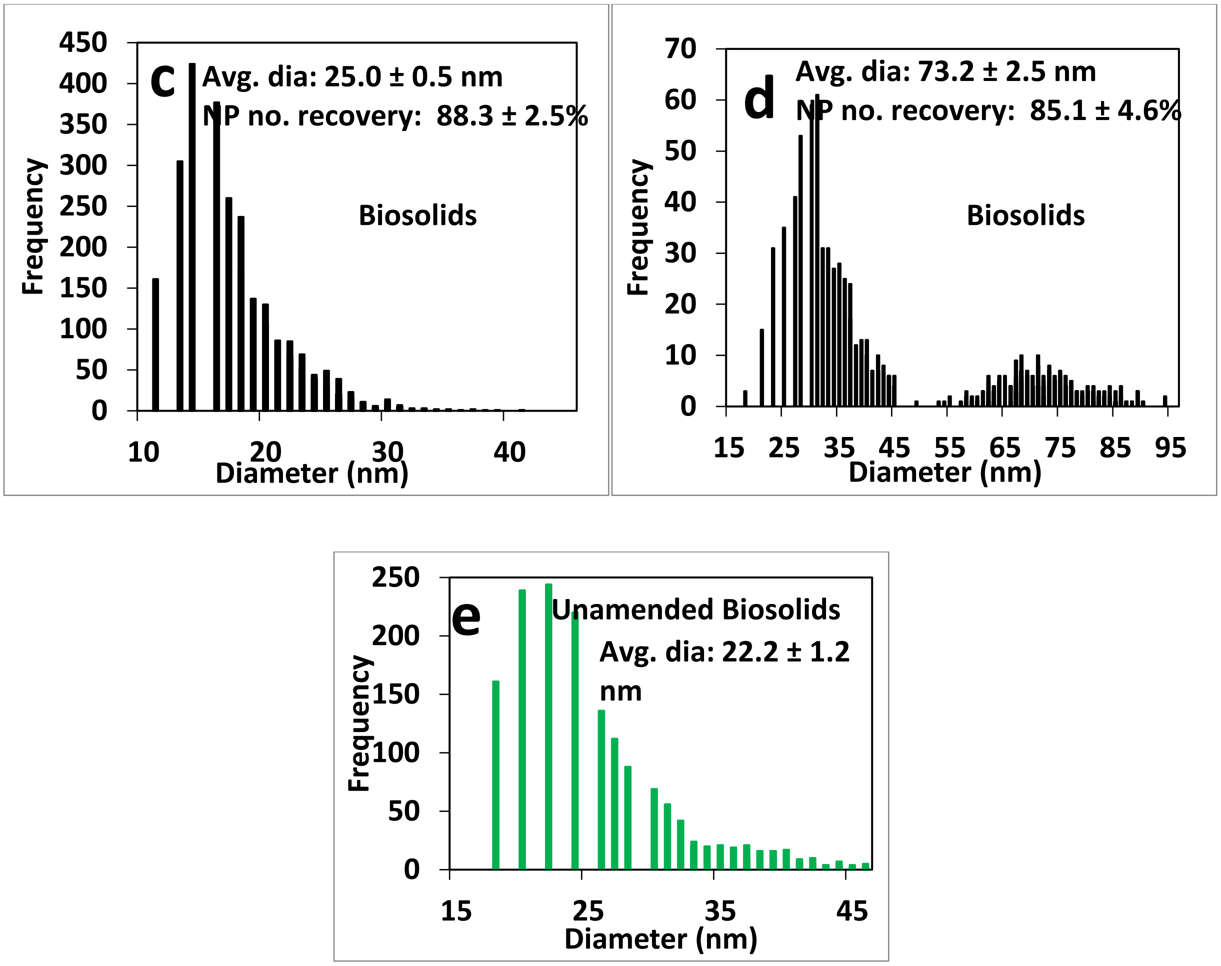

Figure S3-1 DI water and biosolids aqueous extract spiked with PVP coated 30 nm and 80 nm AgNP particles compared with control unspiked biosolids extract using spICP-MS (a & b) 10 ng/L of 30 nm and 80 nm AgNP in DI water (c & d) 10 ng/L of 30nm and 80nm AgNP in biosolids aqueous extract (e) control biosolids extract

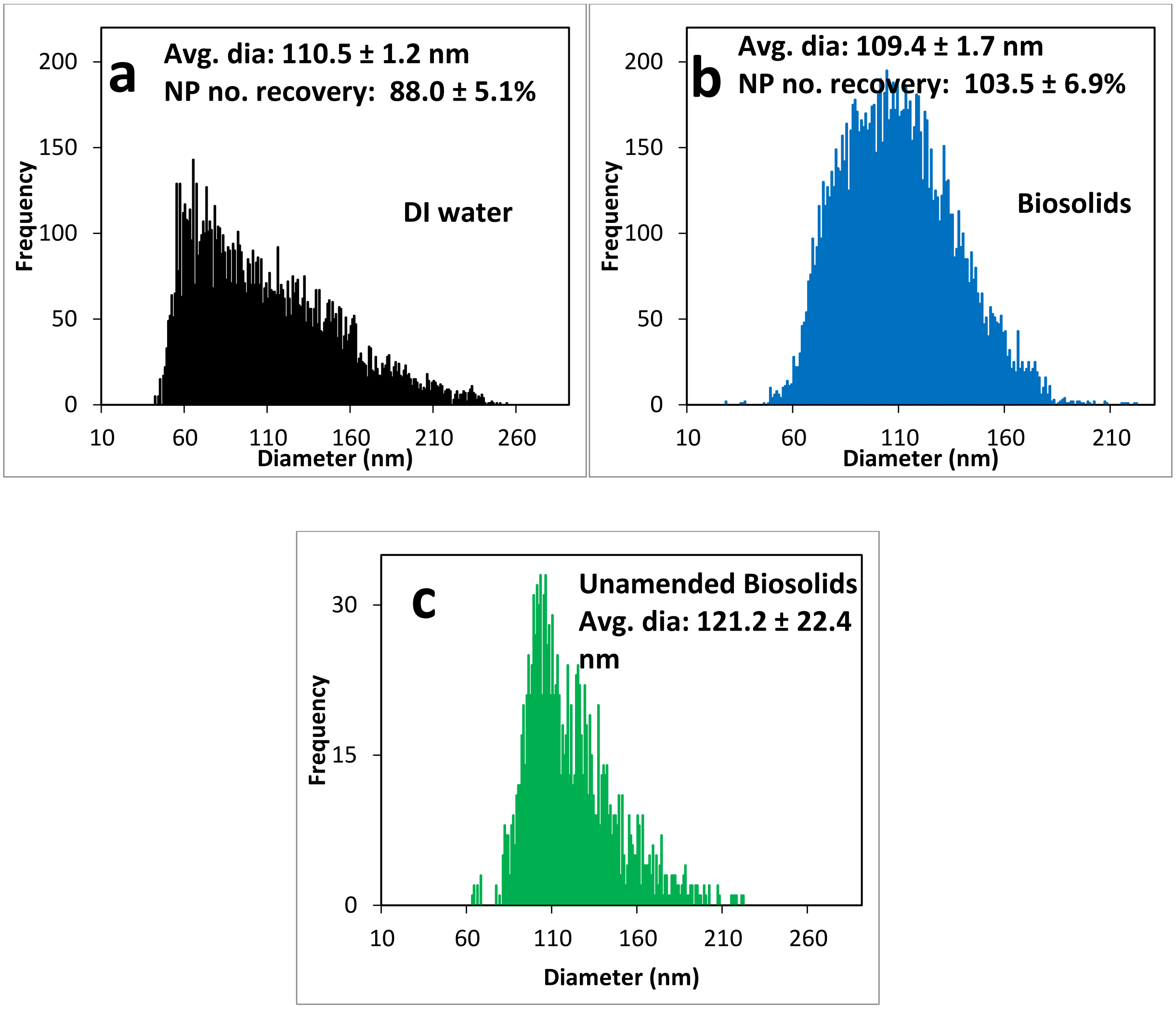

Figure S3-2 DI water and biosolids aqueous extract spiked (particle size spICP-MS: 110.5nm) nCu particles compared with control unspiked biosolids extract (a) 3 µg/L of nCu in DI water & (b) 3 µg/L of nCu in biosolids matrix (c) control biosolids extract

3.7.2. Dissolution of spiked nAg and nCu in biosolids with contact time

To assess the effect of biosolids matrix on pristine nAg, 80nm nAg (100 µg/L) was spiked into biosolids and observed for change in concentration of nAg and dissolved Ag. The biosolid sample was collected, extracted for nAg using enzyme digestion and finally, analysed by spICP-MS. The concentration of nAg decreased from 92.9 ± 1.4 µg/L on day 1 to 7.0 ± 0.4 µg/L on day

30 (Figure S3-3). Whereas, the dissolved Ag concentration increased from 3.8 ± 0.8 µg/L on day 1 to 71.9 ± 4.3 µg/L on day 30. The size of nAg reduces also reduced from71.2 ± 3.2 nm on day 1 to 33.1 ± 1.3 nm on day 30, as contact time with biosolids increases as reported in section 3.4.3. However, the concentration of nAu spiked in biosolids stayed almost constant (95.8 ± 6.3 µg/L) throughout the 30-day period. This suggest that with increased contact time of nAg with biosolids, higher dissolution was observed. Pristine nAg are shown to have dissolution once it gets exposed to environmental conditions [37, 81, 90].

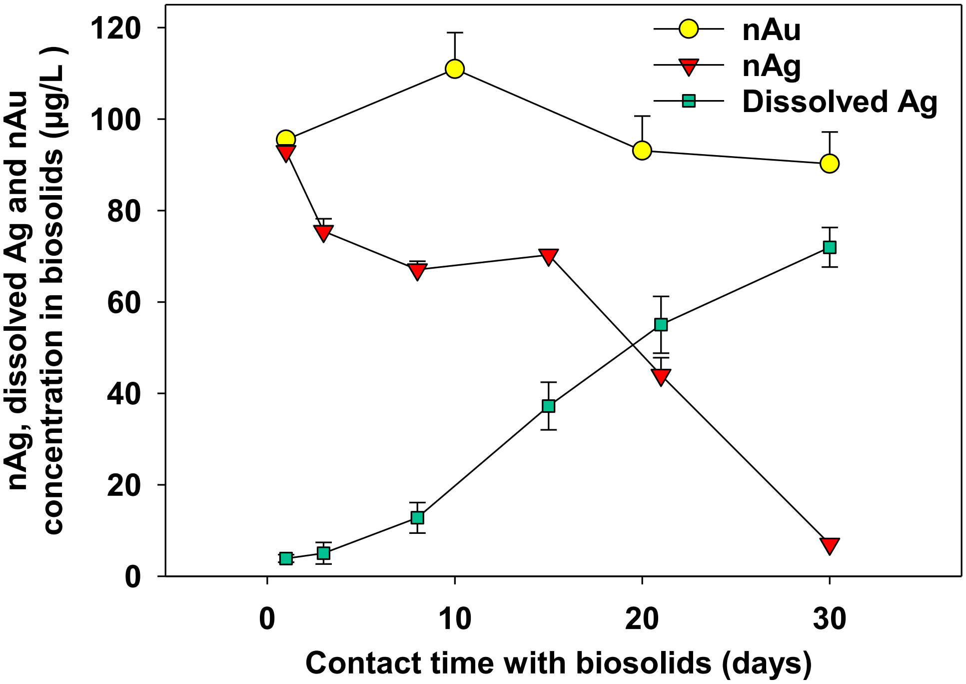

Figure S3-3 Stability of spiked nAg (10 µg/L of 80 nm) mass extraction efficiency using enzyme digestion compared to nAu in contact with biosolids for 30 days

Similar results were observed for 50 nm nCuO (3 mg/L) spiked in biosolids. The concentration of spiked nCu reduced from 1.6 ± 0.2 mg/L on day 1 to 0.1 ± 0.01 mg/L on day 30 (Figure S3-4). The size on nCu reduced from 128.2 ± 0.5 nm on day 1 to 63.9 ± 0.3 nm on day 30. These results indicate dissolution of spiked pristine nCu in contact with biosolids like spiked nAg. nAu particles are generally chemically inert, and thus its recovery was high (~95%) using enzyme-based digestion, whereas, prisitne nAg and nCu particles are more chemically labile, and dissolved to a significant extent in the biosolids matrix leading to lower mass recovery with time. This shows that stability and interactions of NPs with biosolid matrices varies between NP type and the extraction procedure for each NP should be evaluated separately.

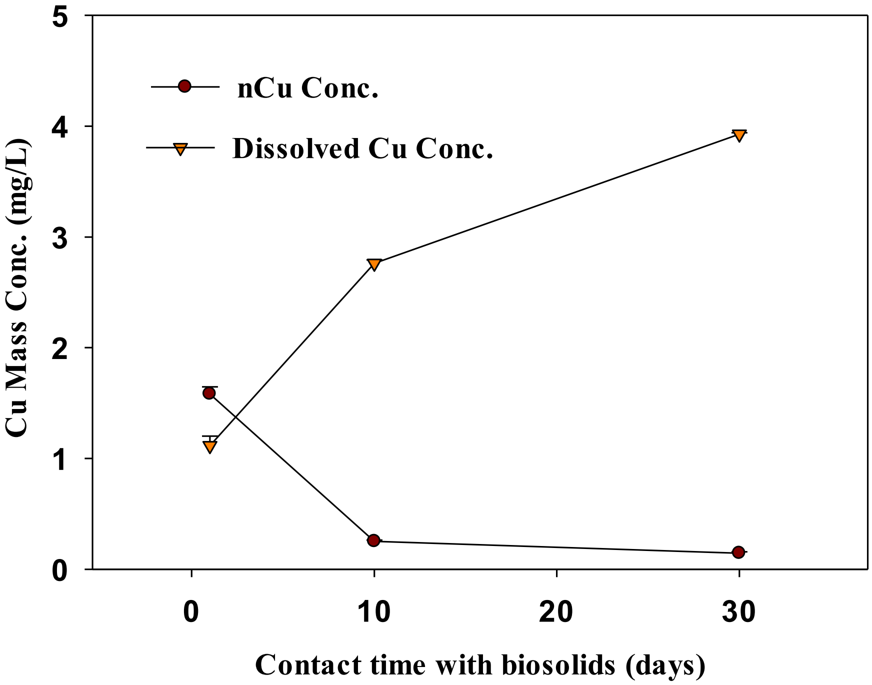

Figure S3-4 Stability of spiked nCu (2 mg/L of 50 nm) in biosolids using enzyme extraction techniques over the period of 30 days.

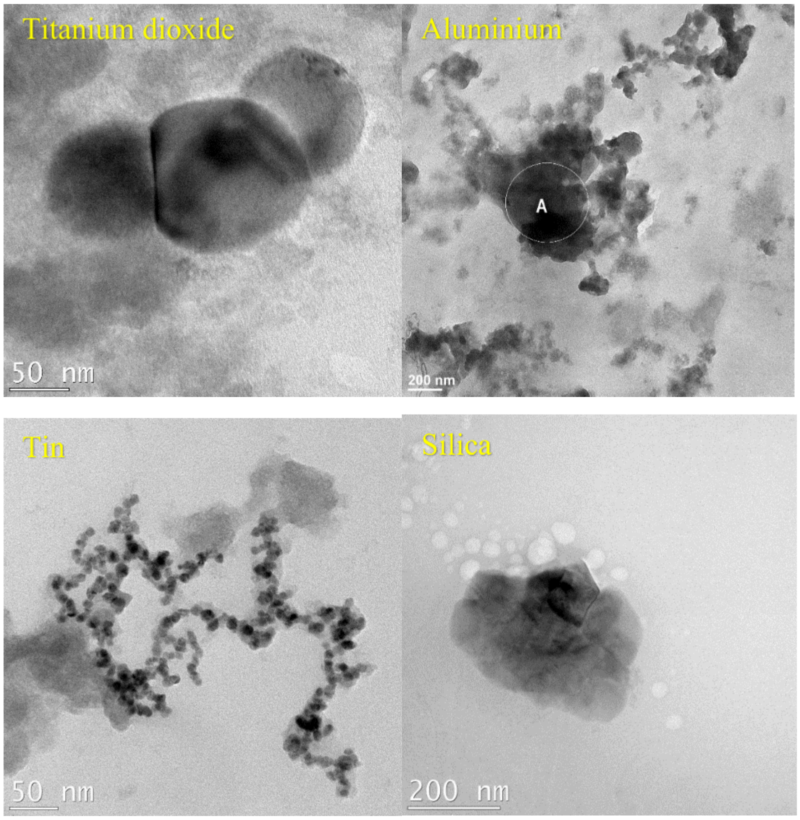

Figure S3-5– TEM images showing different NPs present biosolids samples. Elemental composition was determined by EDX analysis during TEM

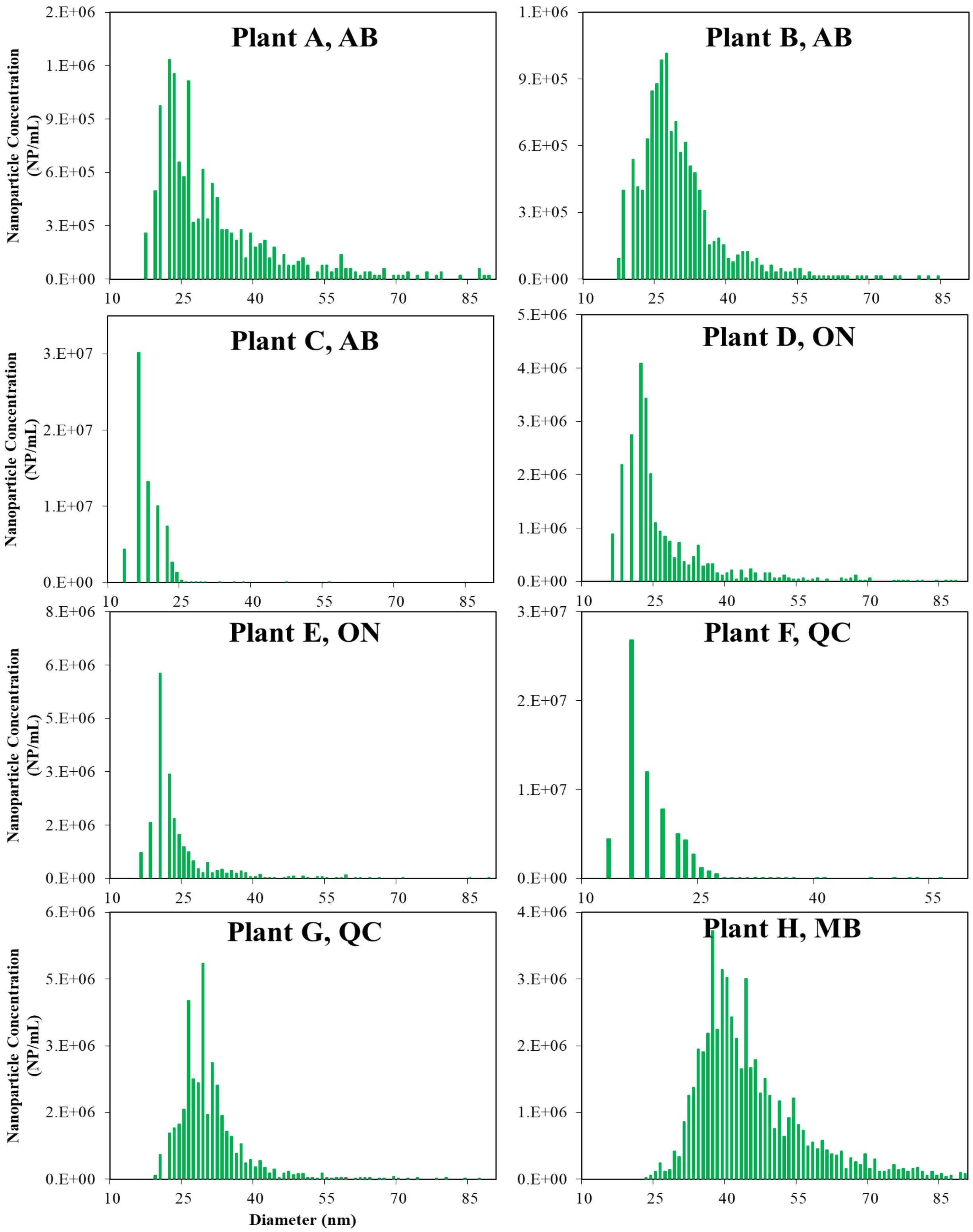

Figure S3-6 Particle size distribution of nAg in biosolids from different WWTPs across Canada.

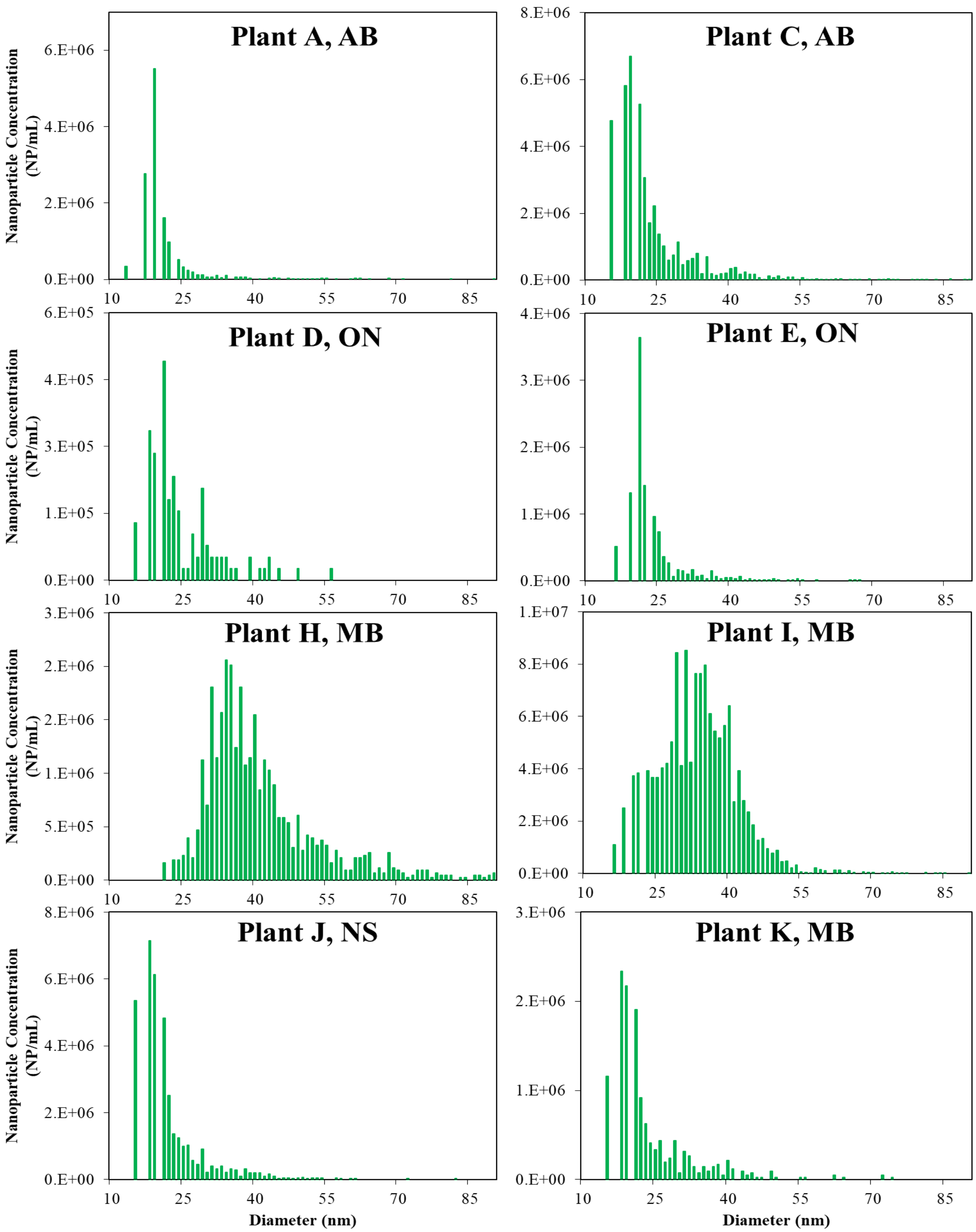

Figure S3-7 Particle size distribution of nAg in sludge from different WWTPs across Canada.

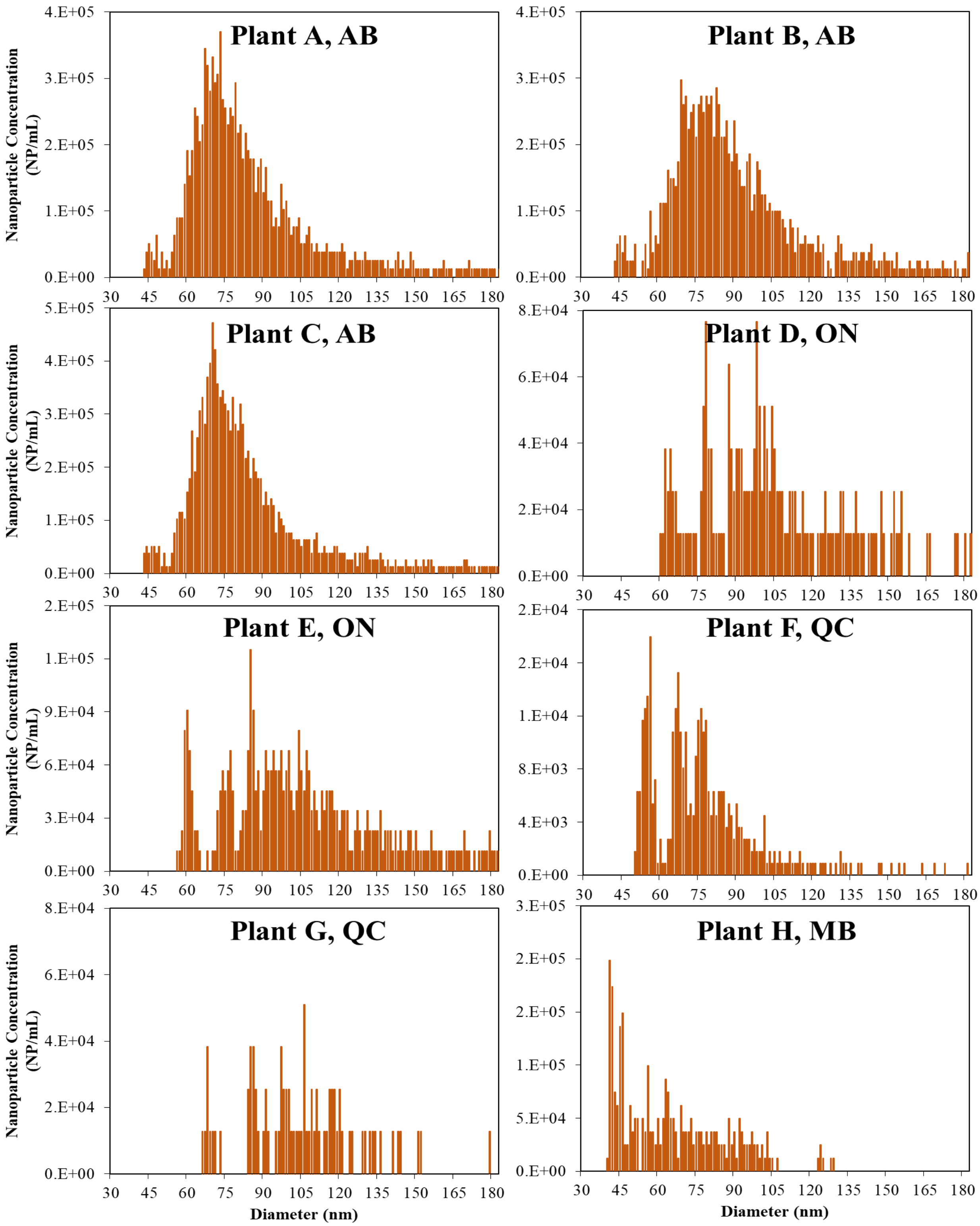

Figure S3-8 – Particle size distribution of nAg in biosolids from different WWTPs across Canada.

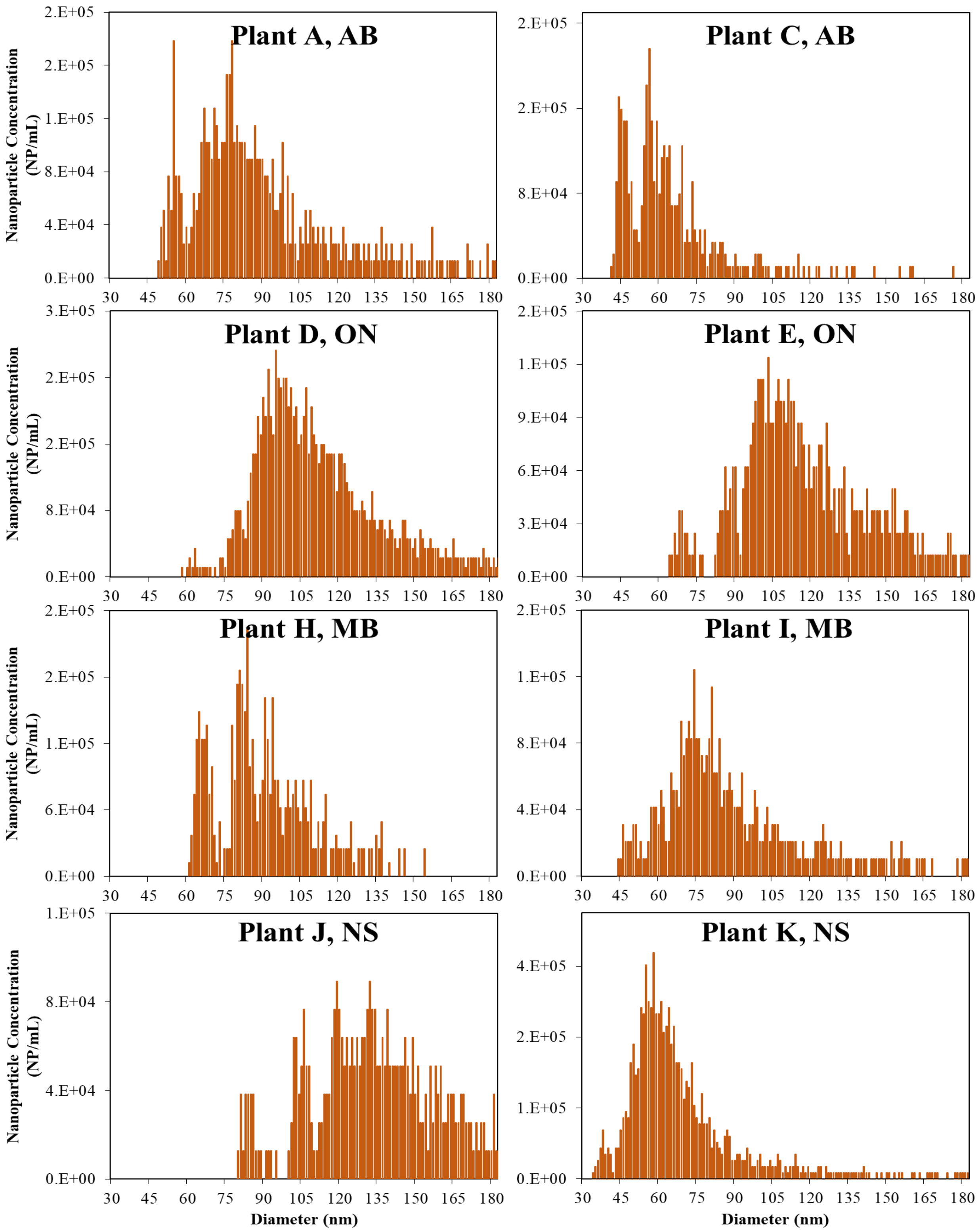

Figure S3-9 Particle size distribution of nAg in sludge from different WWTPs across Canada.

3.8. References

1. Boxall, A.B., et al., *Current and future predicted environmental exposure to engineered nanoparticles.* Central Science Laboratory, Department of the Environment and Rural Affairs, London, UK, 2007. **89**.
2. Keller, A., et al., *Release of engineered nanomaterials from personal care products throughout their life cycle.* Journal of Nanoparticle Research, 2014. **16**(7): p. 1-10.
3. Gottschalk, F. and B. Nowack, *The release of engineered nanomaterials to the environment.* Journal of Environmental Monitoring, 2011. **13**(5): p. 1145-1155.
4. Gottschalk, F., et al., *Modeled environmental concentrations of engineered nanomaterials (TiO2, ZnO, Ag, CNT, fullerenes) for different regions.* Environmental Science & Technology, 2009. **43**(24): p. 9216-9222.
5. Nanotechnology Product Database. *"Introduction to nanotechnology products"*. 2016 [cited 2017 September 4]; Available from: http://product.statnano.com/.
6. Westerhoff, P.K., M.A. Kiser, and K. Hristovski, *Nanomaterial removal and transformation during biological wastewater treatment.* Environmental Engineering Science, 2013. **30**(3): p. 109-117.
7. Navratilova, J., et al., *Detection of Engineered Copper Nanoparticles in Soil Using Single Particle ICP-MS.* International Journal of Environmental Research and Public Health, 2015. **12**(12): p. 15756-15768.
8. Keller, A.A. and A. Lazareva, *Predicted releases of engineered nanomaterials: From global to regional to local.* Environmental Science & Technology Letters, 2013. **1**(1): p. 65-70.
9. Keller, A.A., et al., *Global life cycle releases of engineered nanomaterials.* Journal of Nanoparticle Research, 2013. **15**(6): p. 1692.
10. Barton, L.E., et al., *Transformation of Pristine and Citrate-Functionalized CeO2 Nanoparticles in a Laboratory-Scale Activated Sludge Reactor.* Environmental Science & Technology, 2014. **48**(13): p. 7289-7296.
11. Kiser, M.A., et al., *Biosorption of nanoparticles to heterotrophic wastewater biomass.* Water Research, 2010. **44**(14): p. 4105-4114.
12. Kaegi, R., et al., *Fate and transformation of silver nanoparticles in urban wastewater systems.* Water Research, 2013. **47**(12): p. 3866-3877.
13. Kaegi, R., et al., *Behavior of Metallic Silver Nanoparticles in a Pilot Wastewater Treatment Plant.* Environmental Science & Technology, 2011. **45**(9): p. 3902-3908.
14. Sun, T.Y., et al., *Comprehensive probabilistic modelling of environmental emissions of engineered nanomaterials.* Environmental Pollution, 2014. **185**(Supplement C): p. 69-76.
15. Canadian Water and Wastewater Association (CWWA). *FAQ on Biosolids*. 2012 [cited 2017 January 4th]; Available from: http://www.cwwa.ca/faqbiosolids_e.asp.
16. Sarafadeen, A.O., et al., *Biosolids Land Application.* Pensee, 2014. **76**(9).
17. Liu, J.-f., et al., *Triton X-114 based cloud point extraction: a thermoreversible approach for separation/concentration and dispersion of nanomaterials in the aqueous phase.* Chemical Communications, 2009(12): p. 1514-1516.
18. Liu, J.-f., et al., *Cloud point extraction as an advantageous preconcentration approach for analysis of trace silver nanoparticles in environmental waters.* Analytical Chemistry, 2009. **81**(15): p. 6496-6502.

19. M. Furtado, L., M. Bundschuh, and C. D. Metcalfe, *Monitoring the Fate and Transformation of Silver Nanoparticles in Natural Waters*. Vol. 97. 2016.
20. Choi, S., et al., *A seasonal observation on the distribution of engineered nanoparticles in municipal wastewater treatment systems exemplified by TiO2 and ZnO.* Science of the Total Environment, 2018. **625**: p. 1321-1329.
21. Johnson, A.C., et al., *An assessment of the fate, behaviour and environmental risk associated with sunscreen TiO 2 nanoparticles in UK field scenarios.* Science of the Total Environment, 2011. **409**(13): p. 2503-2510.
22. Kiser, M., et al., *Titanium nanomaterial removal and release from wastewater treatment plants.* Environmental science & technology, 2009. **43**(17): p. 6757-6763.
23. Westerhoff, P., et al., *Occurrence and removal of titanium at full scale wastewater treatment plants: implications for TiO 2 nanomaterials.* Journal of Environmental Monitoring, 2011. **13**(5): p. 1195-1203.
24. Huang, Y., et al., *Fast Multielement Quantification of Nanoparticles in Wastewater and Sludge Using Single-Particle ICP-MS.* ACS ES&T Water, 2021. **1**(1): p. 205-213.
25. Hendren, C.O., et al., *Modeling nanomaterial fate in wastewater treatment: Monte Carlo simulation of silver nanoparticles (nano-Ag).* Science of The Total Environment, 2013. **449**: p. 418-425.
26. Gottschalk, F., T. Sun, and B. Nowack, *Environmental concentrations of engineered nanomaterials: Review of modeling and analytical studies.* Environmental Pollution, 2013. **181**: p. 287-300.
27. Shoults-Wilson, W.A., et al., *Evidence for avoidance of Ag nanoparticles by earthworms (Eisenia fetida).* Ecotoxicology, 2011. **20**(2): p. 385-396.
28. Neal, A.L., et al., *Can the soil bacterium Cupriavidus necator sense ZnO nanomaterials and aqueous Zn2+ differentially?* Nanotoxicology, 2012. **6**(4): p. 371-380.
29. Klaine, S.J., et al., *Nanomaterials in the environment: behavior, fate, bioavailability, and effects.* Environmental Toxicology and Chemistry, 2008. **27**(9): p. 1825-1851.
30. Ma, R., et al., *Fate of Zinc Oxide and Silver Nanoparticles in a Pilot Wastewater Treatment Plant and in Processed Biosolids.* Environmental Science & Technology, 2014. **48**(1): p. 104-112.
31. Iranpour, R., et al., *Regulations for biosolids land application in US and European Union.* Journal of Residuals Science & Technology, 2004. **1**(4): p. 209-22.
32. Holder, A.L., et al., *Nanomaterial disposal by incineration.* Environmental Science: Processes & Impacts, 2013. **15**(9): p. 1652-1664.
33. Förster, H., et al., *Separation of nanoparticles: Filtration and scavenging from waste incineration plants.* Waste Management, 2016. **52**: p. 346-352.
34. Wang, P., et al., *Silver Nanoparticles Entering Soils via the Wastewater–Sludge–Soil Pathway Pose Low Risk to Plants but Elevated Cl Concentrations Increase Ag Bioavailability.* Environmental Science & Technology, 2016. **50**(15): p. 8274-8281.
35. Jesmer, A.H., et al., *The toxicity of silver to soil organisms exposed to silver nanoparticles and silver nitrate in biosolids-amended field soil.* Environmental Toxicology and Chemistry: p. n/a-n/a.
36. Velicogna, J.R., et al., *Phytotoxicity of copper oxide nanoparticles in soil with and without biosolid amendment.* NanoImpact, 2020. **17**: p. 100196.

37. Azodi, M., Y. Sultan, and S. Ghoshal, *Dissolution Behavior of Silver Nanoparticles and Formation of Secondary Silver Nanoparticles in Municipal Wastewater by Single-Particle ICP-MS.* Environmental Science & Technology, 2016. **50**(24): p. 13318-13327.
38. Kent, R.D., J.G. Oser, and P.J. Vikesland, *Controlled Evaluation of Silver Nanoparticle Sulfidation in a Full-Scale Wastewater Treatment Plant.* Environmental Science & Technology, 2014. **48**(15): p. 8564-8572.
39. Barton, L.E., et al., *Heteroaggregation, transformation and fate of CeO2 nanoparticles in wastewater treatment.* Environmental Pollution, 2015. **203**: p. 122-129.
40. Conway, J.R., et al., *Aggregation, Dissolution, and Transformation of Copper Nanoparticles in Natural Waters.* Environmental Science & Technology, 2015. **49**(5): p. 2749-2756.
41. Montaño, M.D., et al., *Current status and future direction for examining engineered nanoparticles in natural systems.* Environmental Chemistry, 2014. **11**(4): p. 351-366.
42. Zhang, C., et al., *Governing factors affecting the impacts of silver nanoparticles on wastewater treatment.* Science of The Total Environment, 2016. **572**: p. 852-873.
43. Reidy, B., et al., *Mechanisms of Silver Nanoparticle Release, Transformation and Toxicity: A Critical Review of Current Knowledge and Recommendations for Future Studies and Applications.* Materials, 2013. **6**(6): p. 2295.
44. Hadrup, N., A.K. Sharma, and K. Loeschner, *Toxicity of silver ions, metallic silver, and silver nanoparticle materials after in vivo dermal and mucosal surface exposure: A review.* Regulatory Toxicology and Pharmacology, 2018. **98**: p. 257-267.
45. Ameh, T. and C.M. Sayes, *The potential exposure and hazards of copper nanoparticles: A review.* Environmental Toxicology and Pharmacology, 2019. **71**: p. 103220.
46. Malhotra, N., et al., *Review of copper and copper nanoparticle toxicity in fish.* Nanomaterials, 2020. **10**(6): p. 1126.
47. Shah, V., et al., *Response of soil bacterial community to metal nanoparticles in biosolids.* Journal of Hazardous Materials, 2014. **274**: p. 399-403.
48. Abdulsada, Z., et al., *Impact of anaerobically digested silver and copper oxide nanoparticles in biosolids on soil characteristics and bacterial community.* Chemosphere, 2021. **263**: p. 128173.
49. Velicogna, J.R., et al., *Soil invertebrate toxicity and bioaccumulation of nano copper oxide and copper sulphate in soils, with and without biosolids amendment.* Ecotoxicology and Environmental Safety, 2021. **217**: p. 112222.
50. Samarajeewa, A.D., et al., *Effect of silver nanoparticle contaminated biosolids on the soil microbial community.* NanoImpact, 2019. **14**: p. 100157.
51. Jesmer, A.H., et al., *The toxicity of silver to soil organisms exposed to silver nanoparticles and silver nitrate in biosolids-amended field soil.* Environmental toxicology and chemistry, 2017. **36**(10): p. 2756-2765.
52. Mitrano, D.M., et al., *Silver nanoparticle characterization using single particle ICP-MS (SP-ICP-MS) and asymmetrical flow field flow fractionation ICP-MS (AF4-ICP-MS).* Journal of Analytical Atomic Spectrometry, 2012. **27**(7): p. 1131-1142.
53. Lee, S., et al., *Nanoparticle size detection limits by single particle ICP-MS for 40 elements.* Environmental science & technology, 2014. **48**(17): p. 10291-10300.
54. Montaño, M., et al., *Improvements in the detection and characterization of engineered nanoparticles using spICP-MS with microsecond dwell times.* Environmental Science: Nano, 2014. **1**(4): p. 338-346.

55. Degueldre, C., P.Y. Favarger, and C. Bitea, *Zirconia colloid analysis by single particle inductively coupled plasma–mass spectrometry.* Analytica Chimica Acta, 2004. **518**(1): p. 137-142.
56. Degueldre, C., P.Y. Favarger, and S. Wold, *Gold colloid analysis by inductively coupled plasma-mass spectrometry in a single particle mode.* Analytica Chimica Acta, 2006. **555**(2): p. 263-268.
57. Pace, H.E., et al., *Determining Transport Efficiency for the Purpose of Counting and Sizing Nanoparticles via Single Particle Inductively Coupled Plasma Mass Spectrometry.* Analytical Chemistry, 2011. **83**(24): p. 9361-9369.
58. Degueldre, C. and P.Y. Favarger, *Thorium colloid analysis by single particle inductively coupled plasma-mass spectrometry.* Talanta, 2004. **62**(5): p. 1051-1054.
59. Montaño, M.D., et al., *Single Particle ICP-MS: Advances toward routine analysis of nanomaterials.* Analytical and Bioanalytical Chemistry, 2016. **408**(19): p. 5053-5074.
60. Montaño, M.D., et al., *Opportunities for examining the natural nanogeochemical environment using recent advances in nanoparticle analysis.* Journal of Analytical Atomic Spectrometry, 2019. **34**(9): p. 1768-1772.
61. Falås, P., et al., *Impact of solid retention time and nitrification capacity on the ability of activated sludge to remove pharmaceuticals.* Environmental Technology, 2012. **33**(8): p. 865-872.
62. Leu, S.-Y., L. Chan, and M.K. Stenstrom, *Toward Long Solids Retention Time of Activated Sludge Processes: Benefits in Energy Saving, Effluent Quality, and Stability.* Water Environment Research, 2012. **84**(1): p. 42-53.
63. Singh, B., Z. Szamosi, and Z. Siménfalvi, *State of the art on mixing in an anaerobic digester: A review.* Renewable Energy, 2019. **141**: p. 922-936.
64. Loeschner, K., et al., *Detection and characterization of silver nanoparticles in chicken meat by asymmetric flow field flow fractionation with detection by conventional or single particle ICP-MS.* Analytical and Bioanalytical Chemistry, 2013. **405**(25): p. 8185-8195.
65. Hineman, A. and C. Stephan, *Effect of dwell time on single particle inductively coupled plasma mass spectrometry data acquisition quality.* Journal of Analytical Atomic Spectrometry, 2014. **29**(7): p. 1252-1257.
66. Dan, Y., et al., *Single particle ICP-MS method development for the determination of plant uptake and accumulation of CeO2 nanoparticles.* Analytical and Bioanalytical Chemistry, 2016. **408**(19): p. 5157-5167.
67. Dan, Y., et al., *Characterization of Gold Nanoparticle Uptake by Tomato Plants Using Enzymatic Extraction Followed by Single-Particle Inductively Coupled Plasma–Mass Spectrometry Analysis.* Environmental Science & Technology, 2015. **49**(5): p. 3007-3014.
68. Tiede, K., et al., *Review of the Risks Posed to Drinking Water by Man-Made Nanoparticels*. 2012, FERA, UK.
69. Schlich, K., et al., *Hazard assessment of a silver nanoparticle in soil applied via sewage sludge.* Environmental Sciences Europe, 2013. **25**(1): p. 17.
70. Caetano, A.L., et al., *Copper toxicity in a natural reference soil: ecotoxicological data for the derivation of preliminary soil screening values.* Ecotoxicology, 2016. **25**(1): p. 163-177.
71. Lützhøft, H.-C.H., et al., *Environmental Effects of Engineered Nanomaterials: Estimations of Predicted No-Effect Concentrations (PNECs).* 2015.

72. Yang, Y., et al., *Metal and nanoparticle occurrence in biosolid-amended soils.* Science of The Total Environment, 2014. **485–486**: p. 441-449.
73. Westerhoff, P., et al., *Characterization, Recovery Opportunities, and Valuation of Metals in Municipal Sludges from U.S. Wastewater Treatment Plants Nationwide.* Environmental Science & Technology, 2015. **49**(16): p. 9479-9488.
74. Canadian Council of Ministers of the Environment (CCME), *Guidance document for the beneficial use of municipal biosolids, municipal sludge and treated septage*. 2012.
75. Bureau de normalisation du Québec (BNQ), *Soil Amendments- Alkaline or Dried Municipal Biosolids*. 2009.
76. United States Environmental Protection Agency (US-EPA), *A Plain English Guide to the EPA Part 503 Biosolids Rule*, in *Land Applications of Biosolids*, U.S.E.P. Agency, Editor. 1994: Washington D. C.
77. Wang, Z., et al., *Biological and Environmental Transformations of Copper-Based Nanomaterials.* ACS Nano, 2013. **7**(10): p. 8715-8727.
78. Li, X., J.J. Lenhart, and H.W. Walker, *Aggregation kinetics and dissolution of coated silver nanoparticles.* Langmuir, 2011. **28**(2): p. 1095-1104.
79. Ma, R., et al., *Size-Controlled Dissolution of Organic-Coated Silver Nanoparticles.* Environmental Science & Technology, 2012. **46**(2): p. 752-759.
80. Levard, C., et al., *Environmental Transformations of Silver Nanoparticles: Impact on Stability and Toxicity.* Environmental Science & Technology, 2012. **46**(13): p. 6900-6914.
81. Liu, J., et al., *Controlled Release of Biologically Active Silver from Nanosilver Surfaces.* ACS Nano, 2010. **4**(11): p. 6903-6913.
82. Kim, B., et al., *Discovery and Characterization of Silver Sulfide Nanoparticles in Final Sewage Sludge Products.* Environmental Science & Technology, 2010. **44**(19): p. 7509-7514.
83. Georgantzopoulou, A., et al., *Ecotoxicological effects of transformed silver and titanium dioxide nanoparticles in the effluent from a lab-scale wastewater treatment system.* Environmental science & technology, 2018. **52**(16): p. 9431-9441.
84. Levard, C., et al., *Sulfidation of Silver Nanoparticles: Natural Antidote to Their Toxicity.* Environmental Science & Technology, 2013. **47**(23): p. 13440-13448.
85. Pradas del Real, A.E., et al., *Fate of Ag-NPs in Sewage Sludge after Application on Agricultural Soils.* Environmental Science & Technology, 2016. **50**(4): p. 1759-1768.
86. Colman, B.P., et al., *Low Concentrations of Silver Nanoparticles in Biosolids Cause Adverse Ecosystem Responses under Realistic Field Scenario.* PLoS ONE, 2013. **8**(2): p. e57189.
87. Jose Ruben, M., et al., *The bactericidal effect of silver nanoparticles.* Nanotechnology, 2005. **16**(10): p. 2346.
88. Kraas, M., et al., *Long-term effects of sulfidized silver nanoparticles in sewage sludge on soil microflora.* Environmental toxicology and chemistry, 2017. **36**(12): p. 3305-3313.
89. Li, L., et al., *Sulfidation as a Natural Antidote to Metallic Nanoparticles Is Overestimated: CuO Sulfidation Yields CuS Nanoparticles with Increased Toxicity in Medaka (Oryzias latipes) Embryos.* Environmental Science & Technology, 2015. **49**(4): p. 2486-2495.
90. Liu, J., K.G. Pennell, and R.H. Hurt, *Kinetics and Mechanisms of Nanosilver Oxysulfidation.* Environmental Science & Technology, 2011. **45**(17): p. 7345-7353.

Connecting text between Chapter 3 and Chapter 4

The widespread use of NPs in several fields increases the probability that they will end up in the environment. A significant fraction of the released NPs from various products end in the wastewater treatment plant. There is a consensus in the literature that more than 70 to 99% of the NP entering the municipal WWTP settle out with sludge. A minor fraction of the NPs entering the municipal WWTP is released with WW effluent to water bodies, however, given the large volumes of WW effluents; the release with effluents still constitutes a significant flux. The reported data on NP size and particle concentration data (including nAg or nCu) in the WW effluent is minimal. In this study, we detect and characterize nAg and nCu using spICP-MS in WW effluent samples by developing methods to concentrate in several Canadian municipal WWTPs.

CHAPTER 4 CONCENTRATION OF SILVER AND COPPER NANOPARTICLES IN WW EFFLUENT FROM MUNICIPAL WASTEWATER TREATMENT PLANTS

Abstract

The widespread use of nanoparticles in several fields increases the probability that they will end up in the environment. A significant fraction of the released NPs from various products end in the wastewater treatment plant. There is a consensus in the literature that more than 70-99% of the NP entering the municipal WWTP settle out with sludge. A minor fraction of the NPs entering the municipal WWTP is released with WW effluent to water bodies, however, given the large volumes of WW effluents; the release with effluents still constitutes a significant flux. This study focuses on the detection and the characterization of nAg and nCu using spICP-MS in wastewater (WW) effluent samples, by using sequential cycles of centrifugal ultrafiltration (CUF) to concentrate NPs into a smaller volume to improve detectability. Sequential cycles of CUF was found to be more efficient than cloud point extraction (CPE) using surfactants, an alternative approach that has been used to concentrate NPs from aqueous samples. WW effluent from 9 different Canadian municipal WWTPs were analysed for nAg and nCu using spICP-MS. Concentration of nCu varied from 0.1 ng/L to 12 ng/L depending on the WWTP effluent with size varying from 34.6 ± 1.3 to 68.0 ± 0.3 nm. Concentration of nAg detected ranged from 0.08 to 0.43 ng/L with mean size 19.3 ± 0.1 to 34.7 ± 7.2 nm lower than previously reported studies. These measured concentrations of NPs in WW effluent are 10^3 to 10^7 folds lower than in WW biosolids. Even though these NP concentration are below PNEC (nAg - 12 ng/L and nCuO -340 ng/L) in freshwater, constant loading can lead to bioaccumulation of NPs in the organisms by constant exposure to WW effluent. The data reported here can be used for future modelling, exposure assessment and toxicology studies.

4.1. Introduction

Engineered nanoparticles (ENPs) are being used in substantial quantities in many commercial products for their novel properties. The rapid growth of nanotechnology leads to unavoidable release of ENPs into the environment after their life. Studies have shown release of ENPs from ENP-enabled products into the environment through various pathways with increasing concerns of NPs to the environmental receptors [1-5]. There is a need to improve the knowledge on the fate and concentration of ENPs in the environment. One of the major routes of release of ENPs to the environment is through municipal wastewater treatment plant (WWTP) effluents discharged into receiving water bodies. In the literature, there is a consensus that more than 70-99% of the NPs entering the WWTP settle out with sludge [6-8]. A minor fraction of the NPs entering the WWTP is released with WW effluent to water bodies, however, given the large volumes of WW effluents; the release with effluents still constitutes a significant flux. A material flow analysis reported that of all the metal NPs used in various products and processes, between 17 and 34% reach the municipal WWTPs [9], of which, 44% are nAg and 18% are nCu [12].

The detected or estimated concentrations of NPs in environmental aquatic samples are usually at ng/L levels. Estimates have been provided from model predictions based on approximate worldwide or regional NP production and consumption volumes, and materials flow analyses from the products to different environmental compartments. Predicted concentrations of $nTiO_2$ in WW effluents varied from 2 to 7 μg/L [2, 3] to 1200 to 1300 μg/L [9] in others studies. nAg concentrations measured in the WW effluents varied between studies: from 1 to 10 ng/L using CPE and measurement with atomic absorption spectroscopy (AAS) [10], to 100 to 200 ng/L using direct spICP-MS analyses [11]. Hadioui et al. (2015) observed nZn of 160 to 210 nm diameter and concentrations of approximately 50 ng/L using spICP-MS [12]. In that study, the detection limits of nZn were improved by removing dissolved metals from the samples by elution through an in-line ion exchange column. Total Ti was analysed in WW effluent by digestion using ammonium persulfate and analysis using ICP-MS for indirect concentration of $nTiO_2$, on the assumption that all TiO_2 are in nanoparticulate form and gave concentrations between 1.6 to 1.8 μg/L [13]. A study on the detection of nAg in a river, immediately downstream of the WW effluent discharge outfall, reported concentrations of 2.0 to 8.6 ng/L compared to 0.9 to 2.3 ng/L upstream of the plant [10]. Another study calculated the concentration of nAg in filtered wastewater influent using field flow fractionation and standard ICP-MS of 1.9 µg/L and 9.3 nm size [14]. A recent study using fast multielement spICP-MS detected 13 metals for size and concentration in various compartments in WWTP in south California, USA [15]. This study used centrifugation as a method to separate solids from complex samples and measured for the metal concentration and particle size distribution in WW effluent with nAg concentration of 1.8 ± 0.01 ng/L with mean size of 13.4 ± 0.1 nm and nCu concentration of 25.6 ± 1.7 ng/L with mean size of 94.3 ± 0.2 nm. Concentrations of other NPs (Cd, Co, Al, Au, Ni, Zn, Ce, Mn, Ti, Fe and Mg) in the waste effluent were also reported in the range of 0.24 ± 0.07 to 70229 ± 4893 ng/g and the sizes varied between 13.4 ± 0.1 and 1734.2 ± 23.4 nm. Another study detected fullerenes using LC-MS at concentrations ranging from 1 to 70,000 ng/L in WW effluent samples from different treatment plants [5]. The LC-MS analysis was performed on concentrated toluene extracts of the retentate of effluent samples, passed through a 0.45 µm filter. The filters were oven dried and ultra sonicated prior to toluene extraction.

WW effluents provide a considerably simpler matrix, in terms of levels of backgrounds colloids and solids for analyses of NPs, compared to biosolids. However, the high extent of attachment and entrapment of NPs in biosolids results in low concentrations of NPs in effluents, posing a different challenge. Concentrating the NPs present in the WW effluent using different techniques and optimizing the process for detecting the NPs is thus required to determine how much NPs are released from municipal WWTPs at the point of release. A few studies have reported metal NP concentrations in municipal WWTP effluents with the assumption that the total metal present in the filtrate passing through a 0.45 µm filter is nanoparticulate. The total metal content in the filtrate is typically characterized by AAS or inductively coupled plasma optical emission spectroscopy (ICP-OES) or ICP-MS after acid digestion. Using this approach, TiO_2 in WW effluent was detected at concentrations of 1 to 100 µg/L [16-18] and nAg in WW effluent at 4 to 10 ng/L [19]. However, this NP concentration characterization technique has significant shortcomings because it does not consider the loss of the NPs on the filters, and accounts for dissolved ions (or complexed to dissolved organic matter) as nanoparticulate. In addition, it does not provide particle size information.

Despite the concentration of the NPs in WW effluent being in the range of ng/L, the significant volume of the WW effluent released into the water sources could pose risks to the environment from discharge of ENPs. Although prior studies have confirmed the presence of nanoparticles in WW effluents, they have emphasized on the development of detection methods rather than a robust assessment of their concentrations in effluents from different municipal WWTPs. Therefore, there is scarcity of information of NP size and concentration data. However, the concentration of the NPs analyzed in filtered wastewater effluent (WW effluent) are expected to be lower due to dilution in the receiving water body and therefore, there is a need to concentrate these environmental samples to enable detection and quantification, even by sensitive analytical techniques.

Cloud point extraction (CPE) is a technique employed to concentrate NPs in environmental water samples [20, 21]. CPE is an extraction method relying on the micelle-analyte (micelle-NP) interactions. The temperature above which micelles formed are immiscible in water is called the lowest critical solution temperature (LCST). CPE involves three fundamental steps: (1) the analytes (NPs) present in the original matrix associate within the micellar aggregates; (2) temperature is increased to above the LSCT, which causes separation of the coacervative phase from the bulk aqueous phase; and (3) the phase separation, such as centrifugation and decanting [22]. The limit of detection of nAg spiked into wastewater samples concentrated by CPE was found to be 12.9 ng/L for influent water and 0.7 ng/L for effluent wastewater measured using graphite furnace atomic absorption spectroscopy [10, 20]. Liu et al. (2009) reported that the presence of humic acids (0−30 mg/L dissolved organic carbon) had no effect on the extraction of nAg using CPE and there was negligible interference from Ag^+ [21]. nCuO spiked at concentration of 20 to 100 µg/L in wastewater were extracted by CPE with recovery efficiency ranging from 80.4% to 108.2 %. Relatively lower recovery of NPs (59.2 to 69.4%) were observed for samples spiked with a lower concentration of 5µg/L [23]. In general, it is important to have effective techniques to concentrate and measure the NPs in complex environmental samples.

nAg concentrations of 1 to 75 ng/L [2, 3, 24], 10 to 300 ng/L [25] and 70 µg/L [9] were predicted in WW effluent. In this study, the concentration of nAg as well as its size distributions in WWTP effluents was measured by inductively coupled plasma mass spectrometer (ICP-MS) in single particle mode. The concentrations of NPs in WW effluents are important for assessing the effects of long term exposure to aquatic organisms, and for risk assessments as well [26, 27]. In addition, this data can be used for the verification of model predictions. Substantial progress has been made recently towards developing comprehensive NP release and fate models, but there is a lack of measurements of NP concentrations in environmental samples to verify model predictions [28-30]. Even if the concentration of NPs in effluents have been found to be low, it still constitutes a substantial mass flux given the large volumes of WW effluents released to receiving water bodies. NPs in receiving water bodies can be bioaccumulated in the food chain and/or accumulated in local environmental compartments such as sediment beds in the proximity of effluent outfalls.

In this study, we characterized the mass and number concentration of nAg and nCu along with their size distributions in effluents from nine urban municipal WWTPs across Canada. There are only few studies which reported both the size and concentration of NPs in the WW effluents [10, 15]. Given the low concentrations of NPs in the effluents, sample preconcentration was required prior to their analysis by spICP-MS. The efficiency of NP concentration by cloud point extraction (CPE) and centrifugal ultrafiltration (CUF) was assessed, and a protocol for sample concentration by CUF was developed. The optimized concentration technique was used to quantify the size and concentration of nAg and nCu in unspiked WW effluents.

4.2. Materials and methods

4.2.1. Wastewater effluent samples

WW effluent were provided by Environment and Climate Change Canada from nine different municipal WWTPs across Canada. One sample was collected in Quebec (QC), and two each (2) were collected from the following provinces: Alberta (AB), Ontario (ON), Manitoba (MB) and Nova Scotia (NS). The samples collected from WWTPs served a population varying from 50,000 to 1.29 million people. Composited samples from a 3-day sampling period from each municipal WWTP were obtained to minimized bias related to heterogeneity in the samples and possible time-based fluctuations in NP concentration. Upon collection, the samples were frozen at a temperature of 80°C until analysis. Freezing and storage of aqueous suspension samples had no impact on the measured nAg concentrations (Table S4-4).

4.2.2. Concentration of spiked nAg using different extraction protocols

Two methods of concentrating NPs in WW effluent were considered in this study: CPE and CUF. CPE was chosen, as it has been reported by several studies as an efficient method NPs in environmentally relevant samples[10, 31, 32]. CUF is previously used to separate NPs from dissolved ions, to indirectly measure concentration of NPs [33-36]. In this study, NPs are directly measured after separation, to assess if it is viable option to concentrate and measure NPs in environmentally relevant samples. The efficiency of a single extraction by both the methods were evaluated by spiking 50 ng/L of 80 nm polyvinylpyrrolidone (PVP)-coated nAg (NanoComposix) in 225 mL of three different WW effluents. The extraction efficiencies of both methods were calculated for one cycle. Optimized method was used for extraction of nCu and nAg from WW effluents from across Canada.

4.2.3. Centrifugal Ultrafiltration (CUF)

Ultrafiltration filters separate particles based on their size. It is used for pre-concentration, fractionation and purification of NPs[28]. In this study, Amicon® Ultra-filter tubes (15 mL) with a filter MWCO of 3 kDa (1-3 nm pore size) was used to separate NPs from the effluent samples

The WW effluents were concentrated in the ultrafilter by centrifugation at 4500g for 30 min. After centrifugation, the ultra-filter was added with deionized (DI) water and sonicated for 30 minutes with DI water to resuspend the NPs from the filter. The retentate was analyzed using spICP-MS for presence of NPs.

4.2.4. Cloud point extraction (CPE)

The NPs in WW effluent were concentrated using procedure from previous reported studies [10, 20, 21, 31, 32]. 40 mL of WW effluent were mixed with 1.0 mL of saturated ethylenediaminetetraacetic acid disodium salt (EDTA) solution, 400 µL of 1 mol/L sodium acetate, 100 µL of 1.25 mol/L acetic acid, and 1 mL of 10% (w/w) TX-114 (LCST = 23 ºC) in a 50 mL tapered polypropylene tubes. The samples were then incubated at 40 ºC for 30 min for mixing of TX-114 with WW effluent. The mixture was then centrifuged at 4 ºC for 10 min at 4500g to enhance phase separation below LCST and was placed on ice to increase the viscosity of the surfactant rich phase. The aqueous supernatant was removed by decanting. The remaining surfactant rich phase is collected and diluted to make the volume up to 10 mL. The concentrated samples were measured using spICP-MS.

4.2.5. Extraction of NPs from unspiked wastewater using CUF

Extraction using CUF method (better extraction efficiency as discussed below in Section **1.4.1** - Method validation: Recovery of spiked nAg using CPE and CUF) was performed for spiked WW effluents to concentrate NPs on multiple sequential CUF's. 225 mL total sample, 15 ml aliquots sequentially concentrated in a CUF. Efficiency of concentration of a 225 mL WW effluent by sequential CUF of sub-samples (15 mL using 15 CUF cycles) was verified by spiking 50 ng/L of 80 nm PVP-coated nAg in DI water and WW effluent (Plant A, AB; Plant D, ON, Plant F, QC and Plant H, MB). Multiple sequential CUF were performed in 225 mL of unspiked WW effluents to increase NP concentration above the limit of detection of spICP-MS.

4.3. Instrumentation and Characterization

4.3.1. spICP-MS analysis

The NP characterization process was performed using PerkinElmer NexION 300x ICP-MS in a single particle mode supported by Syngistix software (ver 1.1). The outputs of this analysis are: NP size distribution, NP concentration and dissolved metal concentration in the samples. An integration dwell time of 100 µs with a sampling time of 100 s were set to measure the samples. Standard reference nAu (NIST) of 60 nm-diameter, or ultra uniform nAu (nanocomposix) of 30 or 55 nm particle diameter, at a concentration of 10^5 particles/mL, were diluted in DI water/ WW effluent from the reactors to find the transport efficiency (4.0 to 9.5%) for the spICP-MS. Table S4-3 shows other main instrumental settings and conditions applied.

The calibration for silver and copper, from a concentration range of 50 ng/L to 2 µg/L, was prepared using standard dissolved silver ions and copper ions of 1000 mg/L (SCP Science PlasmaCAL), respectively. The biosolid aqueous extracts were diluted accordingly, and measured in triplicates using spICP-MS. The spiked nAg, background controls and stock solution, were measured along with the biosolid aqueous extract.

4.3.2. Transmission Electron Microscopy (TEM)

The TEM analysis was carried out using a FEI Tecnai G2 F20 S/TEM equipped with Gatan Ultrascan 4000 4k × 4k CCD Camera System (Model 895). An EDAX Octane T Ultra W/Apollo

XLT2 SDD system was used for energy dispersive X-ray spectroscopy (EDS) measurements. A volume of 10 µL of the sample concentrate was deposited on the Cu/Au TEM grids (Electron Microscopy Sciences, Carbon film 200 mesh Cu/Au grids), which were then air-dried. In order to concentrate the nanoparticles, multiple drops were applied on the samples. Prior to their TEM and EDS analyses, the samples were rinsed with DI water to wash background debris and left to air-dry again.

4.4. Results and discussion

4.4.1. Method validation: Recovery of spiked nAg using CPE and CUF

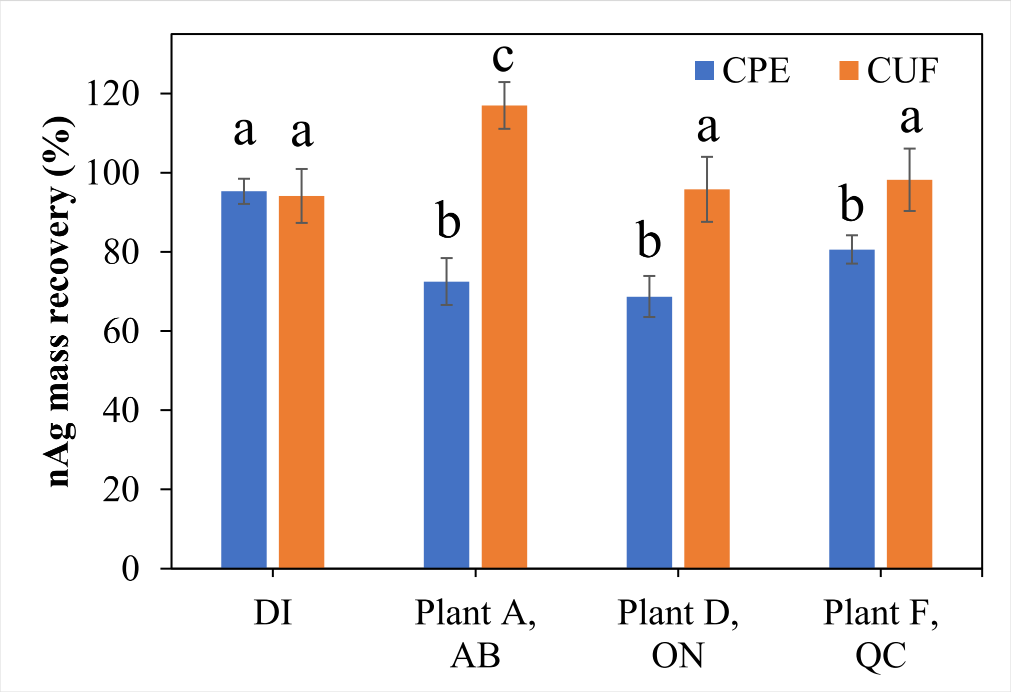

Figure 4-1 Mass recovery of spiked nAg in DI water and 3 different WW effluent using NP extraction techniques CPE and CUF. Error bars represent standard deviation of the 3 replicate samples. Lower case letters (a, b and c) indicate differences between treatments ($p < 0.05$, one-way ANOVA)

50 ng/L nAg spiked in DI water gave similar results for both CPE and CUF with extraction efficiency of 95.3 ± 3.2% and 94.1 ± 6.8%, respectively (not statistically different $p>0.05$). The percentages represent the mass of spiked NPs recovered as measured by sp ICP-MS. Any dissolved

Ag is not accounted for in this assessment. In addition, as the concentration of spiked nAg was close to the limit of detection of ICP-MS, acid digestion of concentrated sample (to compare total metal Ag to recovered nAg) was not possible, since the dilution required to measure acid digested samples (samples with acid percentage close to 1%) in ICP-MS would lead to values below detection limit of 20 ng/L for dissolved Ag. CUF had a similar recovery in DI water (94.1 ± 6.8%) and WW effluent (except for Plant A – stastically different from all CUF measurements) for spiked nAg in WW effluents from plant A, plant D, and plant F with values of 116.9 ± 5.9%, 95.8 ± 8.2%, and 98.2 ± 7.9%, respectively. No aggregation of NPs were observed between stock WW effluent spiked with nAg (69.7 ± 2.6 nm) and recovered nAg using CUF (71.3 ± 1.3 nm) as the particle size distributionsremained unchanged. In contrast, a lower extraction efficiency was observed for CPE in WW effluent compared to CPE in DI water (95.3 ± 3.2%) with 72.5 ± 5.9% in plant A,, 68.7 ± 5.1% in plant D, and 80.8 ± 3.6% in plant F (Figure 4-1). The solution chemistry influences the extraction efficiency in CPE [37] and can be attributed to the complex matrix of WW effluent and its impact on micelle formation [37].

Acid digestion of WW effluents for detection Ag and Cu did not yield results as strong acids used for digestion needs dilution of samples before measurement, leading to concentration below detection limit. In addition, No Ag and Cu was detected in standard mode with acidification of WW effluents (1 to 2% nitric acid) samples suggesting concentration below detection limit.

To concentrate NPs in a WW effluent where the concentration of NPs are below detection limit, multiple cycles of extraction might be required. Multiple cycles of CPE were not performed in WW effluent as the WW composition is not uniform across sample, and thus require optimization of TX-114, EDTA and sodium acetate salts to remove the interferences; leading lower recovery in a single cycle. Additionally, we observed that each cycle of CPE concentration leads to loss of surfactant TX-114 in WW effluent as supernatant is removed, which might be also the reason for lower recovery. These factors made CPE less reliable for our study.

CUF also has somebacks but they turned to be less severe than CPE. CUF after 15 cycles of concentration gave a lower recovery (63.3%) compared to the first cycle (103.6%) as shown in Table 4-1. Studies has shown that approximately 5% dissolution of nAg occurs happens within 12 hours in DI water [34, 38]. Dissolution is a small factor in this study, time period is not significant enough to cause such low recoveries. Furthermore, nAg spiked in WW effluents would be coated with natural organic matter (NOM), which lowers dissolution of nAg. Therefore, these lower recoveries were attributed to attachment of NPs to the filter which were not able to be dislodged by the sonication due to strong attachmen due to multiple cycles. Previous studies have shown NPs having strong attachment to filter membrane regnerated cellulose [39-41]. No NPs were observed in the filtrate WW effluent confirming the attachment to the filter.

Table 4-1 Spiked nAg recovery after 15 cycles using CUF in DI water and four different municipal WWTPs.

WWTPs	**Spiked 50 ng/L nAg recovery after 15 cycles (%)**
DI water	71.2 ± 2.9
Plant A, AB	73.2 ± 7.2
Plant D, ON	58.6 ± 9.5
Plant F, QC	62.3 ± 7.6
Plant H, MB	59.3 ± 5.4

15 sequential concentration cycles of CUF concentration was employed to concentrate both nAg and nCu particles in WW effluent from 9 different Canadian municipal WWTPs. WW effluent were measured raw showed no nAg or nCu signals, whereas, 15 cycle CUF showed the ability to concentrate NPs in WW effluent samples. Figure 4-2 represents plant H having nAg and nCu concentrated from using the 15 cycles of CUF. Similar results of all other plants are shown in supplementary information in Figure S4-1 and Figure S4-2. nAg and nCu concentration, mean size and particle size distribution were different in each plant measured.

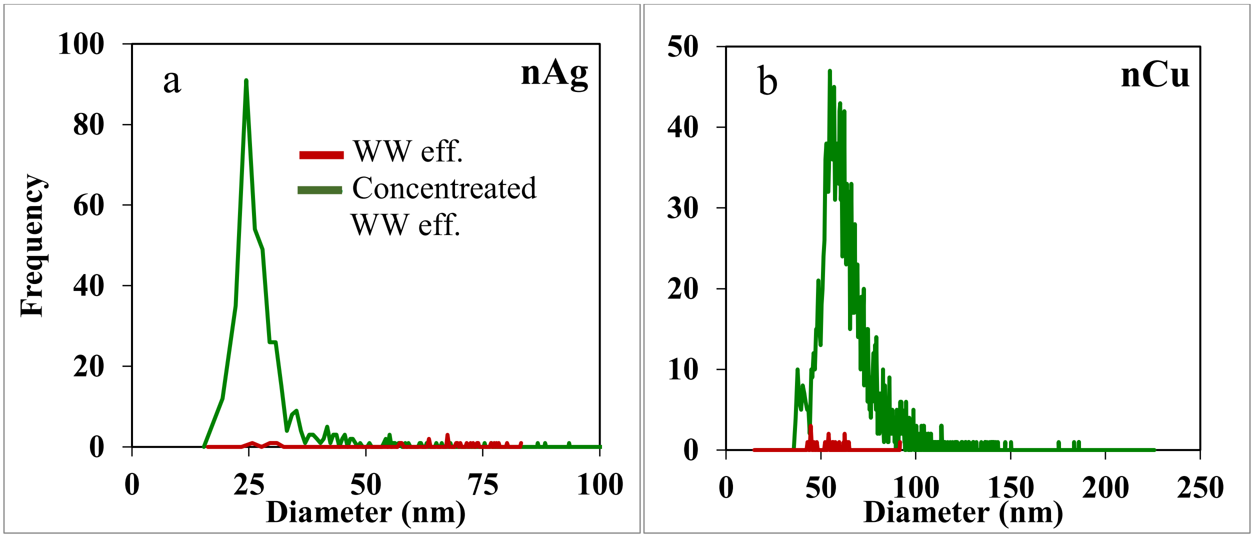

Figure 4-2 Particle size distribution of NPs before and after concentration using 15 cycles using CUF in WW effluent from Plant H, MB measured using spICP-MS a) nAg and b) nCu

4.4.2. Nanoparticle concentration in WW effluent in Canada

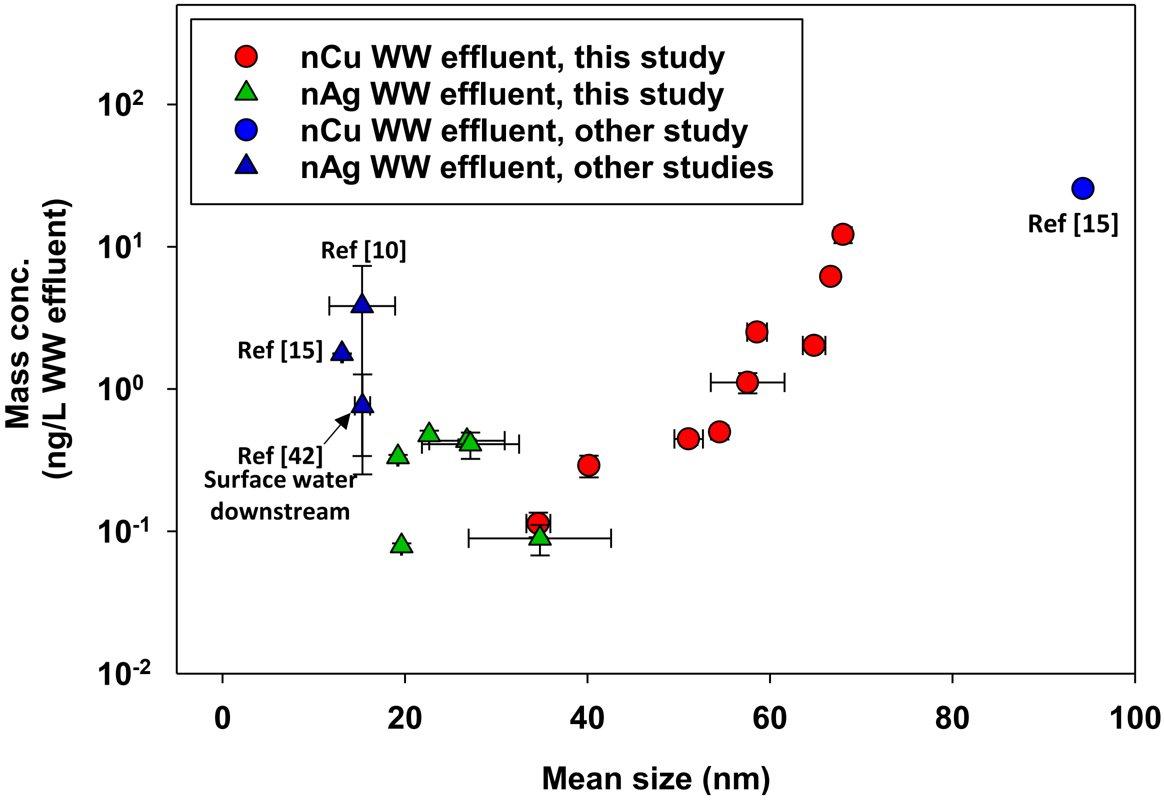

Figure 4-3 Mean size and mass concentration of nAg and nCu in WW effluent aqueous extract using of CUF from municipal WWTP across Canada; blue color represents previously measured data for mean size and mass concentration nAg and nCu in WW effluents. nAg was not detected in Plant D, & E, ON and Plant F, QC and thus, there are fewer data points. Previously reported data with sizes are marked in blue [10, 15, 42].

4.4.2.1. *nAg and nCu in unspiked WW effluent*

Concentration of nAg detected ranged from 0.08 to 0.43 ng/L with mean size 19.3 ± 2.1 to 34.7 ± 7.2 nm (Table S4-1). The size of nAg are similar to the silver sulphide NPs formed from spiked pristine nAg in WW effluent in presence of sulphides and thiols or similar moieties [34]. nAg was not detected in Plant D, & E, ON and Plant F, QC. The error values represent the standard deviation (both triplicates of sample and measurement) mean size of the particle size distribution. The measured nCu mass concentrations were higher in WW effluent compared to nAg. Concentration of nCu varied from 0.1 ng/L to 12 ng/L depending on the municipal WWTP effluent with size varying from 34.6 ± 9.8 to 68.0 ± 14.3 nm (**Table S4-2**). A trend of large nCu particles having high concentration in the WW effluent, whereas, smaller size nCu measured were present at much lower concentrations, can be observed. This is likely because the smaller sized nCu particles were close to limit of size detection of instrument (~30 nm), thereby, possibly having some part of the particle size distribution incorrectly counted as dissolved concentrations.

Model predictions of the concentration of nAg in the WW effluent ranged from 10 ng/L to 100 μg/L [2, 3, 19, 24, 35, 43-45] and nCu ranged from 0.01 to 100 ng/L [46, 47]. The concentration of nCu measured is in the range of previously predicted concentrations, whereas nAg measured (below 1 ng/L) were lower than previously reported studies, showing the need to extract and preconcentrate the NPs before measurement [20, 21, 32, 42, 48]. Being able to reach a low detection limit is crucial, although the lowest detection limit for nAg exists today is ~0.7 ng/L by electro thermal AAS [49-52] and nCu is ~20 ng/L [53, 54], its size distribution is not known at such low concentration [49]. In our study, mass detection limits of close to 2 ng/L for nAg and 5 ng/L for nCu were observed.

A recent study has reported data on the concentration of nAg 1.8 ± 0.01 ng/L with mean size of 13.4 ± 0.1 nm in WW effluents in south California, USA [15]. These measured concentrations were 4 times higher than the peak value reported in our study. Another study had approximately 8 folds higher concentration of nAg in two WWTPs in Germany with average size of 15.3 ± 3.6 nm and average concentrations (calculated average of two WWTPs from different seasons varying from 0.7 to 11 ng/L) of 3.8 ± 3.5 ng/L. Our measured concentrations are similar to the lowest reported effluent concentration of 0.7 ng/L in those two WWTPs in Germany. Whereas, concentrations of nAg (0.3 to 2.5 ng/L) in surface waters in Netherlands were similar to the observed values in our study. Recent study in biosolids showed nAg concentration of 1.2 to 91.1 ng/g (Number concentration: 10^7 to 10^8 NPs/g of dry biosolids) with a mean size of approximately 16 to 41 nm. The size of nAg in WW effluent and biosolids are in the similar range, whereas, the concentration is less than 1% compared to biosolids. This suggest that 99% of nAg entering or reprecipritated during the period in the municipal WWTP is removed through biosolids. Similar results were found in previous studies with 97-99% of nAg separated in municipal WWTP with heteroaggregation, sedimentation and absorption with NOM or colloids [55, 56]. Previous study reported in nine Germany municipal WWTP, the removal efficiency of nAg in municipal

WWTPs is high, achieving a sub 10 ng/L concentration in the effluent as a consequence of some 1.5 μg/L influents [49].

A recent study has reported data on the concentration of nCu 25.6 ± 1.7 ng/L with mean size of 94.3 ± 0.2 nm in WW effluents in south California, US [15]. These measured concentrations were 2.1 times higher than the peak value reported in our study. Study in biosolids matrices detected nCu with mass concentration (3 ng/g to 12 μg/g in dry biosolid) 1000 times higher than in WW effluent measured. Similarly, the mean sizes (47 to 110 nm) in biosolids had larger aggregates or particles sizes compared to WW effluent. This results suggests that the larger nCu particles sizes or aggregates settle down by sedimentation or heteroaggregation with NOM or colloids in sludge or biosolids. The smaller size fraction as compared to biosolids stay suspended in the WW effluent. A study has shown that nCu becomes stable in WW samples due to high NOM reducing sedimentation [57].

The measured concentration of nAg and nCu are well below for any previously reported toxic concentration (~ 50 μg/L) [58-60]. Toxic effects of NPs is contributed by both nanospecific (size and reactive oxygen species genereation) [57, 61-64] and ion release [64-66]. Toxicity of free ions are shown in many organism and complexation may result in reduction of ions [67, 68]. Additionally, silver and copper ions form insoluble or sparingly insoluble inorganic complex that may sediment from the system [57, 69]. Therefore, WW effluent with high organic matter can still be dangerous to aquatic organisms with nanospecific toxic effects. Predicted no observed effect concentration (PNEC) of nAg and nCuO in freshwater is 12 and 340 ng/L, respectively [70]. Even though the measured concentration from our study are below the toxic levels, this constant loading can lead to bioaccumulation of NPs in the organisms by constant exposure to WW effluent. As NPs is a growing industry, production and manufacture of products using NPs will increase leading to higher concentration of NPs released and entering municipal WWTPs.

The box plots indicated variation of size in nAg is much smaller range compared to nCu, with size of nAg in the range of 19.3 ± 2.1 to 34.7 ± 7.2 nm and nCu in the range of .6 ± 9.8 to 68.0 ± 14.3 nm (Figure 4-4a). However, the number concentration of nAg and nCu are in a similar range as seen in Figure 4-4b. A recent study in municpal municipal WWTP biosolids and sludge has shown similar trends of variation of size and number concentration when comparing nAg and nCu. As mentioned before, the sizes of nCu in WW effluent found in this study is in the lower range compared to that in biosolids, suggesting stable particle size staying releasing along with the effluent. However, the size of nAg both in effluent and biosolids are almost the same. These nAg are in the similar range probably due to reprecipitation of dissolved in municipal WWTPs.

Although, CUF followed by spICP-MS is promising results of NP size and concentration in WW effluent, this method may be limited to analyzing particle sizes (specific to each element - 15nm for nAg and 30nm nCu) above the detection limit of the instrument. Consequently, smaller sizes of the NPs below detection limit are considered as dissolved metal or background. Another assumption involved in measuring using spICP-MS, NPs are assumed to circular and uniform, whereas, in reality, these NPs can be composite particles involving multiple elements, complexes with NOM or even heteroaggregated with other colloids or NPs. Even with these downsides, spICP-MS is still one of the most important analytical technique to quantify the presence of NPs in complex matrices.

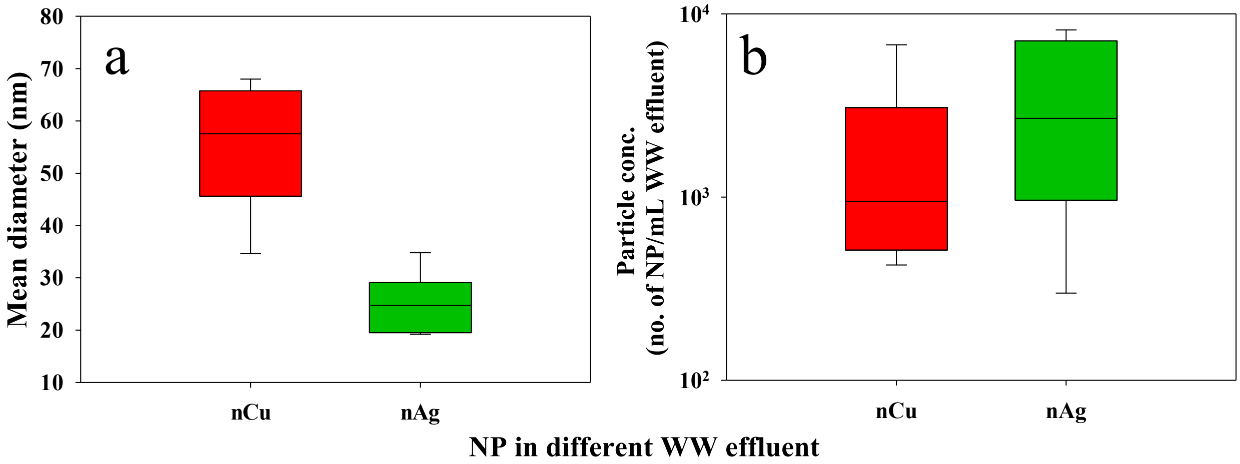

Figure 4-4 Box plot of mean diameter and number concentration of nCu and nAg in WW effluent from municipal WWTP across Canada.

4.5. Implications

WW effluents is a significant point source for NPs release into the environment through surface water discharge. nCu was measured in all 9 WW effluents, whereas, nAg was only detected in 6 of them. The lack of detection of nAg in those WW effluents might be because of a variety of reasons, including separation to WW biosolids, lower than detection limit or no NPs in influent. The measured concentration values of nAg and nCu in WW effluent from municipal WWTPs indicate high removal efficiency similar to previous studies [6, 7, 56]. Comparing the measured concentration of NPs in biosolids from a recent study to our measured concentration in WW effluent, more than 99% are separated along with biosolids during the WW treatment processes, leading to extremely low concentration in the effluent. Furthermore, these separated NPs would accumulate in the WW biosolids usually end up in the landfill, incinerated or agricultural land as fertilizers. Our results also signify that field-scale municipal WWTPs are as effective as lab-scale models in the removal of NPs in sludge [6, 7, 56, 71] .

The most important question is, will the concentration levels around ng/L in WW effluent influence the living organism in the aquatic environment. Ecotoxicological studies have shown that ng/L of NPs can cause harmful effects in prokaryotes, invertebrates and fish [72]. The impact of trace levels of NPs on long term exposure to aquatic organisms in WW effluent should be researched further including possible bioaccumulation. As discussed, most NPs entering the municipal WWTPs heteroaggregate with NOM or other colloids to form large aggregates that settle down along with the sludge. These measured NPs in WW effluent may be natural, or anthropogenic, as presently it is unable to distinguish between them. The nAg and nCu measured in the WW effluent are most likely transformed due to presence of natural organic matter and colloids. Previous study have shown reformation nAg in the WW effluent from dissolved Ag and association with thiols [34]. The data reported here can be used for future modelling, exposure assessment and toxicology studies. Finally, the concentration of NPs measured here a lower than previous reported or predicted data [20, 21, 32, 42, 48].

4.6. Acknowledgements

We acknowledge the assistance of Environment and Climate Change Canada for providing with samples from 11 different municipal WWTPs. The research was supported by the Natural Sciences and Engineering Research Council of Canada and Environment and Climate Change Canada. A. A. R was supported by McGill Engineering Doctoral Award.

4.7. Supplementary information

Table S4-1 nAg measured in various unspiked municipal WWTP effluents using spICP-MS (sample replicates, n = 3 and measurement replicates = 3)

Names used	Most Freq. Size (nm)	Mean Size (nm)	Part. Conc. Measured (NP/mL)	nAg Part. Conc (Considering recovery and Concentration factor) (NP/mL)	nAg mass conc. expected (Considering recovery and concentration factor) (ng/L)]
Plant A, AB	19.4 ± 2.7	26.8 ± 4.1	19807.8 ± 9875.2	2751.1 ± 1371.6	0.43 ± 0.01
Plant C , AB	24.1 ± 5.1	34.8 ± 7.8	2151.4 ± 1005.7	298.8 ± 139.7	0.09 ± 0.02
Plant H, MB	19.9 ± 3.2	27.2 ± 5.3	18941.6 ± 18255.2	2630.8 ± 253.5	0.41 ± 0.09
Plant I, MB	18.0 ± 0.1	22.6 ± 0.0	48768.7 ± 4238.5	6773.4 ± 588.7	0.47 ± 0.04
Plant J, NS	14.5 ± 0.0	19.2 ± 0.1	58868.3 ± 2076.5	8176.2 ± 288.4	0.33 ± 0.01
Plant K, NS	14.3 ± 0.1	19.6 ± 0.1	8516.7 ± 99.2	1182.9 ± 13.8	0.08 ± 0.00

Table S4-2 nCu measured in various unspiked municipal WWTP effluents using spICP-MS (sample replicates, n = 3 and measurement replicates = 3)

Names used	Most Freq. Size (nm)	Mean Size (nm)	Part. Conc. Measured (NP/mL)	nCu Part. Conc (Considering recovery and Concentration factor) (NP/mL)	nCu mass conc. expected (Considering recovery and concentration factor) (ng/L)]
Plant A, AB	57.7 ± 0.2	68.0 ± 0.3	48839.9 ± 6897.8	6783.3 ± 958.0	12.18 ± 1.58
Plant C , AB	41.6 ± 1.2	51.1 ± 1.6	3311.3 ± 560.5	459.9 ± 77.9	0.44 ± 0.04
Plant D, ON	32.5 ± 1.8	40.1 ± 0.5	5487.5 ± 865.0	762.2 ± 120.1	0.29 ± 0.05
Plant E, ON	53.1 ± 1.2	64.8 ± 1.2	9218.2 ± 535.7	1280.3 ± 74.4	2.02 ± 0.04
Plant F, QC	24.8 ± 1.1	34.6 ± 1.3	3064.1 ± 256.7	425.6 ± 35.6	0.11 ± 0.02
Plant H, MB	61.8 ± 0.5	66.7 ± 0.6	29614.4 ± 595.5	4113.1 ± 82.7	6.18 ± 0.06
Plant I, MB	46.3 ± 2.5	57.6 ± 4.0	6832.7 ± 1669.2	949.0 ± 231.8	1.11 ± 0.18
Plant J, NS	48.3 ± 1.7	54.5 ± 0.6	4085.4 ± 590.3	567.4 ± 82.0	0.50 ± 0.06
Plant K, NS	47.6 ± 0.3	58.6 ± 1.1	14760.4 ± 317.5	2050.1 ± 44.1	2.51 ± 0.23

Table S4-3 spICP-MS instrumental parameters used for measurements

Parameter Value	
Sample Uptake Rate	0.28-0.34 mL/min
Nebulizer gas flow	0.97-1.03 L/min

Nebulizer	Meinhard Glass Concentric
Spray Chamber	Meinhard Glass Cyclonic
RF Power	1600 W
Analyte	Ag107
Analysis time	100-150 s
Dwell time	100 µs

Table S4-4 Spiked recovery of 80nm nAg at 100 ng/L before and after freeze storing in at -80 C in WW effluent using CUF

Measurement	Mean Size (nm)	nAg Mass Conc. (ng/L)
Before freezing at -80 C	70.6 ± 0.2	96.0 ± 5.2
After Freeze thaw	69.3 ± 0.7	93.1 ± 3.8

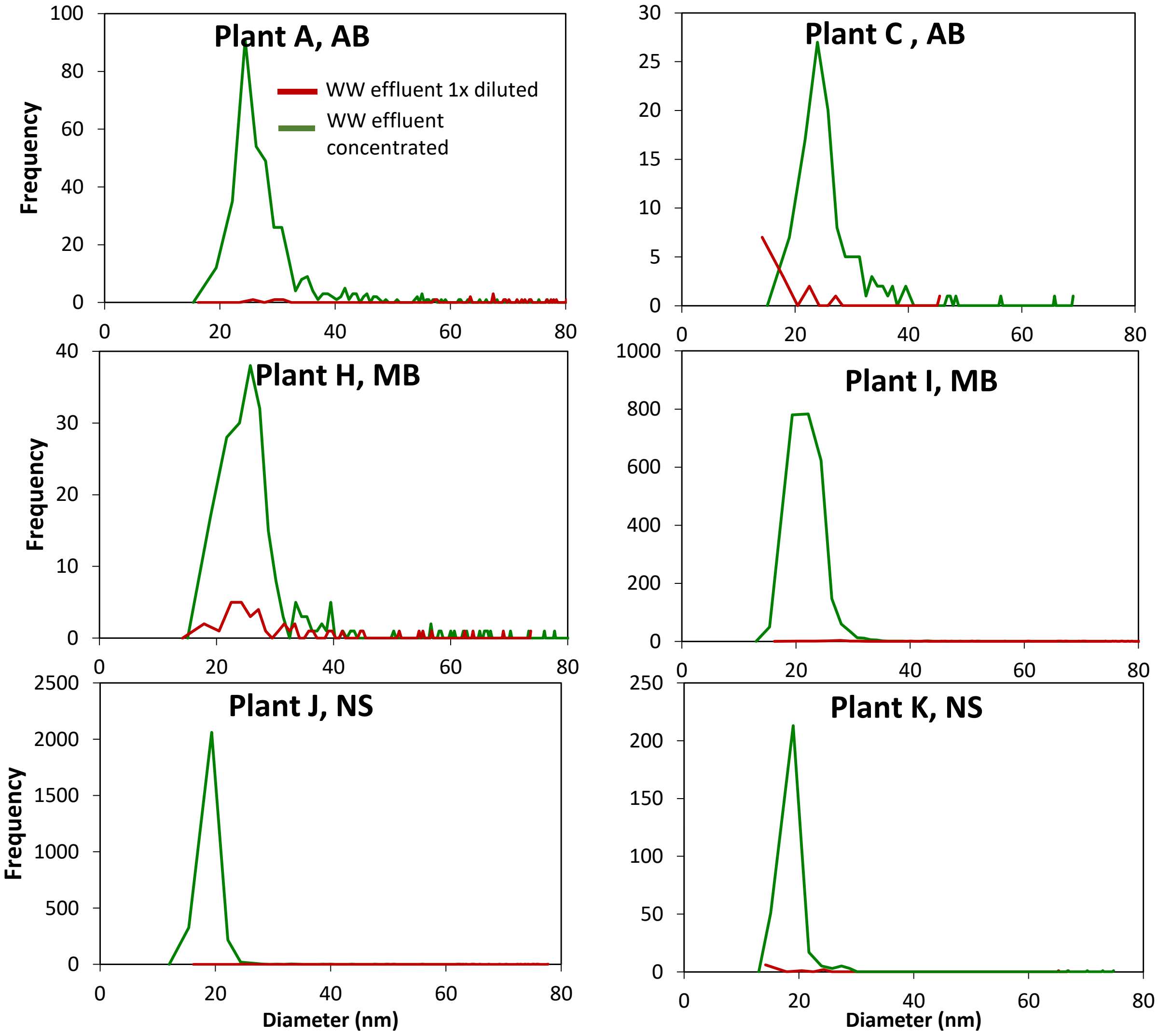

Figure S4-1 nAg measurement using spICP-MS before and after concentrating using CUF from various municipal WWTP effluents

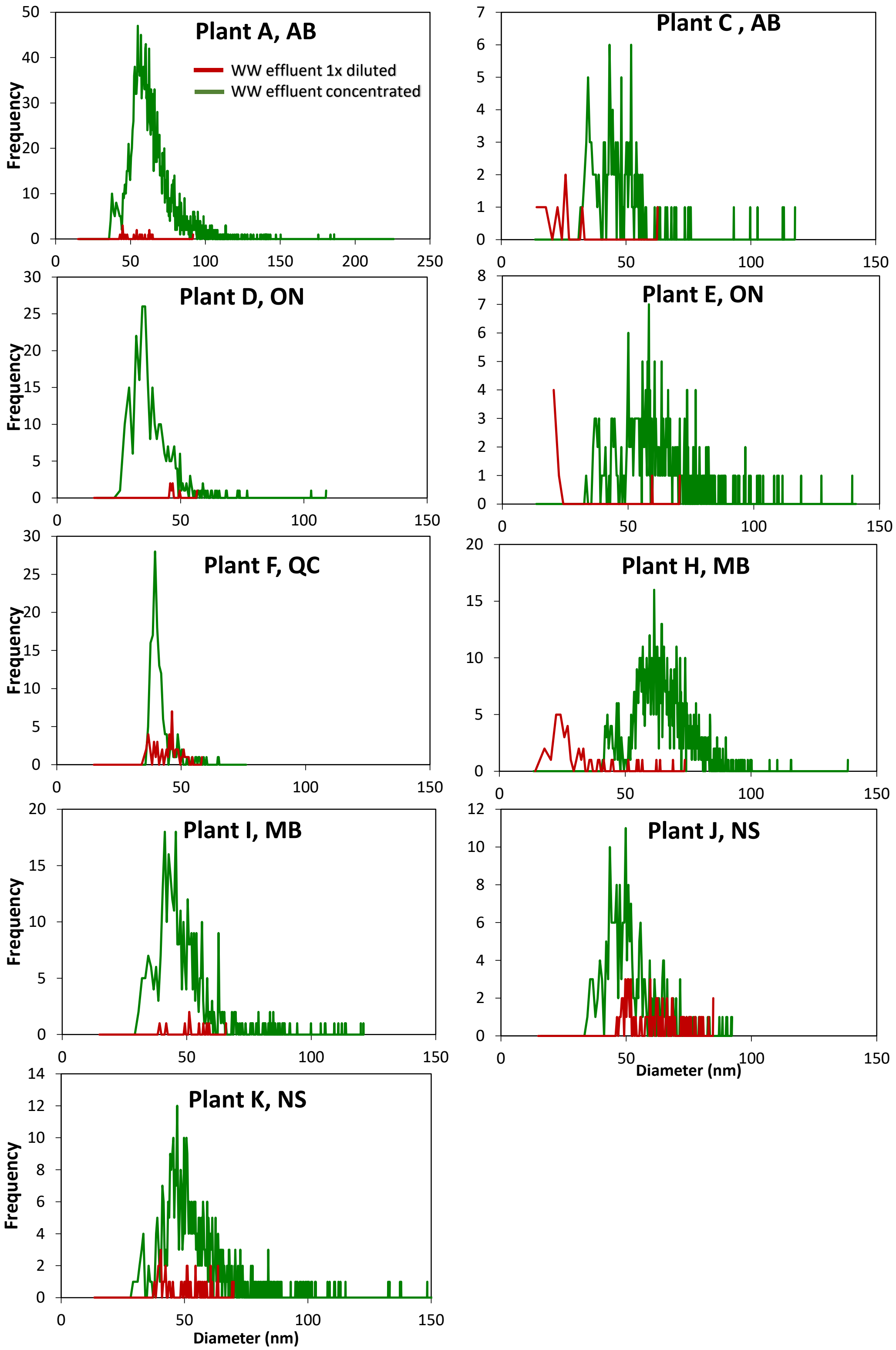

Figure S4-2 nCu measurement using spICP-MS before and after concentrating using CUF from various municipal WWTP effluents

4.8. References

1. Gottschalk, F. and B. Nowack, *The release of engineered nanomaterials to the environment.* Journal of Environmental Monitoring, 2011. **13**(5): p. 1145-1155.
2. Gottschalk, F., et al., *Modeled environmental concentrations of engineered nanomaterials (TiO2, ZnO, Ag, CNT, fullerenes) for different regions.* Environmental Science & Technology, 2009. **43**(24): p. 9216-9222.
3. Gottschalk, F., T. Sun, and B. Nowack, *Environmental concentrations of engineered nanomaterials: Review of modeling and analytical studies.* Environmental Pollution, 2013. **181**: p. 287-300.
4. Westerhoff, P., et al., *Characterization, Recovery Opportunities, and Valuation of Metals in Municipal Sludges from U.S. Wastewater Treatment Plants Nationwide.* Environmental Science & Technology, 2015. **49**(16): p. 9479-9488.
5. Westerhoff, P.K., M.A. Kiser, and K. Hristovski, *Nanomaterial removal and transformation during biological wastewater treatment.* Environmental Engineering Science, 2013. **30**(3): p. 109-117.
6. Kaegi, R., et al., *Behavior of Metallic Silver Nanoparticles in a Pilot Wastewater Treatment Plant.* Environmental Science & Technology, 2011. **45**(9): p. 3902-3908.
7. Ma, R., et al., *Fate of Zinc Oxide and Silver Nanoparticles in a Pilot Wastewater Treatment Plant and in Processed Biosolids.* Environmental Science & Technology, 2014. **48**(1): p. 104-112.
8. Barton, L.E., et al., *Monte Carlo simulations of the transformation and removal of Ag, TiO2, and ZnO nanoparticles in wastewater treatment and land application of biosolids.* Science of The Total Environment, 2015. **511**: p. 535-543.
9. Tiede, K., et al., *Review of the Risks Posed to Drinking Water by Man-Made Nanoparticels*. 2012, FERA, UK. p. 170.
10. Li, L., et al., *To What Extent Can Full-Scale Wastewater Treatment Plant Effluent Influence the Occurrence of Silver-Based Nanoparticles in Surface Waters?* Environmental Science & Technology, 2016. **50**(12): p. 6327-6333.
11. Mitrano, D.M., et al., *Detecting nanoparticulate silver using single-particle inductively coupled plasma–mass spectrometry.* Environmental Toxicology and Chemistry, 2012. **31**(1): p. 115-121.
12. Hadioui, M., V. Merdzan, and K.J. Wilkinson, *Detection and characterization of ZnO nanoparticles in surface and waste waters using single particle ICPMS.* Environmental science & technology, 2015. **49**(10): p. 6141-6148.
13. Khosravi, K., et al., *A novel approach for determining total titanium from titanium dioxide nanoparticles suspended in water and biosolids by digestion with ammonium persulfate.* Analytica Chimica Acta, 2012. **713**: p. 86-91.
14. Hoque, M.E., et al., *Detection and characterization of silver nanoparticles in aqueous matrices using asymmetric-flow field flow fractionation with inductively coupled plasma mass spectrometry.* Journal of Chromatography A, 2012. **1233**: p. 109-115.
15. Huang, Y., et al., *Fast Multielement Quantification of Nanoparticles in Wastewater and Sludge Using Single-Particle ICP-MS.* ACS ES&T Water, 2021. **1**(1): p. 205-213.
16. Kiser, M., et al., *Titanium nanomaterial removal and release from wastewater treatment plants.* Environmental science & technology, 2009. **43**(17): p. 6757-6763.

17. Westerhoff, P., et al., *Occurrence and removal of titanium at full scale wastewater treatment plants: implications for TiO 2 nanomaterials.* Journal of Environmental Monitoring, 2011. **13**(5): p. 1195-1203.
18. Johnson, A.C., et al., *An assessment of the fate, behaviour and environmental risk associated with sunscreen TiO 2 nanoparticles in UK field scenarios.* Science of the Total Environment, 2011. **409**(13): p. 2503-2510.
19. Johnson, A., et al., *Exposure assessment for engineered silver nanoparticles throughout the rivers of England and Wales (CB0433).* Centre for Ecology and Hydrology, UK, 2011.
20. Liu, J.-f., et al., *Triton X-114 based cloud point extraction: a thermoreversible approach for separation/concentration and dispersion of nanomaterials in the aqueous phase.* Chemical Communications, 2009(12): p. 1514-1516.
21. Liu, J.-f., et al., *Cloud point extraction as an advantageous preconcentration approach for analysis of trace silver nanoparticles in environmental waters.* Analytical Chemistry, 2009. **81**(15): p. 6496-6502.
22. Raynie, D.E., *Surfactant-Mediated Extractions, Part I: Cloud-Point Extraction.* LCGC North America, 2016. **34**(1): p. 14-18.
23. Majedi, S.M., B.C. Kelly, and H.K. Lee, *Evaluation of a cloud point extraction approach for the preconcentration and quantification of trace CuO nanoparticles in environmental waters.* Analytica Chimica Acta, 2014. **814**(0): p. 39-48.
24. Hendren, C.O., et al., *Modeling nanomaterial fate in wastewater treatment: Monte Carlo simulation of silver nanoparticles (nano-Ag).* Science of The Total Environment, 2013. **449**: p. 418-425.
25. Keller, A.A. and A. Lazareva, *Predicted releases of engineered nanomaterials: From global to regional to local.* Environmental Science & Technology Letters, 2013. **1**(1): p. 65-70.
26. Pavagadhi, S., M. Sathishkumar, and R. Balasubramanian, *Uptake of Ag and TiO2 nanoparticles by zebrafish embryos in the presence of other contaminants in the aquatic environment.* Water research, 2014. **55**: p. 280-291.
27. Croteau, M.-N., et al., *Silver bioaccumulation dynamics in a freshwater invertebrate after aqueous and dietary exposures to nanosized and ionic Ag.* Environmental science & technology, 2011. **45**(15): p. 6600-6607.
28. Garner, K.L., S. Suh, and A.A. Keller, *Assessing the Risk of Engineered Nanomaterials in the Environment: Development and Application of the nanoFate Model.* Environmental Science & Technology, 2017. **51**(10): p. 5541-5551.
29. Quik, J.T., J.J. de Klein, and A.A. Koelmans, *Spatially explicit fate modelling of nanomaterials in natural waters.* Water research, 2015. **80**: p. 200-208.
30. Praetorius, A., M. Scheringer, and K. Hungerbühler, *Development of Environmental Fate Models for Engineered Nanoparticles・A Case Study of TiO2 Nanoparticles in the Rhine River.* Environmental science & technology, 2012. **46**(12): p. 6705-6713.
31. Hartmann, G., C. Hutterer, and M. Schuster, *Ultra-trace determination of silver nanoparticles in water samples using cloud point extraction and ETAAS.* Journal of Analytical Atomic Spectrometry, 2013. **28**(4): p. 567-572.
32. Liu, J., J. Sun, and G. Jiang, *Use of cloud point extraction for removal of nanosized copper oxide from wastewater.* Chinese Science Bulletin, 2010. **55**(4): p. 346-349.
33. Misra, S.K., et al., *The complexity of nanoparticle dissolution and its importance in nanotoxicological studies.* Science of The Total Environment, 2012. **438**: p. 225-232.

34. Azodi, M., Y. Sultan, and S. Ghoshal, *Dissolution Behavior of Silver Nanoparticles and Formation of Secondary Silver Nanoparticles in Municipal Wastewater by Single-Particle ICP-MS.* Environmental Science & Technology, 2016. **50**(24): p. 13318-13327.
35. Furtado, L.M., et al., *The persistence and transformation of silver nanoparticles in littoral lake mesocosms monitored using various analytical techniques.* Environmental Chemistry, 2014. **11**(4): p. 419-430.
36. Whitley, A.R., et al., *Behavior of Ag nanoparticles in soil: Effects of particle surface coating, aging and sewage sludge amendment.* Environmental Pollution, 2013. **182**: p. 141-149.
37. El Hadri, H. and V.A. Hackley, *Investigation of cloud point extraction for the analysis of metallic nanoparticles in a soil matrix.* Environmental Science: Nano, 2017. **4**(1): p. 105-116.
38. Mitrano, D., et al., *Tracking dissolution of silver nanoparticles at environmentally relevant concentrations in laboratory, natural, and processed waters using single particle ICP-MS (spICP-MS).* Environ. Sci.: Nano, 2014. **1**(3): p. 248.
39. Chook, S.W., et al., *Effective immobilization of silver nanoparticles on a regenerated cellulose–chitosan composite membrane and its antibacterial activity.* New Journal of Chemistry, 2017. **41**(12): p. 5061-5065.
40. Mikelonis, A.M., S. Youn, and D.F. Lawler, *DLVO Approximation Methods for Predicting the Attachment of Silver Nanoparticles to Ceramic Membranes.* Langmuir, 2016. **32**(7): p. 1723-1731.
41. Chen, S.-C., et al., *An experimental study of ultrafiltration for sub-10nm quantum dots and sub-150 nm nanoparticles through PTFE membrane and Nuclepore filters.* Journal of Membrane Science, 2016. **497**: p. 153-161.
42. Peters, R.J.B., et al., *Detection of nanoparticles in Dutch surface waters.* Science of The Total Environment, 2018. **621**: p. 210-218.
43. Mueller, N.C. and B. Nowack, *Exposure modeling of engineered nanoparticles in the environment.* Environmental science & technology, 2008. **42**(12): p. 4447-4453.
44. Boxall, A., et al., *Current and future predicted environmental exposure to engineered nanoparticles.* Central Science Laboratory, Department of the Environment and Rural Affairs, London, UK, 2007: p. 89.
45. Mitrano, D.M., et al., *Silver nanoparticle characterization using single particle ICP-MS (SP-ICP-MS) and asymmetrical flow field flow fractionation ICP-MS (AF4-ICP-MS).* Journal of Analytical Atomic Spectrometry, 2012. **27**(7): p. 1131-1142.
46. Keller, A.A. and A. Lazareva, *Predicted releases of engineered nanomaterials: From global to regional to local.* Environ. Sci. Technol. Lett., 2014. **1**(1): p. 65.
47. Pu, Y., et al., *Fate and Characterization Factors of Nanoparticles in Seventeen Subcontinental Freshwaters: A Case Study on Copper Nanoparticles.* Environmental Science & Technology, 2016. **50**(17): p. 9370-9379.
48. Chao, J.-b., et al., *Speciation Analysis of Silver Nanoparticles and Silver Ions in Antibacterial Products and Environmental Waters via Cloud Point Extraction-Based Separation.* Analytical Chemistry, 2011. **83**(17): p. 6875-6882.
49. Li, L., et al., *Quantification of nanoscale silver particles removal and release from municipal wastewater treatment plants in Germany.* Environmental science & technology, 2013. **47**(13): p. 7317-7323.

50. Hartmann, G., T. Baumgartner, and M. Schuster, *Influence of Particle Coating and Matrix Constituents on the Cloud Point Extraction Efficiency of Silver Nanoparticles (Ag-NPs) and Application for Monitoring the Formation of Ag-NPs from Ag+*. Analytical Chemistry, 2014. **86**(1): p. 790-796.
51. Majedi, S.M. and H.K. Lee, *Recent advances in the separation and quantification of metallic nanoparticles and ions in the environment.* TrAC Trends in Analytical Chemistry, 2016. **75**: p. 183-196.
52. Laborda, F., et al., *Selective identification, characterization and determination of dissolved silver (I) and silver nanoparticles based on single particle detection by inductively coupled plasma mass spectrometry.* Journal of Analytical Atomic Spectrometry, 2011. **26**(7): p. 1362-1371.
53. T. Townsend, A., et al., *The determination of copper, zinc, cadmium and lead in urine by high resolution ICP-MS.* Journal of Analytical Atomic Spectrometry, 1998. **13**(11): p. 1213-1219.
54. Navratilova, J., et al., *Detection of Engineered Copper Nanoparticles in Soil Using Single Particle ICP-MS.* International Journal of Environmental Research and Public Health, 2015. **12**(12): p. 15756-15768.
55. Kaegi, R., et al., *Fate and transformation of silver nanoparticles in urban wastewater systems.* Water Research, 2013. **47**(12): p. 3866-3877.
56. Kiser, M.A., et al., *Biosorption of nanoparticles to heterotrophic wastewater biomass.* Water Research, 2010. **44**(14): p. 4105-4114.
57. Conway, J.R., et al., *Aggregation, dissolution, and transformation of copper nanoparticles in natural waters.* Environmental science & technology, 2015. **49**(5): p. 2749-2756.
58. Navarro, E., et al., *Toxicity of silver nanoparticles to Chlamydomonas reinhardtii.* Environmental science & technology, 2008. **42**(23): p. 8959-8964.
59. Sheng, Z. and Y. Liu, *Effects of silver nanoparticles on wastewater biofilms.* Water research, 2011. **45**(18): p. 6039-6050.
60. European Chemicals Agency. *Acute & chronic ecotoxicity of soluble copper species in view of hazard classification of copper and copper compounds*. 2021; Available from: https://echa.europa.eu/documents/10162/13626/attachment_4_copper_flakes_en.pdf.
61. Shi, J., et al., *To duckweeds (Landoltia punctata), nanoparticulate copper oxide is more inhibitory than the soluble copper in the bulk solution.* Environmental Pollution, 2011. **159**(5): p. 1277-1282.
62. Hanna, S.K., et al., *Accumulation and toxicity of metal oxide nanoparticles in a soft-sediment estuarine amphipod.* Aquatic toxicology, 2013. **142**: p. 441-446.
63. Buffet, P.-E., et al., *A mesocosm study of fate and effects of CuO nanoparticles on endobenthic species (Scrobicularia plana, Hediste diversicolor).* Environmental science & technology, 2013. **47**(3): p. 1620-1628.
64. Hadrup, N., A.K. Sharma, and K. Loeschner, *Toxicity of silver ions, metallic silver, and silver nanoparticle materials after in vivo dermal and mucosal surface exposure: A review.* Regulatory Toxicology and Pharmacology, 2018. **98**: p. 257-267.
65. Blinova, I., et al., *Ecotoxicity of nanoparticles of CuO and ZnO in natural water.* Environmental Pollution, 2010. **158**(1): p. 41-47.
66. Franklin, N.M., et al., *Comparative toxicity of nanoparticulate ZnO, bulk ZnO, and ZnCl2 to a freshwater microalga (Pseudokirchneriella subcapitata): the importance of particle solubility.* Environmental science & technology, 2007. **41**(24): p. 8484-8490.

67. Sunda, W., *Relationship between cupric ion activity and the toxicity of copper to phytoplankton, 168 pp*. 1975, Ph. D. Thesis, Massachusetts Institute of Technology, Cambridge.
68. Moore, M., et al., *Responses of the mussel Mytilus edulis to copper and phenanthrene: interactive effects.* Marine Environmental Research, 1984. **14**(1-4): p. 167-183.
69. Liu, J., et al., *Controlled Release of Biologically Active Silver from Nanosilver Surfaces.* ACS Nano, 2010. **4**(11): p. 6903-6913.
70. Lützhøft, H.-C.H., et al., *Environmental Effects of Engineered Nanomaterials: Estimations of Predicted No-Effect Concentrations (PNECs).* 2015.
71. Comfort, K.K., et al., *Less Is More: Long-Term in Vitro Exposure to Low Levels of Silver Nanoparticles Provides New Insights for Nanomaterial Evaluation.* ACS Nano, 2014. **8**(4): p. 3260-3271.
72. Fabrega, J., et al., *Silver nanoparticles: Behaviour and effects in the aquatic environment.* Environment International, 2011. **37**(2): p. 517-531.

Connecting text between Chapter 4 and Chapter 5

ENPs are being extensively used in a variety of industrial and consumer products such as paints and coatings, leading to NP release in the environment. There is a need to characterize the physio-chemical properties of released NPs to assess the environmental exposures and to inform assessment of risks. The release of NPs from products such as paints and coatings leads to increased concentration of NPs entering into a WWTPs. nAg paints are used in paints and coatings for their antimicrobial properties. In this study, nAg released from painted surface under various aging and aqueous chemistry conditions were characterized for size and concentration by analyses of the aqueous wash samples by ICP-MS in single particle mode (spICP-MS). Finally, a comparative assessment of the on stability and culturability properties of pristine nAg to released nAg from painted surface was carried out.

CHAPTER 5 COMPARISON OF COLLOIDAL AND CHEMICAL STABILITY AND TOXICITY OF SILVER NANOPARTICLES RELEASED FROM PAINTS AND PRISTINE SILVER NANOPARTICLES

Abstract

Engineered nanoparticles (ENPs) are being extensively used in a variety of paints and coatings, and thus, are being released to the environment over time. Little information is available on how the environmental risks of ENPs or its dissolved form released from products differ from pristine (as manufactured) ENPs. Silver nanoparticles (nAg) are commonly present in paints and coatings for their antimicrobial properties. This study aims to quantify the fraction of Ag released as ENPs or as dissolved species from painted surfaces over time due to contact with different pH solutions and/or direct exposure to sunlight; and to compare the colloidal stability and bacterial toxicity of the pristine nAg and released nAg from painted surface embedded in the paint matrix. Our results showed nAg release to increase over time at all pH conditions, with highest nAg concentrations of $2.2 \pm 0.8 \times 10^7$ NP/mL/g observed at acidic pH ~3.5 (at the end of day 16), compared to $3.9 \pm 0.2 \times 10^6$ NP/mL/g in basic pH ~8.5 and $2.1 \pm 0.1 \times 10^6$ NP/mL/g in DI water pH ~5.8. nAg release in acidic pH was 10-folds higher than in neutral pH and 5.6-folds higher than in basic pH. nAg released in acidic pH was smaller in size, with mean diameter of 37.1 ± 2.1 nm compared to 64.6 ± 4.3 nm in neutral pH. The paint-released nAg was also significantly more colloidally stable and resistant to dissolution compared to pristine nAg, at neutral pH. Finally, viability tests with *E. coli D21* suspended in aqueous extracts (neutral pH) of painted surfaces with released Ag, showed that cells were non-culturable after 3 hours, whereas when exposed to pristine nAg, no adverse impact on culturability was found over 42 h. Thus, the physico-chemical properties and ecotoxicological potential of paint-released and pristine nAg are significantly different.

5.1. Introduction

Engineered nanoparticles (ENPs) are used in paints and coatings to enhance their function and performance. About 65,000 to 80,000 metric tons of ENPs are estimated to be used in paints and coatings each year [1]. For example, titanium dioxide ENPs ($nTiO_2$) are used for their photocatalytic activity and UV-protection [2], and silica ENPs ($nSiO_2$) for imparting macro- and micro-hardness, abrasion, scratch and weather resistance in paint [3, 4]. Silver ENPs (nAg) are used in paints and coatings for their antimicrobial properties [5, 6]. Paints with high antimicrobial capacity can be effective in indoor high occupancy areas to control the spread of pathogenic bacteria and viruses, or in outdoor applications to prevent unwanted microbial growth that compromises protection to surfaces and aesthetics [7-14]. The release of ENPs from paints has implications for the paint performance over time and the impact caused by released ENPs on the environment. In particular, ENPs released from outdoor paints can eventually enter wastewater treatment plants, surface water and groundwater via runoff. The knowledge of the concentrations and physico-chemical properties of the released ENPs can provide valuable information about the environmental risk assessment models for evaluating the impacts of ENPs on biota.

ENPs released from functionalized surfaces and products will likely carry some of the product matrix which could influence their environmental transformation, mobility and toxicity [15-18]. ENPs from paint have been shown to be strongly associated with small fragments of the paint matrix, particularly the polymeric binder which is used to colloidally disperse the ENPs in the paint formulation [2, 19, 20]. Precipitation, sunlight (UV) exposure and temperature changes can influence the release of ENPs from painted surfaces as large aggregates [21, 22] or as single ENPs [6]. For instance, exposure of painted surfaces to the environment were reported to result in the chemical transformation of nAg in the paint to nAg_2S, which has low dissolution and toxicity potential [6].

Adeleye et. al. (2016) assessed the release of nCu from painted specimens of wood and aluminum immersed in water for over 180 days. The aqueous sample collected was analysed using microscopic techniques after sample preparation and inductively coupled plasma atomic emission spectroscopy (ICP-AES) by acid digestion [23]. Furthermore, indirect measurement of nCu (without any size information) was determined by filtering the sample through 0.2 µm filter, followed by acid digestion of the filter and quantification using ICP-AES for total metal Cu. Other studies assessed the release of nAg and $nTiO_2$ from painted outdoor facades, by collecting wash water from precipitation, followed by (i) microscopic analysis of wash water and (ii) total metal analysis via acid digestion followed by inductively coupled plasma mass spectrometric analysis (ICP-MS) [6, 24]. Similarly, several other studies quantified NP concentration released from paints or coatings by means of microscopic data (qualitative) and/or acid digestion (indirect quantification) followed by total metal measurement [19, 20, 22, 25-28]. However, these studies report indirect NP concentrations and do not provide adequate or reliable characterization (no particle size distribution (PSD) and NP concentration reported).

A study by Kaegi et al (2010) reported that up to 30% of Ag (total metal analysis) was released over two-month period from an outdoor façade coated with a paint containing nAg, from periodical rainfall events [6]. A recent study on characterization of $nTiO_2$ released from outdoor paints, exposed to snow and rainfall, using single particle ICP-MS (spICP-MS) analysis helped provide information on released NP size, particle size distribution and NP mass concentrations [29]. The study reports released $nTiO_2$ from painted surfaces with sizes ranging from 20 to 60 nm and concentrations less than 0.0001% by weight. Another recent study on the release of $nTiO_2$ from painted surfaces, due to precipitation, using spICP-MS and spICP-time of flight-MS (spICP-TOF-MS) to directly measure the particle size distribution, concentration of NP and association with other metals, reported that $nTiO_2$ was released with size ranging between 15 to 120 nm and associated with Al (20%) and Zr (1%) from the paint [30].

Although the studies above clearly demonstrated ENP releases from paint, the majority of these studies have largely relied either on electron microscopy techniques and/or have reported total metal concentrations released into the aqueous media [6, 19, 20, 22-25, 27, 28], with the exception of few recent studies characterizing NP size and concentration directly [29, 30]. These analytical techniques do not provide adequate or reliable characterization of ENPs released from paints in terms of size, particle size distribution and direct measurements of released NP concentrations. TEM imaging may not provide reliable data for concentrations and size distributions of the ENPs released because of the relatively low numbers of ENPs characterized, in addition to the potential for artefacts related to NP aggregation induced while drying aqueous samples [31, 32]. Measurements of total metal concentration in the aqueous media do not provide information on size, particle size distribution and dissolved metal concentration [6, 20]. Although this is a reliable approach for assessing the mass concentrations of ENPs of insoluble metals such as $nTiO_2$, it offers no information on the size and aggregation state of the ENPs being released. However, in the case of reactive ENPs such as nAg, that can dissolve in aqueous media, the measurement of total Ag in the precipitation in contact with the paint, does not indicate the speciation of Ag released as ENPs or dissolved species. The environmental fate, mobility and toxicity of nAg and dissolved Ag varies significantly, and thus it is important to determine the relative abundance of different forms of nAg released [33-38]. Several studies have discussed the importance of dissolved Ag as one of the major toxicity mechanisms of nAg [39-42]. spICP-MS is a powerful technique for measuring metal NP sizes and concentrations in relatively pure aqueous samples at sub parts per billion concentrations [43-45]. Researchers have analyzed the feasibility of setting spICP-MS size detection limits for frequently used NPs, and a theoretical limit of 10 nm was found suitable for nAg [44]. spICP-MS method has been developed extensively in literature, and the tool has been used for tracking engineered NPs [34, 46-51].

The objectives of this study are to (i) quantify the fraction of Ag released as ENPs or as dissolved species from painted surfaces over time due to contact with different pH solutions and/or direct exposure to sunlight; and to (ii) compare the colloidal stability and bacterial toxicity of the pristine nAg and released nAg from painted surface embedded in the paint matrix. In this study, a paint was synthesized containing a pigment (SiO_2) and metal-free polymeric base-paint and a well-characterized pristine nAg at a known concentration. This custom-made paint with nAg was uniformly applied on plastic paint performance testing surfaces and immersed water in the dark with different pH solutions (acidic pH ~3.5, DI water pH ~5.8 and basic pH ~8.5). The aqueous phase was then analyzed for released nAg and dissolved Ag using spICP-MS. The colloidal stability of pristine nAg used in the formulation was compared to that of nAg released from painted surfaces over time in batch reactors. These suspensions were also used to assess the viability of *E. coli D21* cells exposed to pristine nAg and nAg released from painted surfaces. To compare between the influence of contact with water to that of sunlight exposure in the outdoors on nAg release from the painted surfaces, the painted plastic test surfaces were exposed to sunlight, but were protected from precipitation. The painted surfaces were collected after different sunlight exposure points and immersed in deionized (DI) water for 3 days to assess the release of nAg and dissolved Ag. The water samples were then collected and measured using spICP-MS for nAg size distributions and concentration, as well as dissolved Ag concentration.

5.2. Materials and Methods

5.2.1. Preparation of nAg containing paint

Polyvinylpyrrolidone (PVP)-coated nAg (US Research Nanomaterials) in powder form, with particle diameters in the range of 50 to 80 nm containing PVP at 0.2 % weight to nAg were used to create a custom-made paint by a paint manufacturer. nAg was added to a commercial base paint formulation containing an acrylic polymer binder, without any other metal additives, at a concentration of 0.003% wt. (6.5 µg of nAg/g of dry paint).

To observe the effect of varying pH, polystyrene surfaces (weighing boats, Fisher scientific) of 12 mm thickness and surface dimensions of 8.9 cm × 8.9 cm were used. 1g of wet paint was deposited onto each surface, and spread uniformly using a nylon paint brush (size 8, brush width of 8 mm). This resulted in approximately 0.4 g of dry weight of paint after 3 days of drying. Painted surfaces were exposed to three pH conditions: DI water, acidic conditions (0.1mM nitric acid - pH ~3.5, similar to acid rain pH) [52, 53] and, basic conditions (0.1mM sodium hydroxide - pH ~8.5, similar to basic rain [54]). The painted surfaces were exposed to water of different pH for 16 days at standard room temperature of $20 \pm 3\ ^{\circ}$ and kept covered to avoid light, evaporation and other external interferences.

One of the painted surfaces was subjected to physical wear and tear using sonication, with DI water for 60 minutes. Physical abrasion is typically done to induce degradation from painted surfaces due to wear and tear friction [19]. To maintain similar physical abrasion between replicate surfaces, and minimize human error from affecting the abrasion process, sonication was performed at a fixed frequency and time. Sonication was done in a Fisherbrand^{TM} 11207 ultrasonic bath at 37 hertz frequency for 60 minutes at 10 minutes intervals to maintain the temperature of the water bath between 20 to 25 $^{\circ}$C. The sonicated samples were acid-digested using the digestion protocol (mentioned in section 5.3.3), diluted and measured for total Ag using Perkin Elmer 8000x ICP-OES.

For the sunlight exposure study, the custom-made paint was applied on polyvinyl chloride (PVC) boards of size 7.3 cm × 12.5 cm with 1.5 cm thickness from Plastiver (Trois-Rivières, QC). 1g of wet paint was poured onto each surface, spread uniformly using the paint brush described above. The painted surface was dried for 3 days in the dark and kept covered under a cardboard box to avoid dust and light. The painted boards were weighed before and after the application of paint to measure the dry weight of paint on each surface. Painted PVC boards were exposed to direct sunlight. The boards were stored in a closed container and kept covered after each day of sunlight exposure to avoid direct contact with precipitation. Three painted PVC boards were collected at time points 24, 48, 72, 96 and 120 hours of sunlight exposure (4 months of outdoor exposure June 2019 to September 2019 – only exposed to sunlight). The boards were individually immersed in DI water for 3 days. Wash water from the boards were collected and measured using spICP-MS. The immersion time period of 3 days was the minimum contact time in water for obtaining detectable quantities of nAg in the aqueous phase. Unpainted PVC boards and base paint applied boards were kept as control groups to observe the background concentration of nAg and dissolved Ag from the environment. Aqueous phase samples from the various experiments were periodically collected after gently mixing, to measure released nAg concentration and size and dissolved Ag using spICP-MS.

5.2.2. Colloidal stability of pristine nAg and released nAg from painted surfaces

A comparison of the colloidal stability of nAg released from painted surfaces, and pristine nAg used for the formulation of the paint was performed towards assessing potential differences that may arise in their environmental fate. The released nAg was obtained from the painted surfaces by sonication as mentioned in section 5.2.1, to ensure a high enough concentration of released nAg with attached paint debris. The pristine nAg in DI water was sonicated for 60 minutes (10-minute intervals to maintain the temperature of water bath between 20 to 25 $^{\circ}$C), to stabilize and disperse the ENPs. Suspensions of the released nAg from painted surface and pristine nAg were prepared at a concentration of 10^6 nAg/mL, as verified by spICP-MS. The samples were maintained in an incubator at 20 ºC and mixed continuously at 175 rpm. All systems were prepared in triplicates. Aqueous samples were taken at regular intervals of time and measured for over a period of 15 days using spICP-MS to see the difference between systems.

5.2.3. Culturability of *E. coli D21* exposed to pristine nAg and paint-released nAg

5.2.3.1. *E. coli D21culture conditions*

Escherichia coli D21 (*E. coli D21*), a Gram-negative bacterium was employed as a model bacterium to compare the toxicity of pristine and paint-released nAg. 150 mL of 2.5% (w/v) Luria–Bertani (LB)–Miller growth media (Fisher) was prepared in 250 mL Erlenmeyer flask and autoclaved. Liquid cultures were prepared by inoculating a single colony into the growth media and incubating at 37 °C for 4 h at 150 rpm. Cells were harvested by centrifugation at 5,000 rpm for 10 minutes at 4 °C. The supernatant was decanted and fresh filter sterile 10mM KNO_3 was added to resuspend the cells. The process of resuspension of cells, centrifugation and decanting was repeated twice to remove residual growth media in the cells. Subsequently, the supernatant was decanted, and cells resuspended in filter-sterilized 10 mM KNO_3. The absorbance of the initial cell concentrations was measured at 600 nm in UV-Vis spectrophotometer taking 10mM KNO_3 as reference standard.

5.2.3.2. *nAg exposure experiments*

Preparation of reactor contents: Sterile Erlenmeyer flasks of 500 mL volume were used as microcosms for nAg exposure studies. Four different microcosms were prepared containing: (a) filter sterilized 10 mM KNO_3 (Control); (b) pristine nAg in filter sterilised 10 mM KNO_3 (10 µg of nAg/L); (c) base paint in filter sterilised 10 mM KNO_3; (d) weathered paint aqueous (10 mM KNO_3) suspension obtained by sonication of painted boards (10 µg of nAg/L from weathered paint in DI water). All microcosms were incubated at 37 °C and 150 rpm.

Bacterial culturability: Colony forming units per mL (CFU/mL) counts were determined to characterize the changes in culturable cell population at definite time points. At each time point and for each microcosm, 1 mL of sample was obtained and serial dilutions at 10×, 100×, 1000× were performed using filter sterilized 10 mM KNO_3. 100 µL of the diluted and undiluted stock was plated on LB–Miller media (2.5 % w/v) containing 1.5% (w/v) agar (Fisher) and incubated at 37 °C for 24 h. Thereafter CFUs were enumerated from plates that had between 30–300 CFUs and multiplied with the appropriate dilution factor to obtain the final CFU count. For each sample, culture plates were prepared in triplicate for each of the dilutions.

5.3. Analytical Methods

5.3.1. Inductively coupled plasma mass spectrometric analysis in single particle mode (spICP-MS)

ENP characterization was performed using PerkinElmer NexION 300x ICP-MS in single particle mode supported by Syngistix software (Ver 1.1). This analysis provides the ENP size distribution, ENP concentration and dissolved metal concentration in the samples. An integration dwell time of 100 µs with sampling time of 100-150 s was used to measure the samples. Ultra uniform gold ENPs (nAu) of size 55nm were used for spICP-MS transport efficiency, nAu particles were diluted to a concentration of 10^5 particles/mL in DI water/ paint aqueous extract matrix obtained from the painted surface, to find the transport efficiency (5.0 to 8.5%) for spICP-MS. Other main instrumental settings and conditions are provided in the SI (Table S5-1).

The calibration for silver between the concentration range of 50 ng/L to 2 µg/L was prepared using 1000 mg/L standard stock solution of dissolved silver ions of (SCP Science PlasmaCAL). The spiked nAg, background controls and stock solution were measured along with the released ENPs from painted surfaces. Background controls and base paint did not show any interference with silver measurements at isotope of 107 Da in single particle mode. All measurements were done in triplicates using spICP-MS.

5.3.2. Electron Microscopy

Transmission electron microscopy (TEM) analysis was performed using a FEI Tecnai G2 F20 S/TEM equipped with Gatan Ultrascan 4000 4k × 4k CCD Camera System (Model 895). An EDAX Octane T Ultra W/Apollo XLT2 SDD system was used for energy dispersive X-ray spectroscopy (EDS) measurements. 10 µL of the sample concentrate was deposited on the Cu TEM grids (Electron Microscopy Sciences, Carbon film 200 mesh Cu grids. The grids were allowed to air-dry prior to analysis using TEM and EDS.

Sunlight exposed PVC boards were cut into 1cm × 1cm squares using professional guillotine paper cutter. The cut squares were coated with 5nm platinum in a sputter coater (Leica EM ACE 600). Coated samples were imaged using a scanning electron microscopy (SEM) FEI Quanta 450 FEG.

5.3.3. Sample Digestion and Element Analysis

Paint samples (0.5mL) were acid digested using 5mL of sulfuric acid (95 to 98 % - Fisher Scientific) at 110 ^{0}C for 8 hours in a hot block digester; followed by 2 mL of 70% ICP grade nitric acid (SCP Science) for 1 hour with quality controls; spiked with 100 µg/L of dissolved Ag and 100 µg/L of nAg and background controls. The digested samples were diluted to the required volume and measured using standard mode in Perkin Elmer NexION 300x ICP-MS and Perkin Elmer 8000x ICP-OES. Each paint extract samples were digested in triplicates and each digested sample was measured in triplicates.

5.4. Results and Discussion

The primary particle diameter of pristine nAg measured using TEM was 54.3 ± 7.3 nm (n=109) (Figure S5-1) and the diameters in aqueous (DI water) suspension as determined by spICP-MS was 97.1 ± 6.4 nm. TEM images showed that pristine nAg was aggregated. The size of nAg measured with spICP-MS was larger than TEM due to aggregation of nAg in solution, and each aggregate is measured as single particle.

5.4.1. Effect of pH on release of nAg in custom made paint

Painted polystyrene surfaces immersed in aqueous media released increasing amounts of ENPs with time into the aqueous media under quiescent conditions (Figure 5-1a). Painted polystyrene surfaces in contact with acidic pH ~3.5 released 10 folds higher nAg ($2. \pm 0.08 \times 10^7$ nAg/mL/g on day 16) than those in contact with DI water pH ~5.8 ($2.1 \pm 0.1 \times 10^6$ nAg/mL/g on day 16) and 5.6 folds higher than painted surfaces in contact with aqueous solutions at basic pH ~8.5 ($3.9 \pm 0.2 \times 10^6$ nAg/mL/g on day 16). The mass concentrations of released nAg and dissolved Ag were highest in acidic pH with 7.7 ± 0.4 ng/mL/g and 9.2 ± 0.4 ng/mL/g, compared to the corresponding values measured in DI water (nAg, 3.4 ± 0.1 ng/mL/g and dissolved Ag, 0.7 ± 0.0.8 ng/mL/g) and basic pH (nAg, 5.5 ± 0.4 ng/mL/g and dissolved Ag, 0.3 ± 0.1 ng/mL/g). The aqueous solutions had turbidity of 0 NTU and were clear to the naked eye over the duration of contact. Release of total Ag (nAg painted panels) from painted polystyrene panels observed during the initial precipitation events by Kaegi et al. (2010) [6] was in the similar range at 0.5 to 20 ng/mL, whereas, Zuin et al. (2014) reported 0.1 ng/mL of total Ag release observed from fibre cement panels (nAg painted panels) in water immersion test (pH between 5 to 6) [22]. Overall, only a minute fraction of the nAg in the paint was released into the aqueous solution from painted surface and was determined to be 2.3 ± 0.2 wt% for DI water, 3.8 ± 0.2 % in the basic pH solutions and 5.3 ± 0.5 % in the acidic pH solution, respectively. In case of DI water and basic solution, mechanism of ENP release involves the water permeating through the painted surface reducing the contact between nAg and binder molecules in the paint, leading to release of nAg [55-58]. For acidic solutions, mechanism of ENP release occurs both due to (i) the hydrolysis of the crosslinks (crosslinks - the formation of strong bonds throughout the acrylic polymer network to protect the paint) followed by degradation; as well as (ii) leaching of the nAg due to penetration of water into crosslinks leading to reduced contact of the nAg with the binder [59].

Higher dissolved Ag was observed also for acidic pH ~3.5 systems at 9.2 ± 1.8 ng/mL/g at the end of day 16 as shown in Figure 5-1b. Basic pH ~8.5 systems had minimal dissolution, less than 0.3 ± 0.1 ng/mL/g at the end of day 16 compared to acidic pH ~3.5 with 9.2 ± 1.8 ng/mL/g. Comparable trends were observed elsewhere, with pristine nAg exposed to basic conditions (pH 8.5 to 9) over a long exposure time of 50 days reporting minimal dissolution with precipitation of nAg [60]. In the basic pH ~8.5 conditions, even though the nAg release was higher than that observed in DI water (Figure 5-1a), the dissolution of nAg (3.7 ± 0.8 % dissolved Ag) was inhibited (Figure 5-1c). Other studies have also shown limited dissolution of nAg at basic pH [60, 61]. Liquid stock solution of custom nAg paint before application had 84.2 ± 3.5 % nAg and 15.8 ± 2.9 % dissolved Ag (Figure S5-3), which is comparable to Ag released into DI water after application onto polystyrene surface (82.6 ± 4.9 % nAg and 17.4 ± 5.2 % dissolved Ag) (Figure 5-1c).

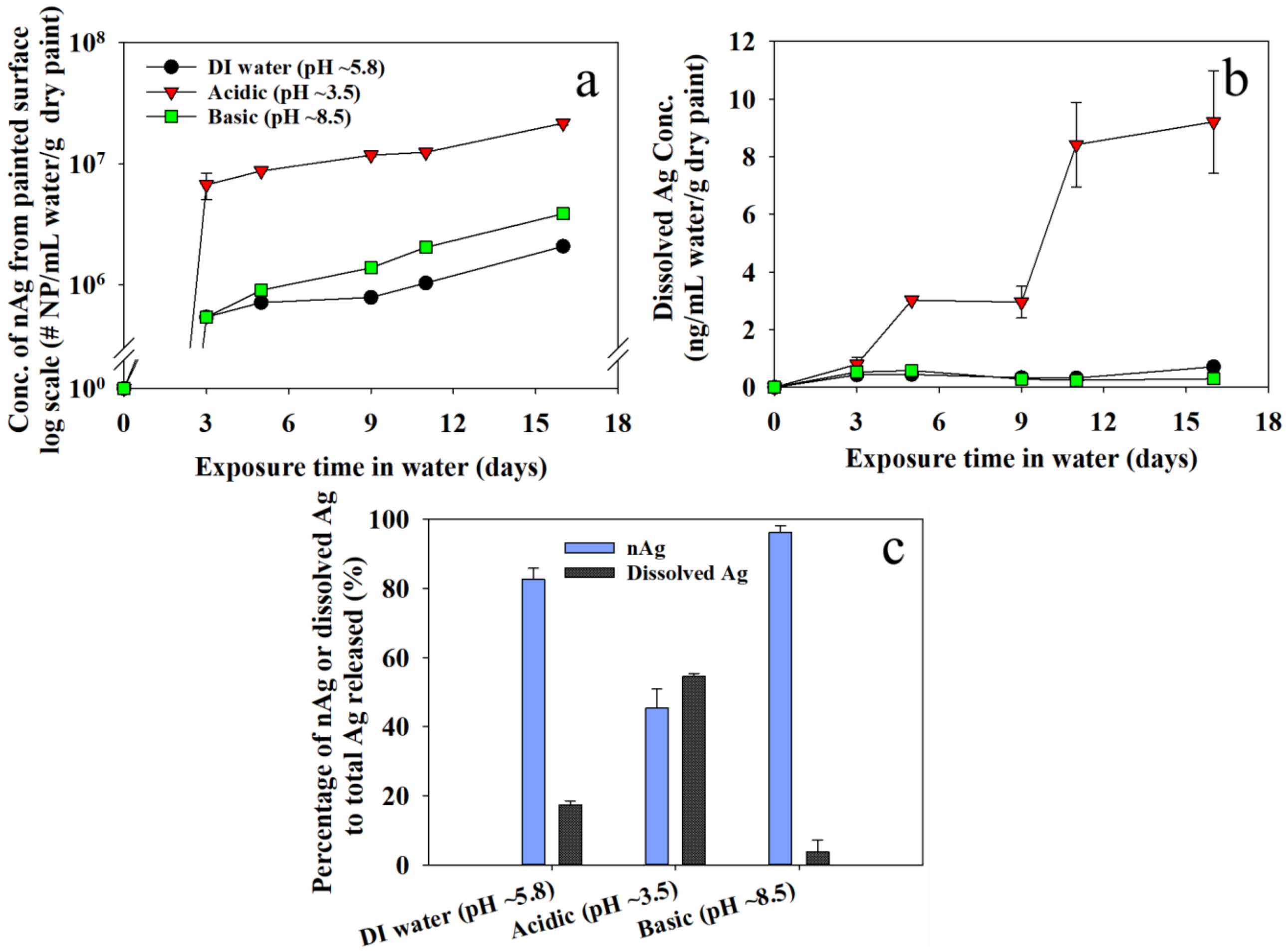

Figure 5-1 Released nAg (a) and dissolved Ag (b) from painted polystyrene surface (custom made paint) exposed to different pH conditions over a period of 16 days (c) shows the variation of dissolved Ag and nAg in DI water pH ~5.8, acidic pH ~3.5 and basic pH ~8.5.

In acidic pH ~3.5 systems, 54.6 ± 4.2% of the total Ag released was dissolved Ag, due to the dissolution of nAg released from the painted surface (Figure 5-1c). The dissolution of the released nAg resulted in smaller-sized nAg with a mean diameter of 37.1 ± 2.1 nm compared to the nAg released into the DI water of 64.6 ± 4.3 nm (Figure 5-2). Although there is no direct evidence, it is also likely that some dissolution of nAg can occur, that remained embedded in the paint on the polystyrene surface. A study on Ag release from nAg embedded in water filter media found 5 to 10 times higher Ag release under acidic conditions (pH 5) compared to neutral(pH 7) or basic pH conditions (pH 9) [62].

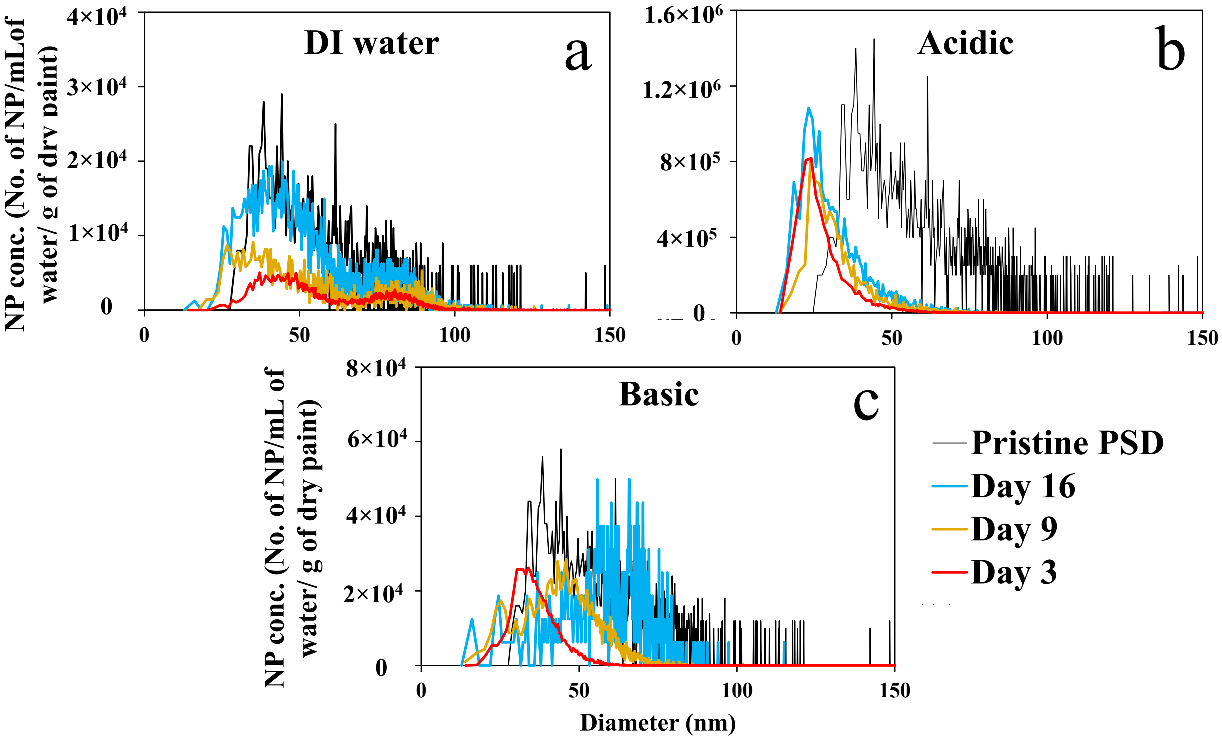

Figure 5-2 Change in particle size distribution (PSD) of released nAg from paint in different pH conditions over a period of 16 days (Day3, 9 and 16) compared to that of pristine nAg PSD obtained using spICP-MS.

In DI water systems, a bimodal size distribution of released nAg was observed at all times. The relative abundance of the smaller sized fraction increased over time suggesting the higher release of smaller particles from paint surface with time(Figure 5-2a). The smaller sized fraction had a mean size of 48.3 ± 3.7 nm with particle concentration of 10^4 particles/mL at 16 days, while the larger sized faction represented aggregates of ENPs of mean size 81.5 ± 5.2 nm with particle concentrations of 10^3 particles/mL at 16 days (Figure 5-2a). In contrast, nAg aggregated over time in the basic pH systems, with particle size increasing from 32.9 ± 1.5 nm at day 3 to 57. 9 ± 4.2 nm at the end of day 16 (Figure 5-2c). Some studies have estimated released NP sizes in basic pH conditions [61, 63, 64]; for instance, Flory et. al (2013) using microscopic and particle sizing techniques (suc as DLS) reported significant aggregation (size up to 4 µm) of pristine nAg at pH 11 [61]. In contrast, several other studies have reported stabilization and lower particle size on exposure to basic pH [60, 65, 66]. These observations suggest that the aggregation of paint released nAg is influenced by interaction of the paint matrix with the basic pH solution.

5.4.2. Effect of sunlight on release of nAg from painted surface

To assess if the releases of nAg to aqueous solutions under quiescent conditions was comparable to releases of nAg from painted surfaces exposed to sunlight parallel outdoor experiments were conducted. PVC rather than polystyrene surfaces were used because the polystyrene surfaces were deformed with continuous sunlight exposure. PVC boards exposed to sunlight over specific periods of time were contacted with water under quiescent conditions for 3 days to assess the readily released fraction of nAg following sunlight exposure. A minimum of 3 days of contact with water was required to obtain measurable amounts of released nAg in the aqueous phase. PVC boards coated with nAg paint with no sunlight exposure released $1.0 \pm 0.04 \times 10^5$ nAg/mL water/g dry paint after 3 days in contact with DI water (Figure 5-3a). After a cumulative 120 h of sunlight exposure, $3.0 \pm 0.1 \times 10^5$ nAg/mL/g was released into the aqueous phase after an identical contact time. This represents a 2.3 fold increase of nAg mass released into the aqueous solution.

Dissolved Ag released from sunlight exposed boards decreased 83.8 % from 6.6 ± 0.9 ng/mL/g with no exposure to sunlight to 1.1 ± 0.02 ng/mL/g after 120 hours of sunlight exposure (Figure 5-3a). A previous study has shown reduced dissolution of nAg in textiles exposed to solar radiation, due to photoreduction of the Ag, leading to almost 100% Ag in metallic form [67].No nAg or dissolved Ag were detected in unpainted PVC boards nor with the ones painted with the metal-free polymeric base paint for the sunlight exposed surfaces, establishing absence of background nAg or dissolved Ag from the environment.

The particle size distribution of nAg released from PVC painted panels show that, with sunlight exposure, the mean size of nAg remained virtually unchanged with 58.7 ± 0.8 nm at 0 h and 53.9 ± 0.3 nm after 120 h exposure (Figure 5-3b). These sizes are similar to primary size of pristine nAg (54.3 ± 7.3 nm) observed in TEM and suggests that the nAg released from sunlight exposed surface are possibly single nAg released along with minute fraction of paint fragments as composite colloids.

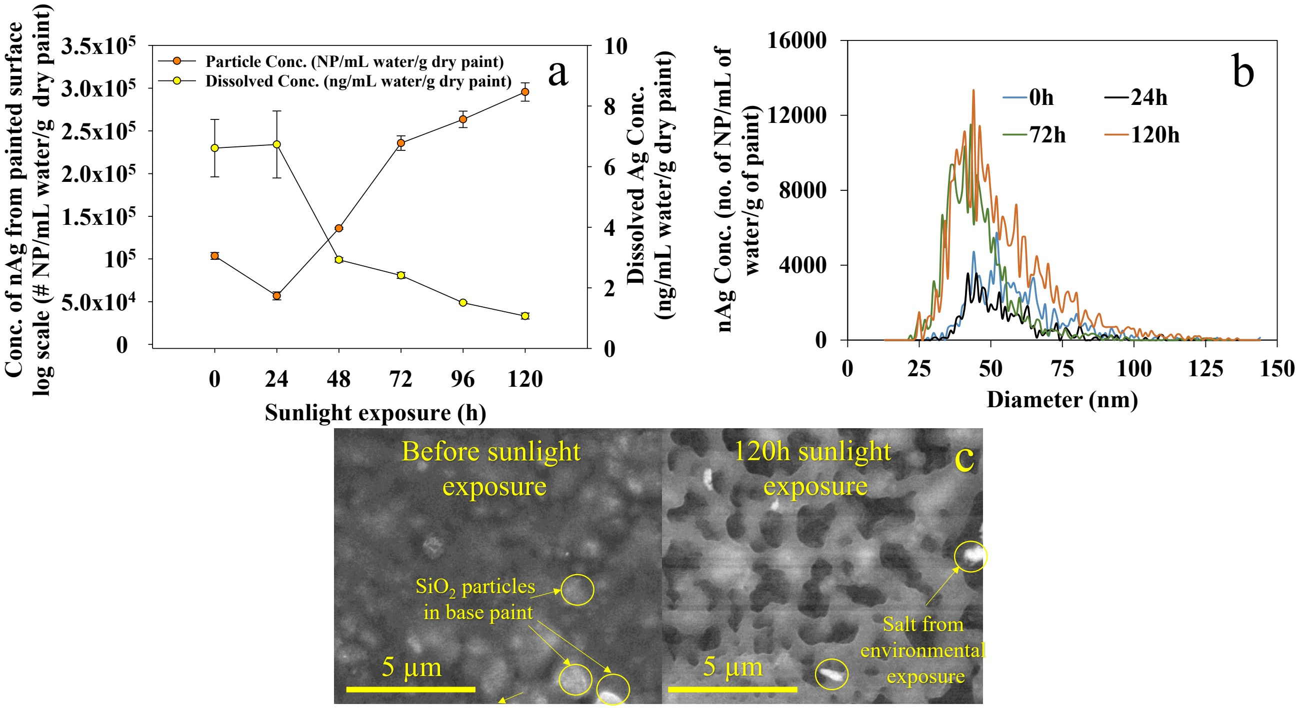

Figure 5-3 a) Release of nAg and dissolved Ag from painted PVC surfaces exposed to sunlight and b) particle size distribution of nAg released from PVC surfaces during the sunlight exposure period of 0 to 120 hours as measured by spICP-MS c) SEM images of PVC painted surface before and after 120h of sunlight exposure showing damage to exposed surface.

SEM images of the 120-h sunlight exposed painted surface revealed fractures in the exposed paint layer (Figure 5-3c). Such deformities in the painted surface have been attributed to photodegradation of the acrylic polymer binder in the paint [2]. ENPs released from sunlight-weathered paints have been shown to be associated with paint and binder fragments, suggesting that the deformations in the surface and photodegradation of the binders contribute to ENP releases. The sunlight exposed surface had salts deposits from the environment. Kaegi et. al. (2010) observed in TEM images that the nAg released from outdoor facades were released as composite colloids associated with organic binders of the paint [6]. Similarly, Al-Kattan et. al.(2015) reported that $nSiO_2$ released from aged (weathered) paint, came associated with paint matrix fragments [25]. Another study by Al-Kattan et. al.(2015) reported that painted panels exposed to simulated sunlight and rainfall released higher amounts of $nTiO_2$ than unexposed panel, due to photocatalytic degradation of the organic paint matrix [19].

The 120-h sunlight-exposed PVC surfaces when immersed in DI water for 3 days released 1.97 times more nAg (57.3 ± 0.9 ng/L more nAg) compared to that released from painted boards immersed in DI water for 8 days without sunlight exposure. This indicates that release of the ENPs from painted surface is not necessarily because of photodegradation of the binder. ENPs are also released during contact with DI water from pores formed during crosslinking reactions of acrylic polymer binder during drying of the wet paint applied on the boards [57, 68, 69]. nAg are released as water permeates into the surface through the pores dislodging them from the binders [57, 58, 69]. Comparing nAg released from PVC and polystyrene painted surfaces upon contact with DI water for 3 days led to comparable concentrations of $1.0 \pm 0.04 \times 10^5$ nAg/mL/g (PVC)and $5.4 \pm 0.21 \times 10^5$ nAg/mL/g (polystyrene). The particle size distributions of released nAg were also observed to be similar.

5.4.3. Colloidal stability and dissolution of pristine nAg and nAg released from painted surfaces

The nAg and nAg-containing paint fragments released from the painted polystyrene surfaces into DI water (pH ~5.8) after sonication were colloidally stable over a period of 15 days (Figure 5-4b) with a constant average mean size of 70.9 ± 3.2 nm (Figure 5-4a) and average nAg concentration in the aqueous phase of 22.6 ± 2.8 ng/mL (Figure 5-4b). However, the mean size of pristine nAg in DI water, changed over time, increasing from 97.1 ± 6.4 nm to 182.0 ± 4.5 nm due to aggregation until day 10, and thereafter, started decreasing to 105.9 ± 19.5 nm by day 15 (Figure 5-4a). The decrease in size by day 15 was associated with a lower concentration as well, reflecting the gravitational settling of larger particles in addition to dissolution of pristine nAg (18.3 ± 0.5 ng/mL at day 0 to 0.27 ± 0.04 ng/mL at day 15) as shown in Figure 5-4c. The particle size distribution of paint-released nAg showed that the released nAg stayed colloidally stable over time, in contrast to the pristine nAg (Figure 5-4b). These patterns are also reflected in the particle size distributions of the two systems (Figure 5-5). TEM images show that the nAg released from paint was associated with chunks of the paint matrix, which may have contributed to its colloidal stability and limited dissolution compared to pristine nAg (Figure S5-2).

Overall, this data suggests that the environmental fate (aggregation potential, colloidal stability, and dissolution patterns) of nAg released from paint would be very different from pristine ENPs. Yet, environmental fate models often use characteristics of pristine ENPs to predict the environmental fate of ENPs released from paints or other products [70]. Robust experimental data on the environmental fate of ENPs released from paints are thus needed to better inform ENP fate models and risk assessments.

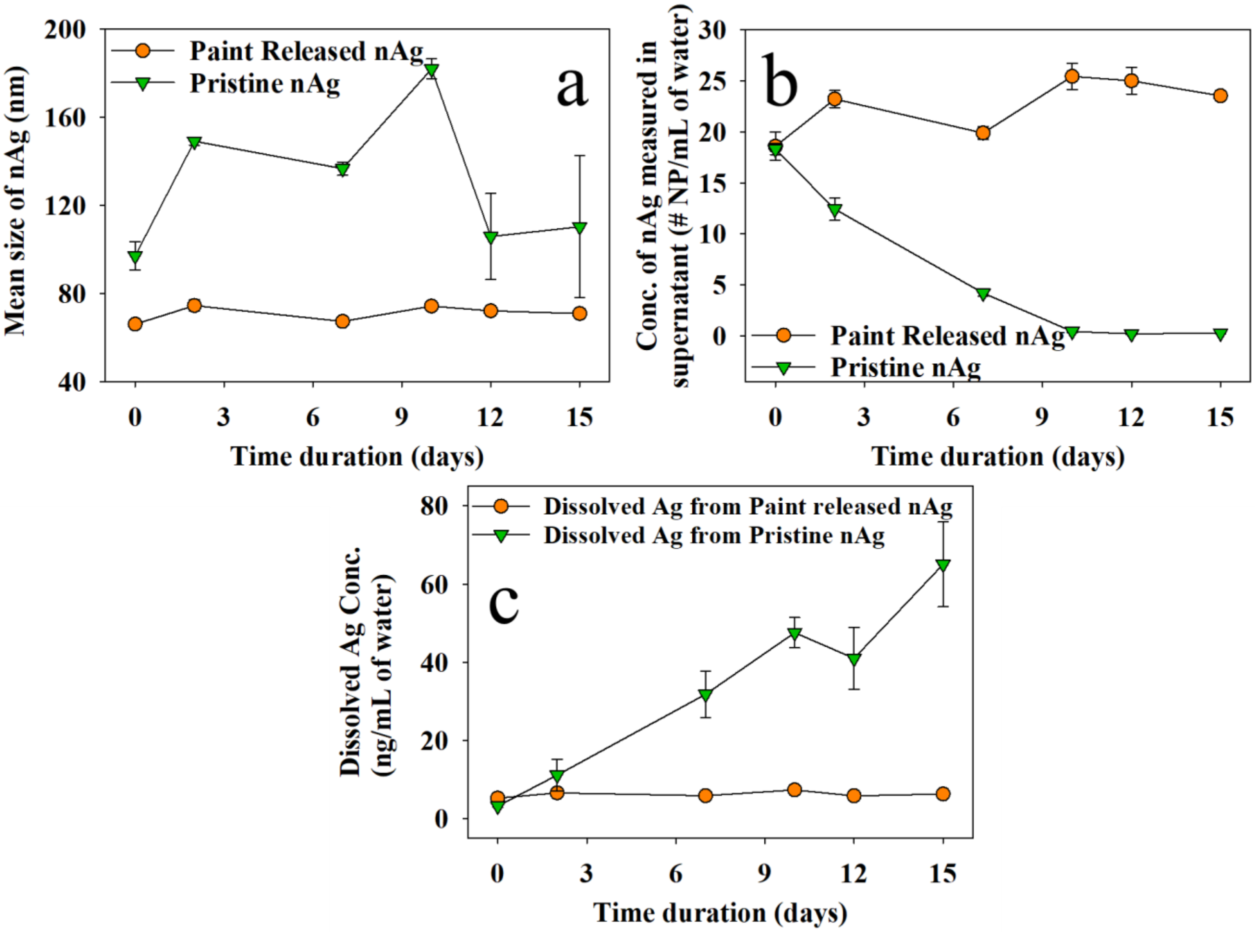

Figure 5-4 Change in (a) mean size (b) nAg concentration, and (c) dissolved Ag concentration over time for pristine nAg and nAg released from the painted polystyrene surface into DI water.

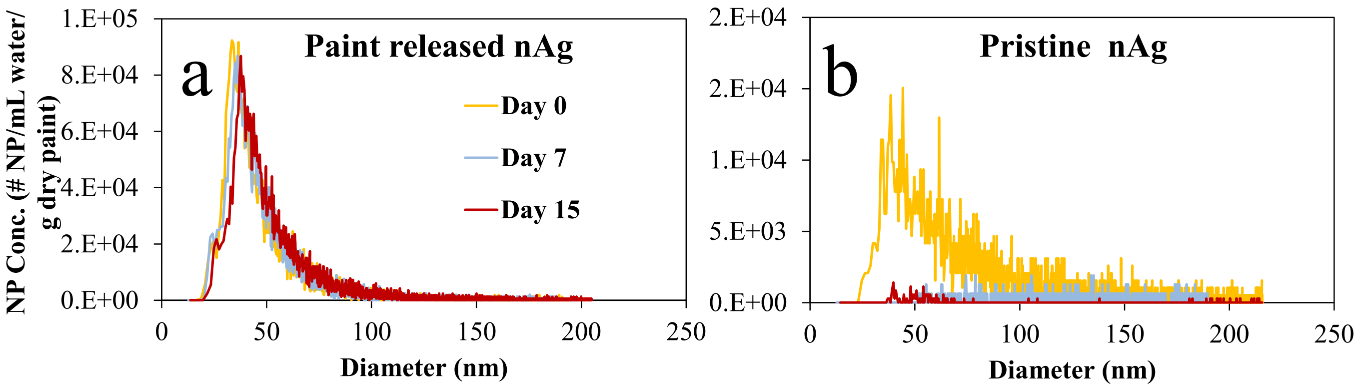

Figure 5-5 Change in particle size distribution of released nAg from paint compared to pristine nAg in DI water over a period of 15 days as measured using spICP-MS.

5.4.4. Culturability of *E. coli D21* in pristine nAg and released nAg from painted polystyrene surfaces

E. coli D21 culturability assays (CFU/mL) for both control systems with filter sterile 10 mM KNO_3 and pristine nAg remained unchanged over 42 h. A faster rate of decline in culturability was observed in microcosms containing aqueous phases collected after sonication of surfaces coated with base paint and nAg-containing paint (Figure 5-6). The CFU/mL in base paint declined by more than two-fold during the first 10 h; by 24 hours no colonies were observed. A more severe decline was observed in case of the nAg released from paint; after 3 h, there were no more viable colonies (Figure 5-6). This indicates that disinfection of *E. coli D21* exposed to nAg released from painted surfaces is much higher than when exposed to pristine nAg only, implying higher bactericidal activity in nAg released from painted surfaces. This observation is in line with studies by Holtz et al. (2012) [7] that depict more than 3-log decrease in bacterial cell counts *(Staphylococcus aureus BEC9393, Enterococcus faecalis ATCC21814, E. coli ATCC 25922 and Salmonella enterica Typhimurium strain LT2)* within 5 hours, when exposed to paints containing nAg. A previous study has reported low or no growth of Gram-positive pathogenic *Staphylococcus aureus* and Gram-negative *E. coli* on glass slides coated with nAg paint- formulations, indicating strong bactericidal activity of nAg containing paint[8]. Possible reasons for the increase in disinfection may be matrix (i.e., paint)–associated effects. These observations indicate the use of nAg in paints can be advantageous to help disinfect various bacteria and viruses from the surface [9, 13, 71, 72].

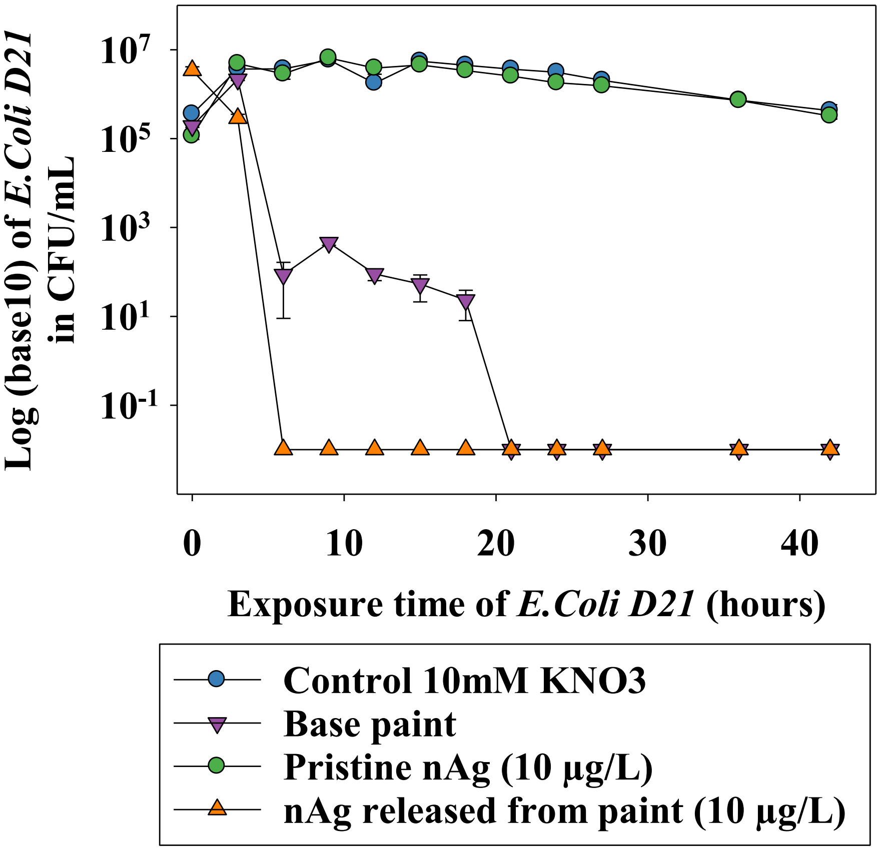

Figure 5-6 Culturability assay of *E. coli D21* exposed to pristine nAg and nAg released from painted surfaces

5.5. Conclusions

The behaviour and characteristics of nAg released from painted surfaces depends on sunlight exposure and pH conditions of the environment. Painted surfaces exposed to sunlight showed increased release of nAg with time due to degradation of the polymeric binder. The mean size of nAg released were in the similar range of mean size calculated using TEM, suggesting that single nAg is released along with a paint fragment. Acid rain precipitation conditions (pH ~3.5) can release more nAg in article and dissolved forms from painted surfaces. However, nAg release in basic pH ~8.5 conditions is associated with greater aggregation with minimal dissolution.

Studies on environmental fate of ENPs have typically been performed with pristine, as-synthesized or as-manufactured NPs, which may not reflect the environmental fate of ENPs released from products with matrix associated with them. This study shows that the nAg released from paint can behave differently compared to pristine nAg with respect to aggregation potential, colloidal stability, dissolution and toxicity, Culturability tests with *E. coli D21* suspended in aqueous extracts (neutral pH) of painted surfaces showed that cells were non-culturable after 3 hours whereas there was no impact on culturability of cells exposed to pristine nAg over 42 h. Thus, nAg can be added to paints and coatings to improve the disinfection capabilities against bacteria and viruses [9, 13, 71, 72]. Our results signify the necessity of toxicity and fate studies using released ENPs from products, rather than pristine ENPs, to capture the associated matrix (i.e, paint) effects.

5.6. Acknowledgment

We acknowledge the assistance of David Liu, McGill University for TEM/EDS and SEM analysis. We thank Société Laurentide for helping us with preparation of custom-made paint. The research was supported by the Natural Sciences and Engineering Research Council of Canada, Environment and Climate Change Canada and Cascades Canada ULC. A. A. R was supported by McGill Engineering Doctoral Award.

5.7. Supplementary information

Table S5-1 Single Particle ICP-MS Instrumental Parameters

Parameter Value	
Sample Uptake Rate	0.28-0.34 mL/min
Nebulizer gas flow	0.97-1.03 L/min
Nebulizer	Meinhard Glass Concentric
Spray Chamber	Meinhard Glass Cyclonic
RF Power	1600 W

Analyte	Ag107
Analysis time	100-150 s
Dwell time	100 µs

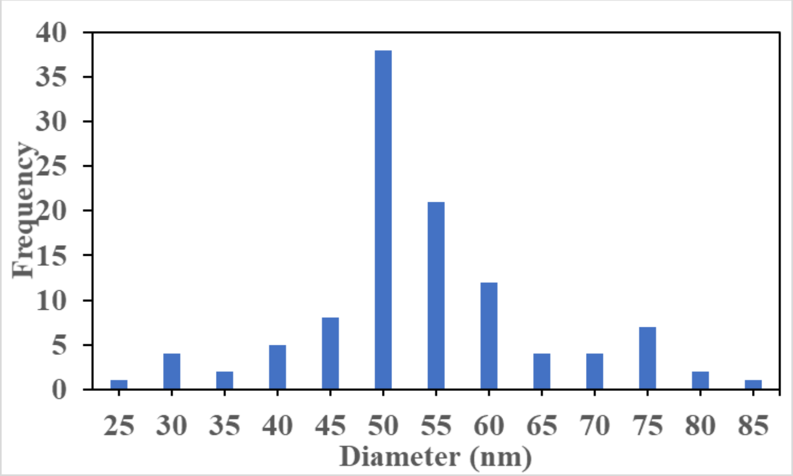

Figure S5-1 Primary particle size distribution from TEM images (n=109) of pristine nAg used in paints.

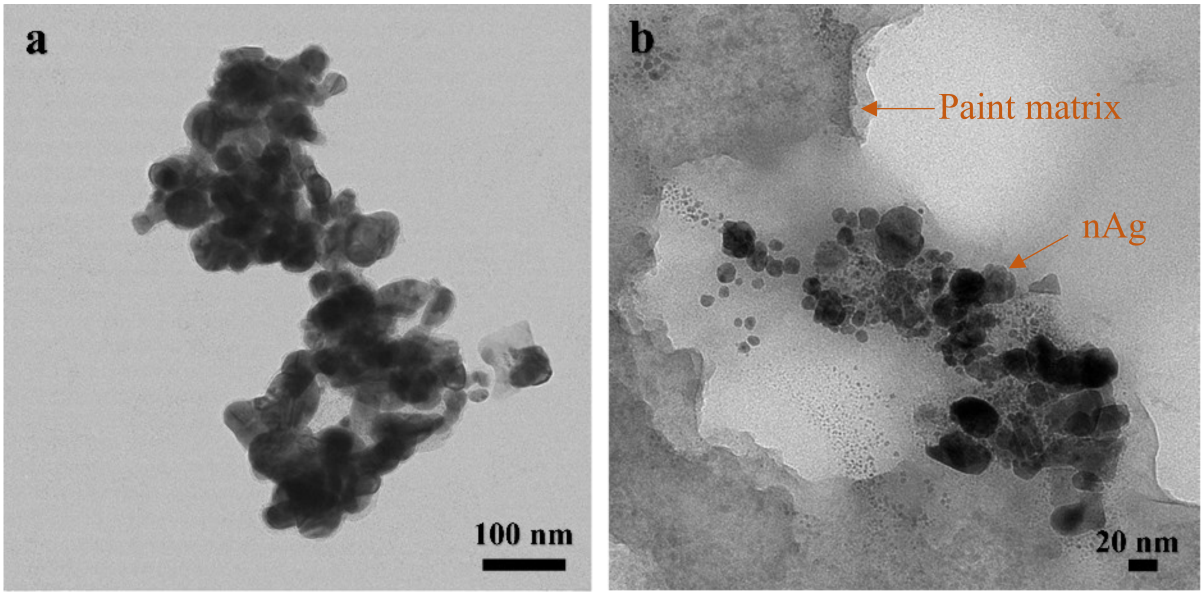

Figure S5-2 TEM images of pristine and released nAg from custom made paint (a) pristine nAg (b) nAg released from painted surface.

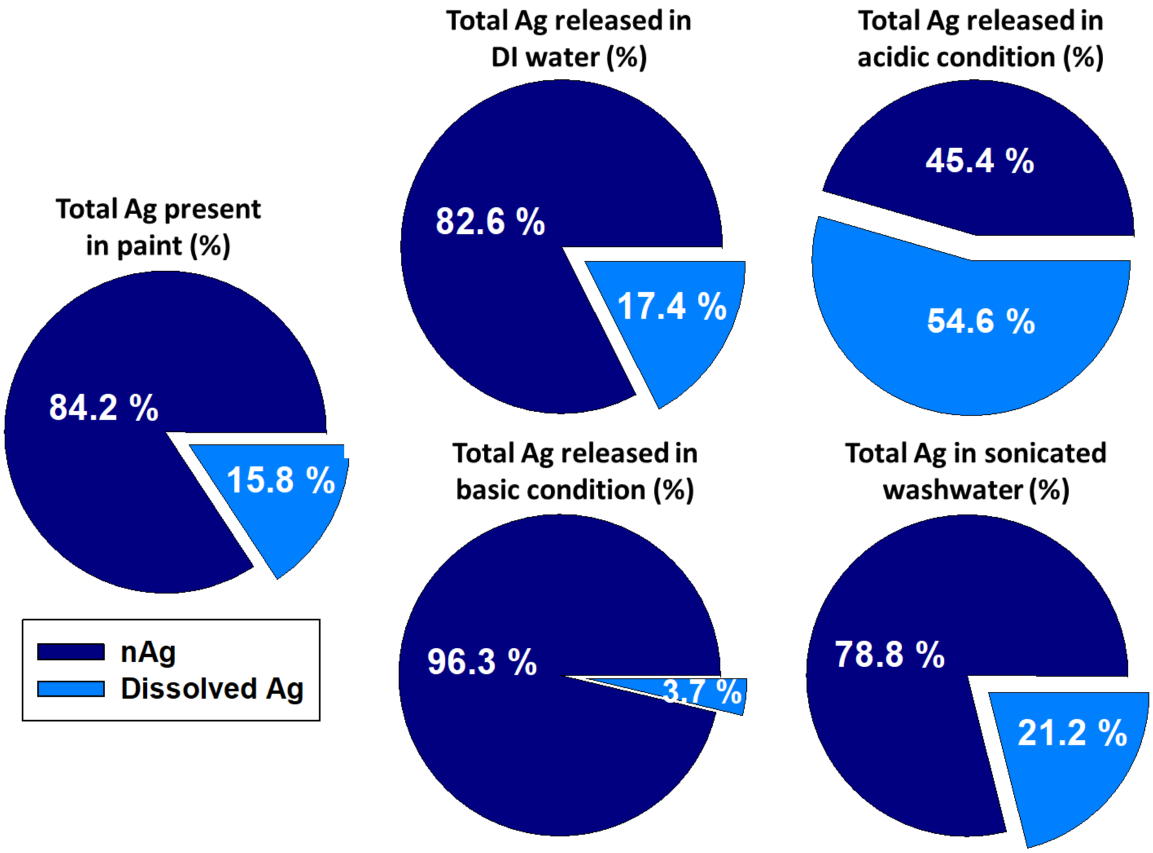

Figure S5-3 Percentage of dissolved Ag and nAg in the total Ag released under different conditions compared to initial state in the paint.

5.8. References

1. Keller, A.A. and A. Lazareva, *Predicted releases of engineered nanomaterials: From global to regional to local.* Environmental Science & Technology Letters, 2013. **1**(1): p. 65-70.
2. Marolt, T., et al., *Photocatalytic activity of anatase-containing facade coatings.* Surface and Coatings Technology, 2011. **206**(6): p. 1355-1361.
3. Künniger, T., et al., *Release and environmental impact of silver nanoparticles and conventional organic biocides from coated wooden façades.* Environmental Pollution, 2014. **184**: p. 464-471.
4. Zhou, S., et al., *The change of the properties of acrylic-based polyurethane via addition of nano-silica.* Progress in Organic Coatings, 2002. **45**(1): p. 33-42.
5. Westerhoff, P.K., M.A. Kiser, and K. Hristovski, *Nanomaterial removal and transformation during biological wastewater treatment.* Environmental Engineering Science, 2013. **30**(3): p. 109-117.

6. Kaegi, R., et al., *Release of silver nanoparticles from outdoor facades.* Environ Pollut, 2010. **158**(9): p. 2900-5.
7. Holtz, R.D., et al., *Nanostructured silver vanadate as a promising antibacterial additive to water-based paints.* Nanomedicine: Nanotechnology, Biology and Medicine, 2012. **8**(6): p. 935-940.
8. Kumar, A., et al., *Silver-nanoparticle-embedded antimicrobial paints based on vegetable oil.* Nature materials, 2008. **7**(3): p. 236-241.
9. Elechiguerra, J.L., et al., *Interaction of silver nanoparticles with HIV-1.* Journal of nanobiotechnology, 2005. **3**(1): p. 6.
10. Tiller, J., C. Sprich, and L. Hartmann, *Amphiphilic conetworks as regenerative controlled releasing antimicrobial coatings.* Journal of Controlled Release, 2005. **103**(2): p. 355-367.
11. Aymonier, C., et al., *Hybrids of silver nanoparticles with amphiphilic hyperbranched macromolecules exhibiting antimicrobial properties.* Chemical Communications, 2002(24): p. 3018-3019.
12. Lu, L., et al., *Silver nanoparticles inhibit hepatitis B virus replication.* Antiviral therapy, 2008. **13**(2): p. 253.
13. Park, S., et al., *Antiviral properties of silver nanoparticles on a magnetic hybrid colloid.* Appl. Environ. Microbiol., 2014. **80**(8): p. 2343-2350.
14. Auyeung, A., et al., *Effective Control of Molds Using a Combination of Nanoparticles.* PloS one, 2017. **12**(1): p. e0169940-e0169940.
15. Saber, A.T., et al., *Nanotitanium dioxide toxicity in mouse lung is reduced in sanding dust from paint.* Particle and Fibre Toxicology, 2012. **9**(1): p. 4.
16. Smulders, S., et al., *Toxicity of Nanoparticles Embedded in Paints Compared with Pristine Nanoparticles in Mice.* Toxicological Sciences, 2014. **141**(1): p. 132-140.
17. Smulders, S., et al., *Toxicity of nanoparticles embedded in paints compared to pristine nanoparticles, in vitro study.* Toxicology Letters, 2015. **232**(2): p. 333-339.
18. Starnes, D.L., et al., *Distinct transcriptomic responses of Caenorhabditis elegans to pristine and sulfidized silver nanoparticles.* Environmental Pollution, 2016. **213**: p. 314-321.
19. Al-Kattan, A., et al., *Release of TiO2 from paints containing pigment-TiO2 or nano-TiO2 by weathering.* Environmental Science: Processes & Impacts, 2013. **15**(12): p. 2186-2193.
20. Al-Kattan, A., et al., *Behavior of TiO2 Released from Nano-TiO2-Containing Paint and Comparison to Pristine Nano-TiO2.* Environmental Science & Technology, 2014. **48**(12): p. 6710-6718.
21. Mizutani, T., et al., *Application of silica-containing nano-composite emulsion to wall paint: A new environmentally safe paint of high performance.* Progress in Organic Coatings, 2006. **55**(3): p. 276-283.
22. Zuin, S., et al., *Leaching of nanoparticles from experimental water-borne paints under laboratory test conditions.* Journal of nanoparticle research, 2014. **16**(1): p. 2185.
23. Adeleye, A.S., et al., *Release and detection of nanosized copper from a commercial antifouling paint.* Water Research, 2016. **102**: p. 374-382.
24. Kägi, R., et al., *Synthetic TiO2 nanoparticle emission from exterior facades into the aquatic environment.* Environmental pollution, 2008. **156**(2): p. 233-239.
25. Al-Kattan, A., et al., *Characterization of materials released into water from paint containing nano-SiO2.* Chemosphere, 2015. **119**: p. 1314-1321.

26. Olabarrieta, J., et al., *Aging of photocatalytic coatings under a water flow: Long run performance and TiO2 nanoparticles release.* Applied Catalysis B: Environmental, 2012. **123-124**: p. 182-192.
27. Zhang, X., et al., *Effects of weathering and rainfall conditions on the release of SiO2, Ag, and TiO2 engineered nanoparticles from paints.* Journal of Nanoparticle Research, 2017. **19**(10): p. 338.
28. Clar, J.G., et al., *Release and transformation of ZnO nanoparticles used in outdoor surface coatings for UV protection.* Science of The Total Environment, 2019. **670**: p. 78-86.
29. Azimzada, A., et al., *Release of TiO2 nanoparticles from painted surfaces in cold climates: characterization using a high sensitivity single-particle ICP-MS.* Environmental Science: Nano, 2020. **7**(1): p. 139-148.
30. Azimzada, A., et al., *Single- and Multi-Element Quantification and Characterization of TiO2 Nanoparticles Released From Outdoor Stains and Paints.* Frontiers in Environmental Science, 2020. **8**(91).
31. Domingos, R.F., et al., *Characterizing manufactured nanoparticles in the environment: multimethod determination of particle sizes.* Environmental science & technology, 2009. **43**(19): p. 7277-7284.
32. Bian, S.-W., et al., *Aggregation and dissolution of 4 nm ZnO nanoparticles in aqueous environments: influence of pH, ionic strength, size, and adsorption of humic acid.* Langmuir, 2011. **27**(10): p. 6059-6068.
33. Furtado, L.M., et al., *The persistence and transformation of silver nanoparticles in littoral lake mesocosms monitored using various analytical techniques.* Environmental Chemistry, 2014. **11**(4): p. 419-430.
34. Furtado, L.M., et al., *Environmental Fate of Silver Nanoparticles in Boreal Lake Ecosystems.* Environ Sci Technol, 2015. **49**(14): p. 8441-50.
35. Barton, L.E., et al., *Heteroaggregation, transformation and fate of CeO2 nanoparticles in wastewater treatment.* Environmental Pollution, 2015. **203**: p. 122-129.
36. M. Furtado, L., M. Bundschuh, and C. D. Metcalfe, *Monitoring the Fate and Transformation of Silver Nanoparticles in Natural Waters*. Vol. 97. 2016.
37. Liu, J., Y.S. Hwang, and J.J. Lenhart, *Heteroaggregation of bare silver nanoparticles with clay minerals.* Environmental Science: Nano, 2015. **2**(5): p. 528-540.
38. Ellis, L.-J.A., et al., *Impact of surface coating and environmental conditions on the fate and transport of silver nanoparticles in the aquatic environment.* Science of The Total Environment, 2016. **568**: p. 95-106.
39. Yang, X., et al., *Mechanism of Silver Nanoparticle Toxicity Is Dependent on Dissolved Silver and Surface Coating in Caenorhabditis elegans.* Environmental Science & Technology, 2012. **46**(2): p. 1119-1127.
40. Ribeiro, F., et al., *Bioaccumulation of silver in Daphnia magna: Waterborne and dietary exposure to nanoparticles and dissolved silver.* Science of The Total Environment, 2017. **574**: p. 1633-1639.
41. Gagné, F., et al., *Sublethal Effects of Silver Nanoparticles and Dissolved Silver in Freshwater Mussels.* Journal of Toxicology and Environmental Health, Part A, 2013. **76**(8): p. 479-490.
42. Reidy, B., et al., *Mechanisms of silver nanoparticle release, transformation and toxicity: a critical review of current knowledge and recommendations for future studies and applications.* Materials, 2013. **6**(6): p. 2295-2350.

43. Mitrano, D.M., et al., *Silver nanoparticle characterization using single particle ICP-MS (SP-ICP-MS) and asymmetrical flow field flow fractionation ICP-MS (AF4-ICP-MS).* Journal of Analytical Atomic Spectrometry, 2012. **27**(7): p. 1131-1142.
44. Lee, S., et al., *Nanoparticle size detection limits by single particle ICP-MS for 40 elements.* Environmental science & technology, 2014. **48**(17): p. 10291-10300.
45. Montaño, M., et al., *Improvements in the detection and characterization of engineered nanoparticles using spICP-MS with microsecond dwell times.* Environmental Science: Nano, 2014. **1**(4): p. 338-346.
46. Laborda, F., et al., *Selective identification, characterization and determination of dissolved silver (I) and silver nanoparticles based on single particle detection by inductively coupled plasma mass spectrometry.* Journal of Analytical Atomic Spectrometry, 2011. **26**(7): p. 1362-1371.
47. Kim, H.-A., et al., *Characterization of silver nanoparticle aggregates using single particle-inductively coupled plasma-mass spectrometry (spICP-MS).* Chemosphere, 2017. **171**: p. 468-475.
48. Telgmann, L., et al., *Single particle ICP-MS as a tool for determining the stability of silver nanoparticles in aquatic matrixes under various environmental conditions, including treatment by ozonation.* Analytical and Bioanalytical Chemistry, 2016. **408**(19): p. 5169-5177.
49. Deng, Y., et al., *Multiple Method Analysis of TiO2 Nanoparticle Uptake in Rice (Oryza sativa L.) Plants.* Environmental Science & Technology, 2017. **51**(18): p. 10615-10623.
50. Azodi, M., Y. Sultan, and S. Ghoshal, *Dissolution Behavior of Silver Nanoparticles and Formation of Secondary Silver Nanoparticles in Municipal Wastewater by Single-Particle ICP-MS.* Environmental Science & Technology, 2016. **50**(24): p. 13318-13327.
51. Montaño, M.D., et al., *Single Particle ICP-MS: Advances toward routine analysis of nanomaterials.* Analytical and Bioanalytical Chemistry, 2016. **408**(19): p. 5053-5074.
52. Wyrwicka, A. and M. Skłodowska, *Influence of repeated acid rain treatment on antioxidative enzyme activities and on lipid peroxidation in cucumber leaves.* Environmental and Experimental Botany, 2006. **56**(2): p. 198-204.
53. Wang, M., et al., *Effect of simulated acid rain on fluorine mobility and the bacterial community of phosphogypsum.* Environmental Science and Pollution Research, 2018. **25**(16): p. 15336-15348.
54. Singh, S., S.P. Elumalai, and A.K. Pal, *Rain pH estimation based on the particulate matter pollutants and wet deposition study.* Science of The Total Environment, 2016. **563-564**: p. 293-301.
55. Croll, S.G. and C.A. Taylor, *Hydrated alumina surface treatment on a titanium dioxide pigment: Changes at acidic and basic pH.* Journal of Colloid and Interface Science, 2007. **314**(2): p. 531-539.
56. Bauer, D., *Degradation of organic coatings. I. Hydrolysis of melamine formaldehyde/acrylic copolymer films.* Journal of Applied Polymer Science, 1982. **27**(10): p. 3651-3662.
57. Dillon, C.E., A.F. Lagalante, and R.C. Wolbers, *Acrylic emulsion paint films: The effect of solution pH, conductivity, and ionic strength on film swelling and surfactant removal.* Studies in Conservation, 2014. **59**(1): p. 52-62.

58. Elliott, J.E., et al., *Structure and swelling of poly(acrylic acid) hydrogels: effect of pH, ionic strength, and dilution on the crosslinked polymer structure.* Polymer, 2004. **45**(5): p. 1503-1510.
59. Rodgers, W., D. Garner, and G. Cheever, *Study of the attack of acidic solutions on melamine-acrylic basecoat/clearcoat paint systems.* Journal of Coatings Technology, 1998. **70**(877): p. 83-95.
60. Zhou, W., et al., *Effects of pH, Electrolyte, Humic Acid, and Light Exposure on the Long-Term Fate of Silver Nanoparticles.* Environmental Science & Technology, 2016. **50**(22): p. 12214-12224.
61. Flory, J., et al., *Influence of pH on the transport of silver nanoparticles in saturated porous media: laboratory experiments and modeling.* Journal of Nanoparticle Research, 2013. **15**(3): p. 1484.
62. Mittelman, A.M., et al., *Silver Dissolution and Release from Ceramic Water Filters.* Environmental Science & Technology, 2015. **49**(14): p. 8515-8522.
63. Illés, E. and E. Tombácz, *The effect of humic acid adsorption on pH-dependent surface charging and aggregation of magnetite nanoparticles.* Journal of Colloid and Interface Science, 2006. **295**(1): p. 115-123.
64. Romanello, M.B. and M.M. Fidalgo de Cortalezzi, *An experimental study on the aggregation of TiO2 nanoparticles under environmentally relevant conditions.* Water Research, 2013. **47**(12): p. 3887-3898.
65. Siddiq, A.M., et al., *Influence of pH on interaction of silver nanoparticles - protein: Analyses by spectroscopic and thermodynamic ideology.* Colloids and Surfaces B: Biointerfaces, 2019. **184**: p. 110524.
66. Akaighe, N., et al., *Transport and deposition of Suwannee River Humic Acid/Natural Organic Matter formed silver nanoparticles on silica matrices: The influence of solution pH and ionic strength.* Chemosphere, 2013. **92**(4): p. 406-412.
67. Mitrano, D.M., et al., *Unraveling the Complexity in the Aging of Nanoenhanced Textiles: A Comprehensive Sequential Study on the Effects of Sunlight and Washing on Silver Nanoparticles.* Environmental Science & Technology, 2016. **50**(11): p. 5790-5799.
68. Zuin, S., et al., *Formulation effects on the release of silica dioxide nanoparticles from paint debris to water.* Science of the Total Environment, 2014. **476**: p. 298-307.
69. Parvate, S. and P. Mahanwar, *Insights into the preparation of water-based acrylic interior decorative paint: tuning binder's properties by self-crosslinking of allyl acetoacetate-hexamethylenediamine.* Progress in Organic Coatings, 2019. **126**: p. 142-149.
70. Quik, J.T., J.J. de Klein, and A.A. Koelmans, *Spatially explicit fate modelling of nanomaterials in natural waters.* Water research, 2015. **80**: p. 200-208.
71. Lara, H.H., et al., *Mode of antiviral action of silver nanoparticles against HIV-1.* Journal of nanobiotechnology, 2010. **8**(1): p. 1.
72. Mori, Y., et al., *Antiviral activity of silver nanoparticle/chitosan composites against H1N1 influenza A virus.* Nanoscale research letters, 2013. **8**(1): p. 93.

Connecting text from Chapter 5 to Chapter 6

nAg used in paints for it antimicrobial properties and the concentration of nAg in paints are much lower compared to $nTiO_2$. However, $nTiO_2$ is one of the major NPs used in paints and coatings for its photocatalytic properties and UV protection. About one third of global $nTiO_2$ produced is used in paints and coating, improving the properties of the paint. The paint is composed of 10 to 30% of its weight as $nTiO_2$. The degradation of painted surfaces releases NPs along with the paint matrix. The behavior of pristine $nTiO_2$ and released $nTiO_2$ from the painted surface should be analysed to assess their fate and toxicity. In this study, release of $nTiO_2$ from painted surfaces using both commercial and custom-made paint under various pH conditions were characterized for size, concentration and particle size distribution by analyses of the aqueous wash samples by ICP-MS in single particle mode (spICP-MS). Finally, culturability test on survival of *E. coli D21* were compared between $nTiO_2$ released from paint, base paint, and pristine $nTiO_2$

CHAPTER 6 RELEASE OF TITANIUM DIOXIDE NANOPARTICLES FROM PAINTED SURFACES TO WATER AND THEIR IMPACTS

Abstract

$nTiO_2$ is one of the major ENPs used in paints for its photocatalytic properties and UV protection. The behavior of pristine $nTiO_2$ and released $nTiO_2$ from the painted surface should be analysed to understand their fate and toxicity. The aim of the study is to quantify the fraction of $nTiO_2$ released from painted surfaces (commercial and custom-made paints) over time due to contact with different pH solutions and/or direct exposure to sunlight; and to compare the colloidal stability and bacterial toxicity of the pristine $nTiO_2$ and released $nTiO_2$ from painted surface embedded (custom-made paint) in the paint matrix. Comparison of four commercial paints with unknown concentration of $nTiO_2$ showed that B-NP ext. (claimed to have NPs) released 11 to 16 times lower $nTiO_2$ of 1 to 2 ng/mL of water/g of dry paint compared to other commercial paints ~ 10 to 30 ng/mL/g. At acidic pH 3.5-4.2, $nTiO_2$ released from commercial paint on surfaces were 20 to 42% more compared to neutral or basic for three paints except for A ext. paint. Custom made paint with $nTiO_2$ at acidic pH of ~3.5 and basic pH ~8.5 lead to aggregation and settling of $nTiO_2$ compared to DI water (pH ~5.8). Sonication of the collected wash water from acidic pH ~3.5 released twice the particle number compared to basic pH ~8.5 and DI water at pH ~5.8 at the end of 11 days. Custom made paint with $nTiO_2$ behaves similarly to commercial paint B-NP ext., with concentrations of ENP released around ~1.7 ng/mL/g in quiescent systems exposed to DI water, acidic and basic conditions. Finally, disinfection tests on survival of *E. coli D21* showed that $nTiO_2$ released from paint were toxic after 6 hours compared to base paint (which recorded survival up to 18 h) and pristine $nTiO_2$, where the *E. coli D21* survival was present through the experiment period of 42 h.

.

6.1. Introduction

Titanium dioxide nanoparticles ($nTiO_2$) are being used as pigments in a variety of products such as paints, enamels, foods, pharmaceuticals, cosmetics and toothpastes for their color, photocatalytic activity and UV-protection [1, 2]. About 30% of the global production of $nTiO_2$ are used in paints and coatings [3, 4]. There is a need to characterize the release of NPs from high-volume products such as paints and coatings, which are considered an important source of NPs entering the WWTPs and surface water. During environmental exposures to precipitation, solar and temperature conditions, the NPs are released along with binders into the environment [5] with some studies showing large aggregates of $nSiO_2$ [5, 6] and others showing NPs less than 15nm nAg being removed from the surface [7]. The concentration of TiO_2 pigment varies 10 to 30% by weight of the paint as noted from safety data sheets. Previous studies have shown that the paint matrix is degraded due to photocatalytic activity, releasing close to 1% of the total TiO_2 in paint from the painted surface due to environmental exposures [5, 7, 8]. Kaegi et al. (2008) [9] have shown that $nTiO_2$ gets released into natural surface waters from painted facades. Even though the percentage of release is low, $nTiO_2$ concentrations as high as 10 mg/L were released during a rainfall event [5, 7, 10].

Many studies have undergone the assessment of release of several NPs. To begin with, a recent study focused on the characterization of $nTiO_2$ released from outdoor paints exposed to rainfall and snow, using single particle mode inductively coupled plasma mass spectrometry (spICP-MS), has reported a release of NPs with sizes ranging between 20 and 60 nm, and concentrations less than 0.0001% released from the painted surfaces [11]. Similarly, another study reported $nTiO_2$ release from painted surface after precipitation, with sizes ranging between 15 and 120 nm, and association with Al (20%) and Zr (1%) from the paint; these results were obtained using spICP-MS and spICP-time of flight-MS (spICP-TOF-MS) to directly measure the particle size distribution, concentration of NP and association with other metals [12]. Furthermore, the release of nCu from painted specimens of wood and aluminum immersed in water was assessed for a period longer than 180 days, where the aqueous sample collected was analysed using microscopic techniques and inductively coupled plasma atomic emission spectroscopy (ICP-AES) by acid digestion [13]. Moreover, nCu was indirectly measured (without any size information) by filtering the sample through a 0.2 µm filter, subsequent acid digestion of the filter and ICP-AES analysis. Several other studies focused on the release of nAg and $nTiO_2$ from painted outdoor facades, by first collecting wash water from precipitation, and then applying a microscopic analysis and acid digestion with subsequent total metal analysis using Inductively coupled plasma mass spectrometric analysis (ICP-MS) [7, 9]. For example, Kaegi et al (2010) reported a release of 30% of Ag over a period of two months from an outdoor façade coated with a paint containing nAg, from periodical rainfall events [7]. Finally, other studies quantified the NP concentration released from paints or coatings using microscopic data and/or acid digestion, followed by total metal measurement [5, 8, 10, 14-17]. However, these latter studies reported indirect NP concentrations, and do not provide adequate or reliable characterization (no particle size distribution and NP concentration reported).

Studies have shown that the stability and toxicity of $nTiO_2$ depend on the particle size and aggregation state [18-21]. Incorporation of $nTiO_2$ in commercial paints and coatings imparts antimicrobial activity and prevents degradation and deterioration of external surfaces and facades [22]. When exposed to UV light, generation of reactive oxygen species (ROS) occurs in surfaces coated with TiO_2-containing paints which inactivates viruses and bacteria [23]. This is also, in part due to the two crystalline forms of $nTiO_2$-anatase and rutile that show different photoactive behavior [24]. Studies on paint and coatings modified to contain $nTiO_2$ reported antiviral and antimicrobial effect in several microorganisms due to photocatalysis, NP size, and ROS generation [25-30].

$nTiO_2$ released from paint surfaces comes along with the paint matrix, resin binders etc., which may perhaps change the toxicity and fate of the nanoparticles in the environment compared to pristine $nTiO_2$. To assess the fate of NPs in the environment, very precise analytical approaches are needed to track the low levels of the particles. Extremely sensitive analytical techniques are required to measure environmentally relevant concentrations of NPs. Although some recent studies have used spICP-MS to characterize $nTiO_2$ [11, 12], the majority of the studies have largely either relied on electron microscopy techniques and/or have reported total metal concentrations released into the aqueous media for NPs [5, 7-10, 13, 14, 16, 17]. spICP-MS is a powerful technique for measuring metal NP sizes and concentrations in relatively pure aqueous samples at sub parts per billion concentrations [31-33]. Researchers have analyzed the feasibility of setting spICP-MS size detection limits for frequently used NPs, and a theoretical limit of 91 nm was found suitable for

TiO_2 [32]. The spICP-MS method has been developed extensively in literature, and the tool has been used for tracking engineering NPs [34-40]. However, titanium measurement at isotope mass 48 (abundance of 73.7%) using spICP-MS in complex water systems is challenging due to interferences in the instrument (^{48}Ca being one of the major one [32, 40, 41]). Titanium isotopic mass of 47 (abundance 7.4%) is used to avoid most of the interferences while measuring in complex water samples. The detection limit of size at isotope 47 of titanium is around 40 nm [42].

The objectives of this study were to (i) quantify the fraction of $nTiO_2$ released from painted surfaces (commercial and custom-made paints) over time due to contact with different pH solutions and/or direct exposure to sunlight; and to (ii) compare the colloidal stability and bacterial toxicity of the pristine $nTiO_2$ and released $nTiO_2$ from painted surface embedded (custom-made paint) in the paint matrix. In this study, we synthesized a paint containing a pigment and metal-free polymeric base-paint and a well-characterized pristine $nTiO_2$ at a known concentration. Four white commercial paints (3 exterior and 1 interior) with unknown $nTiO_2$ were purchased for the study of the effect of pH and for comparison with custom made paint. The paints with $nTiO_2$ (both custom-made and four commercial paints) were uniformly applied on plastic paint performance testing surfaces and immersed water in the dark with different pH solutions (acidic pH ~3.5, DI water pH ~5.8 and basic pH ~8.5). The aqueous phase was then analyzed for $nTiO_2$ to make a comparison between custom-made and commercial paints. The mean size, particle size distribution and concentration of pristine and paint released $nTiO_2$ (custom made), were investigated. To compare between the influence of contact with water to that of sunlight exposure in the outdoors on $nTiO_2$ release from the painted surfaces (custom-made), the painted plastic test surfaces were exposed to sunlight, but were protected from precipitation. The painted surfaces were collected after different sunlight exposure points and immersed in deionized (DI) water for 3 days to assess the release of $nTiO_2$ from painted surface (custom-made) and presence of background $nTiO_2$ from the environment. The water samples were then collected and measured using spICP-MS for $nTiO_2$ size distributions and concentration. The viability of *E. coli D21* cells was assessed by exposing them to pristine $nTiO_2$ and $nTiO_2$ released from painted surfaces (custom made).

6.2. Materials and Methods

6.2.1. Preparation of $nTiO_2$ containing custom made paint and commercial paints

Four white commercial paints (3 exterior and 1 interior) were purchased to study the number of NPs released into water. One of the commercial paint, B-NP ext. claimed that it uses NPs. Other three commercial paints (A ext., D ext. and K int.) did not claim to use NPs. To observe the effect of varying pH, polystyrene surfaces (weighing boats, Fisher scientific) of 12 mm thickness and surface dimensions of 8.9 cm × 8.9 cm were used. 1g of wet paint was deposited onto each surface, spread uniformly using a nylon paint brush (size 8, brush width of 8 mm). This resulted in approximately 0.4 g of dry weight of paint after 3 days of drying. Painted surfaces were exposed to three pH conditions: DI water, acidic conditions (0.1mM nitric acid - pH ~3.5, similar to acid rain pH) [43, 44] and, basic conditions (0.1mM sodium hydroxide - pH ~8.5, similar to basic rain [45]). The painted surfaces were exposed to water of different pH for 16 days and the systems were maintained at standard room temperature of 20 ± 3 $^{\circ}$C and kept covered to avoid light, evaporation and other external interferences.

One of the painted surfaces was subjected to physical wear and tear using sonication, with DI water for 60 minutes. Physical abrasion is typically done to show degradation from painted surfaces due to wear and tear friction [8]. To maintain similar physical abrasion between replicate surfaces, and minimize human error from affecting the abrasion process, sonication was performed at a fixed frequency and time. Sonication was done using Fisherbrand^{TM} 11207 ultrasonic bath at 37 hertz frequency for 60 minutes at 10 minutes intervals to maintain the temperature of the water bath between 20 to 25 $^{\circ}$C. The sonicated samples were acid-digested using the digestion protocol, diluted, and measured using Perkin Elmer 8000x ICP-OES.

Cristal ACTiV^{TM} PC-105 $nTiO_2$ powders (Anatase, ~95% wt.) was used for formulation of custom-made paint. $nTiO_2$ was added to a commercial base paint formulation containing an acrylic polymer binder, without any other metal additives, at a concentration of at a concentration of 10% wt. (221.65 mg of $nTiO_2$/g of dry paint). Custom made paint were applied on polystyrene surfaces like commercial paints and exposed to the same conditions; DI water (~6.5), acidic condition (pH ~3.5), basic conditions (pH ~8.5), and mechanical abrasion using sonication. Aqueous samples were collected at regular intervals of time over a period of 11 days to see the effect of both varying pH and time. spICP-MS was used to measure the samples from aqueous phase.

For the sunlight exposure study, the custom-made paint was applied on polyvinyl chloride (PVC) boards of size 7.3 cm × 12.5 cm with 1.5 cm thickness from Plastiver (Trois-Rivières, QC). 1g of wet paint was poured onto each surface, spread uniformly using the paint brush described above in aqueous chemistry studies. The painted surface was dried for 3 days in the dark and kept covered under a cardboard box to avoid dust and light. The painted boards were weighed before and after the application of paint to measure the dry weight paint on each surface. Painted PVC boards were exposed to direct sunlight. The boards were stored in a closed container and kept covered after each day of sunlight exposure to avoid direct contact with precipitation. Three painted PVC boards were collected at time points 24, 48, 72, 96 and 120 hours of sunlight exposure (4 months of outdoor exposure June 2019 to September 2019). The boards were individually immersed in water for 3 days. Wash water from the boards were collected and measured for $nTiO_2$ using spICP-MS. The immersion period of 3 days was the minimum contact time in water for obtaining detectable quantities of $nTiO_2$ in the aqueous phase. Unpainted PVC boards and base paint applied boards were kept as control groups to observe the background concentration of $nTiO_2$ from the environment.

Aqueous phase samples from the various experiments were periodically collected after gently mixing, to measure released $nTiO_2$ concentration and size using spICP-MS.

6.2.2. Culturability of *E. Coli D21* in pristine $nTiO_2$ and released $nTiO_2$ from painted surface

6.2.2.1. *E. Coli D21 culture conditions*

Escherichia coli D21 (*E. coli D21*), a Gram-negative bacterium was employed as a model bacterium to compare the toxicity of pristine and paint-released nAg. 150 mL of 2.5% (w/v) Luria–Bertani (LB)–Miller growth media (Fisher) was prepared in 250 mL Erlenmeyer flask and autoclaved. Liquid cultures were prepared by inoculating a single colony into the growth media and incubating at 37 °C for 4 h at 150 rpm. Cells were harvested by centrifugation at 5,000 rpm for 10 minutes at 4 °C. The supernatant was decanted and fresh filter sterile 10mM KNO_3 was added to resuspend the cells. The resuspension of the cells, centrifugation and decanting process was repeated twice to remove all growth media left in cells. Subsequently, the supernatant was decanted, and cells resuspended in filter-sterilized 10 mM KNO_3. The absorbance of the initial cell concentrations was measured at 600 nm taking 10mM KNO_3 as reference.

6.2.2.2. *nTiO_2 exposure experiment*

Sterile Erlenmeyer flasks of 500 mL volume were used as microcosms for nTiO_2 exposure. Four different microcosm were prepared containing: (a) filter sterile 10 mM potassium nitrate (KNO_3) (Control); (b) pristine nTiO_2 in filter sterile 10mM KNO_3 (50 mg/L); (c) base paint in filter sterilised 10 mM KNO_3; (d) weathered paint aqueous (10 mM KNO_3) suspension obtained by sonication of painted boards (50 mg of nTiO_2/L from weathered paint in DI water). All the microcosms were incubated in the dark at 37 °C and 150 rpm .

Colony forming unit per mL (CFU/mL) counts were determined to characterize the changes in culturable cell population at definite time points. At each time point and for each microcosm, 1 mL of sample was obtained and serial dilutions at 10×, 100×, 1000× were performed using filter sterilized 10 mM KNO_3. 100 µL of the diluted and undiluted stock was plated on LB–Miller media (2.5 % w/v) containing 1.5% (w/v) agar (Fisher) and incubated at 37 °C for 24 h. Thereafter CFUs were enumerated from plates that had between 30–300 CFU and multiplied with the appropriate dilution factor to obtain the final CFU count. For each sample, culture plates were prepared in triplicate for each of the dilutions.

6.3. Instrumentation and Characterization

6.3.1. spICP-MS analysis

NP characterization was performed using PerkinElmer NexION 300x ICP-MS in single particle mode supported by Syngistix software (ver 1.1). This analysis provides the NP size distribution, NP concentration and dissolved metal concentration in the samples. An integration dwell time of 100 µs with sampling time of 100-150 s was used to measure the samples. Ultra uniform gold NPs (nAu) of size 55nm were used for spICP-MS transport efficiency, at a concentration of 10^5 particles/mL were diluted in DI water/ paint aqueous extract matrix from the painted surface to find the transport efficiency (5.0 to 8.5%) for spICP-MS. Other main instrumental settings and conditions are provided in the SI (Table S6-1).

The calibration for titanium between the concentration range of 100 ng/L to 5 μg/L were prepared using titanium ions of 1000 mg/L (SCP Science PlasmaCAL). The spiked $nTiO_2$, background controls and stock solution were measured along with released NPs from painted surfaces.

6.3.2. Electron Microscopy

Transmission electron microscopy (TEM) analysis was performed using a FEI Tecnai G2 F20 S/TEM equipped with Gatan Ultrascan 4000 4k × 4k CCD Camera System (Model 895). An EDAX Octane T Ultra W/Apollo XLT2 SDD system was used for energy dispersive X-ray spectroscopy (EDS) measurements. 10 μL of the sample concentrate was deposited on the Cu/Au TEM grids (Electron Microscopy Sciences, Carbon film 200 mesh Cu/Au grids. The grids were allowed to be air-dried again prior to analysis using TEM and EDS.

Sunlight exposed PVC boards were cut into 1 cm × 1 cm using professional guillotine paper cutter. The cut boards were coated with 5nm platinum in sputter coater (Leica EM ACE 600). The samples were then imaged using scanning electron microscopy (SEM) FEI Quanta 450 FEG.

6.3.3. Sample Digestion and Element Analysis

Paint samples (0.5mL) were acid digested using 5mL of sulfuric acid (95 to 98 % - Fisher Scientific) at 110 ^{0}C for 8 hours in a hot block digester; followed by 2 mL of 70% ICP grade nitric acid (SCP Science) for 1 hour with quality controls; spiked with 100 μg/L of dissolved Ti (SCP science) and 100 μg/L of $nTiO_2$ (Cristal ACTiV^{TM} PC-105 $nTiO_2$) and background controls. The digested samples were diluted to the required volume and measured using standard mode in Perkin Elmer NexION 300x ICP-MS and Perkin Elmer 8000x ICP-OES. Each paint extract samples were digested in triplicates and each digested sample was measured in triplicates.

6.4. Results and Discussion

6.4.1. Nanoparticle release from commercial paints

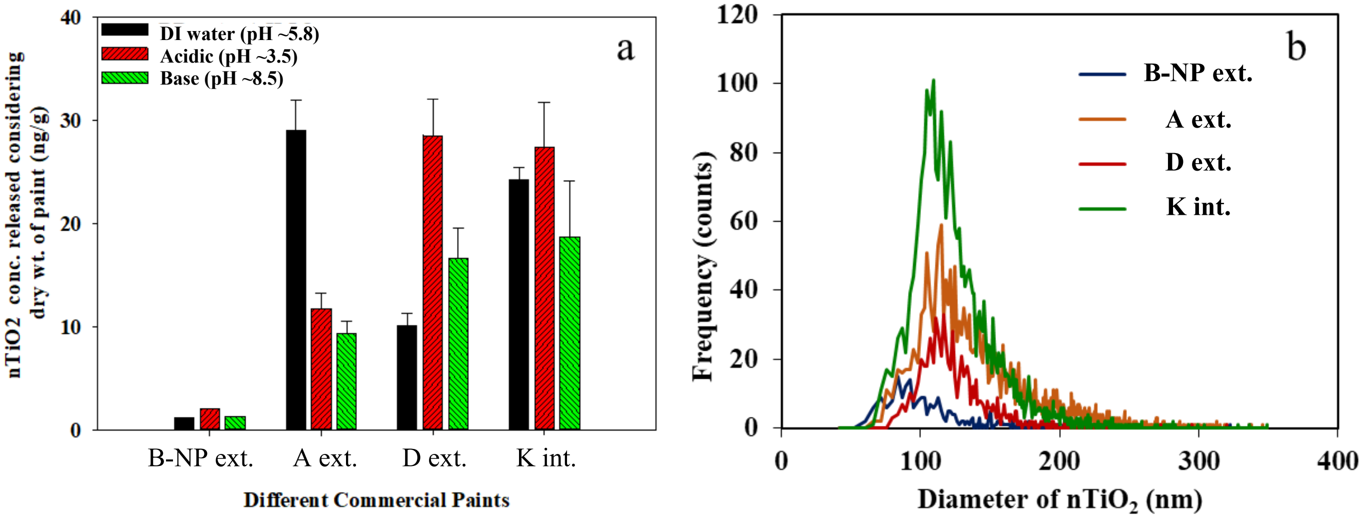

Figure 6-1 nTiO$_2$ released from four commercial paints (a) exposed to different pH conditions and (b) particle size distribution from spICP-MS in DI water after 3 days.

The four commercial paints were exposed to different exposure conditions and showed different release patterns as shown in Figure 6-1a. The mean size of the particles released varied with B-NP ext. (claimed to use nanotechnology) having the lowest mean diameter of 116.2 ± 0.8 nm compared to other three commercial paints (A ext. 157.6 ± 1.4 nm, D ext. 131.9 ± 0.5 nm and K int. 134.5 ± 1.1 nm). The three commercial paints which did not claim to have NPs, had larger particle sizes in the distribution (Figure 6-1b). Larger sizes (150nm to 350nm) of nTiO$_2$ in the three commercial paints (A ext., D ext. and K int.) were absent in paint B-NP ext.; hence suggesting that, the composition of these paints contains nano-sized to micro-sized particles. Commercial paint B-NP ext. released 11 to 16 times lower nTiO$_2$ of 1 to 2 ng/mL of water/g of dry paint compared to other commercial paints with concentration ranging between 10 to 30 ng/mL/g. At acidic pH ~3.5, nTiO$_2$ released from painted surfaces were 20 to 42% more compared to neutral or basic for three paints except for A ext. paint. As different paints released dissimilar amounts of nTiO$_2$ in different exposure conditions, no observable patterns of release were observed for all four commercial paints. The TEM and EDS results confirm the presence of nTiO$_2$ released (varying sizes) from the painted surface from all four commercial paints in contact with water (Figure 6-2).

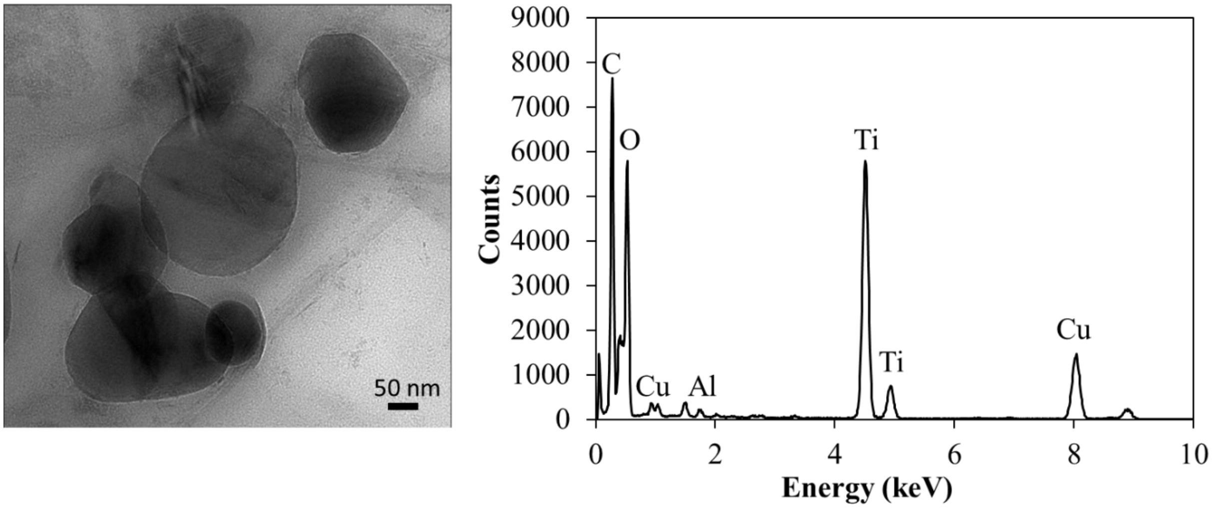

Figure 6-2 TEM and EDS of $nTiO_2$ released from commercial paints B-NP ext. exposed to DI water

The painted surface subjected to physical wear and tear released approximately 222 to 680 µg/mL/g. Paint B-NP ext. (containing NPs) released a 2 x 10^5 - fold more NPs in the supernatant when subjected to sonication, as can be seen in the particle size distribution in Figure 6-3. The mean size of the particle remained the same between the two systems: directly in contact with water and sonicated samples. Whereas, other commercial paints (A ext., D ext. and K int.) subjected to mechanical abrasion in supernatant had a lesser percentage of NP released 10^4 folds higher release compared to Paint B-NP ext. (containing NPs). These results suggest that all four commercial paints have $nTiO_2$, with A ext., D ext. and K int. having a mixture of nano and micron size particles. The use of nanotechnology in paint B-NP ext. helped in keeping the structural integrity of the painted surface when exposed to DI (pH ~6.5), acidic (pH ~3.5) and basic (pH ~8.5) conditions. The larger $nTiO_2$ release in the other three commercial paints are due to the large aggregate formation between nano and micron sized particles.

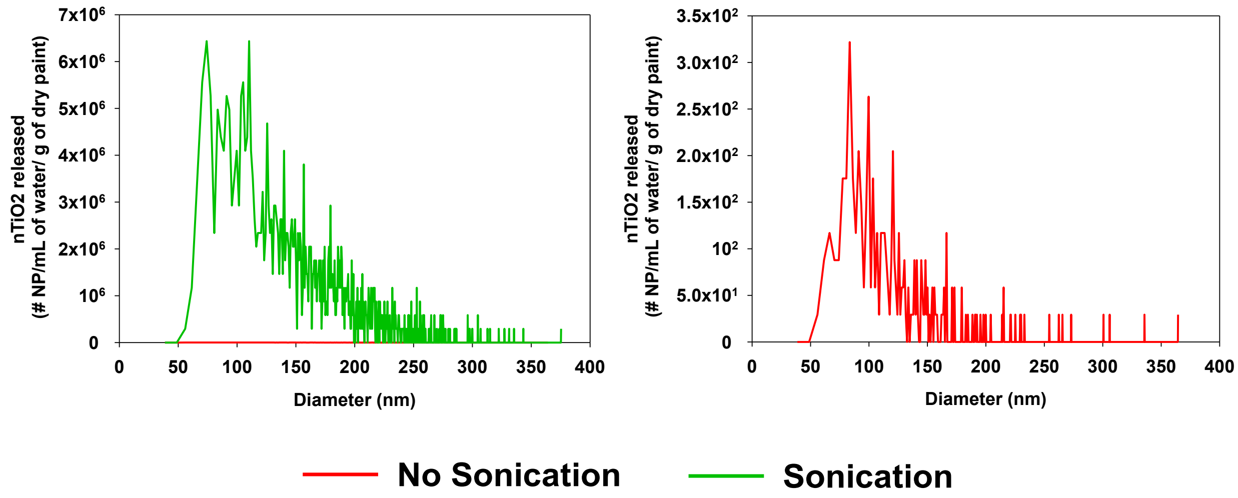

Figure 6-3 Particle size distribution of $nTiO_2$ released from B-NP ext. exposed to DI water and mechanical abrasion by sonication

6.4.2. Nanoparticle release from custom made $nTiO_2$ paint

To comprehend why the release of NPs from *commercial paint claiming to have NPs* is less than other commercial paints studied, custom-made paints were formulated with 10% $nTiO_2$ in dispersion in base acrylic paint with no additives by commercial paint manufacturer. These paints are tested for the same exposure conditions undergone by commercial paints for a period of 11 days. Primary size of pristine $nTiO_2$ was 23.6 ± 5.1 nm (n = 108) using TEM. While spICP-MS analysis shows NPs sizes of 81.1 ± 6.2 nm for $nTiO_2$, indicating larger aggregates in the suspension compared to the primary size by TEM. The pristine $nTiO_2$ were not very stable and settled down after the first day, thus, no particles were found in the supernatant. These results were similar to previous studies which indicate the unstable pristine $nTiO_2$ in the water [21, 46].

Custom made paint with $nTiO_2$ demonstrated release of NPs in quiescent systems over 11 days. Released $nTiO_2$ were aggregated in DI water systems (pH ~6.5), with stable aggregates concentration of 10^5 NP/mL/g, whereas, the painted surface exposed to the acidic (pH ~3.5) and basic (pH ~8.5) conditions resulted in aggregation of the $nTiO_2$ (Figure 6-4a). Previous studies have shown that even at salt concentrations of 0.25mM NaOH (basic condition), 40% of $nTiO_2$ aggregated and sediment in the solution within 5 hours [47]. Similarly, in acidic conditions of pH ~3.5, studies have demonstrated that $nTiO_2$ aggregated and settled out [48]. Similar trends can be observed in $nTiO_2$ release from painted surfaces exposed to quiescent acidic and basic systems due to the ionic strength and pH of the solution [47, 49].

The wash water collected from different pH conditions were sonicated to assess if $nTiO_2$ were settling down due to the varying pH scale. Figure 6-4b shows that the amount of $nTiO_2$ released increases with time, with acidic pH ~3.5 releasing twice the particle number compared to basic pH ~8.5 and DI water at pH ~6.5. These results again indicate aggregation of $nTiO_2$ at acidic pH ~3.5 and basic pH ~8.5. The concentration of $nTiO_2$ released from the painted surface in basic pH ~8.5 and DI water pH ~6.5 stabilized as seen in Figure 6-4b. Whereas, in acidic pH ~3.5, a slight increase in $nTiO_2$ concentration with time was observed, probably due to generation of ROS in $nTiO_2$ leading to degradation of acrylic polymer. Previous studies have reported breakdown of acrylic polymer in the presence of ROS generation [50, 51]. The mean size for paint-released $nTiO_2$ (125.5 ± 10.6 nm) was larger than the mean size of pristine $nTiO_2$ (81.1 ± 6.2 nm) (Figure 6-5). The particle size distribution shows that $nTiO_2$ released from painted surfaces were found to be more agglomerated than pristine $nTiO_2$, possibly due to extensive binding to the paint matrix formation of aggregates and clusters (Figure 6-5). The TEM image of released $nTiO_2$ (Figure S6-1) showed that NPs detach along with the matrix that influences the fate in the environment.

On a weight percent basis of $nTiO_2$ in paint, only a minute concentration (10^{-5} percentage) of $nTiO_2$ was released in quiescent systems as shown in Table 6-1. A recent study has shown only 0.0001% $nTiO_2$ is released from painted surface exposed to precipitation [11]. Aggressively weathered painted surface using sonication released around 2.7% in the stable aqueous fraction of total $nTiO_2$ present in paint (Table 6-1). Previous studies have shown surfaces coated with $nTiO_2$ are durable, water resistant and improved attachment to the surface, probably leading to lower percentage of $nTiO_2$ release from the surface coated with $nTiO_2$ paint [52, 53]. Average mean size of pristine $nTiO_2$ (114.7 ± 2.5 nm) were slightly higher size compared to release NPs from paints (90.4 ± 21.7 nm) probably due to better stabilization using base acrylic paint as seen in previous studies [54, 55].

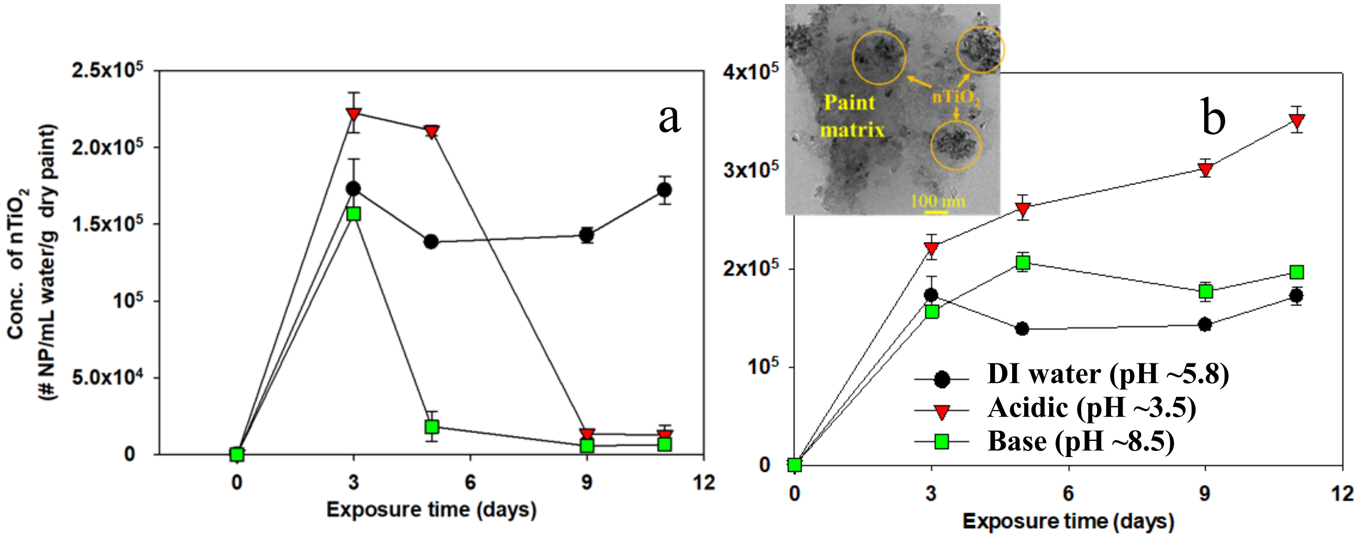

Figure 6-4 Released nTiO$_2$ from painted surface (custom made paint) exposed to different pH conditions over period of 11 days (TEM shows nTiO$_2$ is released with paint matrix from polystyrene surface) (a) without sonication and (b) with sonication of the collected wash water

Table 6-1 Mean size and percentage of released nTiO$_2$ from painted surface (custom made paint)

Exposure Condition	**Mean size of released NPs (nm)**	**nTiO$_2$ released (% wt)**
DI water (pH ~6.5) for 11 days	**125.5 ± 10.6**	**$2.2 \pm 0.1 \times 10^{-5}$**
0.1mM HNO$_3$ (pH ~3.5) for 11 days	**121.5 ± 9.9**	**$4.7 \pm 0.4 \times 10^{-5}$**
0.1mM NaOH (pH ~8.5) for 11 days	**129.6 ± 21.0**	**$2.4 \pm 0.3 \times 10^{-5}$**

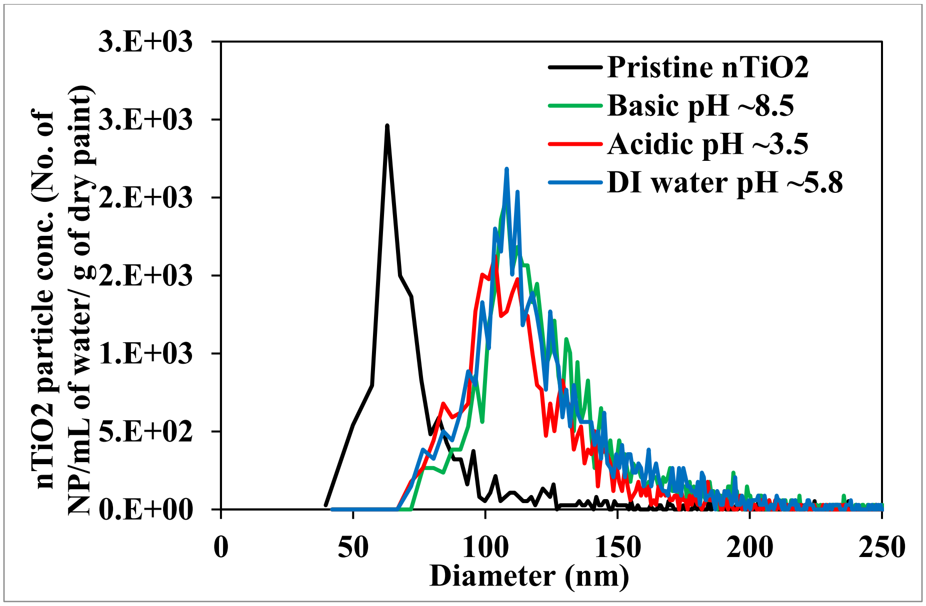

Figure 6-5 Change in particle size distribution of released $nTiO_2$ compared to pristine nTiO2 on Day 3 in different pH conditions.

Table 6-2 Comparing released concentration of $nTiO_2$ from custom made paint and commercial paint.

Exposure conditions (@ 3 days)	Released NP conc. (ng/mL water/g dry paint)				
	Custom paint with $nTiO_2$	B –NP ext.	A ext.	D ext.	K int.
DI water (pH ~6.5)	0.89 ± 0.2	1.1 ± 0.1	29.0 ± 2.5	10.1 ± 1.1	24.2 ± 1.2
0.1mM HNO_3 (pH ~3.5)	1.7 ± 0.3	2.0 ± 0.2	11.7 ± 1.2	28.5 ± 3.1	27.4 ± 3.7
0.1mM NaOH (pH ~8.5)	0.96 ± 0.2	1.3 ± 0.1	9.3 ± 0.9	16.6 ± 2.4	18.7 ± 4.1
Sonication DI water	$1.13 \pm 0.4 \times 10^5$	$2.22 \pm 0.5 \times 10^5$	$4.18 \pm 0.3 \times 10^5$	$6.81 \pm 0.8 \times 10^5$	$4.57 \pm 0.5 \times 10^5$

spICP-MS results indicated that the release of $nTiO_2$ from custom made paint to be similar to that from commercial paint B-NP ext., with concentration of NP release around ~1 ng/mL/g in quiescent systems exposed DI water, acidic and basic conditions. Similar to B-NP ext., $nTiO_2$ release increased with sonication to 10^5 ng/mL/g as seen in the Table 6-2. The results indicate that the structure stability of painted surfaces with $nTiO_2$ is influenced by the physical abrasion of the surface. Average mean size of NPs released from custom-made paint containing $nTiO_2$ is 90.4 ± 21.7 nm, which is lower compared to 131.7 ± 19.5 nm observed in B-NP ext., probably because NP used for formulation of the commercial paint might be of different size range. This suggests that custom made paint and commercial paint behave identically from the standpoint of $nTiO_2$.

6.4.3. Effect of sunlight on release of $nTiO_2$ from painted surface

To assess if the releases of $nTiO_2$ in aqueous solutions under quiescent conditions was comparable to releases of $nTiO_2$ from painted surfaces exposed to sunlight parallel outdoor experiments were conducted. PVC rather than polystyrene surfaces were used because the polystyrene surfaces were deformed with continuous sunlight exposure. PVC boards exposed to sunlight over specific periods of time were contacted with water under quiescent conditions for 3 days to assess the readily released fraction of $nTiO_2$ following sunlight exposure. A minimum of 3 days of contact with water was required to obtain measurable amounts of released $nTiO_2$ in the aqueous phase.

spICP-MS measurements of background control boards and base paint revealed sunlight exposed PVC boards applied with $nTiO_2$ paints increased 3.9 times from $1.2 \pm 0.1 \times 10^5$ ENP/mL/g dry paint with no sunlight exposure to $5.0 \pm 0.1 \times 10^5$ ENP/mL/g after 120 hours of solar radiation (Figure 6-6c). There was a constant particle size distribution for $nTiO_2$ in background base paint and control boards with a slight increase from $1.3 \pm 0.1 \times 10^5$ ENP/mL/g at 24 h to $2.6 \pm 0.1 \times 10^5$ ENP/mL/g at 120 h (Figure 6-6a). These particle peaks can be either anthropogenic or natural $nTiO_2$ in the atmosphere that deposited on the surface. As shown in the previous study on nAg painted surface exposed to sunlight, painted surface exposed to sunlight had surface fissures and fractures. This indicates that acrylic polymer binder used in paints are degraded by sunlight leading to release of higher $nTiO_2$ [1]. Similar results of increased released of NPs were observed from our previous study in nAg exposed to sunlight. Several other studies have shown similar results of increased NP released with SiO_2, TiO_2 and Ag, by measuring metal concentration in the wash solutions using ICP-MS [7, 8, 10, 14].

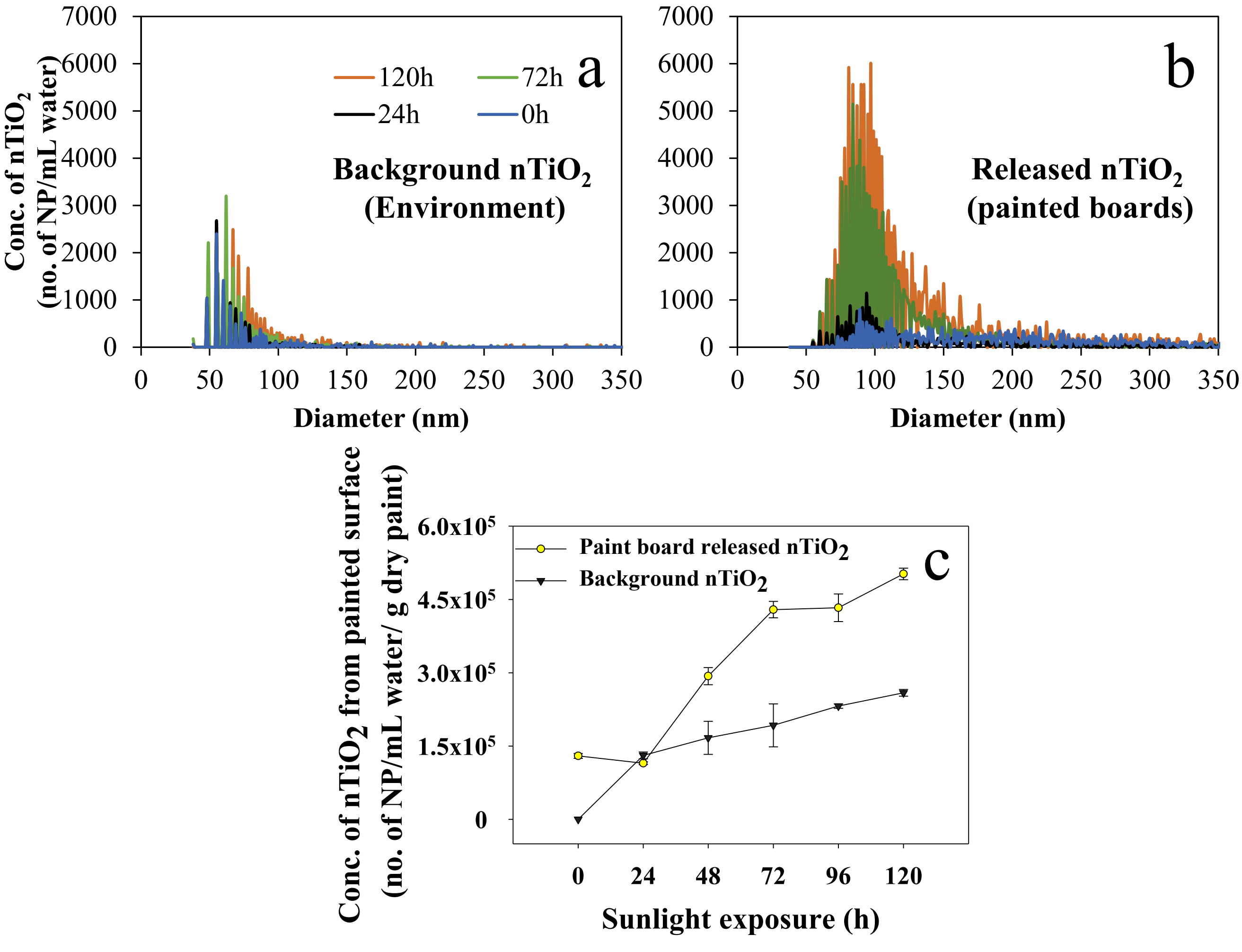

Figure 6-6 $nTiO_2$ release from sunlight exposed PVC surfaces a) Particle size distribution of $nTiO_2$ released from sunlight exposure surfaces over different periods of time (0 to 120h) b) Concentrations of $nTiO_2$ released from painted surface compared to background $nTiO_2$ present in the environment.

The mean size of $nTiO_2$ released from sunlight exposed surfaces remained in similar range 173.7 ± 14.2 nm at 0 h and 162.9 ± 1.1 nm at the end of 120 h (Figure 6-6b). The size of $nTiO_2$ released from the paint is larger compared to the primary size of pristine $nTiO_2$ (81.1 ± 6.2 nm). This is suggestive that the composite colloids of $nTiO_2$ released from sunlight exposed surface are possibly aggregates or cluster. Previous studies have shown that NP released from painted surface usually comes along with painted fragments [7, 8]. This study shows that the aggregates of $nTiO_2$ release from sunlight exposed surfaces, with increased release of NPs with longer sunlight exposure.

The 120 h sunlight-exposed PVC surfaces when immersed in DI water for 3 days released 3.6 times more $nTiO_2$ (3.6 ± 0.8 µg/L more n $nTiO_2$) compared to that released from painted boards immersed in DI water for 8 days with no sunlight exposure. This indicates that larger release of $nTiO_2$ from painted surface is observed from photodegradation of the binder. However, $nTiO_2$ from painted surface are also released during contact with DI water from pores formed during crosslinking reactions of acrylic polymer binder during drying of the wet paint applied on the boards [56-58]. $nTiO_2$ are released as water permeates into the surface through the pores, weaking the attachment to the binders and dislodging them [57-59]. In comparing $nTiO_2$ released from PVC and polystyrene painted surfaces upon contact with DI water for 3 days, comparable concentrations of $1.3 \pm 0.1 \times 10^5$ nAg/mL/g and $1.7 \pm 0.01 \times 10^5$ nAg/mL/g were obtained. The particle size distributions of released $nTiO_2$ were also observed to be similar.

6.4.4. Culturability of *E. coli D21* in pristine $nTiO_2$ and released $nTiO_2$ from painted surface

The controls and base paint systems are as reported in previous study (Chapter 5), as the experiments of nAg and $nTiO_2$ were conducted simultaneously. In reactors with 10mM KNO_3 (control) and pristine $nTiO_2$, *E. coli D21* CFU/mL remained constant over 42 h, suggesting little or no toxicity. However, in reactors containing base paint, bacterial log CFU/mL counts decreased by almost four-fold during the first 10 h; by 20 h, there were no more viable cells remaining as seen in Figure 6-7. In reactors containing $nTiO_2$ released from paint, the rate of decline was more severe – CFU/mL counts reduced by eight-fold within 10 h, after which there were no more viable cells. This indicates higher bacteriostatic activity in $nTiO_2$ released from painted surfaces as opposed to pristine $nTiO_2$ or only paint matrix–a similar observation was reported for nAg as well (submitted). Pagnout et al. [60] observed that similar results: at acidic pH 5.5, small aggregates of $nTiO_2$ (mean hydrodynamic diameter 78 nm) caused more than 99% cytotoxicity to *E.coli* after 20 h exposure. This occurs due to electrostatic interactions between the positively charged $nTiO_2$ and the negatively charged *E. coli* membrane, leading to cell damage.

TEM characterization showed that released NPs from paint detach from the paint matrix (Figure S6-1); the particle size distribution of the released $nTiO_2$ was aggregated compared to its pristine state. Higher surface area of these aggregates led to favorable electrostatic interactions with bacterial cell surfaces, leading either (i) ROS generation, or (ii) paint coatings to cause much higher toxicity than pristine NPs, supporting claims by Jassby et al. [61] who suggest that aggregation and presence of coatings influence NP toxicity. As our exposure studies were performed in the dark, particle-specific effects were more likely to govern toxic response than ROS generation. This leads us to suggest the paint coatings on the released NPs cause both base paint and released NPs to show high toxic response, with the latter showing more acute response due to aggregation as well. This brings to light the importance of considering intrinsic NP properties and coatings when evaluating toxicity of released NPs from paints, particularly when photocatalytic effects are minimal.

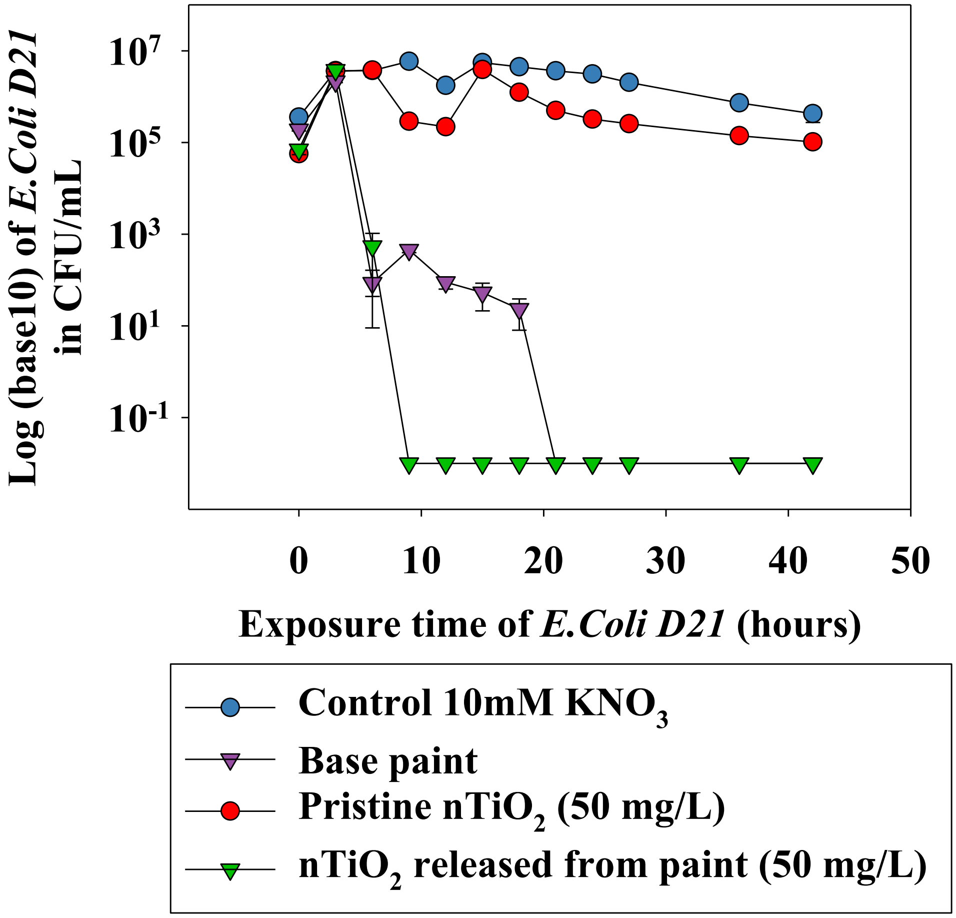

Figure 6-7 Survival rate of E. coli D21 in pristine $nTiO_2$ and $nTiO_2$ released from painted surface

6.5. Conclusions

Paints and coatings are one of the major sources of $nTiO_2$ release to the environment [62]; however, studies of effect of these released NPs are typically done on pristine NPs used in the parent product. The release of $nTiO_2$ and its aggregation state differs depending on the pH conditions of the media, with acidic pH ~3.5 and basic pH ~8.5 causing aggregation. Similar to our previous study with nAg released from painted surfaces at pH ~3.5, higher release of $nTiO_2$ was observed in acidic condition. The released $nTiO_2$ from paint matrix was aggregated compared to its pristine state suggesting the importance of conducting viability studies using the released NPs from paint products. The application of $nTiO_2$ in paints and as an interfacial coating agent causes it to either repel or kill incoming pathogens and prevent their growth on surfaces [63]. With bacterial load on surfaces varying from less than 3 CFU/cm^2 to as high as 1.8 x 10^9 CFU/cm^2, antimicrobial coatings have tremendous applications [64]. An associated disadvantage with paints involves wear-related issues, which cause release and transformation of nTiO$_2$ and associated toxicity. Also, nTiO$_2$ aggregation, particle size, and crystalline structure play a role in determining antimicrobial efficiency [65]. Even though a high concentration (10% w/v) of nTiO$_2$ is used to produce the nano paint (in this study), with exposure to water of different pH, only less than 10^{-5} % of the total NPs was released from the surface, implying satisfactory binding of NP with the resins in the paint matrix. Interestingly, like custom made paint, commercial paint (paint B-NP ext.) claimed to have NPs released lesser nTiO$_2$ compared to other commercial paints. This suggests that using NPs for paint production replacing mixtures of nano-, micron- and larger particles of TiO$_2$ would release lower concentrations to the environment.

6.6. Acknowledgment

We acknowledge the assistance of David Liu, McGill university for TEM/EDS and SEM analysis. Société Laurentide for helping us with preparation of custom-made paint. The research was supported by the Natural Sciences and Engineering Research Council of Canada, Environment and Climate Change Canada and Cascades Canada ULC. A. A. R and A. K were supported by McGill Engineering Doctoral Award.

6.7. Supplementary data

Table S6-1 spICP-MS instrumental parameters used for measurements

Parameter Value	
Sample Uptake Rate	0.28-0.34 mL/min
Nebulizer gas flow	0.97-1.03 L/min
Nebulizer	Meinhard Glass Concentric
Spray Chamber	Meinhard Glass Cyclonic

RF Power	1600 W
Analyte	Ti47, Ti48
Analysis time	100-150 s
Dwell time	100 µs

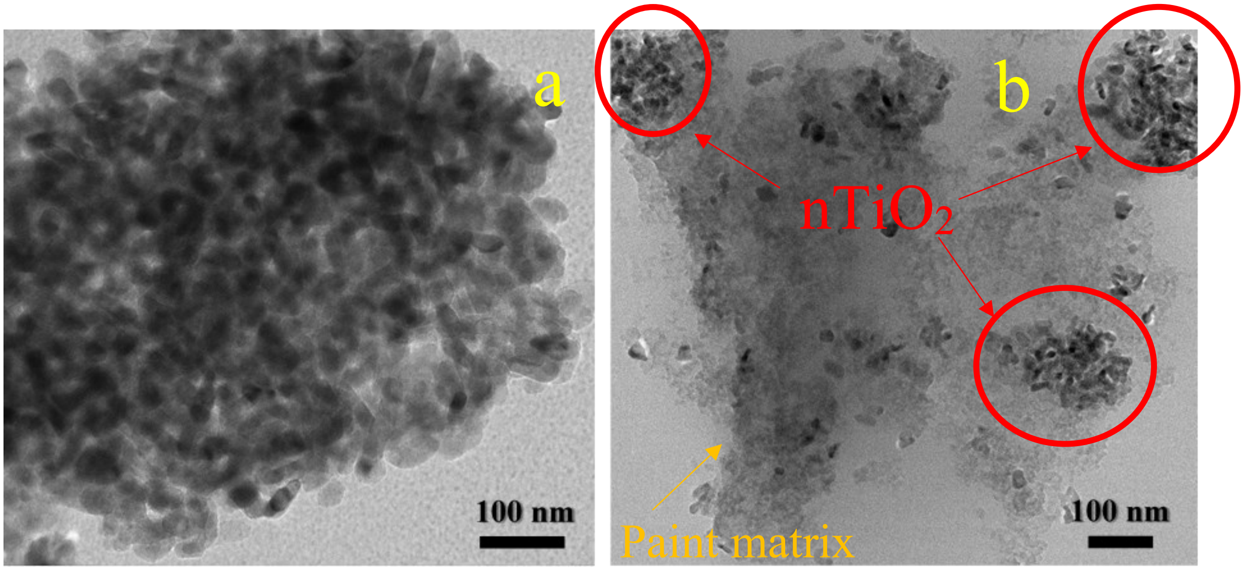

Figure S6-1 TEM images of pristine NPs and NPs released from custom made paint (a) pristine $nTiO_2$ (b) $nTiO_2$ released from painted surface.

6.8. References

1. Marolt, T., et al., *Photocatalytic activity of anatase-containing facade coatings.* Surface and Coatings Technology, 2011. **206**(6): p. 1355-1361.
2. Weir, A., et al., *Titanium dioxide nanoparticles in food and personal care products.* Environmental science & technology, 2012. **46**(4): p. 2242.
3. Keller, A.A. and A. Lazareva, *Predicted releases of engineered nanomaterials: From global to regional to local.* Environmental Science & Technology Letters, 2013. **1**(1): p. 65-70.
4. Piccinno, F., et al., *Industrial production quantities and uses of ten engineered nanomaterials in Europe and the world.* Journal of Nanoparticle Research, 2012. **14**(9): p. 1-11.
5. Zuin, S., et al., *Leaching of nanoparticles from experimental water-borne paints under laboratory test conditions.* Journal of nanoparticle research, 2014. **16**(1): p. 2185.

6. Mizutani, T., et al., *Application of silica-containing nano-composite emulsion to wall paint: A new environmentally safe paint of high performance.* Progress in Organic Coatings, 2006. **55**(3): p. 276-283.
7. Kaegi, R., et al., *Release of silver nanoparticles from outdoor facades.* Environ Pollut, 2010. **158**(9): p. 2900-5.
8. Al-Kattan, A., et al., *Release of TiO2 from paints containing pigment-TiO2 or nano-TiO2 by weathering.* Environmental Science: Processes & Impacts, 2013. **15**(12): p. 2186-2193.
9. Kägi, R., et al., *Synthetic TiO2 nanoparticle emission from exterior facades into the aquatic environment.* Environmental pollution, 2008. **156**(2): p. 233-239.
10. Al-Kattan, A., et al., *Behavior of TiO2 Released from Nano-TiO2-Containing Paint and Comparison to Pristine Nano-TiO2.* Environmental Science & Technology, 2014. **48**(12): p. 6710-6718.
11. Azimzada, A., et al., *Release of TiO2 nanoparticles from painted surfaces in cold climates: characterization using a high sensitivity single-particle ICP-MS.* Environmental Science: Nano, 2020. **7**(1): p. 139-148.
12. Azimzada, A., et al., *Single- and Multi-Element Quantification and Characterization of TiO2 Nanoparticles Released From Outdoor Stains and Paints.* Frontiers in Environmental Science, 2020. **8**(91).
13. Adeleye, A.S., et al., *Release and detection of nanosized copper from a commercial antifouling paint.* Water Research, 2016. **102**: p. 374-382.
14. Al-Kattan, A., et al., *Characterization of materials released into water from paint containing nano-SiO2.* Chemosphere, 2015. **119**: p. 1314-1321.
15. Olabarrieta, J., et al., *Aging of photocatalytic coatings under a water flow: Long run performance and TiO2 nanoparticles release.* Applied Catalysis B: Environmental, 2012. **123-124**: p. 182-192.
16. Zhang, X., et al., *Effects of weathering and rainfall conditions on the release of SiO2, Ag, and TiO2 engineered nanoparticles from paints.* Journal of Nanoparticle Research, 2017. **19**(10): p. 338.
17. Clar, J.G., et al., *Release and transformation of ZnO nanoparticles used in outdoor surface coatings for UV protection.* Science of The Total Environment, 2019. **670**: p. 78-86.
18. Zhang, Y., et al., *Stability of commercial metal oxide nanoparticles in water.* Water Research, 2008. **42**(8): p. 2204-2212.
19. Zhang, Y., et al., *Impact of natural organic matter and divalent cations on the stability of aqueous nanoparticles.* Water Research, 2009. **43**(17): p. 4249-4257.
20. Warheit, D.B., et al., *Health effects related to nanoparticle exposures: Environmental, health and safety considerations for assessing hazards and risks.* Pharmacology & Therapeutics, 2008. **120**(1): p. 35-42.
21. Ottofuelling, S., F. Von Der Kammer, and T. Hofmann, *Commercial Titanium Dioxide Nanoparticles in Both Natural and Synthetic Water: Comprehensive Multidimensional Testing and Prediction of Aggregation Behavior.* Environmental Science & Technology, 2011. **45**(23): p. 10045-10052.
22. Kaiser, J.-P., S. Zuin, and P. Wick, *Is nanotechnology revolutionizing the paint and lacquer industry? A critical opinion.* Science of the total environment, 2013. **442**: p. 282-289.
23. Bogdan, J., J. Zarzyńska, and J. Pławińska-Czarnak, *Comparison of infectious agents susceptibility to photocatalytic effects of nanosized titanium and zinc oxides: a practical approach.* Nanoscale research letters, 2015. **10**(1): p. 1-15.

24. Toma, F.L., et al., *Comparative study on the photocatalytic behaviour of titanium oxide thermal sprayed coatings from powders and suspensions.* Surface and Coatings Technology, 2009. **203**(15): p. 2150-2156.
25. Sousa, V.M., et al., *Photoinactivation of various antibiotic resistant strains of Escherichia coli using a paint coat.* Journal of Photochemistry and Photobiology A: Chemistry, 2013. **251**: p. 148-153.
26. Chung, C.J., et al., *An antimicrobial TiO2 coating for reducing hospital-acquired infection.* Journal of Biomedical Materials Research Part B: Applied Biomaterials: An Official Journal of The Society for Biomaterials, The Japanese Society for Biomaterials, and The Australian Society for Biomaterials and the Korean Society for Biomaterials, 2008. **85**(1): p. 220-224.
27. Ueda, T., D. Yamashina, and K. Kinugawa, *Copper complex titanium oxide dispersion liquid, coating agent composition, and antibacterial/antiviral member*. 2017, Google Patents.
28. Chen, S., et al., *Synergistic antibacterial mechanism and coating application of copper/titanium dioxide nanoparticles.* Chemical Engineering Journal, 2014. **256**: p. 238-246.
29. Kühn, K.P., et al., *Disinfection of surfaces by photocatalytic oxidation with titanium dioxide and UVA light.* Chemosphere, 2003. **53**(1): p. 71-77.
30. Necula, B.S., et al., *In vitro antibacterial activity of porous TiO2–Ag composite layers against methicillin-resistant Staphylococcus aureus.* Acta Biomaterialia, 2009. **5**(9): p. 3573-3580.
31. Mitrano, D.M., et al., *Silver nanoparticle characterization using single particle ICP-MS (SP-ICP-MS) and asymmetrical flow field flow fractionation ICP-MS (AF4-ICP-MS).* Journal of Analytical Atomic Spectrometry, 2012. **27**(7): p. 1131-1142.
32. Lee, S., et al., *Nanoparticle size detection limits by single particle ICP-MS for 40 elements.* Environmental science & technology, 2014. **48**(17): p. 10291-10300.
33. Montaño, M., et al., *Improvements in the detection and characterization of engineered nanoparticles using spICP-MS with microsecond dwell times.* Environmental Science: Nano, 2014. **1**(4): p. 338-346.
34. Laborda, F., et al., *Selective identification, characterization and determination of dissolved silver (I) and silver nanoparticles based on single particle detection by inductively coupled plasma mass spectrometry.* Journal of Analytical Atomic Spectrometry, 2011. **26**(7): p. 1362-1371.
35. Kim, H.-A., et al., *Characterization of silver nanoparticle aggregates using single particle-inductively coupled plasma-mass spectrometry (spICP-MS).* Chemosphere, 2017. **171**: p. 468-475.
36. Telgmann, L., et al., *Single particle ICP-MS as a tool for determining the stability of silver nanoparticles in aquatic matrixes under various environmental conditions, including treatment by ozonation.* Analytical and Bioanalytical Chemistry, 2016. **408**(19): p. 5169-5177.
37. Deng, Y., et al., *Multiple Method Analysis of TiO2 Nanoparticle Uptake in Rice (Oryza sativa L.) Plants.* Environmental Science & Technology, 2017. **51**(18): p. 10615-10623.
38. Azodi, M., Y. Sultan, and S. Ghoshal, *Dissolution Behavior of Silver Nanoparticles and Formation of Secondary Silver Nanoparticles in Municipal Wastewater by Single-Particle ICP-MS.* Environmental Science & Technology, 2016. **50**(24): p. 13318-13327.

39. Furtado, L.M., et al., *Environmental Fate of Silver Nanoparticles in Boreal Lake Ecosystems.* Environ Sci Technol, 2015. **49**(14): p. 8441-50.
40. Montaño, M.D., et al., *Single Particle ICP-MS: Advances toward routine analysis of nanomaterials.* Analytical and Bioanalytical Chemistry, 2016. **408**(19): p. 5053-5074.
41. Reed, R.B., et al., *Overcoming challenges in analysis of polydisperse metal-containing nanoparticles by single particle inductively coupled plasma mass spectrometry.* Journal of Analytical Atomic Spectrometry, 2012. **27**(7): p. 1093-1100.
42. Donovan, A.R., et al., *Single particle ICP-MS characterization of titanium dioxide, silver, and gold nanoparticles during drinking water treatment.* Chemosphere, 2016. **144**: p. 148-153.
43. Wyrwicka, A. and M. Skłodowska, *Influence of repeated acid rain treatment on antioxidative enzyme activities and on lipid peroxidation in cucumber leaves.* Environmental and Experimental Botany, 2006. **56**(2): p. 198-204.
44. Wang, M., et al., *Effect of simulated acid rain on fluorine mobility and the bacterial community of phosphogypsum.* Environmental Science and Pollution Research, 2018. **25**(16): p. 15336-15348.
45. Singh, S., S.P. Elumalai, and A.K. Pal, *Rain pH estimation based on the particulate matter pollutants and wet deposition study.* Science of The Total Environment, 2016. **563-564**: p. 293-301.
46. Tang, Z. and T. Cheng, *Stability and aggregation of nanoscale titanium dioxide particle (nTiO2): Effect of cation valence, humic acid, and clay colloids.* Chemosphere, 2018. **192**: p. 51-58.
47. Keller, A.A., et al., *Stability and Aggregation of Metal Oxide Nanoparticles in Natural Aqueous Matrices.* Environmental Science & Technology, 2010. **44**(6): p. 1962-1967.
48. French, R.A., et al., *Influence of Ionic Strength, pH, and Cation Valence on Aggregation Kinetics of Titanium Dioxide Nanoparticles.* Environmental Science & Technology, 2009. **43**(5): p. 1354-1359.
49. Liu, W., et al., *Comparison on aggregation and sedimentation of titanium dioxide, titanate nanotubes and titanate nanotubes-TiO2: Influence of pH, ionic strength and natural organic matter.* Colloids and Surfaces A: Physicochemical and Engineering Aspects, 2013. **434**: p. 319-328.
50. De Matteis, V., et al., *Toxicity assessment of anatase and rutile titanium dioxide nanoparticles: The role of degradation in different pH conditions and light exposure.* Toxicology in Vitro, 2016. **37**: p. 201-210.
51. Scalarone, D., M. Lazzari, and O. Chiantore, *Acrylic protective coatings modified with titanium dioxide nanoparticles: Comparative study of stability under irradiation.* Polymer Degradation and Stability, 2012. **97**(11): p. 2136-2142.
52. Calia, A., M. Lettieri, and M. Masieri, *Durability assessment of nanostructured TiO2 coatings applied on limestones to enhance building surface with self-cleaning ability.* Building and Environment, 2016. **110**: p. 1-10.
53. Khadem-Hosseini, A., S. Pazokifard, and S.M. Mirabedini, *Durability and mechanical performance of a photo-catalytic water-based nanocomposite coating.* Progress in Organic Coatings, 2017. **112**: p. 254-262.
54. Pica, A., et al., *Acrylic polymer influence on the structure and morphology of AgNPs obtained by chemical method for antimicrobial applications.* Journal of Coatings Technology and Research, 2016. **13**(1): p. 53-61.

55. Sergeev, G.B., et al., *Low-Temperature Synthesis and Properties of Silver Nanoparticles Stabilised by Acrylic Polymers AU - Sergeev, Boris M.* Molecular Crystals and Liquid Crystals Science and Technology. Section A. Molecular Crystals and Liquid Crystals, 2001. **356**(1): p. 121-129.
56. Zuin, S., et al., *Formulation effects on the release of silica dioxide nanoparticles from paint debris to water.* Science of the Total Environment, 2014. **476**: p. 298-307.
57. Parvate, S. and P. Mahanwar, *Insights into the preparation of water-based acrylic interior decorative paint: tuning binder's properties by self-crosslinking of allyl acetoacetate-hexamethylenediamine.* Progress in Organic Coatings, 2019. **126**: p. 142-149.
58. Dillon, C.E., A.F. Lagalante, and R.C. Wolbers, *Acrylic emulsion paint films: The effect of solution pH, conductivity, and ionic strength on film swelling and surfactant removal.* Studies in Conservation, 2014. **59**(1): p. 52-62.
59. Elliott, J.E., et al., *Structure and swelling of poly(acrylic acid) hydrogels: effect of pH, ionic strength, and dilution on the crosslinked polymer structure.* Polymer, 2004. **45**(5): p. 1503-1510.
60. Pagnout, C., et al., *Role of electrostatic interactions in the toxicity of titanium dioxide nanoparticles toward Escherichia coli.* Colloids and surfaces B: Biointerfaces, 2012. **92**: p. 315-321.
61. Jassby, D., J. Farner Budarz, and M. Wiesner, *Impact of aggregate size and structure on the photocatalytic properties of TiO2 and ZnO nanoparticles.* Environmental science & technology, 2012. **46**(13): p. 6934-6941.
62. Varner, K., et al., *Nano titanium dioxide environmental matters: state of the science literature review. US Environmental Protection Agency, Washington, DC*. 2010, EPA/600/R-10/089.
63. Chouirfa, H., et al., *Review of titanium surface modification techniques and coatings for antibacterial applications.* Acta biomaterialia, 2019. **83**: p. 37-54.
64. Page, K., M. Wilson, and I.P. Parkin, *Antimicrobial surfaces and their potential in reducing the role of the inanimate environment in the incidence of hospital-acquired infections.* Journal of materials chemistry, 2009. **19**(23): p. 3819-3831.
65. Verran, J., et al., *Variables affecting the antibacterial properties of nano and pigmentary titania particles in suspension.* Dyes and Pigments, 2007. **73**(3): p. 298-304.

CHAPTER 7 DISCUSSIONS, CONCLUSION AND FUTURE WORK

7.1. Discussion

The overall goal of this thesis is to enchance the knowledge on the release of NPs from nano-enabled products, specifically paints, and develop techniques to detect and measure NPs in one of the major environmental sink (WWTPs). The study explores the difference in stability and culturability between pristine NPs and NPs released from paints. In addition, it discovers methods to concentrate and detect NPs in complex matrices in WWTPs such as WW effluent, sludge and biosolids.

7.1.1. Chapter 3

This study focused on the development and optimization of methods to detect the size, particle size distribution and concentration of metal (Ag and Cu) ENPs in biosolids, through the application of various extraction procedures, and the subsequent analysis of aqueous extracts by spICP-MS. ENPs in aqueous extracts of biosolids were detected with an approximate mean size ranging from 16.0 ± 0.2 to 41.3 ± 0.5 nm for Ag and 42.9 ± 0.3 to 109.7 ± 1.7 nm for Cu, with a concentration in the range of 10^7 to 10^9 NPs/g of dry biosolids from eight municipal WWTPs across Canada. In parallel, NPs in sludge had a similar mean size and number concentration to those in biosolids with 21.8 ± 0.2 to 39.7 ± 2.1 nm for Ag and 67.3 ± 1.1 to 142.8 ± 1.8 nm for Cu, and a concentration of 10^7 to 10^{10} NPs/g of dry sludge.

Significance: This data is an important input to future risk assessment and modelling studies. For all WWTPs, measured nAg and nCu concentrations were lower than the PNEC in soils. The water extractable ENPs are potentially mobile and more available for bio-uptake. Only ~ 0.01 to 5% of the total mass of the metals are easily available in NP form, while the rest of the metals in the biosolids are in the form of un-extracted nano or larger particles, complexes with organic matter or organometal compounds. This contributes to the understanding of how much NPs get released into the environment through the WWTP biosolids and will be a helpful input for policy makers. Furthermore, this study advances analytical capabilities for environmental fate and transformation of NPs in complex environmental matrices.

Critical Analysis: There are some analytical limitations in the detection of nAg and nCu particles in sludge and biosolids. One of the limitations of spICP-MS is that there is element specific detection limit for size (10 nm for nAg and 30 nm nCu) and thus, the mean sizes may be over-estimated if there are significant numbers of particles below the size detection limit. Conversely, larger hetero- and homoaggregates that settle easily are unlikely to be present in the supernatant that is analyzed and thus detected. The sizes of NPs determined in biosolids and sludge using spICP-MS involved the assumption that NPs are spherical, whereas, the NPs found in environmetal samples may be irregular shaped. These assumptions do not affect the particle number concentration nor the mass concentration of analysed NPs. In addition, the concentration and size of NPs detected were confirmed using several quality control steps, including spiking dissolved ions to confirm no background interference of dissolved ions in NP peaks, and NP spiking to understand the matrix effect and dissolution of NPs in the biosolids. It should be noted that when particles are homoaggregated, each homoaggregate would be identified as a discrete particle size contributing to the particle size distribution, and thus the particle size distribution represents a mix of discrete particles sizes and and any homoaggregates present. Furthermore, because spICP-MS is an element-specific technique it cannot distinguish if particles are heteroaggregated, or present as part of larger multi-element composite particles. Furthermore, the NPs detected by spICP-MS may be natural, or anthropogenic, as presently it is unable to distinguish between them. Furthermore, freezing of the samples before measurement did not seem to have an effect on the extraction of the NPs from the samples nor a change in size of NPs extracted.

Finally, the data of NP concentrations measured in sludge and biosolids did not show clear trends of NP size and concentration changes when sludge is converted to biosolids at a specific WWTP or how sizes and concentrations may change with different WW treatment or biosolids preparation techniques . Further analyses of WWTP sludge and biosolids samples for NPs size and concentration from additional WWTPs are required to assess such patterns as well as location-based differences.

7.1.2. Chapter 4

In this study, we detected and characterized nAg and nCu using spICP-MS in WW effluent samples by developing methods to concentrate NPs in several Canadian WWTPs. At first, methods were developed to concentrate NPs by spiking nAg in WW effluent. nAg spiked in DI water gave similar results for both CPE and centrifugal ultrafiltration with extraction efficiency of 95.3 ± 3.2% and 94.1 ± 6.8%, respectively. Similarly, centrifugal ultrafiltration had a higher recovery percentage for spiked nAg in WW effluents from plant A, AB, plant D, ON and plant F, QC with values of 116.9 ± 5.9%, 95.8 ± 8.2%, and 98.2 ± 7.9%, respectively. In contrast, in WW effluent, a lower extraction efficiency was observed for CPE with 72.5 ± 5.9% in plant A, AB, 68.7 ± 5.1% in plant D, ON and 80.8 ± 3.6% in plant F, QC. Centrifugal ultrafiltration after 15 cycles of concentration gave a lower recovery compared to one cycle, with extraction values reducing from 103.6% to 63.3%. These lower recovery rates were attributed to attachment of NPs to the filter which were not able to be dislodged by the sonication. No NPs were observed in the filtrate WW effluent confirming the attachment to the filter. Concentration of nCu varied from 0.1 ng/L to 12 ng/L depending on the WWTP effluent with size varying from 34.6 ± 1.3 to 68.0 ± 0.3 nm. Concentration of nAg detected ranged from 0.08 to 0.43 ng/L with mean size 19.3 ± 0.1 to 34.7 ± 7.2 nm lower than previously reported studies.

Significance: Comparing the measured concentration of NPs in biosolids (Chapter 3) to the measured concentration in WW effluent (Chapter 4), it can be seen that more than 99% of NPs are separated along with biosolids during the WW treatment processes, leading to extremely low concentration in the effluent. These results signify that field-scale WWTPs are as effective as lab-scale models in the removal of NPs in sludge. These measured NPs in WW effluent may be natural, or anthropogenic, and presently it is unable to distinguish between them. Even though these NP concentrations are below PNEC (nAg - 12 ng/L and nCuO - 340 ng/L) in freshwater, constant loading can lead to bioaccumulation of NPs in the organisms by constant exposure to WW effluent. The data reported here can be used for future modelling, exposure assessment and toxicology studies.

Critical Analysis: Similar to Chapter 3, there are some analytical and method limitations of measurement of NPs in WW effluent. Limit of detection of size in spICP-MS is element specific

- close to 10 nm for nAg and close to 30 nm for nCu. The NPs present in WW effluent below these sizes are incorrectly assessed as dissolved concentrations, leading to over estimation of size and a shift in particle size distribution. One of the interesting results obtained was the proportional increase in the mass concentration of nCu along with the size of these particles (trend that was not observed with nAg particles). This might be due to the fact that lower sizes of nCu detected were close to the limit of detection (mentioned before), thereby losing some of the particle concentration as dissolved, whereas nCu at higher concentration had more particles counted contributing to the full particle size distribution. Moreover, the NPs detected in WW effluent may be either anthropogenic or natural and need further research to distinguish between them.

Only nAg and nCu particles were analysed in this study, and a multitude of other manufactured NPs are received and discharged by WWTPs. As reported, only six out of the nine WW effluent measured contained measurable concentration of nAg; however, nCu particles were observed in all the WW effluents. nAg and nCu particles had different element-specific distribution between WWTP sludge and effluent. Therefore, other elemental NPs would also have varying presence and distribution between WW sludge and effluent. Thus, further research must be extended to analyze the presence of other NPs in WWTPs to achieve a more complete understanding of NP concentrations in WWTPs.

7.1.3. Chapter 5

nAg released from painted surfaces under various aging and aqueous chemistry conditions were characterized for size and concentration by analyses of the aqueous wash samples using spICP-MS. nAg releases increased over time at all pH conditions, with highest nAg concentrations observed at acidic pH of 3.5 at $2.2 \pm 0.8 \times 10^7$ NP/mL/g at the end of day 16, compared to basic pH ~8.5 with $3.9 \pm 0.2 \times 10^6$ NP/mL/g or DI water pH ~5.8 with $2.1 \pm 0.1 \times 10^6$ NP/mL/g. Thus, the release of nAg at acidic pH was 10-folds higher than that at neutral pH and 5.6-folds higher than that at basic pH. nAg released with acidic pH were smaller in size, with a mean diameter of 37.1 ± 2.1 nm compared to 64.6 ± 4.3 nm with neutral pH. nAg released from painted surfaces were found to be more colloidally stable compared to pristine nAg in DI water conditions, which dissolved completely after the 15 days of exposure. Finally, culturability test on survival of *E. coli D21* showed that nAg released from paint were toxic after 3 hours compared to base paint (which recorded survival up to 18 h) and pristine nAg, in which *E. coli D21* survival was present through the experiment period of 42 h.

Significance: The physico-chemical properties and ecotoxicological potential of paint-released and pristine nAg are significantly different. This is a step forward in understanding the distinct behaviour of released NPs from products and pristine NPs. Studies on environmental fate and toxicity of NPs have typically been performed with pristine NPs, as-synthesized or as-manufactured NPs, which may not reflect the environmental fate of NPs released from products with matrix associated with them. On the other hand, our results as well as from other studies show that nAg can be added to paints and coatings to improve the disinfection capabilities against bacteria and viruses [1-4]. Our results signify the necessity of toxicity and fate studies using released NPs from products rather than pristine NPs.

Critical Analysis: nAg released from different painted surfaces under various environmentally relevant conditions are associated with some paint matrix, and the following points can be drawn from our analyses. First, the concentration of NPs released might be influenced by the surface on which paint is applied. The study used polystyrene and polyvinyl chloride surfaces, as they did not have any background metal, or inteferences for measurement in spICP-MS, and some differences in the extents of release were observed. Further work is needed to assess the release of NPs from other surfaces. Second, custom-made paint formulated in this study, was based on an industrial standard of 0.003% nAg in a base acrylic polymer. Varying this initial concentration (0.003%) of nAg in paint may influence the concentration of nAg released from painted surface; however, the patterns and behavior of release from various physiochemical conditions (acidic, basic, DI water and sunlight exposure) should remain unaltered. Third, mechanical abrasion was usually used in previous studies to show degradation of paint from painted surfaces. As physical activity for mechanical abrasion may vary between surface to surface, sonication was adopted in our study to maintain similar physical abrasion between surfaces and degrade paint from the surface. There may be some differences in the release patterns based on different types of mechanical abrasion. Fourth, custom-made paint of nAg used for the experimental study contained a base acrylic polymer solution without any other metals whereas, commercial paints may usually contain other pigments, thinner, filler and additives, which might influence the release of NPs. This study is an initial step towards understanding how NPs get released from the painted surface; hence, further research is required to assess the effect of all the other commercial paint ingredients. Finally, the *E.coli* culturability assay was conducted to assess the toxicity of paint released NPs and pristine nAg. However, several other *in-vitro* and *in-vivo* studies on representative cells can be used to assess the toxic nature of the NPs released from paint and its pristine counter parts.

7.1.4. Chapter 6

This chapter involves the analysis of the behavior of pristine $nTiO_2$ and released $nTiO_2$ from the painted surface, to assess their fate and viability. In this study, release of $nTiO_2$ from painted surfaces using both commercial and custom-made paints under various pH conditions was characterized for size, concentration and particle size distribution by analyses of the aqueous wash samples by spICP-MS. Comparison of four commercial paints with unknown concentrations of $nTiO_2$ showed that B-NP ext. (claimed to have NPs) released 11 to 16 times lower $nTiO_2$ of 1 to 2 ng/mL of water/g of dry paint, compared to other commercial paints ~ 10 to 30 ng/mL/g. At acidic pH 3.5-4.2, $nTiO_2$ released from commercial paints on surfaces were 20 to 42% more compared to neutral or basic pH for three paints except for A ext. paint. Since different commercial paints released dissimilar amounts of $nTiO_2$ under different pH conditions, no observable patterns of release were detected for all four paints. Custom-made paint at acidic pH of ~3.5 and basic pH ~8.5 leads to aggregation and settling of $nTiO_2$ compared to DI water (pH ~5.8). Sonication of the collected wash water from acidic pH ~3.5 released twice the particle number compared to basic pH ~8.5 and DI water at pH ~5.8 at the end of 11 days. Custom-made paint with $nTiO_2$ behaves similarly to commercial paint B-NP ext., with concentrations of ENP released around ~1 ng/mL/g in quiescent systems exposed to DI water, acidic and basic conditions. Finally, viability tests on survival of *E. coli D21* showed that $nTiO_2$ released from paint were toxic after 6 hours compared to base paint (which recorded survival up to 18 h) and pristine $nTiO_2$, where the *E. coli D21* survival was present through the experiment period of 42 h.

Significance: Even though a high concentration (10% w/v) of $nTiO_2$ is used to produce the nano paint (in this study), with exposure to water of different pH, only less than 10^{-5} % of NPs applied were released from the surface, implying satisfactory binding of NPs with the resins in the paint matrix. Interestingly, like the custom-made paint, the commercial paint (paint B-NP ext.), claimed to have $nTiO_2$, released lesser NPs compared to other commercial paints. This suggests that using NPs for paint production replacing mixtures of nano-, micron- and larger particles of TiO_2, would release lower concentration to the environment.

Critical Analysis: The main focus of this chapter was to detect the $nTiO_2$ release from painted surfaces, and the exact analysis adopted in the previous chapter for nAg was used to obtain the corresponding results. Studying $nTiO_2$ particles is important since they are the most commonly used NPs in the paint and coating industry. The following points can be drawn from our analyses. First, the commercial paints containing unknown concentrations of $nTiO_2$ showed similar patterns of release compated to custom made paints prepared using known quantities of $nTiO_2$. Second, unlike the results obtained with nAg, the stability and concentration of $nTiO_2$ released from painted surface under environmentally relevant exposure conditions were much less, even at high concentration of $nTiO_2$ in paint. Thus, each NP is likely to have different release rates and extents under same physiso-chemical exposure conditions and thus, needs further work to assess its effects.

7.1.5. General Discussion

Nanotechnology is projected to be a billion-dollar industry with exponential growth over the next decade. The potential areas of use of ENPs are extensive, which can include cosmetics, textiles, electronics, medical, paints and coatings, water treatment, soil remediation, food, packaging and many more. The major types of ENPs used in different fields of expertise include carbon NPs (fullerenes and carbon nanotubes), metal and metal oxide NPs (titanium dioxide, silica, silver, copper, etc.), semiconductor NPs (quantum dots), polymeric NPs (organic based) and lipid-based NPs [5-7]. Based on the research report of nanotechnology market forecast of 2020, global nanotechnology market between 2020 and 2025 is expected to have a compound annual growth rate of more than 14.3% with investments close to \$121 billion [8]. As the usage of NPs is increasing, it is inevitably going to end up in one of the environmental sinks (land air, and water).

In our studies, paint embedded with NPs (nAg and $nTiO_2$) were found to be released from the surface under various physio-chemical conditions. These released NPs bound to small amounts of the paint matrix will reach one of the many environmental sinks, either directly or through a WWTP. The NPs released from paint were found to behave differently from its pristine counterparts, which means that previous studies using prisitine NPs may be inaccurate in predicting its effects (stability and toxicity). Further research is required with NPs released from different products to assess their corresponding effects.

There are many routes of release of NPs from products to the environment, and a very significant route is the release of NPs into municipal wastewater. A 2013 study by Keller and Lazareva [9] suggested that between 17 and 34% of the total metal NPs manufactured and used in various products and processes are released to wastewater treatment plants. Our studies extracted NPs (nAg and nCu) from WWTP sludge and biosolids and measured their size and concentration in the chemically complex matrix.However, methods need to be developed for a multitude of other metal and non-metal NPs present discharged from WWTPs with sludge, biosolids and effluents..

7.2. Conclusion

Overall, this research demonstrates that:

(i) WW sludge and biosolids are one of the main receivers of NPs released into the environment. This is the first report of systematic ENP characterization in sludge and biosolids across several regional WWTPs anywhere in the world. It was found that only a fraction of NPs is easily available in NP form in biosolids, while the rest of the metals are in the form of un-extracted nano or larger particles, which may be complexes with organic matter or organometal compounds.

(ii) The measured concentrations of nAg and nCu are lower than the ones reported in previous modelled and measured studies. In addition, the nAg and nCu measured concentrations in WW effluent from WWTPs, indicate high removal efficiency. Furthermore, our results prove that field-scale WWTPs are as effective as lab-scale models in removing NPs into sludge. Thus, these results can serve as input for future studies focused on modelling, exposure assessment and toxicology of NPs.

(iii) The behaviour of pristine nAg is found to be different than that of nAg released from painted surfaces, in terms of stability, particle size distribution and culturability. For instance, while pristine nAg aggregated and dissolved over time, no significant changes were observed for released nAg from painted surfaces in terms of size, NP distribution and dissolved concentration. In addition, nAg released from painted surfaces were found to be more toxic than pristine nAg.

(iv) The release of $nTiO_2$ from painted surfaces and its aggregation state differ depending on the pH conditions. Nano-enabled commercial paints with $nTiO_2$ released lesser NPs (similar to custom-made $nTiO_2$ paint) compared to other commercials paints with mixture nano-, micron- and larger particles of TiO_2. $nTiO_2$ released from painted surfaces behave differently in stability, particle size distribution and toxicity.

7.3. Future work

Detection and characterization of NPs in complex matrices like WWTPs are difficult. Many of the techniques have limitations for analysis of NPs in environmental samples in complex media, because of their inability to distinguish target NPs from background natural colloids such as clays and mineral oxide particles. spICP-MS is an impressive method for measuring metal NP sizes, particle size distribution and concentrations in relatively pure aqueous samples at sub parts per billion concentrations. This study has developed techniques to detect nAg and nCu particles in WW sludge, biosolids and effluent after extraction or pre-concentration of WW sample. The size, particle size distribution and concentration of nAg and nCu detected from WW samples can be used for future research, modelling and toxicological studies. It is important to investigate the long-term toxic effects of these transformed particles from WWTPs rather than looking into toxic effects of pristine NPs at short term. Furthermore, only two (nAg and nCu) of several NPs used in the nanomaterial industry have been analysed. Other elemental NPs would also have varying presence and partitioning between WW sludge and effluent. Hence, concentration and size data of other NPs in WWTP samples are needed to be analyzed in order to help determine the risk and implement future regulations if needed. In addition, the NPs concentration in WWTP effluents, sludge and biosolids might vary depending on the WWTP facilities and/or, location of WWTPs. Further research and analysis of NP concentration in additional WWTP samples are required to understand the significance of WWTP facilities and/or location of WWTPs.

NPs released from nano-enabled products, such as paints, come along with some product matrix. Our results indicate that both nAg and $nTiO_2$ behaved differently compared to their pristine forms. The matrix of paint, along with which NPs are released, is influencing its fate in the environment. nAg released from paint were observed to be more stable compared to pristine Ag, whereas, $nTiO_2$ released from paint were more aggregated compared to the pristine $nTiO_2$. The culturability studies with *E. Coli D21* assess how released NPs from painted surfaces are different from pristine NPs in their pure form. These results indicate the need to study the release and behavior of NPs from more nano-enabled products. Furthermore, several other *in-vitro* and *in-vivo* studies on representative cells can be used to assess the toxic nature of the NPs released from paint and its pristine counter parts. Further work is required to assess the effect of application surface on the release of NPs and type of NPs used in paints. In addition, further research must focus on how various environmental weathering factors influence NPs release, transformation, toxicity, and behavior from nano-enabled products such as paint.

References

1. Elechiguerra, J.L., et al., *Interaction of silver nanoparticles with HIV-1.* Journal of nanobiotechnology, 2005. **3**(1): p. 6.
2. Lara, H.H., et al., *Mode of antiviral action of silver nanoparticles against HIV-1.* Journal of nanobiotechnology, 2010. **8**(1): p. 1.
3. Park, S., et al., *Antiviral properties of silver nanoparticles on a magnetic hybrid colloid.* Appl. Environ. Microbiol., 2014. **80**(8): p. 2343-2350.
4. Mori, Y., et al., *Antiviral activity of silver nanoparticle/chitosan composites against H1N1 influenza A virus.* Nanoscale research letters, 2013. **8**(1): p. 93.
5. Bhatia, S., *Nanoparticles Types, Classification, Characterization, Fabrication Methods and Drug Delivery Applications*, in *Natural Polymer Drug Delivery Systems: Nanoparticles, Plants, and Algae*, S. Bhatia, Editor. 2016, Springer International Publishing: Cham. p. 33-93.
6. Jeevanandam, J., et al., *Review on nanoparticles and nanostructured materials: history, sources, toxicity and regulations.* Beilstein journal of nanotechnology, 2018. **9**: p. 1050-1074.
7. Weinberg, H., A. Galyean, and M. Leopold, *Evaluating engineered nanoparticles in natural waters.* TrAC Trends in Analytical Chemistry, 2011. **30**(1): p. 72-83.
8. Industryarc, *Nanotechnology Market report – Forecast (2020-2025).* 2020: Report Code: ESR 0048.
9. Keller, A.A. and A. Lazareva, *Predicted releases of engineered nanomaterials: From global to regional to local.* Environmental Science & Technology Letters, 2013. **1**(1): p. 65-70.

APPENDIX

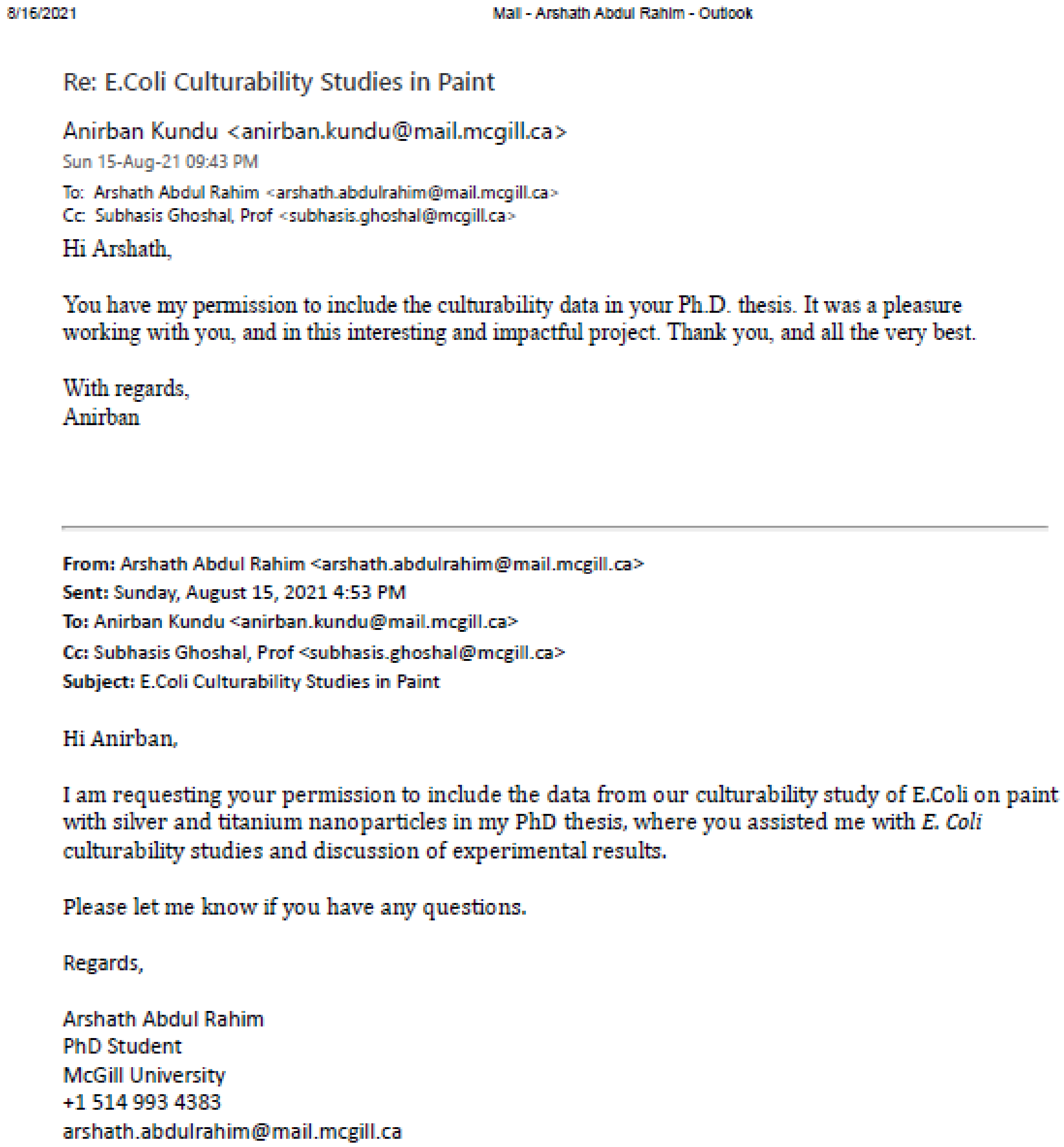

8/16/2021 Mail - Arshath Abdul Rahim - Outlook

Re: E.Coli Culturability Studies in Paint

Anirban Kundu <anirban.kundu@mail.mcgill.ca>
Sun 15-Aug-21 09:43 PM
To: Arshath Abdul Rahim <arshath.abdulrahim@mail.mcgill.ca>
Cc: Subhasis Ghoshal, Prof <subhasis.ghoshal@mcgill.ca>

Hi Arshath,

You have my permission to include the culturability data in your Ph.D. thesis. It was a pleasure working with you, and in this interesting and impactful project. Thank you, and all the very best.

With regards,
Anirban

From: Arshath Abdul Rahim <arshath.abdulrahim@mail.mcgill.ca>
Sent: Sunday, August 15, 2021 4:53 PM
To: Anirban Kundu <anirban.kundu@mail.mcgill.ca>
Cc: Subhasis Ghoshal, Prof <subhasis.ghoshal@mcgill.ca>
Subject: E.Coli Culturability Studies in Paint

Hi Anirban,

I am requesting your permission to include the data from our culturability study of E.Coli on paint with silver and titanium nanoparticles in my PhD thesis, where you assisted me with *E. Coli* culturability studies and discussion of experimental results.

Please let me know if you have any questions.

Regards,

Arshath Abdul Rahim
PhD Student
McGill University
+1 514 993 4383
arshath.abdulrahim@mail.mcgill.ca

Figure A1 Permission email from second author in regards to using the data where second author assisted first author with E. Coli culturability studies and discussion of experimental results.

McGill University
Environmental Health and Safety
Room 426, McTavish 3610 Montreal, Quebec H3A 1Y2

THIS IS TO CERTIFY THAT

Arshath Abdul Rahim

Department of Civil Engineering & Applied Mechanics

SUCCESSFULLY COMPLETED CORE TRAINING IN

Workplace Hazardous Materials Information System (W.H.M.I.S.)

ON 20-Jul-17

Joseph Vincelli
Joseph Vincelli
EHS Operations Manager
Valid Until Sunday, July 19, 2020

Wayne Wood
Director, EHS

Figure A2 Workplace Hazardous Materials Information System (W.H.M.I.S) certificate required to work in the Benedek Environmental Engineering lab